The rotation of Iberia during the Aptian and consequences for pervasive Cretaceous remagnetization

Zhihong Gong

GEOLOGICA ULTRAIECTINA

Mededelingen van de Faculteit Geowetenschappen

Universiteit Utrecht

No. 292

Members of the Dissertation Committee:
Prof. Dr. R. van der Voo
Department of Geological Sciences,
University of Michigan, Ann Arbor, USA

Prof. Dr. R. L. M. Vissers
Faculty of Geosciences,
Utrecht University, Utrecht, The Netherlands

Prof. Dr. M. J. R. Wortel
Faculty of Geosciences,
Utrecht University, Utrecht, The Netherlands

Prof. Dr. C. J. Spiers
Faculty of Geosciences,
Utrecht University, Utrecht, The Netherlands

Dr. J. Dinarès-Turell
Instituto Nazionale di Geofisica e Vulcanologia
Rome, Italy

This study was supported by:
The Vening Meinesz Research School of Geodynamics (VMSG), with financial aid from the Department of Earth Sciences of the Faculty of Geosciences, Utrecht University, The Netherlands.

The research for this thesis was carried out at:
Paleomagnetic laboratory 'Fort Hoofddijk'
Faculty of Geosciences, Utrecht University
Budapestlaan 17, 3584 CD, Utrecht
The Netherlands

The author can be reached through e-mail: gong@geo.uu.nl

ISBN: 978-90-5744-158-5

Graphic design: GeoMedia, Faculty of Geosciences,
Utrecht University

The rotation of Iberia during the Aptian and consequences for pervasive Cretaceous remagnetization

De rotatie van het Iberisch schiereiland tijdens het Aptien en de gevolgen voor pervasieve remagnetizatie gedurende de Krijt periode

(met een samenvatting in het Nederlands)

PROEFSCHRIFT

ter verkrijging van de graad van doctor
aan de Universiteit Utrecht
op gezag van de rector magnificus, prof. dr. J.C. Stoof,
ingevolge het besluit van het college voor promoties
in het openbaar te verdedigen
op donderdag 20 november 2008 des middags te 12.45 uur

door

Zhihong Gong

geboren op 19 december 1974
te Shenchi, People's Republic of China

Promotor:
Prof. Dr. C. G. Langereis

Co-Promotor:
Dr. M. J. Dekkers

天行健，君子以自强不息；
地势坤，君子以厚德载物。
—《周易》

Bibliography

Chapter 1:
Gong, Z., Langereis, C.G. and Mullender, T.A.T. (2008). The rotation of Iberia during the Aptian and the opening of the Bay of Biscay, *Earth Planet. Sci. Lett*., 273, 80-93.

Chapter 2:
Gong, Z., van Hinsbergen, D.J.J., Vissers, R.L.M., Dekkers, M.J.. Early Cretaceous syn-rotational extension in the Organyà basin: What was the palinspastic position of Iberia during its rotation? *Submitted to Tectonophysics*.

Chapter 3:
Gong, Z., Dekkers, M.J., Dinarès-Turell, J., Mullender, T.A.T., (2008). Remagnetization mechanism of Lower Cretaceous rocks from the Organyà Basin (Pyrenees, Spain). *Studia Geoph. Geod.* 52, 187-210.

Chapter 4:
Gong, Z.,van Hinsbergen, D.J.J., Dekkers, M.J.. Diachronous pervasive remagnetization in northern Iberian basins during Cretaceous rotation and extension. *Submitted to Earth Planet. Sci. Lett.*

Chapter 5:
Gong, Z., Dekkers, M.J., Heslop, D., Mullender, T.A.T.. End-member modeling of isoth-ermal remanent magnetisation (IRM) acquisition curves: a novel approach to diagnose remagnetization. *Submitted to Geophy. J. Int.*

Contents

Prologue

In the early Mesozoic, the super-continent Pangaea broke up into Laurasia and Gondwana (e.g. Scotese, 2001; Torsvik et al., 2008). The Iberian Peninsula together with Eurasia was a part of Laurasia (e.g. Dercourt et al., 1986; Gibbons and Moreno, 2002). In the Cretaceous, Iberia was separated as a micro-plate from Eurasia and Africa along the Azores-Gibraltar plate boundary in the South and the North Pyrenean Fault Zone in the North (e.g. Srivastava et al., 1990b; Olivet, 1996; Vergés et al., 2002; Sibuet et al., 2004). Subsequently Iberia rotated ~35° counter-clockwise (CCW) with respect to Eurasia, contemporaneous with the opening of the Bay of Biscay (e.g. Carey, 1958; Bullard, 1965; Van der Voo, 1969; Sibuet et al., 2004). To constrain this rotation more precisely, in particular with respect to its age and duration, several controversial and partially conflicting views have been proposed. The inconsistencies arise mainly from (1) the low resolution age dating; (2) paucity of paleomagnetic data; (3) possible remagnetization (secondary paleomagnetic components overprinted the primary natural remanent magnetization which was locked-in at the timing of the formation of the rock); (4) very low intensities of the natural remanent magnetization (NRM). Meanwhile, most paleomagnetic studies argue that there would be a two-stage rotation. Other studies, based on oceanic magnetic anomalies in the Bay of Biscay (Pichon and Sibuet, 1971; Srivastava et al., 1990b; Srivastava et al., 1990a; Roest and Srivastava, 1991; Brothers et al., 1996; Olivet, 1996; Sibuet et al., 2004), agree that the opening of the Bay of Biscay occurred between M0r to A33o (Aptian to Campanian), and caused the ~37° CCW rotation of Iberia. However, the timing of the Iberian rotation based on sea-floor anomalies alone is poorly constrained because of the "Cretaceous Quiet Zone", the Cretaceous Normal Superchron. Therefore, to answer when, how, and where Iberia rotated, integrated high-resolution stratigraphic and detailed paleomagnetic data are required.

In the Iberian Peninsula, many Mesozoic extensional and transtensional basins which formed during the rotation of Iberia and the opening of Bay of Biscay, are reported to be remagnetized (e.g. Schott and Peres, 1987; Galdeano et al., 1989; Moreau et al., 1992; Pares and Roca, 1996; Moreau et al., 1997; Juárez et al., 1998; Dinarès-Turell and García-Senz, 2000; Villalaín et al., 2003; Márton et al., 2004; Soto et al., 2008). The widespread Iberian remagnetization combined with fairly poor age constraints increased the controversy on their mechanism(s) and whether the remagnetizations are regional, i.e. basin scale, or continent-wide over entire Iberia. Most of the Mesozoic basins have a supposedly Cretaceous remagnetization (Galdeano et al., 1989; Moreau et al., 1992; Juárez et al., 1994; Juárez et al., 1998; Dinarès-Turell and García-Senz, 2000) which usually was argued to have been acquired during the Cretaceous Normal Superchron because of the invariably normal polarity overprint. The remagnetization mechanisms are loosely tied to the 'Cretaceous thermal event' reported in Iberia. To answer when and why the Iberian remagnetization happened, detailed remagnetization studies in Iberia are needed.

Meanwhile seen in a worldwide perspective, the "remagnetization syndrome" is considered to be much more widespread than previously anticipated. To diagnose remagnetization, the classical approaches focus on the analysis of paleomagnetic directions and utilize field tests (e.g. fold test) as much as possible. Such analysis – while worthwhile – is not entirely independent. Therefore in several cases hysteresis parameters (coercive force, remanent coercive force, saturation magnetization, and remanent saturation magnetization acquired from hysteresis loops and back field demagnetization curves) are plot in the 'Day plot' (Day et al., 1977) and the results may show so-called the remagnetized and non-remagnetized trends (Channel and McCabe, 1994) helping to identify the remagnetization. However, for samples with either low intensity magnetization or a mixed magnetic mineralogy, this method may be equivocal. Therefore, additional criteria, independent from the paleomagnetic directions, are required to identify and understand the remagnetization.

To accomplish these aims, this Ph.D project was carried out in the Organyà Basin, northern Spain (Fig. 1). Why did we select the Organyà Basin as study area? There are two major reasons: (1) The Organyà Basin is a typical inverted Pyrenean basin. The basin experienced extension during the Berriasian-middle Albian, post-rift sedimentation during late Albian-Cenomanian, and inversion during the late Santonian followed by the Pyrenean orogeny until the Miocene (Dinarès-Turell and García-Senz, 2000; García-Senz, 2002). The ages of the sediments in the Organyà Basin are well constrained by biostratigraphy in stages and sub-stages (Becker, 1999; Bernaus et al., 1999; Bernaus, 2000; Bernaus et al., 2000; Bernaus et al., 2003). So, the paleomagnetic data to be gathered when shown

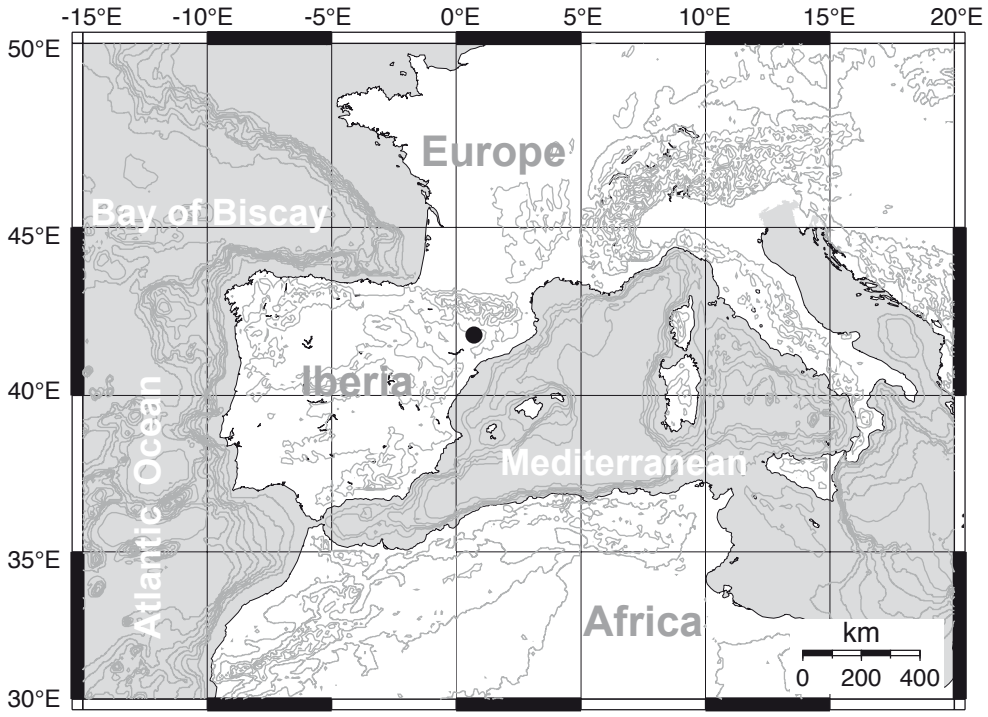

Pro-Fig. 1. Position of Iberia, Bay of Biscay in a bathymetry and topographic map. The black dot indicates the location of the Organyà Basin (the actual basin is smaller than the size of the dot).

to be primary are narrowly constrained in age. In the Organyà Basin, the lower Cretaceous Berriasian-Barremian limestones were earlier reported to be remagnetized while the Aptian-Cenomanian marls (with some limestone intercalations) have a primary remagnetization (Dinarès-Turell and García-Senz, 2000). Therefore, the Organyà Basin is a very appropriate location for studying the timing of the rotation of Iberia with respect to Eurasia. (2) The ~ 4.5 km thick Cretaceous hemipelagic and pelagic deposits in the Organyà Basin consist of limestones and marls. The remagnetization is considered to be a chemical remagnetization, however, the remagnetization mechanism was not explored in detail. So the basin also provides a very good opportunity to scrutinize the remagnetization mechanisms and further develop identification methods for remagnetization.

The approaches we used for this study derive mainly from the paleomagnetic and rock magnetic fields. In the Cretaceous rotation of Iberia study, a new demagnetization protocol especially for low-intensity magnetization samples was developed. It consists of thermal demagnetization (up to 150˚C for limestones and 210˚C for marls) followed by alternating field demagnetization (until 100 mT). In the Organyà Basin, our paleomagnetic results have a higher quality (small uncertainties in age and α_{95}) and quantity (more than 1100 drilled cores) than many other published paleomagnetic datasets. Based on the paleomagnetic datasets in Iberia and Oceanic magnetic anomaly data from the Bay of Biscay, we can constrain the Iberian rotation better in time and magnitude. To reconstruct the palinspastic position Iberia during the rotation, the paleo-stress regime in the Organyà Basin was derived from the anisotropy of magnetic susceptibility (AMS). The obtained original extension direction is used for this purpose along with other geological and geophysical constraints.

To answer when and why these pervasive Iberian remagnetization occurred, the small circle intersection (SCI) method (Waldhör and Appel, 2006) is applied to restore the syn-tectonic remagnetized direction in the Organyà Basin and several other Iberian basins. Several rock magnetic methods have been designed to diagnose the remagnetization, each with their advantages and disadvantages. Here we developed a novel method based on end-member modeling (e.g. Weltje, 1997; Heslop and Dillon, 2007) of isothermal remanent magnetization (IRM) acquisition curves. This new approach can be a very useful tool to diagnose remagnetization in weakly magnetic sediments.

References

Becker, E., 1999. Orbitoliniden-Biostratigraphie der Unterkreide (Hauterive-Barrême) in den spanischen Pyrenäen (Profil Organyà, Prov. Lérida). Rev. Paléobiol., Genève 18, 359-489.

Bernaus, J.M., Arnaud-Vanneau, A., Caus, E., 1999. La sedimentación "Urgoniense" en la cuenca de Organyà (NE España). Libro homenaje a José Ramírez del Pozo. De Geol. Y Geofis. Españoles del Petróleo AGGEP, 71-80.

Bernaus, J.M., 2000. L'Urgonien du Bassin d'Organyà (NE de l'Espagne): micropaléontologie, sédimentologie et stratigraphie séquentielle. Mém. H. S. 33, 138.

Bernaus, J.M., Caus, E., Arnaud-Vanneau, A., 2000. Aplicación de los análisis micropaleontológicos cuantittivos en estratigrafía secuential: El Cretácico inferior de la cuenca

de Organyà (Pirineos, España). Rev. Soc. Geol. España 13, 55-63.

Bernaus, J.M., Arnaud-Vanneau, A., Caus, E., 2003. Carbonate platform sequence stratigraphy in a rapidly subsiding area: the Late Barremian – Early Aptian of the Organya basin, Spanish Pyrenees. Sedimentary Geology 159, 177-201.

Brothers, L.A., Engel, M.H., Elmore, R.D., 1996. A laboratory investigation of the late diagenetic conversion of pyrite to magnetite by organically complexed ferric iron. Chemical Geology 130, 1-14.

Bullard, E., Everett, J., Gilbert Smith, A., 1965. A symposium on continental drift. in, Phil. Trans. R. Soc. Lond. Ser. A.,41-51.

Carey, S.W., 1958. A tectonic approach to continental drift. in, Symposium on Continental Drift.Hobart (Tasmania),177-355.

Channel, J.E.T., McCabe, C., 1994. Comparison of magnetic hysteresis parameters of unremagnetized and remagnetized limestones. J. Geophys. Res. 99, 4613-4623.

Day, R., Fuller, M.D., Schmidt, V.A., 1977. Hysteresis properties of titanomagnetites: Grain size and composition dependence. Phys. Earth Planet. Int. 13, 260-266.

Dercourt, J., Zonensshain, L.P., Ricou, L.E., Kazmin, V.G., Lepichon, X., Knipper, A.L., Grandjacquet, C., Sbortshikov, I.M., Geyssant, J., Leprevier, C., Peckersky, D.H., Boulin, J., Sibuet, J.C., Savostin, L.A., Soroktin, O., Westphal, M., Bazhenov, M.L., Lauer, J.P., Biju-Duval, B., 1986. Geological Evolution of the Tethys Belt from the Atlantic to Pamirs since the Lias. Tectonophysics 123, 241-315.

Dinarès-Turell, J., García-Senz, J., 2000. Remagnetization of Lower Cretaceous limestones from the southern Pyrenees and relation to the Iberian plate geodynamic evolution. J. Geophys. Res. 105, 19405-19418.

Galdeano, A., Moreau, M.G., Pozzi, J.P., Berthou, P.Y., Malod, J.A., 1989. New Paleomagnetic Results from Cretaceous Sediments near Lisbon (Portugal) and Implications for the Rotation of Iberia. Earth Planet. Sci. Lett. 92, 95-106.

García-Senz, J., 2002. Cuencas extensivas del Cretacico Inferior en los Pireneos Centrales – formacion y subsecuente inversion. [PhD thesis]. University of Barcelona, Barcelona.

Gibbons, W., Moreno, M.T., 2002. The geology of Spain. The Geological Society, London, pp. 649.

Heslop, D., Dillon, M., 2007. Unmixing magnetic remanence curves without a priori knowledge. Geophys, J. Int. 170, 556-566.

Juárez, M.T., Osete, M.L., Melendez, G., Langereis, C.G., Zijderveld, J.D.A., 1994. Oxfordian Magnetostratigraphy of the Aguilon and Tosos Sections (Iberian Range, Spain) and Evidence of a Preoligocene Overprint. Physics of the Earth and Planetary Interiors 85, 195-211.

Juárez, M.T., Lowrie, W., Osete, M.L., Meléndez, G., 1998. Evidence of widespread Cretaceous remagnetisation in the Iberian Range and its relation with the rotation of Iberia. Earth and Planetary Science Letters 160, 729-743.

Márton, E., Abranches, M.C., Pais, J., 2004. Iberia in the Cretaceous: new paleomagnetic results from Portugal. J. Geodyn. 38, 209-221.

Moreau, M.G., Canerot, J., Malod, J.A., 1992. Paleomagnetic study of Mesozoic sediments from the Iberian Chain (Spain) Suggestions for Barremian remagnetization and implications for the rotation of Iberia. Bull. Soc. Géol. France 163, 393-402.

Moreau, M.G., Berthou, J.Y., Malod, J.-A., 1997. New paleomagnetic Mesozoic data from the Algarve (Portugal): fast rotation of Iberia between the Hauterivian and the Aptian. Earth Planet. Sci. Lett. 146, 689-701.

Olivet, J.L., 1996. Kinematics of the Iberian Plate. B Cent Rech Expl 20, 131-195.

Pares, J.M., Roca, E., 1996. The significance of tectonic-related Tertiary remagnetization along the margins of the Valencia Trough. J. Geodyn. 22, 207-227.

Pichon, X.L., Sibuet, J.C., 1971. Western extension of boundary between European and Iberian Plates during the Pyrenean orogeny. Earth Planet. Sci. Lett. 12, 83-88.

Roest, W.R., Srivastava, S.P., 1991. Kinematics of the plate boundaries between Eurasia, Iberia and Africa in the North Atlantic from the Late Cretaceous to the present. Geology 19, 613-616.

Schott, J.J., Peres, A., 1987. Paleomagnetism of the Lower Cretaceous redbeds from northern Spain: evidence for a multistage acquisition of magnetization. Tectonophysics 139, 239-253.

Scotese, C., 2001. Atlas of Earth History, PALEOMAP Project. Arlington, TX, pp. 52.

Sibuet, J.C., Srivastava, S.P., Spakman, W., 2004. Pyrenean orogeny and plate kinematics. J. Geophys. Res. 109, B08104, doi: 10.1029/2003JB002514.

Soto, R., Villalaín, J., J., Casas-Sainz, A., M., 2008. Remagnetizations as a tool to analyze the tectonic history of inverted sedimentary basins: A case study from the Basque-Cantabrian basin (north Spain). Tectonics 27, doi:10.1029/2007TC002208.

Srivastava, S.P., Roest, W.R., Kovacs, L.C., Oakey, G., Levesque, S., Verhoef, J., Macnab, R., 1990a. Motion of Iberia since the Late Jurassic: results from detailed aeromagnetic measurements in the Newfoundland Basin. Tectonophysics 184, 229-260.

Srivastava, S.P., Schouten, H., Roest, W.R., Klitgord, K.D., Kovacs, L.C., Verhoef, J., Macnab, R., 1990b. Iberian plate kinematics: a jumping plate boundary between Eurasia and Africa. Nature 344, 756-759.

Torsvik, T., Muller, R.D., Van der Voo, R., Steinberger, B., Gaina, C., 2008. Global plate motion frames: Toward a unified model. Rev. Geophys. 46, RG3004, doi:10.1029/2007RG000227.

Van der Voo, R., 1969. Paleomagnetic evidence for the rotation of the Iberian Peninsula. Tectonophysics 7, 5-56.

Vergés, J., Fernàndez, M., Martínez, A., 2002. The Pyrenean orogen: pre -, syn -, and post – collisional evolution. Journal of the virtual explorer 8, 57 – 76.

Villalaín, J.J., G., F.-G., M., C.A., A., G.-I., 2003. Evidence of a Cretaceous remagnetization in the Cameros Basin (North Spain): implications for basin geometry. Tectonophysics 377, 101-117.

Waldhör, M., Appel, E., 2006. Intersections of remanence small circles: new tools to improve data processing and

interpretation in palaeomagnetism. Geophys, J. Int. 166, 33 – 45.
Weltje, G.J., 1997. End-member modeling of Compositional data: numberical-statistical algorithms for solving the explicit mixing problem. Mathematical Geology 29, 503-549.

Samenvatting (Summary in Dutch)

Het onderzoek beschreven in dit proefschrift spitst zich toe op het Organyà Bekken (Pyreneeën, Spanje), en kan in grote lijnen gegroepeerd worden involgens twee deel- onderwerpen: 1) de rotatie van het Iberisch schiereiland gedurende de Krijt periode en de daaraan gerelateerdezogeheten palinspastische reconstructie, en 2) de gevolgen hiervan voor de registratie van de natuurlijke remanente magnetiszatie (NRM), met name de mate waarin de gesteenten zijn geremagnetiszeerd (dit betekent dat zij een NRM signaal bevatten dat jonger is dan de leeftijd van de betreffende gesteente formatie). Remagnetisatie wordt allereerst onderzocht in het Organyà Bekken zelf. Vervolgens vormt een combinatie en vergelijking van deze gegevens met die verkregen uit verscheidene andere Mesozoïsche Iberische bekkens de basis om de ouderdom van de remagnetizsatie zo exactprecies als mogelijk te bepalen. Als laatste wordt een nieuwe aanpak voorgesteld om remagnetisatie vast te stellente herkennen onafhankelijk van de analyse van paleomagnetische richtingen. De eerste twee hoofdstukken van het proefschrift houden zich bezig met het eerste onderwerp, terwijl het tweede onderwerp wordt behandeld in de drie daaropvolgende hoofdstukken.

In **Hoofdstuk 1** wordtbeschrijft de analyse van de ouderdom en de grootte van de rotatie in het Krijt van het Iberisch schiereiland bepaald aan de hand van. eEen gedetailleerde paleomagnetische studie van mariene sedimenten van Krijt ouderdom uit het Organyà Bekken in is combinatie met informatie verkregen uit oceanische magnetische anomalien in de Golf van Biscaje. De paleomagnetische gegevens uit meer dan 1100 monsterkernen geven aan dat de Iberische rotatie geeindigd was vóór het Albien. Het begintijdstip van de rotatie kan echter niet worden bepaald omdat de betreffende gesteenten zijn geremagnetiszeerd. Ook de overige bestaande paleomagnetische datasets van het Iberisch schiereiland maken het niet mogelijk om het begin van de Iberische rotatie vast te stellenprecies geven. Echter, de magnetische anomalie M0r uit de Golf van Biscaje geeft als begintijdstip de basis van het Aptien. Dit betekent datheeft de gehele Iberische rotatie van ~ 35 ° tegen de klok in ten opzichte van Eurazië, heeft plaatsgevonden tijdens het Aptien. De rotatie is sneller geweest in het vroeg- Aptien en lijkt langzamer te gaan tijdens het midden- en laat-Aptien.

De interpretatie van de anisotropie van de lage-veld magnetische susceptibiliteit (AMS) van het Organyà Bekken vormt het onderwerp van **Hoofdstuk 2**. Drie verschillende AMS typenmaaksels kunnen worden onderscheiden, variërend van intermediair tot tektonischmaaksels. Deze zijn geïnterpreteerd in termen van paleospanningen die hebben geheerst in het Organyà Bekken. De richtingsverdeling van de maximale anisotropie-as suggereert dat een compressieve druk in verband met de verkorting als gerolg van de Pyreneeën orogenese meer intens was in het oostelijke deel van het bekken. Dit is in lijn met de structurele geologische waarnemingen. In het centrale en westelijke deel kan een originele N-Z extensionele richting worden herleid, hetgeen impliceert dat de latere verkorting hier volledig is geaccomodeerd in de basale overschuiving. De N-Z extensie-richting staat loodrecht op de huidige Bòixols overschuiving aan de zuidrand van het Organyà Bekken. De gereconstrueerde extensie-richting is ongeveer NO -ZWE, die mogelijk de extensie-richting tijdens de Iberische rotatie kan representeren. Dit zou impliceren dat het Organyà Bekken ten westen van het rotatie-draaipunt gepositioneerd was. In dit kader wordt de palinspastische positie van Iberië besproken tijdens haar rotatie en opeenvolgendeopvolgende oostwaartse beweging naar de positie van vóór de aanvang van de Pyreneesche orogenese.

Voor de studie beschreven in **Hoofdstuk 3** zijn vier transects genomen in het Organyà Bekken van het westen naar het oosten om een driedimensionaal beeld te krijgen van de verdeling van de remagnetisatie. Onafhankelijk van het transect zitis de overgang tussen geremagnetiseerde en niet-geremagnetiseerde strata in het bovenste deel van de Prada kalksteenfe, de Prada C KalksteenFormatie. Vanaf de oudste mergelformatie, de Cabó Formatie, tot de jongst ontsloten formatie, lijken de gesteenten altijd een primaire NRM te dragen. Dit houdt in dat het onderste deel van de stratigrafie geremagnetiszeerd is en het bovenste deel niet. De bijbehorende gesteentemagnetische studie toont dat de drager van de remanentier voornamelijk magnetiet is, met kleine bijdragen van hematiet en goethiet. Een breuk-breccietest uitgevoerd in het onderste gedeelte van de geremagnetiszeerde stratigrafie, suggereert dat de remagnetisatie ten minste ouder moet zijn dan het Eoceen toen zogeheten back-thrusting actief was in het Organyà Bekken. Begraving in een verhoogd geothermisch regime is een mogelijk mechanisme

voorvoorgesteld als remagnetisatie. Transport van een grote hoeveelheid externe vloeistoffenfluïde fase is onwaarschijnlijk, dit betekent dat deDaarom zijn zogenoemde intern gebufferde vloeistoffen waarschijnlijk het meest belangrijk geweest zijn. De rol van de aanwezige drukoplossing in de gesteenten bij het remagnetiszatie proces is niet duidelijk.

In **Hoofdstuk 4** richten we onze aandacht op het zo nauwkeurig mogelijk bepalen van het tijdstip van de remagnetiszatie in het Organyà Bekken alsmede drie andere gebieden in Iberië: het Cabuérniga Bekken, het Iberische Gebergte, en het Cameros Bekken. Voor de drie laatstgenoemde locaties zijn gepubliceerde paleomagnetische data gebruikt. Ondanks de variabele laaghelling kan de paleomagnetische richting tijdens remagnetisatie worden achterhaald met behulp van de 'kleincirkel-intersectie' (SCI) methode. In het Organyà Bekken heeft de op deze wijzezo bepaalde paleomagnetische richting tijdens de remagnetiszatie een declinatie (D) van 316.8°, en een inclinatie (I) van 54.8° (metbetrouwbaarheid α_{95} =van 3.3°). Deze richting ligt dichtbij de paleomagnetische richting van de transitionele Prada C Formatie bij volledige laagstand correctie, hetgeen zeer goed in overstemming is met de geologische informatie uit het Organyà Bekken waarmee de geloofwaardigteid van toepassing van de SCI methode is gebleken. Hiermee is dtoepasbaarheid van de De ouderdommen van remagnetisatie is nu bepaald op: de grens tussen het Barremien en het Aptien voor het Organyà Bekken, het vroeg-midden Aptien voor het Cabuérniga Bekken, het midden-laat Aptien voor het Iberische Gebergte, en tussen post-Aptien en pre-Santonien voor het Cameros Bekken. Omdat Iberië vrij snel geroteerd is, is het resultaat een mozaïek van geremagnetiszeerde gebieden. Het voorgestelde remagnetisatie mechanisme voor deze geologische setting is vermoedelijk een gebeurtenis beperkt tot het betreffende bekken tijdens de rifting fase. Een dunne korst verschafte de verhoogde geothermische gradiënt die vereist is om de temperatuur voor de geochemische reacties te bereiken relatief dicht bij het aardoppervlak, met de remagnetisatie als gevolg. Een puls van vloeistoffenfluïde fase over het gehele Iberische schiereiland die doorgaans vaak impliciet als oorzaak voor de remagnetiszatie werd aangenomen, is daarom onwaarschijnlijk.

In **Hoofdstuk 5** wordt een nieuwe aanpak ontwikkeld om remagnetiszatie in kalksteen te kunnen herkennen. Deze methode is gebaseerd op 'end-member' modelleren van sets van isotherme remanente magnetisatie (IRM) acquisitie curves van de geremagnetiseerde en de niet-geremagnetiseerde kalkstenen in het Organyà Bekken. End-member modellering doet geen vooronderstelling omtrent de vorm van de end-membersi. Een model met drie-end-membersileden is geïnterpreteerd als een adequate beschrijving van de gegevens. End-membersi zijn twee magnetische mineralen met een lage coërciviteitskracht en één mineraal met een hoge magnetische coërciviteitskracht (hematiet). Na normaliszatie voor de bijdrage van het hoog-coërcivitieve end-member-, kunnen de geremagnetiseerde en niet-geremagnetiseerde kalkstenen op een consistente manier onderscheiden worden aan de hand van de relatieve bijdrages van de laag-coërcivitieve end-membersi-. Vandaar dat deze nieuwe aanpak een nuttig instrument kan zijn om remagnetisatie te herkennen in monsters met een lage intensiteit, onafhankelijk van informatie betreffende paleomagnetische richtingen.

摘要 (Summary in Chinese)

本论文选择西班牙比利牛斯山脉的奥甘尼亚盆地 (Organyà) 为重点研究区，在前两章主要研究了白垩纪伊比利亚半岛的旋转和其有关的古地理位置及古板块重建，后三章研究了构造旋转对天然剩磁记录，尤其是对岩石重磁化的影响。重磁化现象是指岩石保存的古磁场信号比其形成时的古磁场晚。本文首先研究了奥甘尼亚盆地的重磁化，然后扩展到其它几个伊比利亚中生代盆地。最后，我们提出一种不同于古地磁方向分析的检验重磁化的新方法。

第一章：通过对白垩纪奥甘尼亚盆地海洋沉积物的古地磁研究，结合比斯开湾 (Bay of Biscay) 洋底磁异常资料，本章厘定了伊比利亚半岛旋转的时间和规模。1100多个岩心的奥甘尼亚盆地古地磁数据分析结果表明，伊比利亚半岛的旋转结束略早于阿尔布期。但是由于受岩石重磁化的影响，无法进一步确定旋转的准确时间。综合整理、分析现有的其它来自伊比利亚的古地磁数据，仍然不能精确地确定伊比利亚开始旋转的时间。但比斯开湾磁异常M0r表明伊比利亚旋转开始于阿普第期。因此，整个伊比利亚半岛旋转发生在阿普第期，相对于欧亚大陆逆时针旋转了约35 °。旋转速度在阿普第早期很快，在阿普第中后期似乎放缓。

第二章：对奥甘尼亚盆地各向异性低场磁化率的分布进行了分析。奥甘尼亚盆地展示了三种类型的各向异性磁化率组构，包括于中间和构造磁组构。这些磁组构可以解释为奥甘尼亚盆地古应力。最大各向异性轴方向的分布表明：盆地东部记录与挤压有关，因为比利牛斯造山运动相对更激烈。此解释符合本地的地质结构。在盆地西部，推断为原始南北伸展方向，这意味着后期挤压完全消失于盆地中部的断层。南北伸展方向垂直于当今在南缘奥甘尼亚盆地的保克算奥（Bòixols）逆冲断层。恢复的盆地伸展方向大约是东北-西南。它可以代表伊比利亚半岛旋转的伸展方向。这意味着奥甘尼亚盆地处于伊比利亚旋转支点的西部。在这一框架下，对有关伊比利亚半岛从其旋转和向东运动到比利牛斯造山作用开始前时的古地理位置及古板块的重建进行了讨论。

第三章：通过对奥甘尼亚盆地由西向东的四个横断面的研究，建立重磁化分布的三维视图。从重磁化到非重磁化的过渡层，独立于横断面，发生在普拉达地层的最上层（普拉达C石灰石）。从卡保泥灰岩地层的最下层到较年轻的地层，岩石一直携带天然剩磁。这意味着下部地层被重磁化，但上层部分没有被重磁化。相关的岩石磁学结果表明，磁性矿物主要是磁铁矿和少量的赤铁矿及针铁矿。最底部重磁化岩的断层角砾岩测试表明，重磁化开始至少早于始新世，当时在奥甘尼亚盆地逆冲断层活跃。埋藏在上升的地热中被认为是主要的磁化机制。大量的外来流体导致重磁化不太可能。因此，所谓的内部缓冲流体肯定占主导地位。观察到的压力溶解对岩石重磁化的影响目前尚不清楚。

第四章：我们把注意力集中到确定重磁化在奥甘尼亚盆地和其他三个伊比利亚地区（卡布尔尼嘎盆地，伊比利亚山脉，卡么若斯盆地）的时间。对于后三个地区可以利用已发表的古地磁数据进行分析。尽管地层可能发生倾斜，但重磁化期间的古地磁方向可以通过小圆圈相交（ SCI ）方法恢复。在奥甘尼亚盆地，恢复的古地磁方向是D = 316.8°，I = 54.8 ° (α_{95} = 3.3°)，接近于过渡地层普拉达C的全面倾斜校正的古地磁方向，这和奥甘尼亚盆地的地质证据非常吻合，并验证了小圆圈相交（ SCI ）方法的实用性。重磁化的开始时代分别为：在奥甘尼亚盆地为阿普第期开始，在卡布尔尼嘎盆地为阿普第早中期，在伊比利亚山脉为阿普第中晚期，在卡么若斯盆地为阿普第期之后但在桑托阶之前。由于伊比利亚半岛的快速旋转导致马赛克镶嵌式的重磁化盆地发生。重磁化机制拟议为重磁化局限于盆地范围并发生于盆地扩展期间。变薄的地壳引起地温梯度升高，因而在浅层就可以达到地球化学反应所需温度，从而导致重磁化。因此，伊比利亚半岛范围的流体造成重磁化的假定不太可能。

第五章：提出一种诊断重磁化灰岩的新方法。这种方法是对奥甘尼亚盆地重磁化和非重磁化的灰岩的等温剩磁曲线进行端员建模。端员建模不作任何端员形状假设。三个端员建模用于解释说明数据。在本项研究中，三个端员包括两个低矫顽磁性矿物端员和一个高矫顽磁性矿物端员（赤铁矿）。标准化高矫顽磁性矿物后，通过低矫顽磁性矿物端员的研究，重磁化和非重磁化灰岩可以很容易分辨。因此，这一新方法不同于传统的古地磁方向分析方法，它可提供非常有用的工具来诊断磁化强度低样品中的重磁化。

Summary (in English)

The research described in this thesis focuses on the Organyà Basin (Pyrenees, Spain) and can be categorized into two main topics: 1) the Cretaceous rotation of Iberia and the related palinspastic reconstruction, and 2) the implications for the recording of the natural remanent magnetization (NRM), notably the extent to which the rocks are remagnetized (they contain an NRM signal that is younger than the age of the rock unit it is retrieved from). Remagnetization is first studied in the Organyà Basin and then combined with the record in several other Mesozoic Iberian basins to provide constraints on its timing. Finally a new approach to recognize remagnetization independent of paleomagnetic directional analysis is proposed. The first two chapters deal with the first topic while the second topic is addressed in the three subsequent chapters.

In **Chapter 1** the timing and magnitude of the Iberian rotation is well constrained by a detailed paleomagnetic study of the Cretaceous marine sediments from the Organyà Basin combined with ocean floor magnetic anomaly information from the Bay of Biscay. The paleomagnetic data obtained from more than 1100 cores constrain the end of the Iberian rotation to just before the Albian. The onset of the rotation, however, cannot be determined because the pertinent rocks are remagnetized. Also analysis of all other existing paleomagnetic datasets from Iberia, does not allow pinpointing precisely the beginning of the Iberian rotation. However, the magnetic anomaly M0r from the Bay of Biscay indicates its start at the base of the Aptian. Therefore, the entire Iberian rotation of ~35° counterclockwise with respect to Eurasia occurred during the Aptian. The rotation is faster in the early Aptian and seems to slow down during the middle and late Aptian.

In **Chapter 2** the distribution of the anisotropy of the low-field magnetic susceptibility (AMS) was analyzed for the Organyà Basin. Three types of AMS fabrics could be distinguished ranging from so-called intermediate to tectonic magnetic fabrics. These were interpreted in terms of the paleostresses that have acted in the Organyà Basin. The directional distribution of the maximum anisotropy axis suggests that a compressional overprint is related to shortening because the Pyrenean orogeny was more intense in the eastern part of the basin, which is in line with structural geological observations. In the western sites an original N-S extenstional direction could be inferred, implying that the later shortening was entirely accommodated in the basinal thrust in the central portion of the basin. The N-S extensional direction is perpendicular to the present-day Bòixols thrust at the southern margin of the Organyà Basin. The restored extension direction is approximately NE-SW, which can represent the extensional direction during the Iberian rotation. This would imply a position of the Organyà Basin westerly of the Iberian rotation pivot point. In this frame work, the palinspastic position of Iberia during its rotation and eastward movement to its position before the onset of the Pyrenean orogeny is discussed.

In **Chapter 3** four transects were taken from west to east in the Organyà Basin to develop a three-dimensional view of the remagnetization distribution. Independent of transect, the transition between remagnetized and non-remagnetized strata occurs in the topmost Prada Formation, the Prada C limestone. From the lowermost Cabó marl Formation to younger formations, the rocks appear always to carry a primary NRM. This implies that the lower part of the stratigraphy is remagnetized and the upper part is not remagnetized. The related rock magnetic study shows the remanence carriers are mainly magnetite with minor contributions of hematite and goethite. A fault-breccia test that could be carried out in the lowermost portion of the remagnetized rocks suggests that the remagnetization must predate the Eocene when back-thrusting was active in the Organyà Basin. Burial in an elevated geothermal regime is argued to be the remagnetization mechanism. A vast amount of external fluids is unlikely. Therefore, so-called internally buffered fluids must have been dominant. The role of pressure solution observed in the remagnetized rocks is not clear.

In **Chapter 4** we focus our attention to constraining the timing of the remagnetization in the Organyà Basin and three other areas in Iberia: the Cabuérniga Basin, the Iberian Range, and the Cameros Basin. For the latter three localities, published paleomagnetic data were used. Despite variable tilting, the paleomagnetic directions during remagnetization can be restored with the small circle intersection (SCI) method. In the Organyà Basin, the restored paleomagnetic field direction during remagnetization is D = 316.8°, and I = 54.8° (with a_{95} = 3.3°), close to the paleomagnetic direction of the transitional Prada C Formation upon full tilt correction which complies very well with the geological evidence in the Organyà Basin, lending

credibility to the SCI method. The ages of the remagnetization are now constrained to: the Barremian/Aptian boundary for the Organyà Basin, early-middle Aptian for the Cabuérniga Basin, middle-late Aptian for the Iberian Range, and between post-Aptian and pre-Santonian for the Cameros Basin. Because Iberia rotated fairly rapid a mosaic of remagnetized basins is the result. The proposed remagnetization mechanism for this setting is likely a basin-confined event during the rifting phase. A thinned crust provided the elevated geothermal gradient required to reach the temperature for the geochemical reactions that induced the remagnetization at shallow depth. An Iberia-wide fluid pulse as often implicitly assumed causing the remagnetization is therefore unlikely.

In **Chapter 5** a new approach to diagnose remagnetization in limestones is developed. This method is based on end-member modeling of sets of isothermal remanent magnetization (IRM) acquisition curves from the remagnetized and non-remagnetized limestones in the Organyà Basin. End-member modeling does not make any assumption on the shape of the end-members and a three-end-member model was interpreted to adequately describe the data. End-members are two low-coercivity magnetic minerals and one high-coercivity magnetic mineral (hematite). After normalizing for the contribution of the high-coercivity end-member, remagnetized and non-remagnetized limestones can be consistently discriminated by the relative contributions of the low-coercivity end-members. Hence, this new approach may provide a useful tool to diagnose the remagnetization in low intensity samples, independent from an analysis of paleomagnetic directions.

PART 1

Rotation of Iberia

CHAPTER 1

The rotation of Iberia during the Aptian and the opening of the Bay of Biscay

Z. Gong, C.G. Langereis, T.A.T. Mullender.
Paleomagnetic Laboratory Fort Hoofddijk, Dept. of Earth sciences, Utrecht University, Budapestlaan 17, 3584 CD Utrecht, The Netherlands
Reprinted from Earth and Planetary Science Letters, 273 (2008), 80-93, with permission from Elsevier.

Abstract

The Cretaceous rotation of the Iberian plate in a geodynamical active setting between Africa and Europe is contemporaneous with the opening of the northern Atlantic Ocean, and provides fundamental temporal and kinematical constraints on the evolution of the Bay of Biscay and the Pyrenees. Here, we report new paleomagnetic data from 50 sites (1109 drilled cores) from marine sediments of the Cretaceous Organyà basin in the southern Pyrenees, to constrain the timing and magnitude of the rotation of Iberia. Berriasian to Barremian directions in exclusively limestone lithology are remagnetized, in agreement with previous Organyà basin studies. The Aptian to Cenomanian marls and limestones in the Organyà Basin, however, provide primary magnetisations asserted by rock magnetic experiments and positive fold tests. Our results constrain the rotation of Iberia to be finished just before the Albian. Paleomagnetic data cannot well constrain the onset of the rotation, but sea-floor anomaly studies restrict the onset of the rotation to anomaly M0, or the Barremian-Aptian boundary. This implies that the entire rotation of Iberia happened in one single phase, and is confined to the Aptian. This is in contrast to earlier studies that suggested a two-phase rotation of Iberia, but we argue that the large errors in published ages are not in disagreement with our results. In summary, we constrain the ~35° rotation of Iberia to the Aptian period which implies a rotation rate of 2.7 – 5.1 °/Myr, depending on the (controversial) duration of the Aptian.

Keywords: Paleomagnetism, Iberia rotation, Bay of Biscay, Cretaceous, Aptian

1 Introduction

The rotation of Iberia with respect to Eurasia has been studied for decades since the hypothesis of Carey (1958) and the model of Bullard et al. (1965). Carey (1958) proposed on the basis of geological data alone that the Iberia block had been rotated 30° to 40° counter-clockwise (CCW) resulting in the opening of the 'Biscay Sphenochasm' during the post-Palaeozoic, with a pivot point in the western Pyrenees. Bullard et al. (1965) used numerical fits with a least squares criterion for reconstruction of the continents around the Atlantic ocean – including their continental shelves – and they supported the rotation hypothesis of Carey.

Constraining the timing and the amount of counter-clockwise rotation constituted an important topic of paleomagnetic studies during the 1960s that culminated in the landmark paper of Van der Voo (1969). Van der Voo and co-workers (Van der Voo, 1967, 1969; Van der Voo and Zijderveld, 1971) reported a CCW rotation of ~35° between the late Triassic and late Cretaceous, in agreement with Carey's hypothesis (Carey, 1958). Constraining the rotation more precisely, in particular with respect to its age and timing, has shown to be controversial and several partially conflicting views have been put forward. The inconsistencies arise mainly from (1) the low resolution age dating frequently in combination with a paucity of paleomagnetic data, and (2) the often poor paleomagnetic results caused by possible remagnetization and/or very low intensities of the natural remanent magnetisation (NRM). For example, one study published a single result for the entire Barremian-Aptian interval which was based on five sites (63 samples) (Moreau et al., 1992) and another study yielded one result for the entire Aptian-Albian interval, based on four sites (35 samples) (Moreau et al., 1997), which limits constraining the timing of the rotation phase. Meanwhile, many rock units in the Iberian Peninsula were reported to be remagnetized (Schott and Peres, 1987; Galdeano et al., 1989; Moreau et al., 1992; Juárez et al., 1994; Villalain et al., 1994; Pares and Roca, 1996; Juárez et al., 1998; Dinarès-Turell and García-Senz, 2000; Gong et al., 2008). Most of them have a supposedly Cretaceous remagnetization (Galdeano et al., 1989; Moreau et al., 1992; Juárez et al., 1994; Juárez et al., 1998; Dinarès-Turell and García-Senz, 2000; Gong et al., 2008) which usually was argued to have been acquired during the Cretaceous Normal Superchron (CNS) because of the invariably normal polarity overprint. In general, most studies agreed on the total amount of the rotation of 35-40° (Galdeano et al., 1989; Van der Voo, 1993). In addition, all paleomagnetic studies so far have seemed to reach consensus on a two-stage rotation. For example, Galdeano et al. (Galdeano et al., 1989) suggested a ~26° fast Barremian CCW rotation and a ~13° CCW rotation during the Albian and the Maastrichtian. For a more detailed compilation and review of all relevant paleomagnetic studies we refer to Dinarès-Turell and García-Senz (2000).

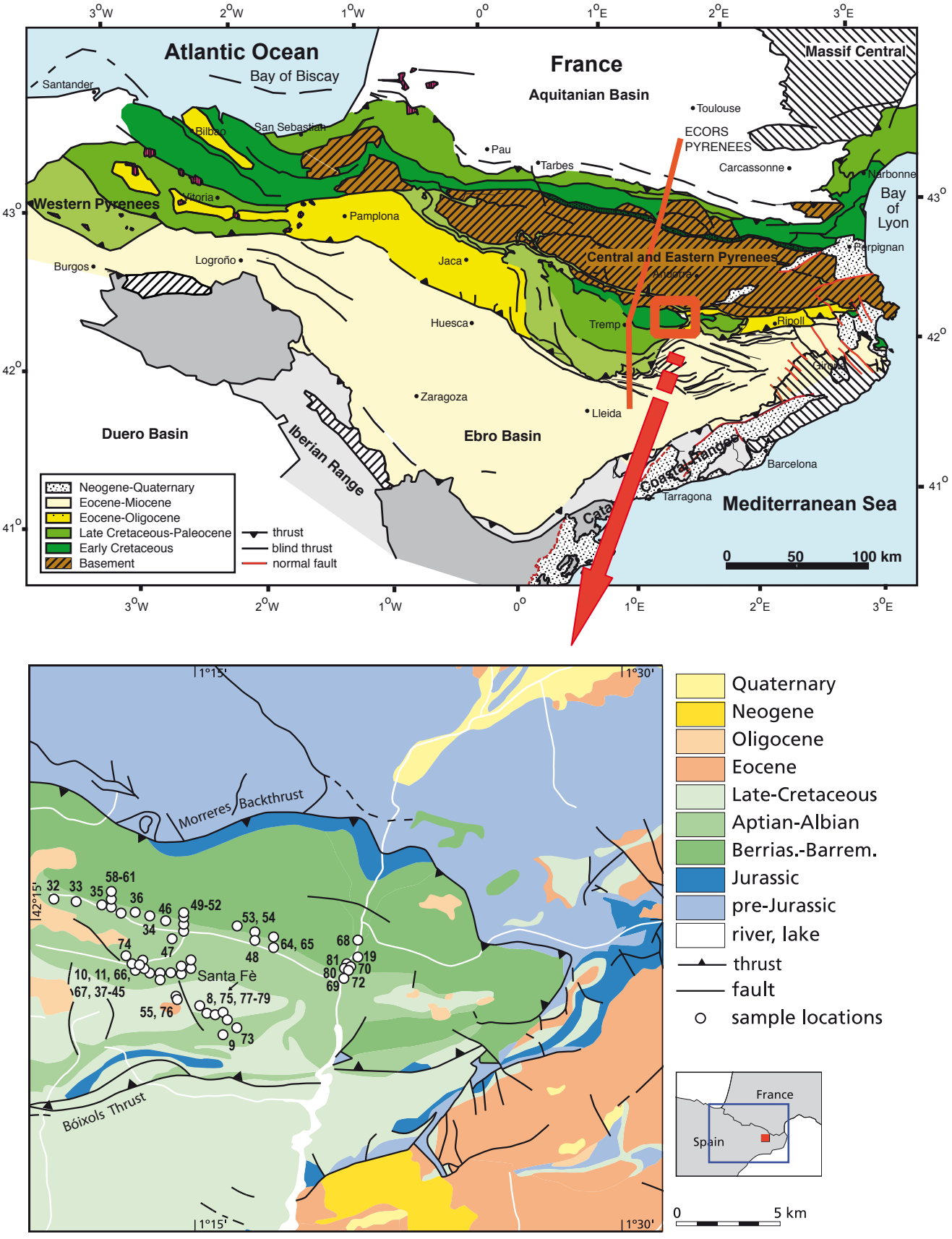

Figure 1 Geological map of the Pyrenees modified after Jaume Vergés (Vergés et al., 2002) and the Organyà Basin with the locations of the sampling sites; numbers refer to those reported in the Supplementary Table. At the bottom right, the Organyà Basin and the Pyrenees map area are indicated by a red and blue square on the topographic map, respectively.

Other studies were based on oceanic magnetic anomalies in the Bay of Biscay (Pichon and Sibuet, 1971; Srivastava et al., 1990b; Srivastava et al., 1990a; Roest and Srivastava, 1991; Olivet, 1996; Sibuet et al., 2004), which have recently been argued to be caused by serpentinisation during mantle exhumation, rather than by actual sea-floor spreading (Sibuet et al., 2007). These studies show different details and slightly dissimilar reconstructions, but all agree that the opening of the Bay of the Biscay happened during the Cretaceous between chrons M0 and A33o, i.e. between 125 Ma and ~83 Ma according to the most recent geological time scale (Ogg et al., 2004).

There are two major types of kinematic reconstruction models for the opening of the Bay of Biscay. The differences are mainly in deriving the Euler poles of the rotation of Iberia, which are required for the reconstructions. Sibuet et al. (2004)

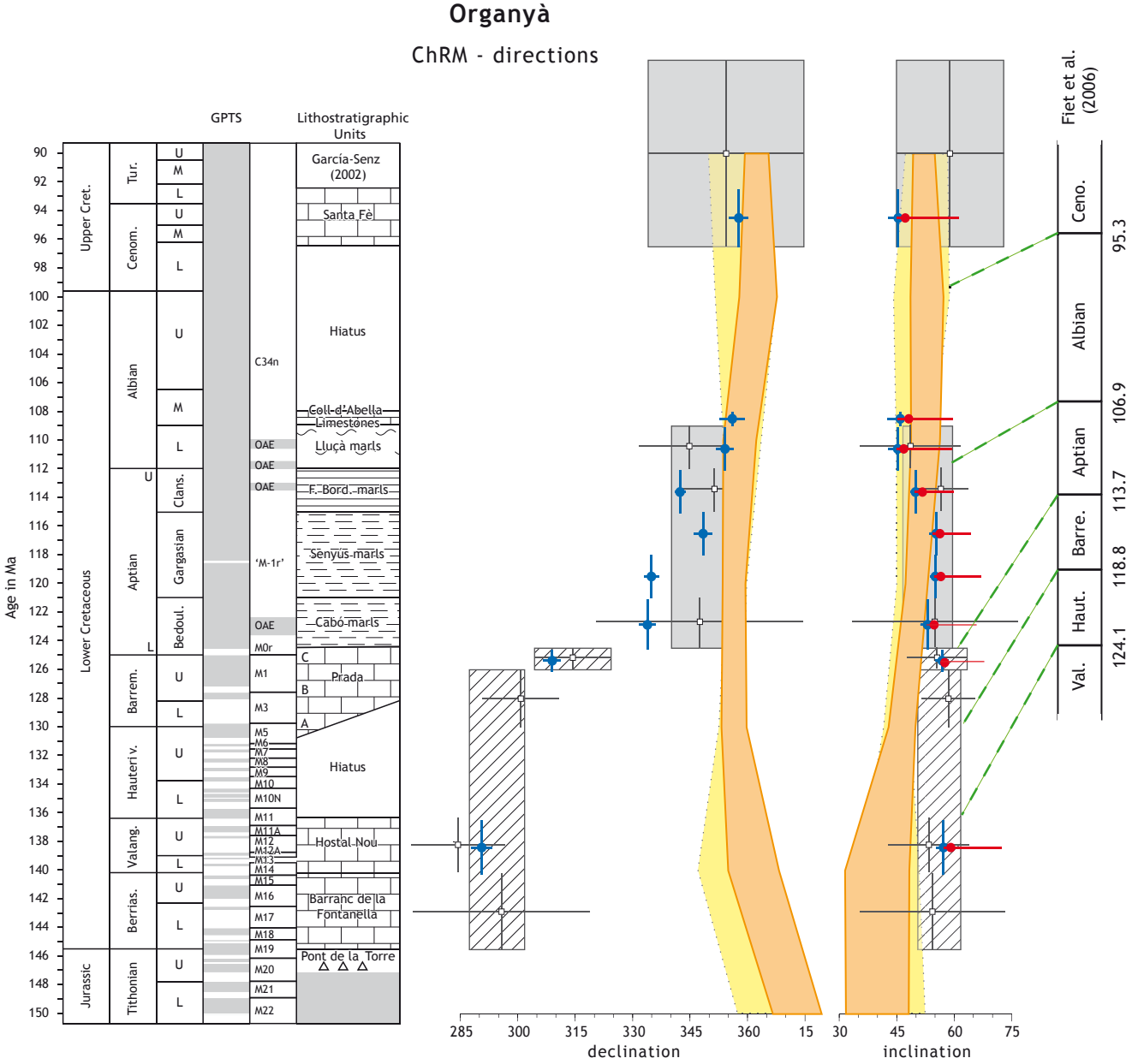

Figure 2 Characteristic remanent magnetisation (ChRM) directions versus lithology and formations in the Organyà Basin, correlated to the new geological time scale (Ogg et al., 2004), including the geomagnetic polarity time scale (GPTS); grey (white) is normal (reversed) polarity; chron nomenclature follows CK92 (Cande and Kent, 1992); vertical bars denote age errors. The time scale from (Fiet et al., 2006) is shown on the right. Blue closed circles indicate the mean formation directions (declination, inclination) and their errors (blue horizontal bars, ΔD_x, ΔI_x) from the present study (Table 1), whereas blue open circles denote remagnetised directions that are not used for the rotation of Iberia. The small open squares denote mean formation directions recalculated from Dinarès-Turell and García-Senz (2000); the grey shaded rectangles represent their published group means; obliquely shaded rectangles denote remagnetised directions (see text); the directional errors (ΔD_x, ΔI_x) are recalculated according to Table 1. The red closed circles are inclinations after applying the elongation/inclination (E/I) method using the TK03.GAD model (Tauxe and Kent, 2004); red horizontal bars shows the 95% bootstrap error range. Expected directions from the apparent polar wander paths (APWP) for Eurasia from Torsvik et al. (2008) and Besse & Courtillot (2002) are plotted in light orange and light yellow, respectively.

convincingly argue that a best fit of M0 (Srivastava et al., 2000) across the Atlantic and in the Bay of Biscay provides a better and more robust kinematic model. Their conclusion leads to a CCW rotation of Iberia of ~37°. Because precise age and timing of a CCW rotation of Iberia based on sea-floor anomalies alone are poorly constrained because of the Cretaceous Normal Superchron (CNS), or the Cretaceous Quiet Zone in sea-floor anomaly terms, integrated high-resolution stratigraphic and paleomagnetic data are required to better constrain the rotation in time and magnitude.

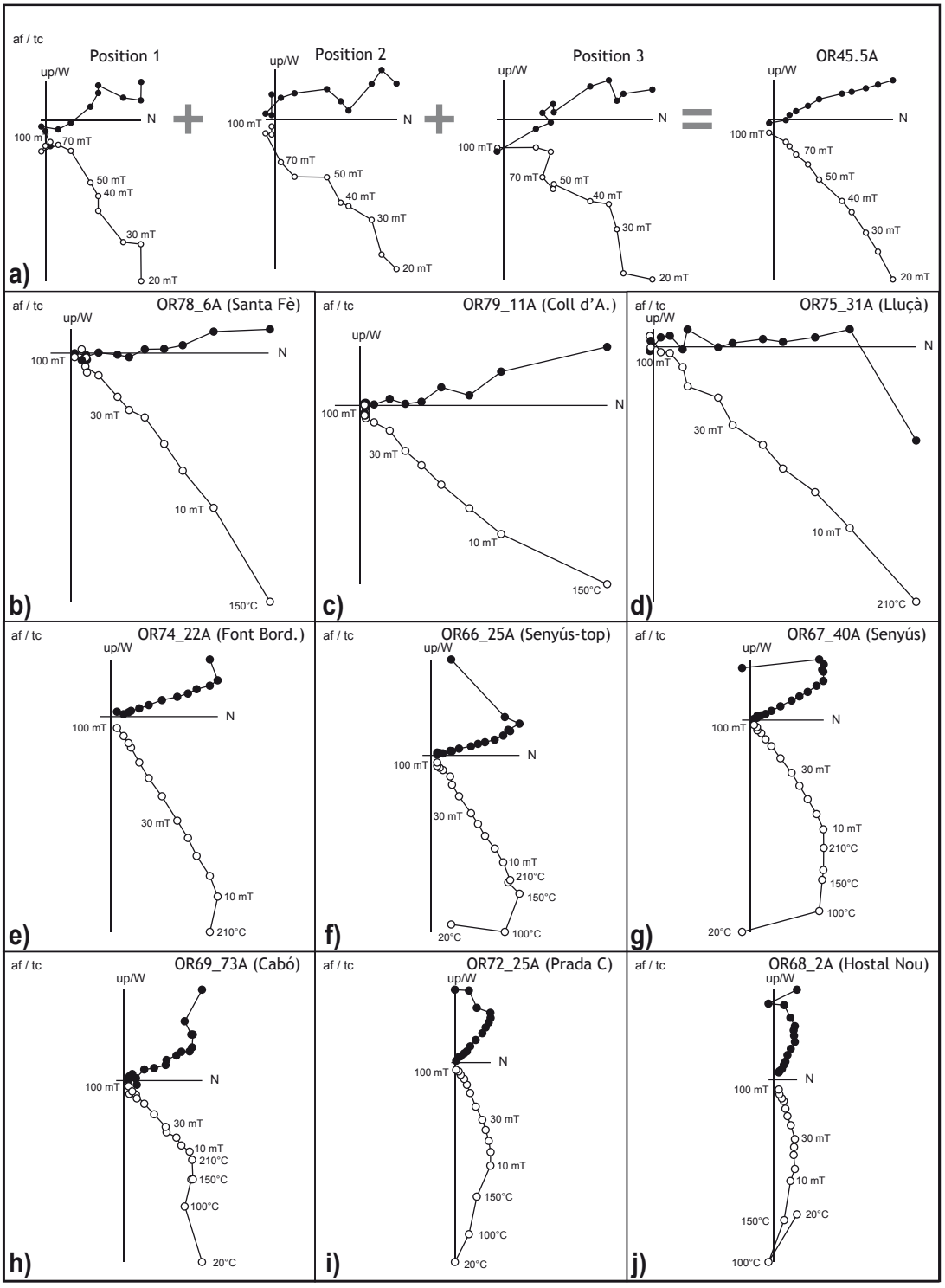

Figure 3 a). Orthogonal vector diagrams (Zijderveld, 1967) of an example of our "3 position protocol"; the results of 3 independent positions on our automated cryogenic magnetometer are merged to reduce the noise observed in single position measurements, yielding a significantly improved demagnetisation diagram; b-j). demagnetisation results from the different formations in the Organyà Basin, after bedding tilt correction (TC). We used a thermal (initial heating to 150-210 °C) plus AF (up to 100 mT) demagnetisation method which proved to give the best demagnetisation results. Closed (open) circles indicate the projection on the horizontal (vertical) plane.

In this study, we use the new geological time scale (GTS2004, (Gradstein et al., 2004)) for the Cretaceous (Ogg et al., 2004) which we apply also to obtain new numerical ages for earlier studies to improve the age control. We do realise, however, that this time scale – especially in terms of numerical ages – is not without debate (Fiet et al., 2006; Tucholke and Sibuet, 2007). The strongly deviating time scale of (Fiet et al., 2006), particularly in terms of the duration of the Aptian, will be discussed in more detail below.

The study area, the Organyà basin, is well dated by biostratigraphy (García-Senz, 2002), in stages and sub-stages for every formation. We furthermore massively sampled ~50 sites with a total of more than 1100 drilling cores (Supplementary Table), yielding specimens which were measured on the robotised cryogenic magnetometer at Fort Hoofddijk, Utrecht, the Netherlands. This robot produces significantly better – both in quality and quantity – data on the low intensity marls and limestones of the Organyà basin, and an adapted (3-position) protocol was developed especially for these low-intensity limestones. For this study, we demagnetised 1109 specimens of which 960 demagnetisations gave a reliable and interpretable result, an average success rate of 85%, although this success rate varies between formations, from 57% to 100% (Supplementary Table).

2 Geological setting of the Organyà basin

The Organyà Basin is located in the Bóixols thrust sheet in the southern Pyrenees and is filled with a ~ 4.5 km thick series of Mesozoic hemi-pelagic and pelagic sediments, mainly Cretaceous limestones and marls (Fig. 1). It is an inverted extensional basin, which underwent Berriasian to middle Albian extension and rifting – most intense during the Aptian. Subsequent inversion and uplift after the middle Albian resulted in a stable platform during middle Cenomanian to early Santonian, which was finally included in the Pyrenean Orogeny during late Santonian – Maastrichtian (Dinarès-Turell and García-Senz, 2000; García-Senz, 2002; Gong et al., 2008).

During the extensional history, the tectonic evolution inside the Organyà Basin is recorded in five phases: the Tithonian-Valanginian rift initiation, the Hauterivian uplift and erosion leading to a hiatus, the Barremian moderate rifting, the early and middle Aptian (Bedoulian – Gargasian) intense rifting, and late Aptian (Clansayesian) – middle Albian late rifting. The first rifting that resulted in the formation of the Berriasian-Valanginian platform carbonates (400 – 500 m thickness) lasted ~9.1 Myr, leading to an average sedimentation rate in the centre of the basin of around 5 cm/kyr. The depositional environment is interpreted as coastal lagoonal (García-Senz, 2002). The hiatus in the Organyà Basin sequence during the subsequent Hauterivian uplift and erosion phase is also recorded at other places in the central Iberian rift systems (Salas et al., 2001) and in the North-Iberian basins (Hiscott et al., 1990). The Barremian to earliest Aptian moderate rifting lasted ~5.5 Myr, subsidence increased slightly and the accumulation rate of the platform carbonates rose to ~20 cm/kyr (pending unrecognised hiati). Apparently, the subsidence rate, eustatic forces and sediment influx were in near equilibrium so that throughout the series (Prada Fm.) shallow platform carbonate conditions

Table 1 For every formation sampled, the number of demagnetisations (specimens) is given (N_{demag}) and the number of ChRM directions(N_{ChRM}); the Vandamme cut-off reduces the number of accepted ChRM directions for calculation of the mean declination (D), the inclination of the original distribution (I_{org}), and their cone of confidence (a_{95}) and precision parameter (k); I_{APWP} is the inclination expected from the APWP (Torsvik et al., 2008), while I_{EI} is the inclination resulting from intersection of the distribution with TK03.GAD (Tauxe and Kent, 2004). The inclination (I) results from 5000 bootstraps of TK03.GAD, with 95% lower and upper bounds (I_l, I_u). For each direction we determine the virtual geomagnetic pole (VGP), with a mean VGP latitude (latp) and longitude (longp) and corresponding cone of confidence (A95) and precision parameter (K), from which we determine the errors in declination (ΔD_x) and inclination (ΔI_x) (Butler, 1992) as plotted in Figure 2.

Formations	ChRM directions & Vandamme cut-off (vD)							TK03.GAD				VGPs from unflattened dataset						
	N_{demag}	N_{ChRM}	D	I_{org}	α_{95}	k	I_{APWP}	I_{EI}	$I_l <$	I	$< I_u$	λ_l	latp	longp	a_{95}	K	ΔD_x	ΔI_x
Santa Fè	107	85	357.8	46.4	2.4	42.5												
vD		**80**	**357.7**	**45.4**	2.1	60.3	**52.5**	48.0	45.0	**47.2**	61.2	28.4	76.5	189.2	2.2	54.1	**2.50**	**2.62**
Coll d'Abella	115	66	352.0	46.0	3.6	22.8												
vD		**60**	**356.0**	**45.9**	2.7	45.9	**52.6**	47.6	45.1	**48.1**	59.6	29.1	77.2	197.3	2.9	41.8	**3.32**	**3.39**
Lluçá	101	101	354.4	45.4	2.0	49.3												
vD		**99**	**354.1**	**45.2**	2.0	53.3	**52.4**	46.9	44.9	**46.8**	59.3	28.0	75.4	202.9	2.0	49.6	**2.27**	**2.41**
Font Bordonera	111	108	342.4	49.9	1.1	148.5												
vD		**108**	**342.4**	**49.9**	1.1	148.5	**51.7**		49.7	**51.7**	59.9	32.3	73.0	242.4	1.2	129.0	**1.42**	**1.29**
Senyús top	73	71	349.0	55.4	1.7	95.5												
vD		**69**	**348.4**	**55.3**	1.6	116.6	**51.0**		54.4	**56.3**	64.2	36.9	79.9	245.4	1.9	79.6	**2.37**	**1.83**
Senyús	139	133	334.1	55.1	1.5	70.2												
vD		**129**	**334.9**	**55.1**	1.3	97.8	**50.3**		54.8	**56.5**	67.0	37.1	70.4	265.6	1.5	71.0	**1.88**	**1.44**
Cabó	225	185	333.0	55.1	2.7	12.0												
vD		**162**	**333.8**	**52.9**	1.5	38.0	**49.2**		52.7	**54.3**	65.6	34.8	68.2	257.9	1.8	38.0	**2.19**	**1.82**
Prada C	169	136	309.7	56.5	2.1	26.0												
vD		**113**	**308.8**	**56.7**	1.1	95.7	**48.2**		56.4	**57.5**	67.6	38.1	51.0	282.1	1.4	69.6	**1.78**	**1.31**
Hostal Nou	85	75	289.7	57.1	2.1	64.0												
vD		**70**	**290.6**	**57.2**	1.7	96.4	**41.0**		57.3	**59.1**	72.3	39.9	39.1	294.0	2.1	65.1	**2.74**	**1.88**

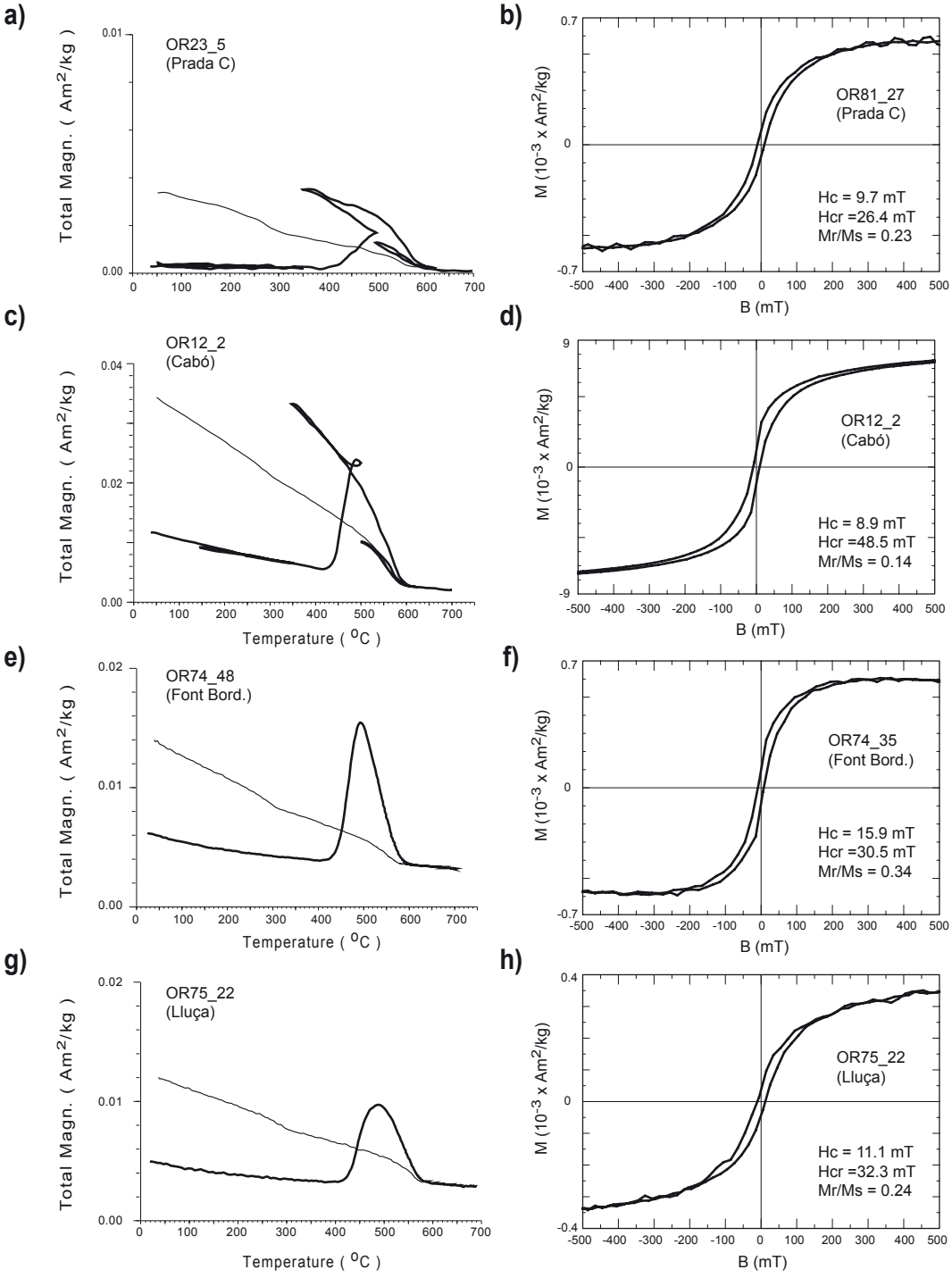

Figure 4 Thermomagnetic curves (Curie balance (Mullender et al., 1993)) and hysteresis loops for characteristic samples. In the thermomagnetic curves, thick (thin) lines indicate the heating (cooling) curves. Hysteresis loops are corrected for the paramagnetic contribution.

are maintained. The maximum rifting phase occurred during the Aptian and is typified by the limestones grading into marls and accumulation rates in the centre of the basin increased to ~27 cm/kyr, while conditions became coastal-marine. Apparently, relief was enlarged so that more detrital material could be transported into the basin. In the areas that remained coastal, in the South of the basin, syn-rift unconformities have been recognised. The top of the Albian sediments was eroded, producing an upper Albian to lower Cenomanian hiatus, and an angular Cenomanian unconformity.

During the Cenomanian inversion, the extensional fault system in the southern Organyà Basin inverted to a compressional fault system. Following the inversion phase and substantial erosion, the Cenomanian platform carbonates were deposited. This stable platform phase continued until the early Santonian. During late Santonian – Maastrichtian times, the

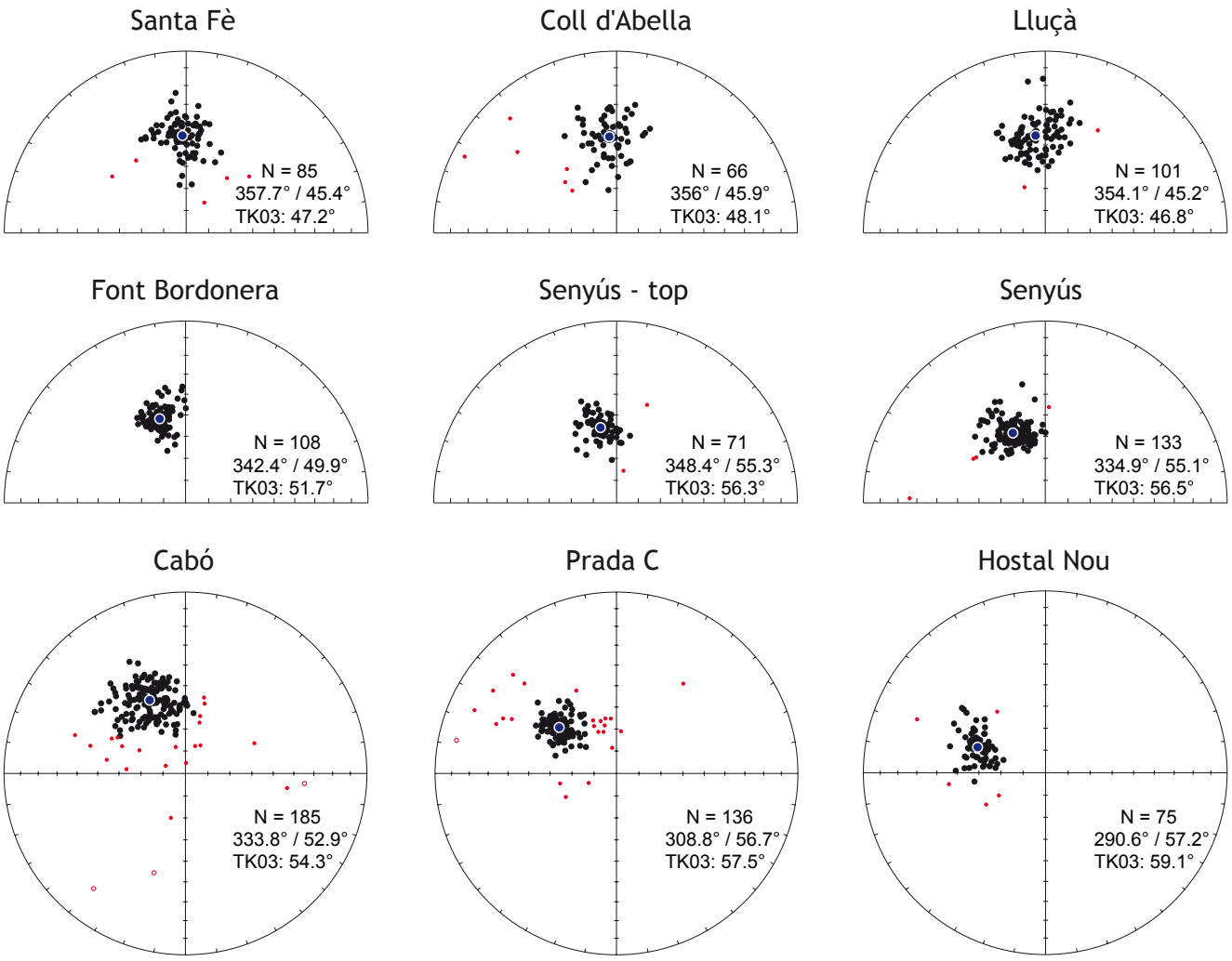

Figure 5 Equal-area projections of the ChRM distributions of all formations in the Organyà Basin; only the Senyús formation has been split into two parts with different lithology (marls vs. limestones in the top of the formation). Red symbols are individual directions rejected by the Vandamme cut-off (Vandamme, 1994); blue symbols denote mean directions; their cone of confidence (a_{95}) is too small to be visible. The means per formation are given as number (N) of ChRM directions used, mean declination/inclination, and unflattened inclination according to TK03.GAD.

basement fault system inverted to become the Bóixols thrust system, along with the Santa Fè syncline.

The main structure inside the Organyà Basin is the Santa Fè syncline, which includes Aptian – Albian marls and limestones, and upper Cretaceous platform carbonates exposed at both limbs. The Cretaceous marine sediments in the OB are subdivided into nine formations (Berástequi et al., 1990; García-Senz, 2002; Bernaus et al., 2003) (Supplementary Table). The ages of the specific formations are derived from biostratigraphy (ammonites, planktonic and benthonic foraminifers) (Becker, 1999; Bernaus et al., 1999; Bernaus, 2000; Bernaus et al., 2000; Bernaus et al., 2003), and summarised by García-Senz (2002).

3 Methods

The palaeomagnetic samples in the OB were taken by a portable gasoline-powered drill, covering all formations throughout the whole basin (Fig. 1, Supplementary Table). Many additional sites with respect to our earlier study (Gong et al., 2008) were drilled (all sites with site number > 65), particularly in the top of the Prada C limestones and in the Aptian-Albian marl formations, as well in the overlying Santa Fè limestones (Fig. 2). In this paper, we report the palaeomagnetic results of 15 sites (802 cores) drilled for this study, and we combined 35 sites (307 cores) from our previous field campaigns (Fig. 1, Supplementary Table).

Initially, to select the best demagnetisation method for the low intensity Organyà samples, we performed detailed stepwise thermal and alternating field (AF) demagnetisation. Based on those results, we decided to use combined thermal plus AF stepwise demagnetisation to process the new Organyà samples. Limestones were thermally demagnetised to 150°C and marls up to 210°C, then followed by AF demagnetisation in small steps to a maximum field of 100 mT. Thermal demagnetisation was processed in a laboratory-built furnace and the natural remanent magnetisation (NRM) measured with a 2G Enterprises DC-SQUID magnetometer. AF demagnetisation was done in the so-called "three position" protocol (Fig. 3a) by an in-house developed robot, which let the samples pass-through a 2G Enterprises SQUID magnetometer (noise level 10^{-12} Am^2). Zijderveld diagrams (Zijderveld, 1967) and

principal-component analysis (Kirschvink, 1980) were used to determine the characteristic remanent magnetisation (ChRM) directions.

After the ChRM component analysis, we have analysed the directions of all sites, and combined them to formation distributions and their means, if possible. If, for example, a group of sites within one formation clearly not showed a common true mean direction (McFadden and Lowes, 1981) we have combined the data in more groups, e.g. the lower and upper part of the Senyús marls. We have also determined the VGPs for every locality/formation and the corresponding K and A95 parameters, from which we have determined the directional errors in declination (ΔD_x) and inclination (ΔI_x) according to Butler (Butler, 1992) (Table 1, Fig. 2).

On the combined data we have used the Vandamme cut-off (Vandamme, 1994): a variable cut-off angle is calculated for each record by iteration. This has been argued to be a better estimate than using a fixed cut-off angle (McElhinny and McFadden, 1997) and the method permits a considerable improvement to VGP scatter estimates, especially for low and high latitudes where a fixed cut-off angle tends to over under) estimate the VGP scatter. Effectively, it eliminates data points that have a larger secular variation than the data distribution permits. Applied to our data, it appears that very few data points were omitted, typically not more than a few per cent. We realise that the method not only eliminates outliers of secular variation, but also 'inconsistent directions', possibly caused by erroneous orientations in the field or in the laboratory. Nevertheless, we consider the Vandamme cut-off an objective way to disregard data points that do not fit the distribution but have otherwise good Zijderveld diagrams.

To correct for the sediment inclination error, the data set – after applying the Vandamme cut-off to avoid elongation bias – was processed with the elongation/inclination (E/I) method, based on the statistical field model TK03.GAD (Tauxe and Kent, 2004). Flattening factor (f) ranges from 0.3 to 1.0 were applied. The method requires a rather large data set (preferably

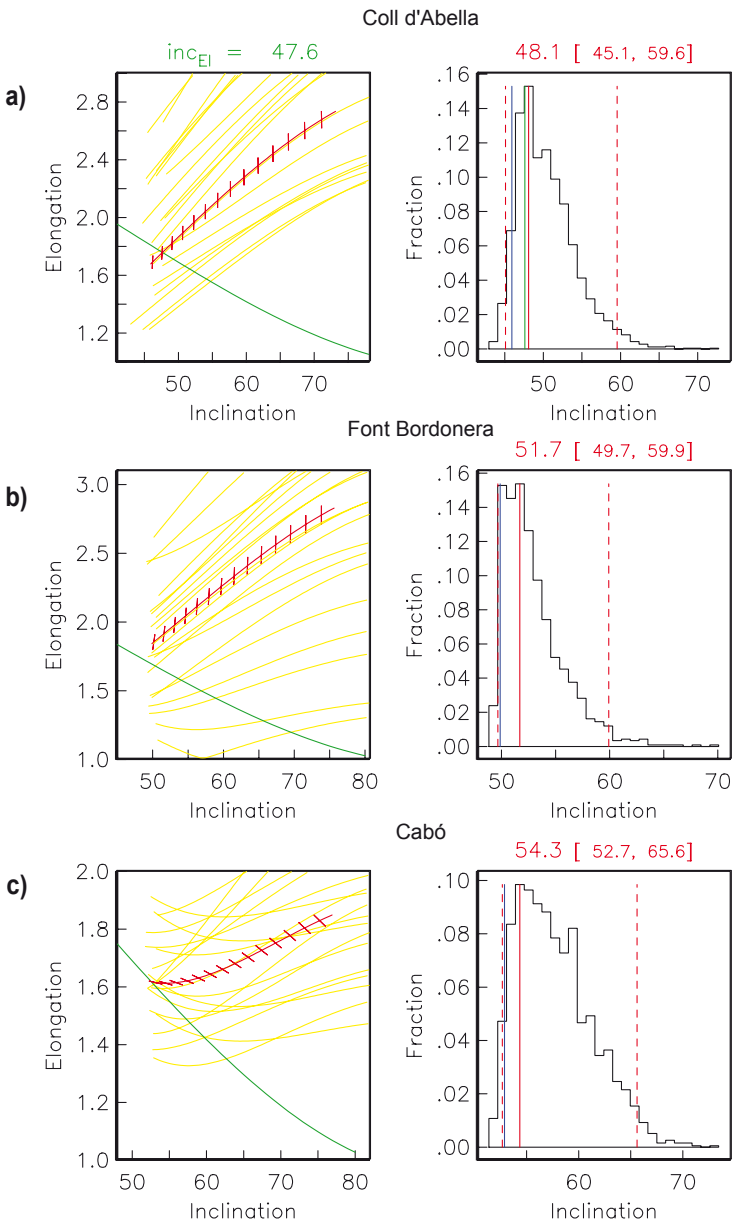

Figure 6 Left panels: plots of elongation versus inclination for the TK03.GAD model (green line) and for various formations (red barbed line) for different values of f. The barbs indicate the direction of elongation with horizontal being E-W and vertical being N- S. Also shown are results (yellow lines) from 20 (out of 5000) bootstrapped data sets. The crossing points (if the dataset intersects the model) represent the inclination/elongation pair most consistent with the TK03.GAD model, given as I_{EI} (in green) above the panel. Right panels: histogram of crossing points from 5000 bootstrapped data sets. The most frequent inclination (solid red vertical line; dashed red vertical lines denote the 95% bootstrap error) is given as value (and range) on top of the panel; the inclinations of the original distribution (blue vertical line) or the intersection with the model (green vertical line) are indicated.

N > ~100) to represent a statistically robust distribution of geomagnetic field behaviour.

The rock magnetic measurement consisted of determining thermomagnetic curves and hysteresis loops to identify the magnetic component carriers. The thermomagnetic experiments were processed in air on a modified horizontal translation type Curie balance with noise level 2×10^{-8} Am^2 (Mullender et al., 1993). An alternating gradient force magnetometer (AGFM: MicroMag Model, Princeton Measurements Corporation (USA), noise level $2\times10^{-9}Am^2$) was used for hysteresis loops of selected samples from each of the different formations.

4 Results

4.1 Rock magnetic results

Thermomagnetic curves have been determined on selected samples from different formations. Generally speaking, the total magnetisation is mainly dominated by ferrimagnetic minerals. The slope change between 550°C and 600°C indicates a main contribution of magnetite. In the Organyà Basin, there is only one type of thermomagnetic curve (Fig. 4): it appears that around 420°C, but occasionally at a lower temperature, chemical alteration occurs because the heating and cooling curves are not reversible. Most likely, pyrite is oxidised to magnetite. This indicates that the thermal demagnetisation results higher than 400°C are not stable. There is no clear evidence for magnetic sulphides. Essentially, the samples from all formations show the same thermomagnetic pattern.

The hysteresis loops reveal two typical groups after slope correction (Fig. 4). Wasp-waisted loops (Fig. 4d) indicate a mixture of low and high coercivity minerals. They are almost closed below 500 mT. This may signify a (minor) contribution of a high-coercivity mineral, like haematite or goethite. The remaining hysteresis loops (Fig. 4b, f, h) are saturated (Fig. 4f) or almost saturated (Fig. 4b, h) well below 500 mT, indicating pseudo single domain magnetite particles. The non-saturated loops (Fig. 4b, 4h) likely have a small amount of haematite or goethite.

4.2 Demagnetisation results

Since the thermal plus AF demagnetisation method gave the best results, most of the Organyà Basin samples were processed this way. After thermally removing (most of the) the viscous or present-day overprint component (by heating limestones up to 150° and marls up to 210°), most of the demagnetisation diagrams reveal only one ChRM component, between ~30 mT and up to 80-100 mT, at which the magnetisation is completely removed. This suggests, in accordance with the rock magnetic experiments, that the ChRM component is essentially carried by magnetite. Representative Zijderveld diagrams of each formation are shown in Fig. 3. The ChRM in the Organyà Basin mainly has a north-west declination and positive inclination. All results indicate a normal polarity throughout the whole basin. This is expected for the Aptian to Cenomanian sites, since this is consistent with NRM acquisition during the Cretaceous Normal Superchron. Typically, the marls have NRM intensities ranging from 2 – 50 mA/m, while those of the limestones range 0.2 – 3.0 mA/m. Even samples with very low intensities give in general good to excellent demagnetisation results, thanks to the 3 position procedure on the robotised magnetometer. We have applied quality criteria to the demagnetisation diagrams,

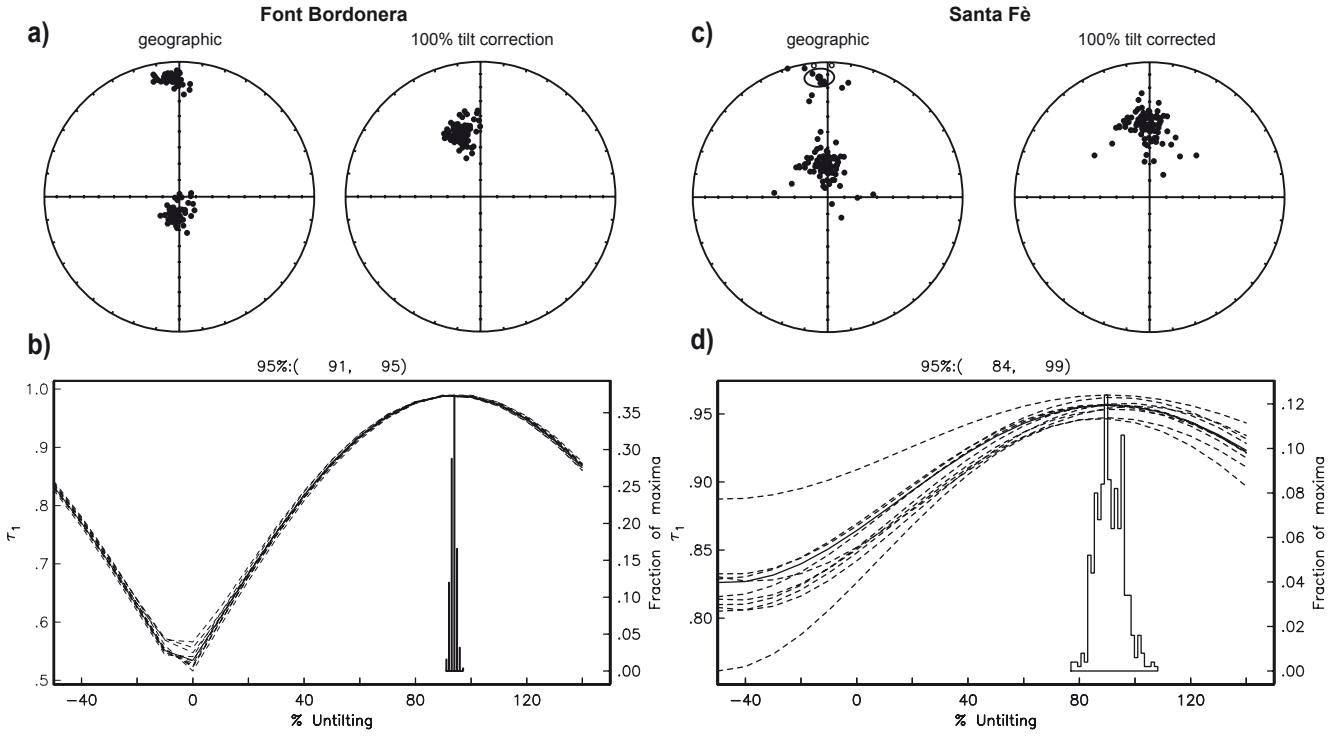

Figure 7 Non-parametric fold tests (Tauxe and Watson, 1994) on the Font Bordonera and Santa Fè formations; a) and c) are equal-area plots of the ChRM directions from both limbs in geographic coordinates and after tilt correction; b) and d) give the results of the fold test as some bootstrapped examples of the first eigenvalues (τ_1) upon progressive untilting. The 95% bootstrap error interval is indicated.

mostly based on a maximum angular deviation (MAD) of less than 15°, but also on erratic behaviour, acquisition of a gyroremanent magnetisation (GRM) (Dankers and Zijderveld, 1981) at higher (> 50mT) fields or simply too low intensities that did not permit deriving a reliable component. In a few cases, re-examination of sites showed that they were sampled (too) close to a fault, explaining a random or evidently 'strange' direction. These samples or sites have been omitted from further consideration.

In this study, 960 ChRM directions from all 50 sites are lumped per formation. The number of well determined individual directions for each formation varies from 66 to 185 (Table 1). After applying the Vandamme cut-off, 960 ChRM directions were left for the mean directions of 8 formations (9 levels) (Table 1, Fig. 5). From the original directions, the Vandamme cut-off retains some 93% of the data; the directional change after applying the cut-off is less than 4°, and mostly less than 1°, which is caused by the large amount of data per level or formation. In the Font Bordonera formation, no data are omitted, while in the Coll d'Abella member, 14% of the data points are disregarded. The datasets for each formation have very low α_{95}, ranging from 1.1 to 2.7, both before or after the Vandamme cut-off.

According to previous studies (Dinarès-Turell and García-Senz, 2000; Gong et al., 2008), the Hostal Nou and Prada C formations are remagnetised because of burial diagenesis. Therefore, they cannot be used for a directional study. The younger formations (from Cabó to Santa Fè) have primary magnetisations (Gong et al., 2008). Their formation mean directions, therefore, represent directional changes, and may characterise the rotation of Iberia.

To correct for a possible inclination error, the E/I method was used for systematically unflattening the Organyà Basin formation directions (Table 1). Only the distributions from the Lluçà Fm. (N = 99), Coll d'Abella member (N = 60) and Santa Fè Fm. (N = 80) formations intersect the model upon unflattening, giving a slight but not significant correction for the inclination (I_{EI} in Table 1, Fig. 6). A bootstrap is then applied (N=5000), giving a distribution (histogram, Fig. 6) of the flattening factor f with a 95% significance bootstrap interval. Most sites meet the requirement of a sufficiently large amount of data points. In all cases, the inclination is not significantly corrected, suggesting no inclination error occurs in these limestones and marls. We conclude the NRM has been mainly acquired after early compaction and dewatering of the sediments. This may be interpreted as a post-depositional remanent magnetisation (pDRM) process, or the NRM may have been acquired through early diagenetic formation (Van Hoof and Langereis, 1991), e.g. by precipitation of iron oxides through bacterial mediation (Van Hoof et al., 1993).

4.3 Fold tests

In the Organyà Basin, the Font Bordonera and Santa Fè formations are the only available formations which are accessible on both limbs of the Santa Fè syncline. These formations have been sampled for a fold test.

The Font Bordonera formation has been sampled both at the south limb (site OR 73) and the north limb (site OR 74) of the Santa Fè syncline. The equal area plots of directions from both limbs before and after tilt correction (Fig. 7) show that in geographic coordinates the two sites have significantly different directions, while after tectonic tilt correction the directions of both sites form a single cluster. The non-parametric fold test of Tauxe and Watson (1994) (Fig. 7a,b) is considered to be positive because closest grouping is reached at 91% – 95% untilting, close to full unfolding. The small deviation from 100% significance may be caused by orientation or bedding plane errors. This fold test checks for maximum clustering, but this need not always be the ideal case (McFadden, 1998), while also a well-recorded secular variation distribution would have a slight elongation at this latitude, which is not necessarily compatible with maximum clustering. Hence, we conclude that the Font Bordonera Formation has a pre-folding origin of the NRM, even though the tilt corrected means just fail to have a common true mean direction (ctmd), after (McFadden and Lowes, 1981). We use full untilting for joining the two distributions into a single one that represents the directions in the Font Bordonera marls.

For the fold test of the Santa Fè formation, two sites (OR 55 and OR 76) were drilled from the North limb, while three sites (OR 08, OR 77 and OR 78) were sampled from the South limb of the Santa Fè syncline. In geographic coordinates, declinations of both limbs of this formation (Fig. 7c) are quite similar with values around 356°. However, the inclination of the North limb is around 12° ± 7° compared to the 69.8° ± 2.2° from the South limb. The highest clustering (at the 95% bootstrap level) (Fig. 7d) occurs between 84% and 99%, which we consider a positive fold test. After 100% tilt adjustment, the directions of both limbs (Fig. 7c) are very similar and their means share a common true mean direction (ctmd) with classification B (according to (McFadden and Jones, 1981)). Therefore, also the Santa Fè Formation carries a pre-folding NRM.

5 Discussion

5.1 The Rotation of Iberia recorded in the Organyà Basin

The Berriasian to Barremian limestones of the Barranc de la Fontanella, Hostal Nou and Prada formations (this study and (Dinarès-Turell and García-Senz, 2000)) have very consistent ChRM directions, but they cannot be used for the rotation of Iberia. They are shown to be remagnetized because firstly, they show no reversed polarities – which should be expected from a continuous section before the CNS – and rock magnetic experiments provide ample evidence for remagnetisation (Dinarès-Turell and García-Senz, 2000; Gong et al., 2008). This remagnetisation is a wide-spread regional event, reported in many studies as either a pervasive or partial overprint. It is usually assumed to have been caused during the Aptian-Albian rifting phase, or at least during the CNS because of its invariably normal polarity (Schott and Peres, 1987; Galdeano et al., 1989; Turner et al., 1989; Juárez et al., 1994; Villalain et al., 1994; Pares and Roca, 1996; Juárez et al., 1998; Dinarès-Turell and García-Senz, 2000; Villalaín et al., 2003; Gong et al., 2008). In addition to showing a rotation seemingly much larger than reported in literature, also the inclinations of the Berriasian to Barremian sites are significantly steeper than expected from the apparent polar wander paths (APWP) (Figs. 2, 8). The directions from the top of the Prada C limestones have mean

declinations of ~309-314° (this study and Dinarès-Turell and García-Senz (2000)) and are very close to those reported from Hauterivian-Barremian sediments near Lisbon (Galdeano et al., 1989). Our results shares a ctmd with that of Dinarès-Turell and García-Senz (2000), but inclinations are still steeper than expected (although we note that also the Lisbon sediments are anomalously steep, Fig. 8; also, the results of Dinarès-Turell and García-Senz (2000) share a cmtd with those of Galdeano et al. (1989).

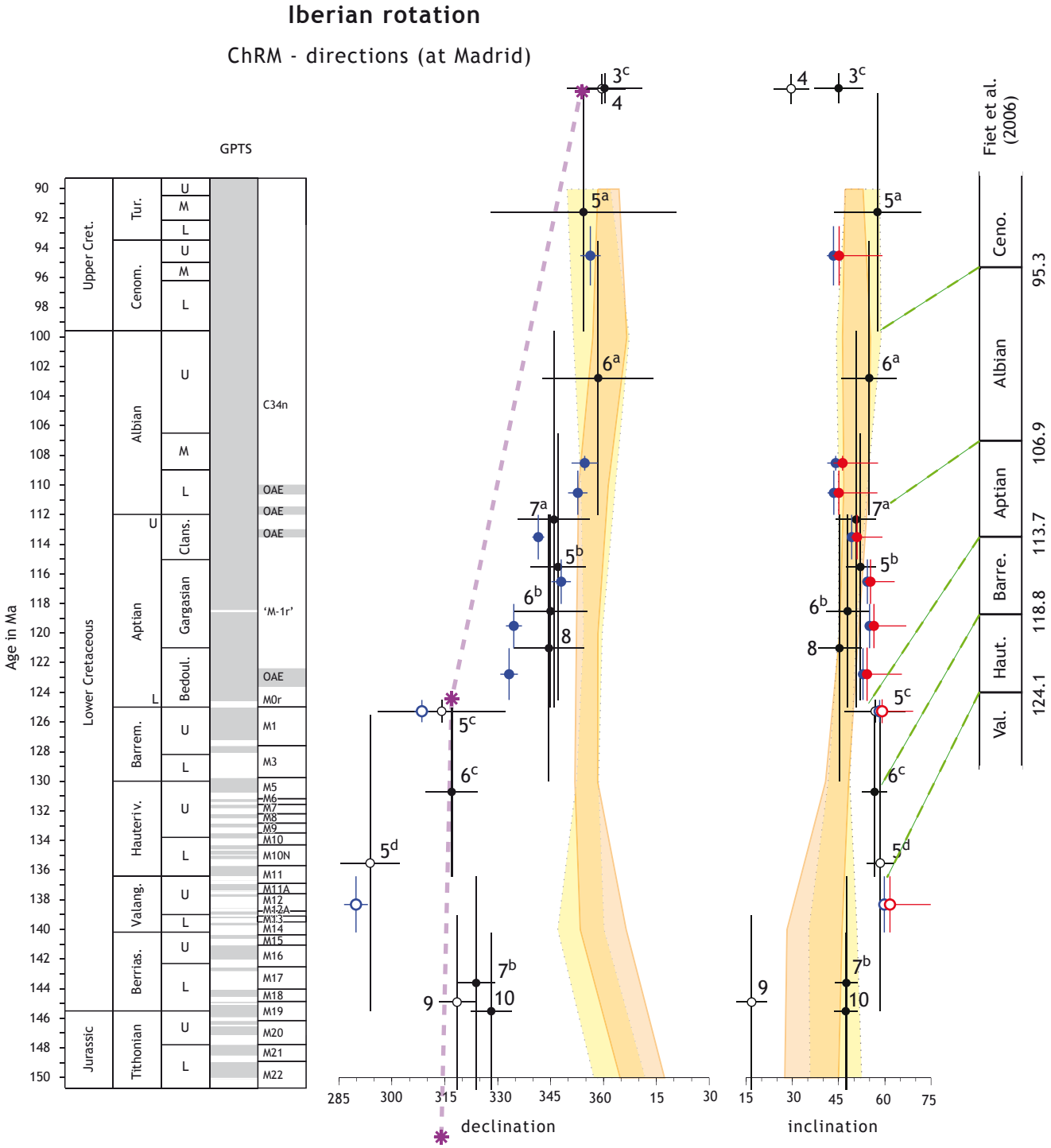

Figure 8 Paleomagnetic directions from Iberia, corrected to Madrid (40.4°N, 3.7°W). The solid (open) blue and red symbols indicate the data from our study (see caption to Figure 2) and solid black symbols indicate literature data; open symbols indicate rejected data. Numbers refer to those listed in Table 2; vertical error bars denote age uncertainty, horizontal error bars denote ΔD (= a_{95}/cos (I)) and ΔI (=a_{95}). The yellow and orange shaded APWPs (Besse and Courtillot, 2002; Torsvik et al., 2008) are as in caption to Figure 2. The purple asteriks give the declinations as derived from the sea-floor anomaly data from the Bay of Biscay (Srivastava et al., 2000; Sibuet et al., 2004), notably the M0 anomaly at the Barremian/Aptian boundary, and the A33o anomaly in the late Cretaceous. The anomaly record constrains the rotation well in magnitude, but poorly in time because of the Cretaceous Normal Superchron. The geological time scale (Ogg et al., 2004) is shown on the left, while the new time scale from Fiet et al. (2006) is on the right of the figure.

Table 2 Summary of all relevant data from this study and literature. The latitude and longitude of each study (lats, longs) is given, and the original published directions with their published Fisher parameters. Asterix in N denotes number of samples, otherwise n is number of accepted sites (out of N total number of sites). Directions (D, I) have been recalculated (via pole correction) to Madrid, and are plotted in Figure 8. Age information is as given in the original study, with the exception of the radiometric ages[1] which are taken from a recent review (Solé et al., 2003). Numerical minimum (hi-age) and maximum (lo-age) are taken from the most recent geological time scale (Ogg et al., 2004) and may change in future studies. Numbers in the first column denote the same study (1- 13), letters (a, b, c, d) are the different intervals from that study. Directions in italics (4, 9) have been rejected (open symbols in fig. 8), the reasons for rejection are in the text.

	Study	Remarks	lats	longs	Published					Madrid		Age information		
					N	*D*	*I*	a_{95}	*k*	*D*	*I*	Stage / radiometric age	lo-age	hi-age
1	Van der Voo & Zijderveld, 1971	Lisbon basalts, Portugal	38.75	-9.30	33/34	352.0	40.0	3.0	70.4	353.6	41.4	72 Ma[1]	74.0	70.0
2	Storetvedt et al., 1990	Monchique Complex, Portugal	37.32	-8.55	27*	181.0	-42.0	4.5	39.4	2.3	46.1	72 Ma[1]	73.0	71.0
3[a]	Van der Voo, 1969	Monchique Syenite, Portugal	37.32	-8.55	8*	182.0	-37.0	6.5	73.6	3.6	41.6	72 Ma[1]	73.0	71.0
3[b]	Van der Voo, 1969	Lisbon basalts, Portugal	38.75	-9.30	17*	354.0	40.5	4.5	63.8	355.6	42.2	72 Ma[1]	74.0	70.0
3[c]	Van der Voo, 1969	Sintra granite, Portugal	38.75	-9.30	25*	359.0	42.5	5.0	34.5	0.5	44.6	83 Ma[1]	84.0	82.0
4	Storedvedt et al., 1987	Sintra granite, Portugal	38.80	-9.38	34*	*358.0*	*27.3*	3.3	57.0	360.1	29.6	83 Ma[1]	84.0	82.0
5[a]	Dinarès-Turell & García-Senz, 2000	Sites 1-3	42.23	1.22	3/4	354.4	58.9	14.1	77.1	354.3	57.6	Cenomanian-Santonian	99.6	83.5
	this study	Santa Fè	42.23	1.22	80*	357.7	47.2	2.1	60.3	356.3	45.2	M. Cenomanian - L. Turonian	96.5	92.5
6[a]	Galdeano et al., 1989	Near Lisbon, Portugal	38.45	-9.21	3/3	358.0	53.0	9.0	187.0	358.5	54.9	Albian-Cenomanian	112.0	93.5
	this study	Col d'Abella	42.23	1.22	60*	356.0	48.1	2.7	45.9	354.7	46.3	M. Albian	109.0	108.0
	this study	Lluça	42.23	1.22	99*	354.1	46.8	2.0	53.3	352.7	45.1	L. Albian	112.0	109.0
7[a]	Moreau et al., 1997	Limestones, Algarve, Portugal	37.06	-7.76	4/4	345.7	47.8	6.5	220.0	346.0	50.6	Aptian - Albian	125.0	99.6
	this study	Font B.	42.23	1.22	108*	342.4	51.7	1.1	148.5	341.5	51.0	U. Aptian	115.0	112.0
5[b]	Dinarès-Turell & García-Senz, 2000	Sites 5-20	42.23	1.22	13/17	347.7	53.1	4.8	74.4	347.1	52.1	Aptian - Lower Albian	124.5	106.5
	this study	Senyus top	42.23	1.22	69*	348.4	56.3	1.6	116.6	348.0	55.3	M. Aptian (top)	118.0	115.0
6[b]	Galdeano et al., 1989	Near Lisbon, Portugal	38.45	-9.21	2/2	344.0	47.0	7.0	32.0	345.0	47.9	Aptian	125.0	112.0
	this study	Senuys	42.23	1.22	129*	334.9	56.5	1.3	97.8	334.6	56.4	M. Aptian	121.0	118.0
8	Moreau et al., 1992	Iberian Chain, Spain	40.50	0.00	5/5	345.5	44.5	7.0	124.0	344.5	45.3	Barremian - Aptian	130.0	112.0
	this study	Cabo	42.23	1.22	162*	333.8	54.3	1.5	38.0	333.2	54.2	L. Aptian	124.5	121.0
	this study	Prada C (II)	42.23	1.22	113*	308.8	57.5	1.1	95.7	308.5	59.1	Barremian-Aptian bnd.	126.0	124.5
5[c]	Dinarès-Turell & García-Senz, 2000	Sites 21-23 (transitional)	42.23	1.22	3/3	314.4	55.5	9.9	155.8	314.1	56.8	lowermost Aptian	126.0	124.5
6[c]	Galdeano et al., 1989	Near Lisbon, Portugal	38.45	-9.21	3/3	317.0	58.0	4.0	1000.0	317.0	56.6	Hauterivian - Barremian	136.4	125.0
5[d]	Dinarès-Turell & García-Senz, 2000	Sites 24-34 (remagnetised)	42.23	1.22	11/11	294.6	56.1	4.4	108.0	293.8	58.5	Berriasian - Barremian	145.5	125.5
	this study	Hostal Nou	42.23	1.22	70*	290.6	59.1	1.7	96.4	289.8	61.6	Valanginian	140.2	136.4
7[b]	Moreau et al., 1997	Limestones, Algarve, Portugal	37.06	-7.76	6/6	323.8	46.5	3.7	330.0	323.9	47.5	Tithonian - Valanginian	150.8	136.4
9	Schott & Peres, 1987	Red beds, northern Spain	42.01	-2.56	6/8	*319.0*	*18.0*	5.0	157.0	318.5	16.8	Kimmeridgian - Valanginian	150.8	139.0
10	Galbrun et al., 1990	Limestones, Algarve, Portugal	37.06	-7.76	40*	328.0	45.9	3.9	32.3	328.2	47.3	Tithonian-Berriasian	150.8	140.2
11	Steiner et al., 1985	Sites AG 2-5	41.30	-1.05	4 / 4	322.0	44.6	6.0	239.0	321.3	45.3	Oxfordian	161.2	155.7
12	Juárez et al., 1998	All sites minus AT1, PO2	41.30	-1.05	11/13	326.8	42.2	4.0	281.0	323.3	41.2	Oxfordian	161.2	155.7
13	Juárez et al., 1994	Sites TO3, AG1,2,4	41.30	-1.05	268*	324.1	40.6	2.9	9.9	326.1	42.7	Oxfordian	161.2	155.7

The younger rocks from Aptian to Cenomanian, however, can be argued to have primary components (Dinarès-Turell and García-Senz, 2000; Gong et al., 2008). In addition, our new and positive fold tests confirm that certainly the upper Aptian (Font Bordonera marls) and Cenomanian (Santa Fè limestones) formations have original (or at least pre-folding) magnetisations. The declinations in the Aptian sites, however, are not according to the expected declinations derived from the APWPs of Eurasia (Besse and Courtillot, 2002; Torsvik et al., 2008) but show a clear counter-clockwise (CCW) rotation with respect to Eurasia. Since the Organyà Basin is located on the Iberian block (but see discussion below), we assume that these CCW rotations represent the rotation of Iberia, also since they are consistent with published data in terms of timing and magnitude. On the contrary, declinations of the Albian and Cenomanian sites plot within the expected Eurasian range. In particular, our new results from the lower Albian Lluça marls and from the middle Albian Col d'Abella limestones are in excellent agreement with the Eurasian APWP. This indicates that the rotation of Iberia was fully completed just before the Albian, contrary to earlier reports (Juárez et al., 1998; Dinarès-Turell and García-Senz, 2000). According to Table 1, the formation mean declinations change from ~334° in the lower Aptian to ~ 356° in the uppermost Aptian. It indicates a minimum of ~ 22° rotation in the Organyà Basin in the Cabó (lower Aptian) and Senyús marls (middle & upper Aptian) which is completed in the Lluçà marls (lower Albian). In addition, the inclinations from Albian to Cenomanian rocks have an excellent agreement with those derived from the APWPs of Eurasia. Therefore, from the Organyà Basin data we can very well constrain the age of the end of the rotation as the Aptian – Albian boundary. However, we cannot accurately constrain the beginning of the rotation from the OB because of the remagnetisation of the pre-Aptian limestones. The top of the Prada C formation gives a transitional direction with a declination of ~309-314° which is close to, but still slightly less than reported declinations for lower Cretaceous and Jurassic sections in Iberia, which we discuss below.

5.2 Paleomagnetic data from Iberia

For comparison and to better constrain the rotation of Iberia, all relevant published paleomagnetic data from 160 Ma to 70 Ma (Vandenberg, 1980; Galdeano et al., 1989; Galbrun et al., 1990; Moreau et al., 1992; Moreau et al., 1997; Dinarès-Turell and García-Senz, 2000) were recalculated with respect to Madrid (Table 2, Fig. 8). Unfortunately, most of the published data have large age and directional uncertainties, contrary to our data which were sampled at much higher age resolution, and using a considerably larger amount of sites and samples. Consequently, we report smaller errors in both directions and ages. In figure 8, we plot the (correspondingly numbered) data of Table 2 between 83 and 150 Ma. We have rejected some results for incorporation in our assessment of the rotation of Iberia. Partly because these are remagnetised (the OB lower Cretaceous limestones), partly on the basis of anomalously shallow inclinations from igneous rocks (Schott and Peres, 1987; Storetvedt et al., 1987), suggesting that they may have not been properly corrected for the paleo-horizontal. On the basis of paleomagnetic results, we cannot well constrain the beginning of the rotation because of a) the transitional/remagnetised data from OB and b) the large age interval reported for the Lisbon sediments, which is not better constrained than Hauterivian-Barremian (Galdeano et al., 1989).

Meanwhile, our Organyà Basin data are clearly consistent with published Iberian data sets – they fit within the (large) published age errors – and clearly show the pattern of the rotation of Iberia. Therefore, we deduce that the basin must have been part of Iberia during the entire Cretaceous rotation. This need not contrast with the reconstruction model of Sibuet et al. (2004) in which the Organyá Basin belongs to a microplate separated from Europa by back-arc spreading and consequently incorporated into the Iberian plate. An extensive discussion on the consequences of our new results on (the timing of) subduction/collision of the transitional domain between Iberia and Europe and on Pyrenean orogeny is beyond the scope of this study, however, and will be discussed in a subsequent paper.

5.3 Reconstruction of the opening of Bay of Biscay

The sea-floor magnetic record of the Bay of Biscay has been the subject of many studies (Srivastava et al., 1990b; Srivastava et al., 1990a; Roest and Srivastava, 1991; Sibuet and Collette, 1991; Olivet, 1996; Srivastava et al., 2000; Sibuet et al., 2004) because of its importance in northern Atlantic Ocean spreading. In a recent study by Sibuet et al. (2004), two 'end-member' models have been critically compared. The two models correspond to two different modes of opening for the Bay of Biscay during this time. The first model argues for a scissors-type opening of the bay with a pole of rotation, presently located just off the coast near Gijon, northern Spain (43.85° N, 5.83° W; (Srivastava et al., 2000)). It is based on the fit of anomaly M0 identifications across the North Atlantic and constrained by maintaining the direction of motion between the plates along the Azores-Gibraltar fracture zone. The second model (Olivet, 1996) relies on the geological assumption that prior to Chron A33o, there was a large left-lateral strike-slip motion between Iberia and Eurasia in an east-west direction. The correspondence of geomorphological features located between Iberia and its adjacent plates is satisfactory in both reconstructions: a good fit between the shape of the northern and southern Bay of Biscay continental margins. Sibuet et al. (2004) convincingly argue, however, that a best fit of M0 across the Atlantic (Srivastava et al., 2000) and in the Bay of Biscay provides a better and more robust kinematic model. This model also strengthens the earlier interpretation of Sibuet and Collette (1991) for the existence of a triple junction at the mouth of the Bay of Biscay, since its opening, until Chron A33o. Sibuet et al. (2004) conclude that there is no significant rotation between anomaly M25 (Kimmeridgian, 154.5 Ma) and anomaly M0 (lower boundary of the Aptian, 125 Ma). The deduced directions translate to ~314° (M25) and ~317° (M0), which is paleomagnetically indistinguishable and in good agreement with published data (Table 2). More importantly, the beginning of the rotation is very well constrained at M0 (declination = 317°), while the end of the rotation cannot be constrained better than having ended at Chron A33o (earliest Campanian, 83.4 Ma; corresponding to a declination of 354°) because of the CNS which produces a quiet zone in marine magnetic anomaly terms.. The M0 value of the declination is in excellent agreement with the

published declination of 317° from the Hauterivian-Barremian Lisbon sediment (Galdeano et al., 1989), and very close to the transitional declinations in Organyà of 309-314° (Table 2, Fig. 8). Apparently, the transitional remagnetised directions are very close to their expected primary direction.

We conclude that the onset of the rotation of Iberia is very well constrained by M0, at the Barremian-Aptian boundary (125 Ma), and agrees within error with published paleomagnetic data. The end of the rotation phase is now very well constrained by our new Albian data, at the Aptian-Albian boundary (112 Ma). It appears therefore that the entire rotation has occurred during the Aptian. The Aptian in the new Geological Time Scale is longer than in most previous versions (see (Gradstein et al., 2004)). According to magnetic anomaly data, the total rotation between M0 (317°) and A33o (354°) is 37°. If we average the Tithonian-Barremian paleomagnetic results, before the Aptian, we find a declination of ~323°; if we include the Oxfordian results (Juárez et al., 1998) we find the same value of ~323° (Table 2). If we average the post Aptian (Albian-Cenomanian) data, we find a declination of ~356°, while including the data from younger (Campanian) igneous rocks (Table 2) yields an average declination of 357.5° well within palaeomagnetic errors. The total rotation based on paleomagnetic data is therefore ~33-34° which compares very well with the ~37° from magnetic anomalies. Our best estimate for the Iberian rotation is therefore ~35°, in remarkable agreement with the first estimate (~35°) by Van der Voo (1969) almost 40 years ago.

To estimate the rate of rotation, we need to know the duration of the Aptian, however this duration is very controversial (Fiet et al., 2006; Tucholke and Sibuet, 2007). The new GTS2004 argues for a longer duration than in older time scales, of 13.0 ± 2.0 Myr, whereas the recent study of Fiet et al. (2006) convincingly argues for a significantly shorter duration of 6.8 ± 0.4 Myr. In addition, they propose an age for the Barremian/Aptian boundary – equivalent to the age of the base of M0 – of 113.7 ± 0.4 Ma, in contrast to the GTS2004 age of 125.0 ± 1.0 Ma. The Fiet et al. study is based on K-Ar dating of glauconites which are in exellent agreement with cyclostratigraphically derived ages (Gale, 1995; Fiet et al., 2001) and Rb/Sr glauconite ages (Rousset et al., 2004). This also would imply a younger age for the M0 anomaly than presently assumed, and interestingly, a recent study on volcanic rocks from Tarim (China) documents an age of 113.3 ± 1.6 Ma for an interval that is assumed to represent the M0 subchron (Gilder et al., 2003).

Hence, the rotation rate according to the GTS2004 Aptian duration would be ~2.7°/Myr, but the time scale of Fiet et al. (2006) implies a faster average rotation rate of ~5°/Myr. This is comparable to or lower than rotation rates found, for example, in the Calabrian arc (Scheepers et al., 1994) or the Aegean arc (Duermeijer et al., 1998; Duermeijer et al., 2000). This rotation rate implies an average half spreading rate of ~2.9 cm/yr, in line with observed rates of up to 3.3 cm/yr (Sibuet et al., 2004; Sibuet et al., 2007).

Finally, an interesting observation is that the rotation seems to progress faster in the early Aptian (Fig. 8) and seems to slow down during the middle and upper Aptian. Approximately half of the rotation takes place during the early Aptian (~3.5 Myr), the other half during the remainder of the Aptian (~9 Myr). This could imply that the initial rifting was faster than the final phase of opening of the Bay of Biscay. In their work, Sibuet et al. (2004) cannot recognise distinct phases as no recognisable magnetic anomalies exist in the M0-A34 quiet magnetic zone, but they underline a change of kinematic phase in the Bay of Biscay, both by the abrupt change in the direction of magnetic trends, at about a third of the distance from chron M0 in the direction of the Bay of Biscay axis and by an associated change in direction of the triple junction branches.

We must note, however, that there are several pitfalls in timing the rotation more precisely. Firstly, it is possible that there is some gap or hiatus between the top of the Prada C limestones and the subsequent Cabó marls (García-Senz, 2002). Secondly, the GTS2004 does not allow robust age constraints on the substages of the Aptian, but progress in (e.g. cyclostratigraphic) dating (Fiet et al., 2006) may well improve determination of substage duration in the future, thereby shedding more light on rifting or opening rates. These processes likely have an expression in the geology of the Pyrenees, but the assessment of causes and effects is at present hampered by the still uncertain relation between (bio)stratigraphic and radiometric ages during this important time interval. The consequences for Pyrenean orogeny, however, will be discussed elsewhere in a subsequent paper.

Acknowledgements

We thank reviewers Rob Van der Voo and Jean-Claude Sibuet who helped to improve our earlier manuscript. We also thank Mark Dekkers, Guillaume Dupont-Nivet, Reinoud Vissers and Douwe van Hinsbergen for stimulating discussions. Mark Dekkers and Iuliana Vasiliev are thanked for their help in the field. Thanks are due to Jaume Vergés for supplying the geological map of the Pyrenees and Rien Rabbers for helping the Organyà Basin map. This work was carried out under the program of the Vening Meinesz Research School of Geodynamics (VMSG), with financial aid from the Department of Earth Sciences of the Faculty of Geosciences.

References

Becker, E., 1999. Orbitoliniden-Biostratigraphie der Unterkreide (Hauterive-Barrême) in den spanischen Pyrenäen (Profil Organyà, Prov. Lérida). Rev. Paléobiol., Genève 18, 359-489.

Berástequi, X., García-Senz, J., Losantos, M., 1990. Tecto-sedimentary evolution of the Organyà extensional basin (central south Pyrenean unit, Spain) during the Lower Cretaceous. Bull. Soc. Géol. France 8, 251-264.

Bernaus, J.M., Arnaud-Vanneau, A., Caus, E., 1999. La sedimentación "Urgoniense" en la cuenca de Organyà (NE España). Libro homenaje a José Ramírez del Pozo. De Geol. Y Geofis. Españoles del Petróleo AGGEP, 71-80.

Bernaus, J.M., 2000. L'Urgonien du Bassin d'Organyà (NE de l'Espagne): micropaléontologie, sédimentologie et stratigraphie séquentielle. Mém. H. S. 33, 138.

Bernaus, J.M., Caus, E., Arnaud-Vanneau, A., 2000. Aplicación de los análisis micropaleontológicos cuantittivos

en estratigrafía secuential: El Cretácico inferior de la cuenca de Organyà (Pirineos, España). Rev. Soc. Geol. España 13, 55-63.

Bernaus, J.M., Arnaud-Vanneau, A., Caus, E., 2003. Carbonate platform sequence stratigraphy in a rapidly subsiding area: the Late Barremian – Early Aptian of the Organya basin, Spanish Pyrenees. Sedimentary Geology 159, 177-201.

Besse, J., Courtillot, V., 2002. Apparent and true polar wander and the geometry of the geomagnetic field over the last 200 Myr. J. Geoph. Res. 107, doi:10.1029/2000JB000,050.

Bullard, E., Everett, J., Gilbert Smith, A., 1965. A symposium on continental drift. in, Phil. Trans. R. Soc. Lond. Ser. A.,41-51.

Butler, R.F., 1992. Paleomagnetism: magnetic domains to geologic terranes. Blackwell Scientific Publications, Boston, pp. 319.

Cande, S.C., Kent, D.V., 1992. A new geomagnetic polarity time scale for the late Cretaceous and Cenozoic. Journal of Geophysical Research 97, 13917-13951.

Carey, S.W., 1958. A tectonic approach to continental drift. in, Symposium on Continental Drift.Hobart (Tasmania),177-355.

Dankers, P., Zijderveld, J.D.A., 1981. Alternating field demagnetizatiof rocks, and the problem of gyromagetic remanence. Earth and Planetary Science Letters 53, 89-92.

Dinarès-Turell, J., García-Senz, J., 2000. Remagnetization of Lower Cretaceous limestones from the southern Pyrenees and relation to the Iberian plate geodynamic evolution. J. Geophys. Res. 105, 19405-19418.

Duermeijer, C.E., Krijgsman, W., Langereis, C.G., Ten Veen, J.H., 1998. Post-early Messinian counterclockwise rotations on Crete: implications for Late Miocene to Recent kinematics of the southern Hellenic arc. Tectonophysics 298, 177-189.

Duermeijer, C.E., Nyst, M., Meijer, P.T., Langereis, C.G., Spakman, W., 2000. Neogene evolution of the Aegean arc: paleomagnetic and geodetic evidence for a rapid and young rotation phase. Earth and Planetary Science Letters 176, 509-525.

Fiet, N., Beaudoin, B., Parize, O., 2001. Lithostratigraphic analysis of Milankovitch cyclicity in pelagic Albian deposits of central Italy: implications for the duration of the stage and substages. Cretaceous Research 22, 265-275.

Fiet, N., Quidelleur, X., Parize, O., Bulot, L.G., Gillot, P.Y., 2006. Lower Cretaceous stage durations combining radiometric data and orbital chronology: Towards a more stable relative time scale? Earth and Planetary Science Letters 246, 407-417.

Galbrun, B., Berthou, P.Y., Moussin, C., Azema, J., 1990. Magnetostratigraphy of the Jurassic-Cretaceous Boundary in Carbonate Marine Shelf – the Bias Do Norte Section (Algarve, Portugal). Bul.Soc.Géol.France 6, 133-143.

Galdeano, A., Moreau, M.G., Pozzi, J.P., Berthou, P.Y., Malod, J.A., 1989. New Paleomagnetic Results from Cretaceous Sediments near Lisbon (Portugal) and Implications for the Rotation of Iberia. Earth and Planetary Science Letters 92, 95-106.

Gale, A.S., 1995. Cyclostratigraphy and correlation of the Cenomanian stage in Western Europe, Orbital Forcing Timescales and Cyclostratigraphy. Geological Society Special Publications 85, 177-197.

García-Senz, J., 2002. Cuencas extensivas del Cretacico Inferior en los Pireneos Centrales – formacion y subsecuente inversion. [PhD thesis]. University of Barcelona, Barcelona.

Gilder, S., Chen, Y., Cogne, J.P., Tan, X.D., Courtillot, V., Sun, D.J., Li, Y.G., 2003. Paleomagnetism of Upper Jurassic to Lower Cretaceous volcanic and sedimentary rocks from the western Tarim Basin and implications for inclination shallowing and absolute dating of the M-0 (ISEA?) chron. Earth and Planetary Science Letters 206, 587-600.

Gong, Z., Dekkers, M.J., Dinarès-Turell, J., Mullender, T.A.T., 2008. Remagnetization mechanism of Lower Cretaceous rocks from the Organyà Basin (Pyrenees, Spain). Studia Geoph. Geod. 52, 187-210.

Gradstein, F.M., Ogg, J.G., Smith, A.G., Agterberg, F.P., Bleeker, W., Cooper, R.A., Davydov, V., Gibbard, P., Hinnov, L.A., House, M.R., Lourens, L., Luterbacher, H.P., McArthur, J., Melchin, M.J., Robb, L.J., Shergold, J., Villeneuve, M., Wardlaw, B.R., Ali, J., Brinkhuis, H., Hilgen, F.J., Hooker, J., Howarth, R.J., Knoll, A.H., Laskar, J., Monechi, S., Plumb, K.A., Powell, J., Raffi, I., Röhl, U., Sadler, P., Sanfilippo, A., Schmitz, B., Shackleton, N.J., Shields, G.A., Strauss, H., Van Dam, J., van Kolfschoten, T., Veizer, J., Wilson, D., 2004. A geologic time scale 2004. Cambridge University Press, Cambridge, pp. 589.

Hiscott, R.N., Wilson, R.C.L., Gradstein, F.M., Pujalte, V., García-Mondéjar, J., Boudreau, R.R., Wishart, H.A., 1990. Comparative stratigraphy and subsidence history of Mesozoic rift basins of the North Atlantic. AAPG Bull. 74, 60-76.

Juárez, M.T., Osete, M.L., Melendez, G., Langereis, C.G., Zijderveld, J.D.A., 1994. Oxfordian Magnetostratigraphy of the Aguilon and Tosos Sections (Iberian Range, Spain) and Evidence of a Preoligocene Overprint. Physics of the Earth and Planetary Interiors 85, 195-211.

Juárez, M.T., Lowrie, W., Osete, M.L., Meléndez, G., 1998. Evidence of widespread Cretaceous remagnetisation in the Iberian Range and its relation with the rotation of Iberia. Earth and Planetary Science Letters 160, 729-743.

Kirschvink, J.L., 1980. The least-squares line and plane and the analysis of palaeomagnetic data. Geophysical Journal of the Royal Astronomical Society 62, 699-718.

McElhinny, M.W., McFadden, P.L., 1997. Palaeosecular variation over the past 5 Myr based on a new generalized database. GJI 131, 240-252.

McFadden, P.L., Jones, D.L., 1981. The fold test in palaeomagnetism. Geophysical Journal, Royal Astronomical Society 67, 53-58.

McFadden, P.L., Lowes, F.J., 1981. The discrimination of mean directions drawn from Fisher distributions. Geophysical Journal, Royal Astronomical Society 67, 19-33.

McFadden, P.L., 1998. The fold test as an analytical tool. Geophysical Journal International 135, 329-338.

Moreau, M.G., Canerot, J., Malod, J.A., 1992. Paleomagnetic study of Mesozoic sediments from the Iberian Chain (Spain) Suggestions for Barremian remagnetization and

implications for the rotation of Iberia. Bull. Soc. Géol. France 163, 393-402.
Moreau, M.G., Berthou, J.Y., Malod, J.-A., 1997. New paleomagnetic Mesozoic data from the Algarve (Portugal): fast rotation of Iberia between the Hauterivian and the Aptian. Earth and Planetary Science Letters 146, 689-701.
Mullender, T.A.T., Van Velzen, A.J., Dekkers, M.J., 1993. Continuous drift correction and separate identification of ferrimagnetic and paramagnetic contribution in thermomagnetic runs. Geophys. J. Int. 114, 663-672.
Ogg, J.G., Agterberg, F.P., Gradstein, F.M., 2004. The Cretaceous Period, in: Smith, A.G. (Eds.), A Geologic Time Scale 2004. Cambridge University Press, Cambridge, pp. 589.
Olivet, J.L., 1996. Kinematics of the Iberian Plate. Bulletin des Centres de Recherches Exploration-Production Elf Aquitaine 20, 131-195.
Pares, J.M., Roca, E., 1996. The significance of tectonic-related Tertiary remagnetization along the margins of the Valencia Trough. Journal of Geodynamics 22, 207-227.
Pichon, X.L., Sibuet, J.C., 1971. Western extension of boundary between European and Iberian Plates during the Pyrenean orogeny. Earth Planet. Sci. Lett. 12, 83-88.
Roest, W.R., Srivastava, S.P., 1991. Kinematics of the plate boundaries between Eurasia, Iberia and Africa in the North Atlantic from the Late Cretaceous to the present. Geology 19, 613-616.
Rousset, D., Leclerc, S., Clauer, N., Lancelot, J., Cathelineau, M., Aranyossy, J.F., 2004. Age and origin of Albian glauconites and associated clay minerals inferred from a detailed geochemical analysis. Journal of Sedimentary Research 74, 631-642.
Salas, R., Guimerà, J., Martín-Closas, C., Meléndez, A., Alonso, A., 2001. Evolution of the Mesozoic Central Iberian Rift System and its Cainozoic inversion (Iberian chain). in, In: Ziegler P.A., Cavazza W., Robertson A.H.F. and Crasquin-Soleau (eds) Peri-Tethyan rift/wrench basins and passive margins. Mém. Mus. Natn. Hist. nat. Paris.145-185.
Scheepers, P.J.J., Langereis, C.G., Zijderveld, J.D.A., Hilgen, F.J., 1994. Paleomagnetic Evidence for a Pleistocene Clockwise Rotation of the Calabro-Peloritan Block (Southern Italy). Tectonophysics 230, 19-48.
Schott, J.J., Peres, A., 1987. Paleomagnetism of the Lower Cretaceous redbeds from northern Spain: evidence for a multistage acquisition of magnetization. Tectonophysics 139, 239-253.
Sibuet, J.C., Collette, B.J., 1991. Triple junctionsof Bay of Biscay and North-Atlantic – new Constraints on the Kinematic Evolution. Geology 19, 522-525.
Sibuet, J.C., Srivastava, S.P., Spakman, W., 2004. Pyrenean orogeny and plate kinematics. J. Geophys. Res. 109, B08104, doi: 10.1029/2003JB002514.
Sibuet, J.C., Srivastava, S.P., Manatschal, G., 2007. Exhumed mantle-forming transitional crust in the Newfoundland – Iberia rift and associated magnetic anomalies. J. Geophys. Res. 112, B06105, doi: 10.1029/2005JB003856.
Solé, J., Pi, T., Enrique, P., 2003. New geochronological data on the Late Cretceous alkaline magmatism of the northeast Iberian Peninsula. Cret. Res. 24, 135-140.
Srivastava, S.P., Roest, W.R., Kovacs, L.C., Oakey, G., Levesque, S., Verhoef, J., Macnab, R., 1990a. Motion of Iberia since the Late Jurassic: results from detailed aeromagnetic measurements in the Newfoundland Basin. Tectonophysics 184, 229-260.
Srivastava, S.P., Schouten, H., Roest, W.R., Klitgord, K.D., Kovacs, L.C., Verhoef, J., Macnab, R., 1990b. Iberian plate kinematics: a jumping plate boundary between Eurasia and Africa. Nature 344, 756-759.
Srivastava, S.P., Sibuet, J.C., Cande, S., Roest, W.R., Reid, I.D., 2000. Magnetic evidence for slow seafloor spreading during the formation of the Newfoundland and Iberian margins. Earth and Planetary Science Letters 182, 61-76.
Storetvedt, K.M., Mogstad, H., Abranches, M.C., Mitchell, J.G., Serralheiro, A., 1987. Palaeomagnetism and isotopic age data from Upper Cretaceous igneous rocks of W. Portugal; geological correlation and plate tectonic aspects. Geophys. J. RAS 88, 241-263.
Tauxe, L., Watson, G.S., 1994. The fold test: an eigen analysis approach. Earth and Planetary Science Letters 122, 331-341.
Tauxe, L., Kent, D., 2004. A simplified statistical model for the geomagnetic field and the detection of shallow bias in paleomagnetic inclinations: was the ancient magnetic field dipolar?, in: Meert, J. (Eds.), Timescales of the Paleomagnetic Field. Am. Geophys. Union, Washington, DC, pp. 320.
Torsvik, T., Muller, R.D., Van der Voo, R., Steinberger, B., Gaina, C., 2008. Global plate motion frames: Toward a unified model. Rev. Geophys. in press.
Tucholke, B.E., Sibuet, J.C., 2007. Leg 210 synthesis: Tectonic, magmatic, and sedimentary evolution of the Newfoundland – Iberia rift. in, Proceedings of the Ocean Drilling Program, Scientific Results. College Station TX 7784509547, USA.
Turner, P., Turner, A., Ramos, A., Sopeña, A., 1989. Palaeomagnetism of Permo-Triassic rocks in the Iberian Cordillera, Spain: acquisition of secondary and characteristic remanence. J. Geol. Soc. (Lond.) 146, 61-76.
Van der Voo, R., 1967. The rotation of Spain: palaeomagnetic evidence from the Spanish Meseta. Palaeogeography, Palaeoclimatology, Palaeoecology 3, 393-416.
Van der Voo, R., 1969. Paleomagnetic evidence for the rotation of the Iberian Peninsula. Tectonophysics 7, 5-56.
Van der Voo, R., Zijderveld, J.D.A., 1971. Renewed palaeomagnetic study of the Lisbon volcanics and implications for the rotation of the Iberian Peninsula. Journal of Geophysical Research 76, 3913-3921.
Van der Voo, R., 1993. Paleomagnetism of the Atlantic, Tethys and Iapetus Oceans. Cambridge University Press, Cambridge, pp. 411.
Van Hoof, A.A.M., Langereis, C.G., 1991. Reversal records in marine marls and delayed acquisition of remanent magnetization. Nature 351, 223-225.
Van Hoof, A.A.M., Van Os, B.J.H., Rademakers, J.G., Langereis, C.G., De Lange, G.J., 1993. A paleomagnetic and geochemical record of the Upper Cochiti reversal and

two subsequent precessional cyles from Southern Sicily. Earth Planet. Sci. Lett. 117, 235-250.
Vandamme, D., 1994. A new method to determine paleosecular variation. Phys. Earth Planet. Int. 85, 131-142.
Vandenberg, J., 1980. New palaeomagnetic data from the Iberian Peninsula. Geologie en Mijnbouw 59, 49-60.
Vergés, J., Fernàndez, M., Martínez, A., 2002. The Pyrenean orogen: pre -, syn -, and post – collisional evolution. Journal of the virtual explorer 8, 57 – 76.
Villalain, J.J., Osete, M.L., Vegas, R., Garciaduenas, V., Heller, F., 1994. Widespread Neogene Remagnetization in Jurassic Limestones of the South-Iberian Palaeomargin (Western Betics, Gibraltar Arc). Physics of the Earth and Planetary Interiors 85, 15-33.
Villalaín, J.J., G., F.-G., M., C.A., A., G.-I., 2003. Evidence of a Cretaceous remagnetization in the Cameros Basin (North Spain): implications for basin geometry. Tectonophysics 377, 101-117.
Zijderveld, J.D.A., 1967. A.C. Demagnetization of rocks: analysis of results, in: Runcorn, S.K. (Eds.), Methods in Palaeomagnetism. Elsevier, New York, pp. 254-286.

Supplementary Table Table of formations, ages, sites sampled in the Organyà Basin (with OR sites/numbers as plotted in Figure 1), and their GPS positions (UTM coordinates), bedding plane (strike & dip). number of samples used for statistics (N_{stat}), number of demagnetised specimens (N_{demag}) and the number of cores drilled ($N_{drilled}$) per site and formation. The percentage givens is the success rate of samples used for the statistics vs. the number of demagnetisations. Biostratigraphic ages are taken from García-Senz (2002). numerical ages are according to the new geological time scale (Ogg et al.. 2004).

Formation	Lithology	Age (biostratigraphic)	Age_hi (Ma)	Age_lo (Ma)	Thickness (m)	Sed. rate (cm/kyr)
Santa Fè	limestones	Cenomanian	96.5	92.5	40	1.0
	hiatus	L. Cenomanian	108.0	96.5		
		M. Albian				
Col d'Abella	limestones	Middle Albian	109.0	108.0	150	15
Lluçá	dark grey marls	Lower Albian	112.0	109.0	705	24
Font Bordonera	marls & m. limest.	Clansayesian	115.0	112.0	530	18
Senyus top	marls & limestones	Garagasian	118.0	115.0	775	13
Senuys	marls	Garagasian	121.0	118.0		
Cabó	marls	Bedoulian	124.5	121.0	950	27
Prada C	dark limestones	Upper Barremian	126.0	124.5	300	20
Prada A,B	limestones	Barremian	130.0	126.0	900	23
	hiatus	L. Barremian	136.4	130.0		
		Hauterivian				
Hostal Nou	limestones	Valanginian	140.2	136.4	200	5.3
Barranc de la Fontanella	limestones	Berriasian	145.5	140.2	200 - 300	3.8 - 5.7

Site	GPS (N)	GPS (E)	Strike/Dip	N_{stat}	N_{demag}	$N_{drilled}$
Santa Fè						
OR08	4674362	355777	270 / 26	9	11	10
OR55	4674578	355247	77 / 40	7	7	8
OR76	4674578	355247	77 / 40	5	22	22
OR77	4674379	355782	270 / 26	25	27	27
OR78	4674407	355761	270 / 26	39	40	40
			79%	**85**	**107**	**107**
Coll d'Abella						
OR79	4674302	356117	269 / 47	66	115	68
			57%	**66**	**115**	**68**
Lluçá						
OR75	4674262	356235	267 / 42	101	101	52
			100%	**101**	**101**	**52**
Font Bordonera						
OR09	4673823	356638	267 / 45	13	15	10
OR73	4673853	357082.72	259 / 53	39	39	39
OR74	4676913	353328	110 / 45	56	57	72
			97%	**108**	**111**	**121**
Senyús top						
OR38	4676146	353737	94 / 45	8	9	9
OR66	4676543	353580	99 / 43	63	64	64
			97%	**71**	**73**	**73**
Senyús						
OR10	4676608	353783	103 / 47	11	12	9
OR11	4676651	354627	104 / 65	11	11	9
OR37	4676149	353474	107 / 39	12	12	13
OR39	4676608	353783	105 / 46	6	6	6
OR40	4676609	353688	108 / 43	4	4	4
OR41	4676520	353678	105 / 51	5	7	9
OR42	4676502	353673	106 / 45	8	10	10
OR43	4676657	354225	96 / 41	13	13	13
OR44	4676651	354627	105 / 48	7	7	8
OR45	4676634	354604	103 / 53	8	8	8
OR67	4676613	353782	97 / 43	48	49	49
			96%	**133**	**139**	**138**

Site	GPS (N)	GPS (E)	Strike/Dip	N_{stat}	N_{demag}	$N_{drilled}$
Cabó						
OR32	4679374	350548	110 / 45	10	11	12
OR33	4679420	350608	111 / 44	2	6	8
OR34	4678412	352887	96 / 50	7	8	10
OR35	4679435	350663	107 / 50	2	2	8
OR36	4679145	352279	98 / 47	8	9	11
OR46	4678324	353738	104 / 48	10	10	11
OR47	4677797	354093	101 / 39	11	11	11
OR48	4677654	356981	97 / 41	9	9	10
OR50	4678049	355024	114 / 48	9	9	9
OR51	4678088	355021	114 / 51	8	8	8
OR52	4678226	354979	111 / 43	8	9	9
OR60	4679751	351232	105 / 48	6	6	7
OR61	4679114	351293	95 / 45	7	8	8
OR64	4677510	358140	106 / 50	9	9	9
OR65	4677405	358088	109 / 49	8	8	8
OR69	4676084	362557	103 / 51	71	102	105
			82%	**185**	**225**	**244**
Prada C						
OR19	4676683	363264	111 / 53	12	13	9
OR49	4678686	354971	111 / 57	7	7	8
OR53	4678016	356794	109 / 42	6	7	6
OR54	4677963	357415	89 / 46	6	6	8
OR58	4679986	351233	116 / 50	7	8	8
OR59	4679914	351326	118 / 54	2	3	3
OR70	4676392	362829	103 / 63	0	28	84
OR72	4676280	362699	105 / 65	33	34	34
OR80	4676302	362719	108 / 68	31	31	31
OR81	4676386.16	362759.93	105 / 66	32	32	32
			80%	**136**	**169**	**223**
Hostal Nou						
OR68	4677635	363525	110 / 60	75	85	83
			88%	**75**	**85**	**83**
			Total *85%*	**960**	**1125**	**1109**

CHAPTER 2

Early Cretaceous syn-rotational extension in the Organyà basin: What was the palinspastic position of Iberia during its rotation?

Z. Gong, D. J. J. van Hinsbergen, R. L. M. Vissers, M. J. Dekkers
Dept. of Earth Sciences, Utrecht University
(submitted to Tectonophysics)

Abstract

In this study we interpret the palaeostress pattern in the Organyà Basin (southern Pyrenees, northern Spain) as inferred from the anisotropy of magnetic susceptibility (AMS) of 39 sites distributed over the entire basin. Combined with information from other Cretaceous Iberian basins, such analysis adds to constrain kinematic reconstructions of the Cretaceous rotation of Iberia allied with the opening of the Bay of Biscay and the northward propagation of the North Atlantic.

The Organyà Basin is an inverted Cretaceous basin in the hanging wall of the Bóixols thrust. The lithologies are mainly weakly deformed pelagic and hemi-pelagic limestones and marls which recorded the Aptian 35° counterclockwise rotation of Iberia. Three types of AMS fabrics could be distinguished, all representing typically intermediate and tectonic fabrics. EW magnetic lineations dominate in the eastern part of the basin and are related to crustal shortening during the Pyrenean orogeny. This interpretation is consistent with structural cross-sections across the basin showing more intense shortening in the east. In the central part of the basin, approximately NS oriented magnetic lineations are observed, interpreted as the original extensional direction during basin foundering. So, in line with results from previous studies, AMS can still unveal the original extensional direction in an inverted sedimentary basin, something which may be difficult to reconstruct from geological data alone. The original extension direction in the Organyà basin is perpendicular to the Bóixols thrust bounding the basin to the south.

Correction for the Aptian rotation of Iberia leads us to infer a NE-SW oriented extension direction at the onset of the rotation of Iberia. This extension direction is inconsistent with current plate kinematic reconstructions of the Cretaceous rotation and motion of Iberia. We therefore suggest a scenario in which the stage pole, describing the onset of opening of the Bay of Biscay and related Iberian rotation, was located near the northeastern corner of the Iberian mainland. During the later Aptian, ongoing rotation of Iberia and opening of the Bay of Biscay occurred according to a stage pole located near northern France. At this stage, the motion of the Iberian continent was in part accomodated by stretching of the west Iberian margin, leading to an additional component of eastward motion and to the development in the Pyrenean realm of a strike-slip environment, prior to N-S convergence and shortening in the Pyrenees since the latest Cretaceous.

Keywords: Anisotropy of magnetic susceptibility, Organyà Basin, Pyrenees, Iberian rotation, Bay of Biscay, Cretaceous

1 Introduction

The anisotropy of the magnetic susceptibility (AMS) of weakly deformed rocks in sedimentary basins has been shown to be a sensitive proxy of either paleostress or low-strain trajectories (Jelinek, 1977; Hirt et al., 1993; Tarling and Hrouda, 1993; e.g. Borradaile and Henry, 1997; Soto et al., 2007). Many previous studies have documented the usefulness of AMS in detecting subtle fabrics, developed even in virtually undeformed sedimentary rocks that do not show any microscopic evidence of deformation such as brittle mesostructures (e.g. Borradaile and Hamilton, 2004; Cifelli et al., 2005; Soto et al., 2007). As a result, the AMS of inverted basin sediments may preserve kinematic and dynamic information on the extensional history of the basin fill (van Hinsbergen et al., 2005; Soto et al., 2007). The AMS analysis of weakly deformed basin sediments thereby provides a strong tool to infer the initial kinematics of inverted basin-bounding normal faults, i.e., to reveal whether these faults were essentially oblique (transtensional) or purely extensional, whilst such early-stage fault kinematics can often no longer be inferred from the reactivated and overprinted basin margin structure.

There are several inverted sedimentary basins exposed in the northern part of the Iberian Peninsula. These basins mainly formed during an Aptian to early Albian phase in which Iberia rifted and rotated counterclockwise (CCW) away from Europe allied with opening the Bay of Biscay to the North and progressive ~E-W spreading and northward opening of the Atlantic Ocean to the West (e.g. Carey, 1958; Bullard, 1965; Sibuet et al., 2004; Gong et al., 2008b). The basins were inverted along their basin-bounding faults during the latest Cretaceous to middle Miocene compression, leading to the Pyrenean fold-and-thrust belt (e.g. Muñoz et al., 1992; Muñoz, 1992; Golonka, 2004). Among these inverted northern Iberian basins are the

Basque-Cantabrian basin in the northwest, and the Central Pyrenean basin including the Organyà basin in the southern Pyrenees (Fig.1).

In a recent AMS and structural study of the Basque-Cantabrian basin, Soto et al. (2007) have shown that the pre-inversion extension direction in present-day coordinates was NE-SW, perpendicular to a major NW-SE trending, inverted basin-bounding normal fault, the Rumaceo fault. The Organyà basin in the southern Pyrenees to the east has a comparable geological history of Aptian-Albian extension and late Cretaceous and younger inversion (García-Senz, 2002).

Different plate kinematic evolution models (e.g. Carey, 1958; Srivastava et al., 1990a; Sibuet and Collette, 1991; Olivet, 1996; Srivastava et al., 2000; Sibuet et al., 2004) have been proposed for the opening of the Bay of Biscay and the consequent palinspastic positions of the Iberian plate with time. There are some important inconsistencies between these reconstructions that essentially arise from the inferred positions of the various rotation poles. On the other hand, whilst the kinematics of the opening of the Bay of Biscay and allied rotation of Iberia is still under discussion, most workers agree on the amount of rotation of Iberia with respect to Eurasia: ~35° CCW (Carey,; Bullard, 1965; Van der Voo, 1969; Choukroune, 1992; Sibuet et al., 2004; Gong et al., 2008b).

A possible way to test the reliability of the rotation poles used in plate kinematic reconstructions of Iberia is to use coeval tensional directions of the paleo-stress field on the north Iberian margin at the onset of the ~35° CCW Iberia rotation during the Aptian (Gong et al., 2008b). With this aim in mind, we present below the results of an AMS study of the Organyà Basin to (1) validate the conclusions of van Hinsbergen et al. (2005) and Soto et al. (2007) that AMS contains information on the pre-inversion tectonic directions; (2) to investigate whether the magnetic fabrics in the Organyà Basin can in all likelihood be related to the Aptian-early Albian extension or, alternatively to a younger overprint during the late Cretaceous and younger inversion history and (3) what the angular relationship is between the extension directions inferred from the AMS fabrics and the inverted basin-bounding normal fault now exposed as the Bóixols thrust. We then proceed to place the results of this study in the context of existing plate kinematic reconstructions describing the rifting and rotation of Iberia and contemporaneous opening of the Bay of Biscay and the Atlantic Ocean, and propose a qualitative alternative to these current reconstructions.

2 Geological setting

In the early Jurassic, opening of the South and Central Atlantic involved breakup of the Pangaea supercontinent into Laurasia and Gondwana (e.g. Scotese, 2001; Torsvik et al., 2008). At that stage, the Iberian Penisula together with Eurasia formed part of Laurasia. During the Cretaceous, progressive breakup and spreading of the North Atlantic Ocean led to separation of the Iberian microplate from Eurasia and Africa along the Azores-Gibraltar plate boundary in the South and the North Pyrenean Fault Zone in the North (e.g. Srivastava et al., 1990b; Olivet, 1996; Vergés et al., 2002; Sibuet et al., 2004). During this breakup process, the triangular Bay of Biscay opened leading to ~35° CCW rotation of Iberia (e.g. Carey, 1958; Bullard, 1965; Van der Voo, 1969; Choukroune, 1992; Sibuet et al., 2004; Gong et al., 2008b). Recently, Gong et al. (2008b) have confined the amount and age of the Cretaceous Iberian rotation with respect to Eurasia to 35° CCW during the Aptian. During this rifting episode, the Pyrenean extensional basins formed on the margins of Iberia and Eurasia. During and/or after the rotation of Iberia, transtensional rifting along the southwestern Eurasia margin resulted in Albian-Turonian alkali-basaltic magmatism and low-pressure high-temperature metamorphism, and in the Albian exhumation and emplacement of upper mantle slices in pull-apart basins presently exposed in the North Pyrenean Zone along the North Pyrenean Fault (Montigny et al., 1986; Vissers et al., 1997; Lagabrielle and Bodinier, 2008).

Northward motion of Africa since the late Cretaceous eventually led to closure of the Pyrenean extensional basins and collision between Iberia and Eurasia, which culminated in the Pyrenean orogeny (Golonka, 2004). N-S contraction lasted from late Santonian to middle Miocene times (Muñoz, 1992) and inverted the pre-Santonian extensional structures.

The syn-rotational rifting along the northern Iberian margin resulted in several extensional sedimentary basins including the Basque-Cantabrian Basin, the North Pyrenean Basin and the Central Pyrenean Basin (García-Senz, 2002; Gibbons and Moreno, 2002). These basins experienced several pulses of extension followed by inversion and subsequent flexural subsidence during the Pyrenean orogeny. The Central Pyrenean Basin became detached along an underlying Triassic evaporite horizon and transported some 100 km southward onto the Iberian foreland, whilst the North Pyrenean Basin was fragmented and thrusted northward onto the European foreland (e.g. Choukroune and and the ECORS Team, 1989; Muñoz, 1992; Beaumont et al., 2000; Rosenbaum et al., 2002). Compression started during the Maastrichtian and progressively led to the development of a typical foreland fold-and-thrust belt, with inversion of the rift-related normal faults including the Bóixols fault (e.g. García-Senz, 2002).

The Organyà Basin forms part of the Central Pyrenean Basin and is exposed in the hanging wall of the Bóixols thrust (Fig.1). The basin was subjected to Berriasian – middle Albian extension and rifting, followed by inversion and shortening during the Pyrenean Orogeny (Juárez et al., 1998; Dinarès-Turell and García-Senz, 2000; García-Senz, 2002; Gong et al., 2008a). The detailed geological structure of the Organyà Basin has been elegantly illustrated by García-Senz (2002) in a number of longitudinal and transverse cross-sections (Fig. 2). The internal structure of the Organyà Basin is dominated by the asymmetric Santa Fé syncline, which has a thicker northern limb than its southern limb (Fig. 2). The wavelength and amplitude of this fold increases from east to west, in proportion to the thickening of the Cretaceous series. The dominant structure exposed reflects the compressive deformation whilst the structure at depth reveals the presence of normal faults related to the previous extensional stage (García-Senz, 2002).

Around 4.5 km of hemi-pelagic to pelagic Cretaceous sediments were deposited in the Organyà Basin (Fig. 2). The formations have been very well dated using biostratigraphy (Becker, 1999; Bernaus et al., 1999; Bernaus, 2000; Bernaus

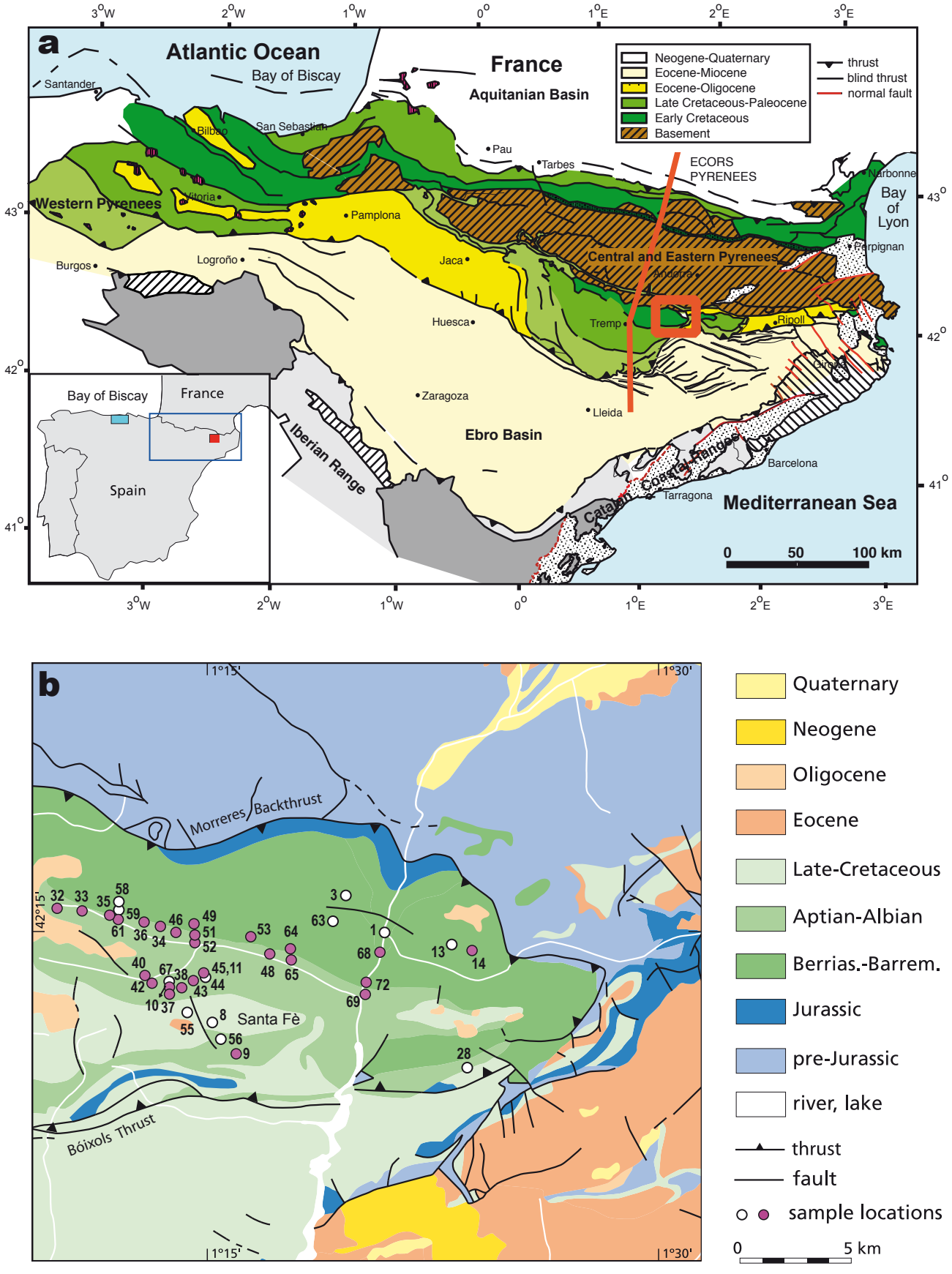

Figure 1 (a) Geological map of the Pyrenees modified after (Vergés et al., 2002). Red and blue solid rectangles in inset map show locations of respectively the Organyà and Basque – Cantabrian basins. (b) Detailed map of the Organyà Basin showing locations of sampling sites (purple and white dots indicate successful and unsuccessful sites, respectively). Site numbers correspond to those reported in Table 1.

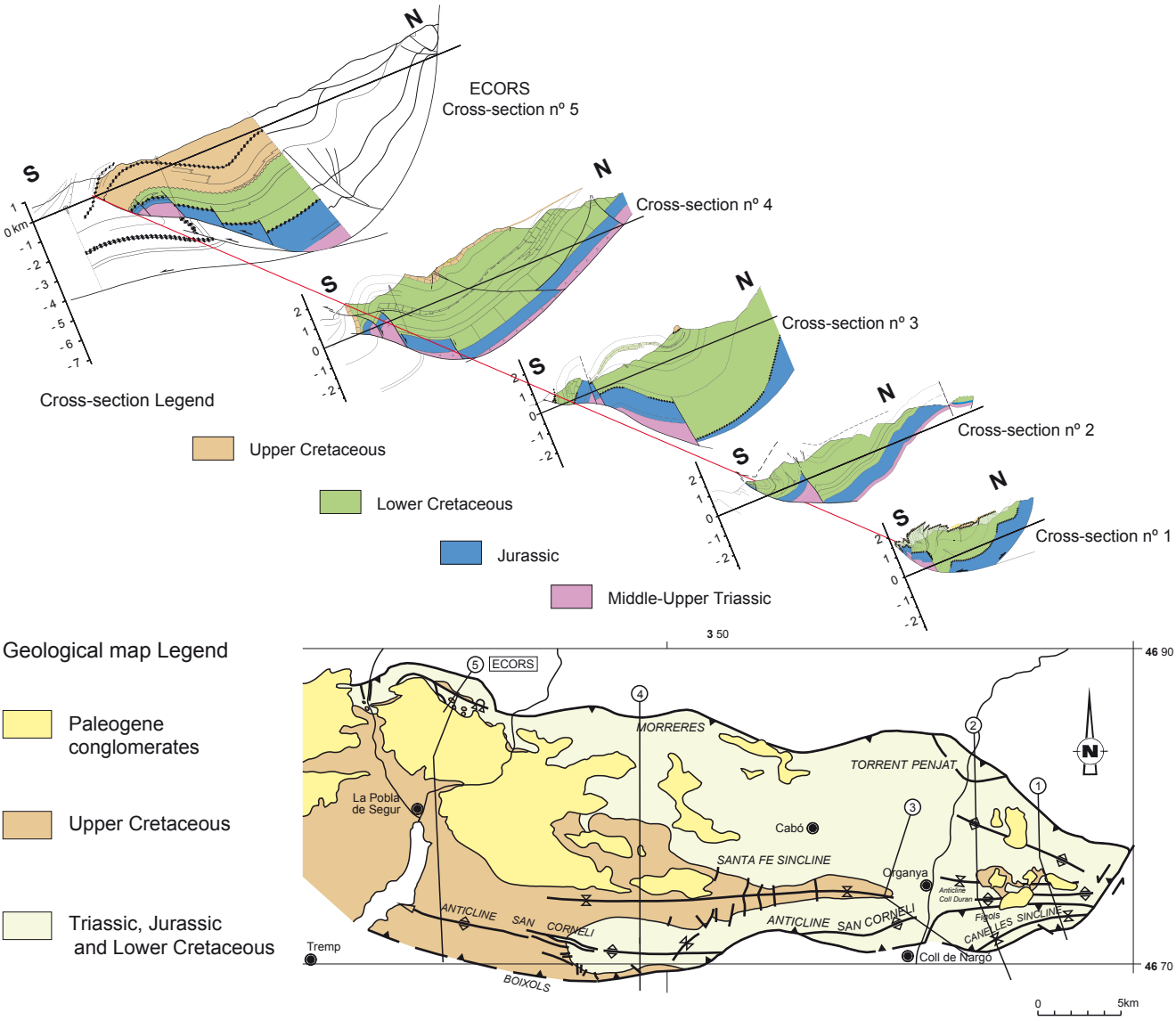

Figure 2 Oblique projection of five cross-sections across the Bóixols sheet, modified after García-Senz (2002), illustrating the change in structural geometry of the Organyà Basin from west to east suggesting higher shortening strains in the eastern part of the basin. Locations of sections are shown on the map.

et al., 2000; Bernaus et al., 2003). The early stages of rifting lasted around 20 Myr and resulted in the deposition of Berriasian-Barremian and earliest Aptian platform carbonates, in a depositional environment interpreted as coastal lagoonal (García-Senz, 2002). The net subsidence was apparently balanced by sediment influx such that throughout the series (Prada Fm.) shallow platform carbonate conditions were maintained. During the Barremian-early Aptian, represented by the transition from the Prada limestones into the Aptian Cabó marls, subsidence rates increased and the net sedimentation rate approximately doubled. Conditions became coastal-marine whilst a higher influx of detrital material suggests increasing topography. In the areas that remained coastal, in the South of Organyà Basin, syn-rift unconformities have been recognized. A hiatus occurs in the upper Albian coinciding with a general rise of the northern Iberian plate (Hiscott et al., 1990). The stage of most intense rifting, reflected by the accelerated subsidence in the Organyà basin during the Aptian, has been shown to coincide with the counterclockwise rotation of Iberia (Gong et al., 2008b).

3 Sampling and methods

Thirty-nine sites (336 oriented cores yielding at least one standard-sized paleomagnetic specimen) covering the entire Organyà Basin, were drilled using a portable gasoline-powered drill and oriented with a magnetic compass (Fig. 1, Table 1). One specimen from each core was processed for the present AMS study. The anisotropy of the low-field magnetic susceptibility was determined with a KLY-3S AC susceptometer (AGICO, Brno, Czech Republic). It operates at a frequency of 875 Hz with a r.m.s. field of 300 A/m and has a sensitivity level of 3 x 10^{-8} SI for a standard-sized specimen. The anisotropy is determined by rotating the sample in three perpendicular planes while the magnetic moment in the applied field is

monitored, allowing the calculation of the principal axes of the susceptibility tensor according to the procedures described in Jelínek(1977). This involves calculation of a tri-axial ellipsoid with principal axes K_{max}, K_{int} and K_{min} describing its shape and properties. We express the magnetic fabric by the parameters *P'* (the corrected anisotropy degree) proposed by Jelínek (1981), the shape parameter *T* (varying between prolate (-1) and oblate (+1)), the magnetic lineation *L* (K_{max}/K_{int}) and the magnetic foliation *F* (K_{int}/K_{min}). To verify whether the differences between the estimated principal susceptibilities as compared to measuring errors are sufficiently meaningful to consider the specimen as anisotropic, the *F*-test is used (Jelínek, 1977). It compares the measurement variance (reduced to 9 positions) to the derived parameters (5 degrees of freedom). In this study, an *F*-distribution on 5 and 9 degrees of freedom with a level of 95% significance ($F_{5, 9; 95}$ = 3.4817; (Jelínek, 1977)) is used to evaluate measurement quality. Only the individual samples with an *F*-test statistic above 3.4817 are considered to be reliable and used for further analysis.

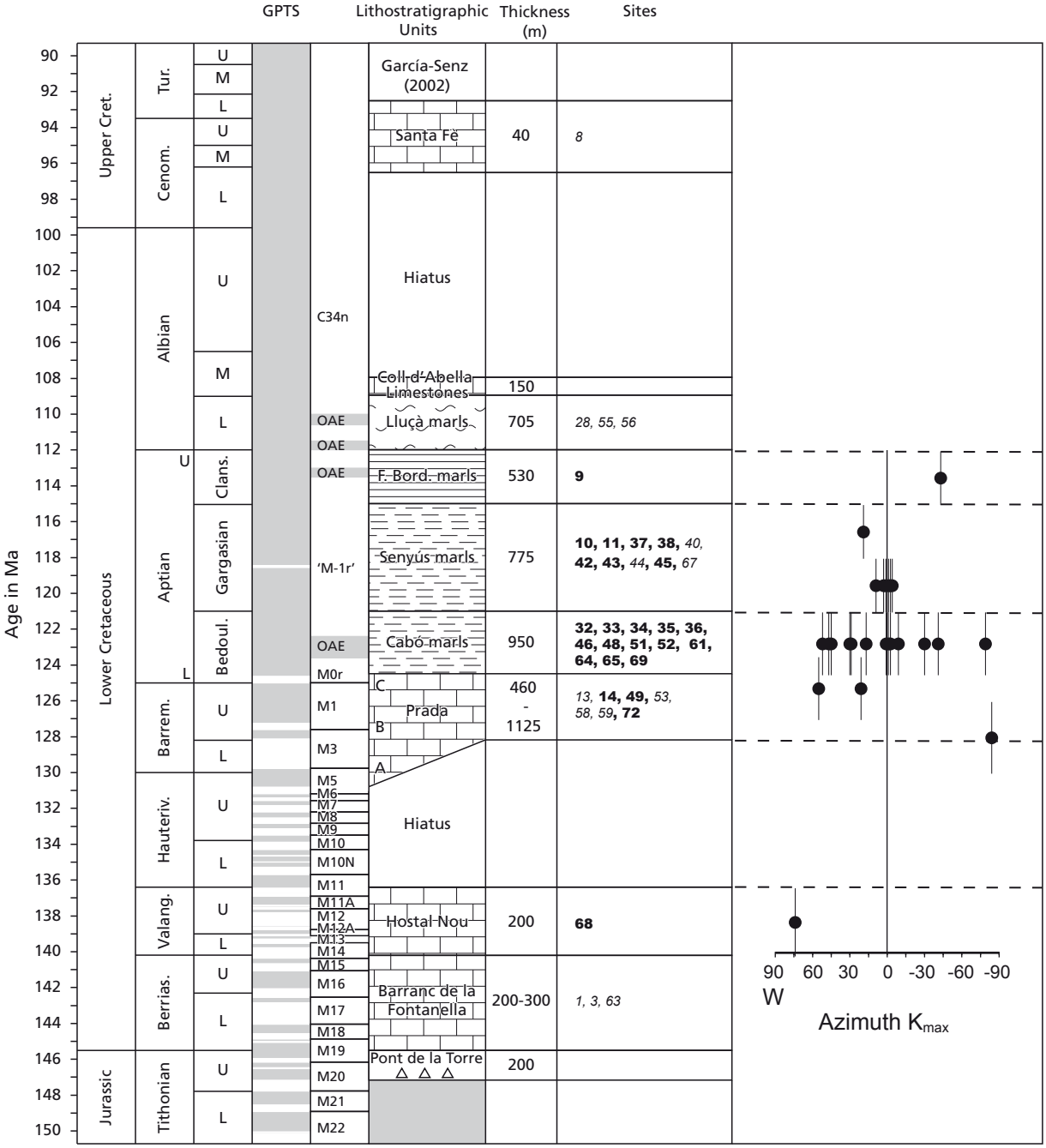

Figure 3 Stratigraphic column showing the lithology of the Organyà Basin, with lithostratigraphic units and formation thicknesses after García-Senz (2002). Geological and geomagnetic polarity time scales (GPTS) after Gradstein et al. (2004). Grey (white) indicates normal (reversed) polarity. Chron nomenclature follows CK92 (Cande and Kent, 1992). Graph to the right shows azimuthal direction of the magnetic lineation (K_{max}) versus lithology (time). Successful sites in bold, unsuccessful sites in italics. Black solid dots indicate site mean azimuthal directions from successful sites. Vertical bars indicate inferred age errors.

4 AMS results

Most of the specimens yielded technically reliable results: 308 out of 336 passed the F-test criterion. Twenty five out of thirty nine sites, from the Berriasian to the Aptian (Fig. 3), gave a sufficient number of reliable specimens (at least 6) useful for interpretation (Supplementary Figs. 1, 2, 3, 4). The site mean susceptibility ranges from 4 x 10^{-6} SI to 1287 x 10^{-6} SI (Table 2). There is no clear relationship between mean susceptibility and the AMS ellipsoid parameters.

Irrespective of lithology and stratigraphic position, most of the sites (Table 2) have low values for the lineation L of < 1.02, with one exceptional site (OR14) yielding values of up to 1.05. Similarly, foliation values F are in most of the cases < 1.03; however, the same exceptional site gave values of up to 1.05. In addition, there is no clear trend in oblateness versus prolateness of the AMS ellipsoids with lithology or stratigraphic position.

When plotted on a per-site basis (Fig. 4), three main types of AMS fabrics can be distinguished that we relate to an increasing tectonic imprint on the originally sedimentary fabric (in bedding-corrected coordinates). In line with AMS studies from other Iberian basins (Soto et al., 2007), a purely sedimentary fabric has not been retrieved from the Organyà Basin. We recognize a Type 1 AMS fabric with the lowest tectonic signature (Figs. 4a-e) which has the minimum susceptibility axis K_{min} (sub)vertical in bedding corrected coordinates, i.e., K_{min} is oriented perpendicular to the bedding. K_{int} and K_{max} are nicely clustered, with K_{max} approximately N-S oriented, although some are oriented NW-SE or NE-SW. We will address this in the discussion below. Note that the shapes of the AMS ellipsoids are either prolate or oblate (Table 2). Eighteen of the twenty five AMS sites, mostly from the Cabó and Senyús marls and two (OR49 and OR72) from limestone sites, belong to Type 1.

Table 1 Sample sites in the Organyà Basin (locations shown in Figure 1), with GPS positions (in UTM coordinates, georeference: ED50), lithostratigraphic units, age, lithology (L = limestone; M = marl; ML = marly limestone), and bedding plane orientation given as strike and dip). Unsuccessful sites shown in italics.

Site	GPS (N)	GPS (E)	Unit / Formation	Age	Lithology	Strike / Dip
OR08	*4674362*	*355777*	*Santa Fe*	*Cenomanian*	*light L*	*268 / 29*
OR28	*4671112*	*364194*	*Lluçà*	*Aptian-Albian*	*dark M&ML*	*251 / 96*
OR55	*4674578*	*355247*	*Lluçà*	*Aptian-Albian*	*dark M*	*77 / 40*
OR56	*4674384*	*355887*	*Lluçà*	*Aptian-Albian*	*dark M*	*276 / 43*
OR09	**4673823**	**356638**	**Font Bordonera**	**Aptian**	**dark M**	**267 / 45**
OR10	**4676608**	**353783**	**Senyús**	**Aptian**	**dark M**	**103 / 47**
OR11	**4676651**	**354627**	**Senyús**	**Aptian**	**dark M**	**104 / 65**
OR37	**4676149**	**353474**	**Senyús**	**Aptian**	**dark M&ML**	**107 / 39**
OR38	**4676146**	**353737**	**Senyús**	**Aptian**	**dark M**	**94 / 45**
OR40	*4676609*	*353688*	*Senyús*	*Aptian*	*dark M*	*108 / 43*
OR42	**4676502**	**353673**	**Senyús**	**Aptian**	**dark M**	**106 / 45**
OR43	**4676657**	**354225**	**Senyús**	**Aptian**	**dark M**	**96 / 41**
OR44	*4676651*	*354627*	*Senyús*	*Aptian*	*dark M*	*105 / 48*
OR45	**4676634**	**354604**	**Senyús**	**Aptian**	**dark M**	**103 / 53**
OR67	*4676613*	*353782*	*Senyús*	*Aptian*	*dark M*	*97 / 43*
OR32	**4679374**	**350548**	**Cabó**	**Aptian**	**dark M**	**110 / 45**
OR33	**4679420**	**350608**	**Cabó**	**Aptian**	**dark M**	**111 / 44**
OR34	**4678412**	**352887**	**Cabó**	**Aptian**	**dark M**	**96 / 50**
OR35	**4679435**	**350663**	**Cabó**	**Aptian**	**dark M**	**107 / 50**
OR36	**4679145**	**352279**	**Cabó**	**Aptian**	**dark M**	**98 / 47**
OR46	**4678324**	**353738**	**Cabó**	**Aptian**	**dark M**	**104 / 48**
OR48	**4677654**	**356981**	**Cabó**	**Aptian**	**dark M&ML**	**97 / 41**
OR51	**4678088**	**355021**	**Cabó**	**Aptian**	**dark M**	**114 / 51**
OR52	**4678226**	**354979**	**Cabó**	**Aptian**	**dark M**	**111 / 43**
OR61	**4679114**	**351293**	**Cabó**	**Aptian**	**dark M**	**95 / 45**
OR64	**4677510**	**358140**	**Cabó**	**Aptian**	**dark M**	**106 / 50**
OR65	**4677405**	**358088**	**Cabó**	**Aptian**	**dark M**	**109 / 49**
OR69	**4676084**	**362557**	**Cabó**	**Aptian**	**dark M**	**103 / 51**
OR49	**4678686**	**354971**	**Prada C**	**Barremian-Aptian**	**dark L**	**111 / 57**
OR53	*4678016*	*356794*	*Prada C*	*Barremian-Aptian*	*dark L*	*109 / 42*
OR58	*4679986*	*351233*	*Prada C*	*Barremian-Aptian*	*dark L*	*116 / 50*
OR59	*4679914*	*351326*	*Prada C*	*Barremian-Aptian*	*dark L*	*118 / 54*
OR72	**4676280**	**362699**	**Prada C**	**Barremian-Aptian**	**dark L**	**105 / 65**
OR13	*4678521*	*363736*	*Prada B, A*	*Barremian*	*dark L*	*98 / 42*
OR14	**4678273**	**365704**	**Prada B, A**	**Barremian**	**dark L**	**296/18**
OR68	**4677635**	**363525**	**Hostal Nou**	**Valanginian**	**dark L**	**110 / 60**
OR01	*4678605*	*363464*	*Barranc de la Fontanella*	*Berriasian*	*light L*	*106 / 46*
OR03	*4679885*	*361263*	*Barranc de la Fontanella*	*Berriasian*	*dark L*	*97 / 56*
OR63	*4679700*	*361298*	*Barranc de la Fontanella*	*Barremian*	*dark L*	*91 / 57*

Site OR72 shows larger within-site dispersion than the other sites of this type.

What we label as a Type 2 AMS intermediate fabric (Figs. 4f-h) has well grouped K_{max}, while K_{int} and K_{min} occur in a girdle perpendicular to K_{max}. This type is dominated by prolate AMS ellipsoids with T < 0 in all of the pertinent sites (Table 2). The magnetic foliation is lost at the scale of the site (Aubourg et al., 2004). Two marl sites (OR33 and OR61) and a remagnetized limestone site (OR 68) belong to this group. This type of

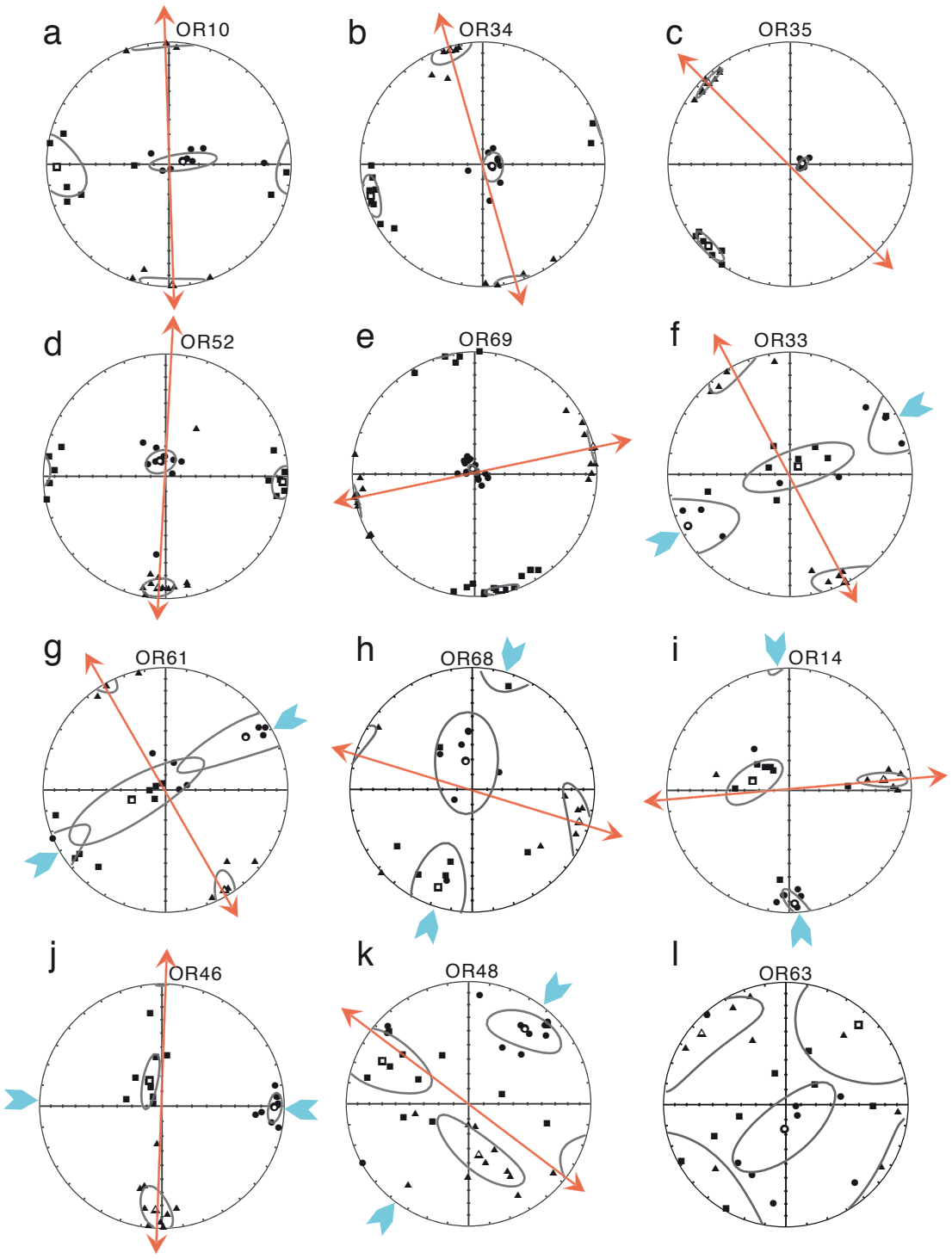

Figure 4 Stereoplots (equal area, lower-hemisphere projection) showing representative AMS data after tectonic correction. Maximum, intermediate and minimum principal anisotropy axes are indicated by respectively triangles, squares and circles. Solid symbols show individual directions, open symbols are mean directions, with 95 % confidence zones indicated. Red and blue arrows represent inferred extension and compression directions. (a-e) Examples of Type 1 fabrics with K_{min} perpendicular to bedding. (f-h) Examples of Type 2 fabrics with clustered K_{max}, and K_{int} and K_{min} tending to spread over a girdle. (i,j) Examples of Type 3 fabrics, with clustered K_{min} almost parallel to bedding. (k) Example of transitional fabric. (l) Example of unsuccessful fabric. For further interpretation and discussion see text.

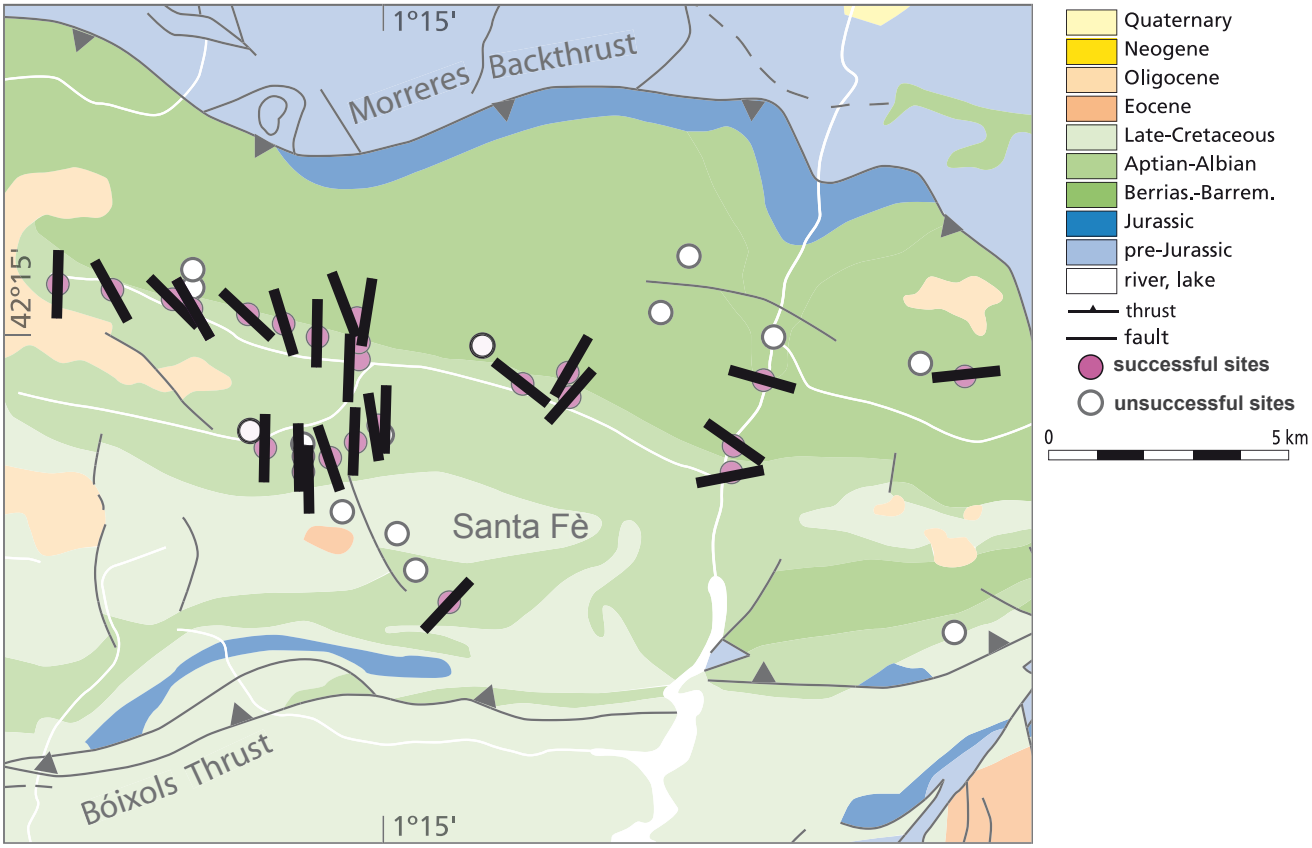

Figure 5 Orientation of the magnetic lineation (K_{max}) after tectonic correction, as a function of position in the Organyà Basin. E-W lineations are dominant in the east, N-S lineations predominate in the western and central part of the basin, and NE-SW and NW-SE lineations tend to occur in the northern and southern marginal regions of the basin.

magnetic fabric is generally considered to result from the early stages of layer-parallel shortening (Tarling and Hrouda, 1993).

Type 3 AMS fabrics (Fig. 4i, j) are characterized by predominantly oblate ellipsoids, with K_{min} well grouped and almost parallel to the bedding, while K_{max} and K_{int} are less clustered. In this case, the positions of K_{min} and K_{int} are usually interchanged with respect to those of type 2 and a newly formed magnetic foliation is developed highly oblique to the bedding (Bakhtari et al., 1998; Aubourg et al., 2004). Three marl sites (OR40, OR42 and OR46) and one limestone site (OR14) belong to this group.

Finally, site OR48 from the Cabó marls and site OR 53 from the Prada limestone have a poorly defined AMS fabric (Figs. 4k, l). The fabric obtained from site OR 48 (Fig. 4k) is transitional between Type 2 and Type 3, and is characterized by prolate ellipsoids with K_{min} reasonably well grouped while K_{max} and K_{int} show a girdle perpendicular to K_{min}. The magnetic fabric in Fig. 4l shows the results from an unsuccessful site (OR 53).

All of the AMS fabrics obtained from the Organyà Basin sediments are interpreted as either tectonic fabrics or as fabrics intermediate between a purely sedimentary and a tectonic fabric. The tectonic overprint is considered to gradually increase from Type 1 to Type 3. In the next section we address the tectonic interpretation of the AMS results.

5 Discussion

5.1 Deformation history of the Organyà Basin

The magnetic lineations recorded by the AMS fabrics in the lower Cretaceous pre- and syn-rift sediments of the Organyà Basin show two dominant directions, i.e., N-S and E-W. NE-SW and NW-SE oriented lineations may be transitional between these two endmembers (Fig. 5). A plot of the azimuth of the lineation versus stratigraphy (Fig. 3) shows that the lineation direction in the Organyà Basin does not systematically vary with lithology or age. The geographic distribution, however, of these lineations (Fig. 5) does show a distinct trend, with E-W lineations being dominant in the east, N-S lineations dominant in the western-central part of the basin, and NE-SW or NW-SE lineations that seem to be confined to the northern and southern marginal regions of the basin.

The E-W trending lineations in the eastern part of the Organyà Basin are in line with the large-scale deformational structure of the basin illustrated by García-Senz (2002): the N-S cross sections (Fig. 2) across the basin strongly suggest that the strain accommodated by the Organyà basin fill increases from west to east. The E-W trending lineation can thus straightforwardly be interpreted to result from (late Cretaceous and Cenozoic) N-S contraction and basin inversion. As outlined previously in this paper, and as illustrated in Fig. 2, the late Cretaceous – Cenozoic contraction and inversion was for an important part localised along a decollement in the underlying Triassic evaporites. In the east of the basin, the

Table 2 AMS parameters from the successful sites in the Organyà Basin. N = number of specimen (F-test >3.4817); K_m = mean susceptibility; K_{max}, K_{int} and K_{min} denote normed principal susceptibilities; st. Errors = Standard Error for $K_{max;}$ $L = K_{max}/K_{int}$ (magnetic lineation); $F = K_{int}/K_{min}$ (magnetic foliation); $P = K_{max}/K_{min}$ (the degree of AMS); $P` = (15/2)\ [(K_{max} - K)^2 + (K_{int} - K)^2 + (2\ K_{min} - K)^2]/(3^* K)^2$ denotes the eccentricity degree; $T = 2\ln F/\ln P - 1$ denotes the shape parameter (Jelinek, 1981).

Sites	N	K_m (*10-6SI)	K_{max}	K_{int}	K_{min}	st. Errors	L	F	P	P′	T
OR9	9	10.50	1.009	1.008	0.983	0.003	1.001	1.026	1.027	1.013	0.943
OR10	8	71.39	1.005	1.000	0.995	0.001	1.005	1.005	1.010	1.004	-0.060
OR11	8	82.99	1.003	1.001	0.996	0.000	1.002	1.005	1.007	1.003	0.363
OR14	7	4.62	1.045	0.996	0.955	0.013	1.045	1.046	1.093	1.039	0.007
OR32	9	519.63	1.008	1.001	0.992	0.002	1.007	1.009	1.016	1.007	0.108
OR33	8	409.70	1.009	0.997	0.994	0.001	1.012	1.003	1.015	1.007	-0.576
OR34	10	473.99	1.012	1.004	0.983	0.001	1.008	1.021	1.030	1.013	0.454
OR35	7	576.03	1.010	1.005	0.985	0.000	1.005	1.021	1.025	1.012	0.624
OR36	9	608.83	1.010	1.000	0.991	0.002	1.010	1.009	1.019	1.008	-0.007
OR37	10	34.87	1.007	1.001	0.992	0.002	1.006	1.009	1.014	1.006	0.225
OR38	9	23.01	1.009	0.998	0.993	0.005	1.012	1.005	1.017	1.008	-0.374
OR42	10	42.95	1.007	0.998	0.995	0.001	1.009	1.003	1.012	1.005	-0.440
OR43	11	81.96	1.004	0.999	0.996	0.001	1.005	1.003	1.008	1.003	-0.229
OR45	11	152.67	1.009	0.998	0.993	0.001	1.011	1.005	1.016	1.007	-0.386
OR46	9	615.01	1.010	1.005	0.985	0.001	1.005	1.020	1.025	1.011	0.603
OR48	11	907.68	1.005	1.000	0.995	0.001	1.006	1.004	1.010	1.004	-0.139
OR49	6	644.02	1.007	0.998	0.995	0.001	1.009	1.003	1.012	1.006	-0.497
OR51	8	1286.67	1.014	0.995	0.991	0.002	1.020	1.004	1.023	1.011	-0.693
OR52	11	714.47	1.011	0.999	0.990	0.002	1.012	1.009	1.021	1.009	-0.150
OR61	8	410.05	1.009	0.997	0.994	0.002	1.011	1.004	1.015	1.007	-0.532
OR64	8	659.34	1.007	1.003	0.990	0.001	1.004	1.013	1.017	1.008	0.503
OR65	9	473.99	1.009	1.005	0.986	0.001	1.005	1.019	1.023	1.011	0.583
OR68	7	42.70	1.011	0.998	0.992	0.002	1.013	1.006	1.019	1.009	-0.331
OR69	19	119.46	1.024	1.012	0.964	0.001	1.011	1.050	1.062	1.028	0.631
OR72	20	28.77	1.009	1.003	0.988	0.002	1.005	1.015	1.021	1.009	0.484

largely E-W trending Bóixols thrust changes orientation to a NE-SW trend which, during inversion, must have induced a strong component of transpression leading to strain partitioning between motion along the decollement and shortening of the overlying sediments. The resulting larger shortening strains in the east are obvious from the structural cross-sections of García-Senz (2002) and confirmed by our AMS data.

The N-S oriented magnetic lineations, however, obtained from the center of the basin in the western part of the study area, are parallel to the inversion-related contraction direction and are therefore likely not related to this event. Because these directions are orthogonal to the Bóixols thrust – shown by strong contrasts in stratigraphic thicknesses across the fault to be an inverted lower Cretaceous normal fault (Muñoz, 1992; García-Senz, 2002) – it seems most likely that these lineations reflect the (syn-depositional) extension direction during basin foundering. At this point we can make three inferences. First, the original extension direction is still maintained in the inverted basin centre, which probably means that virtually all contraction during late Cretaceous and Cenozoic inversion was accommodated by motion along the basal decollement, with only passive folding of the overlying basin sediments. Secondly, the pre-inversion extension direction we find in the Organyà basin confirms the conclusion of Soto et al. (2007) and van Hinsbergen et al. (2005) that studying the AMS of inverted basins allows recognition and reconstruction of the original extension direction in an inverted basin. Thirdly, analogous to the results obtained by Soto et al. (2007) in the Basque-Cantabrian basin, the N-S extensional direction in the Organyà basin interpreted from the AMS fabrics is oriented perpendicular to the Bóixols inverted normal fault, suggesting that the syn-depositional extension direction during early Cretaceous rifting was also perpendicular to the main basin-bounding fault. Because extension of the Organyà Basin started at the onset of the Cretaceous Iberian rotation (Gong et al., 2008b), we correct for the 35° counterclockwise rotation of Iberia with respect to Eurasia, thus restoring a ~NE-SW extension direction, and interpret this direction as the extension direction in the Organyà Basin at the early stages of the rotation of Iberia and the opening of the Bay of Biscay.

5.2 Palinspastic reconstruction

The Cretaceous tectonic evolution of the Organyà Basin is contemporaneous with the Iberian counter-clockwise rotation (Gong et al., 2008b) and opening of the Bay of Biscay (Sibuet et al., 2004). As illustrated and discussed below, this extensional setting of the Organyà Basin (and the South Pyrenean basin in general) conflicts with current plate kinematic reconstructions and the inferred positions of Iberia with respect to Europe with time.

Current plate kinematic reconstructions describing the rotation and motion of Iberia with respect to Europe mainly differ in the estimated locations of the associated Euler poles, and in the consequent pre-rotation position of Iberia with respect to Eurasia. Srivastava et al. (2000) propose a scissor-type opening model for the Bay of Biscay based on its ocean

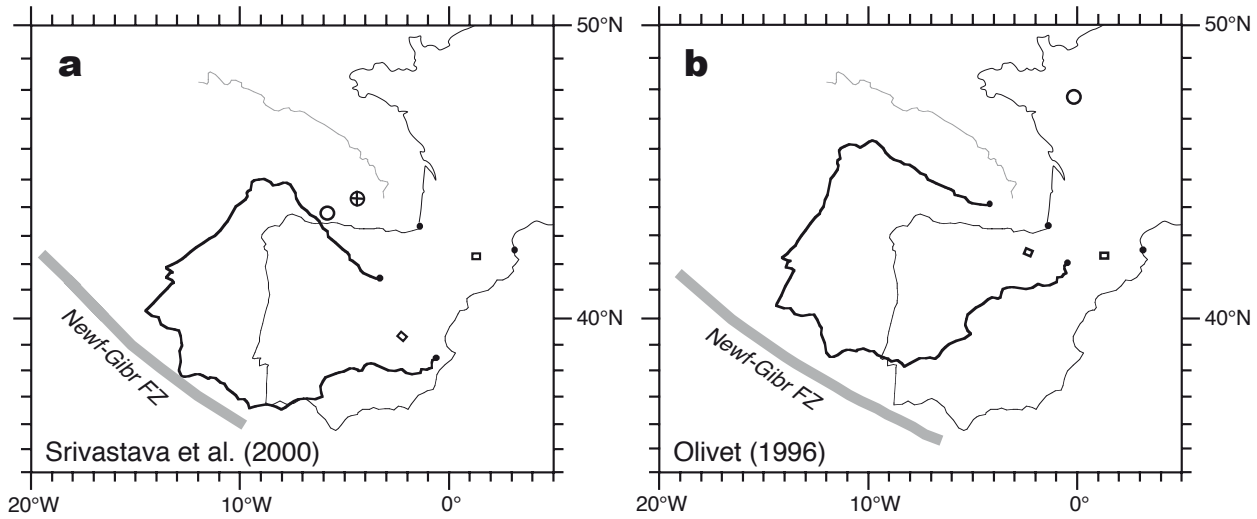

Figure 6 Reconstructed positions of Iberia at M0 times according to the two main endmember kinematic models of Srivastava (2000) and Olivet (1996), modified after Sibuet et al. (2004). Open circles denote total reconstruction poles for Iberia with respect to Eurasia, small rectangles show approximate positions of the Organyà Basin. (a) Kinematic model of Srivastava et al (2000), with total reconstruction pole (43.85° N, 5.83° W, -44.76°) of Sibuet et al. (2004). Circle with cross denotes M0-A33o stage pole (44.35° N, 4.30° W, 37.21°) adopted from Sibuet et al. (2004). (b) Kinematic model of Olivet (1996), with total reconstruction pole located in NW France (47.79° N, 0.22° W, -26.81°).

floor magnetic anomaly pattern and that of the central Atlantic, whereas Olivet (1996) mainly on the basis of geological data suggests a left-lateral strike slip opening model. These two models can be considered to represent endmember scenarios. The first model (Srivastava et al., 2000), which is based on the fit of anomaly M0 identifications across the North Atlantic and Bay of Biscay and constrained by maintaining the direction of motion between the plates along the Azores-Gibraltar fracture zone, infers a total reconstruction pole for the motion of Iberia with respect to Eurasia located in the Bay of Biscay north of Gijon (Fig. 6a). The second model (Olivet, 1996) assumes a total reconstruction pole in northwestern France to account for a dominant left-lateral strike-slip component in the motion between Eurasia and Iberia inferred from geological data, with Iberia moving in a southeasterly direction prior to chron A33o (Fig. 6b). Both of the reconstructions fit the shape of the northern and southern Bay of Biscay continental margins and the geomorphological features located between Iberia and its adjacent plates. However, Sibuet et al. (2004) argue that the model of Srivastava et al. (2000) fits the M0 better and provides a more robust reconstruction. Sibuet et al (2004) have proposed a stage pole for Iberia with respect to Eurasia for the period M0-A33o (125 Ma – ~80 Ma; ages following Gradstein et al. (2004)) located in the eastern Bay of Biscay at 44.35° N, 4.30° W, 37.21° (Fig. 6a). The model of Srivastava (2000) and Sibuet et al. (2004) implies that the basins in the Pyrenean realm should undergo compression, whilst the geological data clearly indicate an extensional tectonic setting. This inconsistency led Sibuet et al. (2004) to suggest that the Pyrenean basins developed in a backarc setting above a north-dipping slab of subducting Neotethys oceanic lithosphere separating the Pyrenean realm from Iberia. Gong et al. (2008b), however, have shown that the Aptian sediments in the Organyà basin did record the Iberian rotation, hence that the basin must have formed part of Iberia.

The Olivet (1996) reconstruction, on the other hand, poses some problems as well, as this model implies roughly NNW-SSE oriented extension in the Pyrenean domain, which is at variance with the restored NE-SW oriented extension direction based on our AMS data and associated normal fault orientations in the Organyà basin. The total reconstruction pole, in addition, has a rotation angle of about 27° which, in view of the inferred pole position in northern France, results in an even smaller vertical axis rotation of Iberia close to 25°, i.e., significantly less that the 35° of Aptian CCW rotation documented by paleomagnetism (Gong et al., 2008b). Sibuet et al. (2004) moreover argue that the M0 position of Iberia inferred by the Olivet (1996) model induces misfits of the M0 anomalies. This latter problem is further discussed below.

Albeit on different aspects, it follows that both models for the kinematics of Iberian plate motion are at variance with the geological data, which calls for a further analysis aiming to circumvent such inconsistencies. In our view, there are three aspects involved that deserve attention.

First, the stage pole inferred by Sibuet et al. (2004) to describe the Cretaceous rotation of Iberia with respect to Eurasia is a finite stage pole relating the position of Iberia at chron M0 to the position of Iberia at chron A33o. We emphasize that most of that period coincides with the Cretaceous Normal Superchron, or the Cretaceous Quiet Zone in sea-floor anomaly terminology. The study by Gong et al. (2008b) clearly confines the rotation of Iberia to the Aptian, such that the kinematics of Iberia motion for the M0-A33o interval may well have involved different substages that combine into the net M0-A33o stage pole, obviously without any anomaly record whatsoever in the ocean floor until chron A33o, except of course for the slightly (4 Ma) older A34 anomaly. Note that Sibuet et al. (2004) likewise recognize that the Iberian paleomagnetic data may well serve to refine the kinematic model for the M0-A33o interval.

A second aspect concerns the assumption made in all plate kinematic reconstructions that plates are rigid and do not deform. In the case of Iberia, however, there are at least two pieces of evidence suggesting that significant deformation

may have affected the northern and western margins. First, a major EW-trending structure exists along the northwestern and northern margin of Iberia which seems to merge eastward with the North Pyrenean Zone. This structure was clearly active during Cenozoic NS-directed shortening since A33o (Sibuet et al., 2004) and accomodated limited subduction of the oceanic Bay of Biscay underneath Iberia (e.g. Boillot, 1984; Sibuet et al., 2004). In view of the geological evidence in the North Pyrenean basins for major motions along the North Pyrenean Fault during the late Mesozoic it seems perfectly possible that this discontinuity north of the Iberian margin was already active at that time as well. Secondly, marine studies of the western Iberian margin focussing on the Iberia-Newfoundland break-up history have provided evidence for a complex breakup process involving at least two stages, i.e., a first Tithonian-Barremian (i.e., pre M0) stage leading to mantle exhumation and, notably, a second stage of extension dated as latest Aptian, reflected by at least five 10 km-scale half graben structures (Péron Pinvidic et al., 2007). Although quantitative data on the magnitude of this late Aptian stretching phase are lacking, these data suggest that the Iberian mainland was effectively stretched away from the M0 anomaly.

A third aspect of possible relevance is the notion made by Gong et al. (2008b) that the Aptian rotation of Iberia itself seems to have involved two stages, i.e., an early Aptian stage of relatively rapid rotation followed by slower rotation during the remainder of the Aptian. We note that this possible decrease in the rate of rotation of Iberia coincides with the late Aptian stretching affecting the western Iberian margin (Péron Pinvidic et al., 2007). In addition we also note that rift-related normal faults in the Organyà basin are unconformably sealed by Cenomanian strata (Fig. 2), consistent with increasing late Cretaceous localization of the Iberian motion along the North Pyrenean Zone (e.g. Peybernès and Souquet, 1984; Choukroune, 1992; Lagabrielle and Bodinier, 2008).

With the above aspects in mind, we now proceed to reconsider the late Mesozoic rotation history of Iberia. Whilst a detailed quantitative analysis of the Iberia plate kinematics lies outside the scope of the present study, we suggest the following qualitative three-stage scenario as a plausible alternative to the two main models discussed above. In this scenario it is assumed

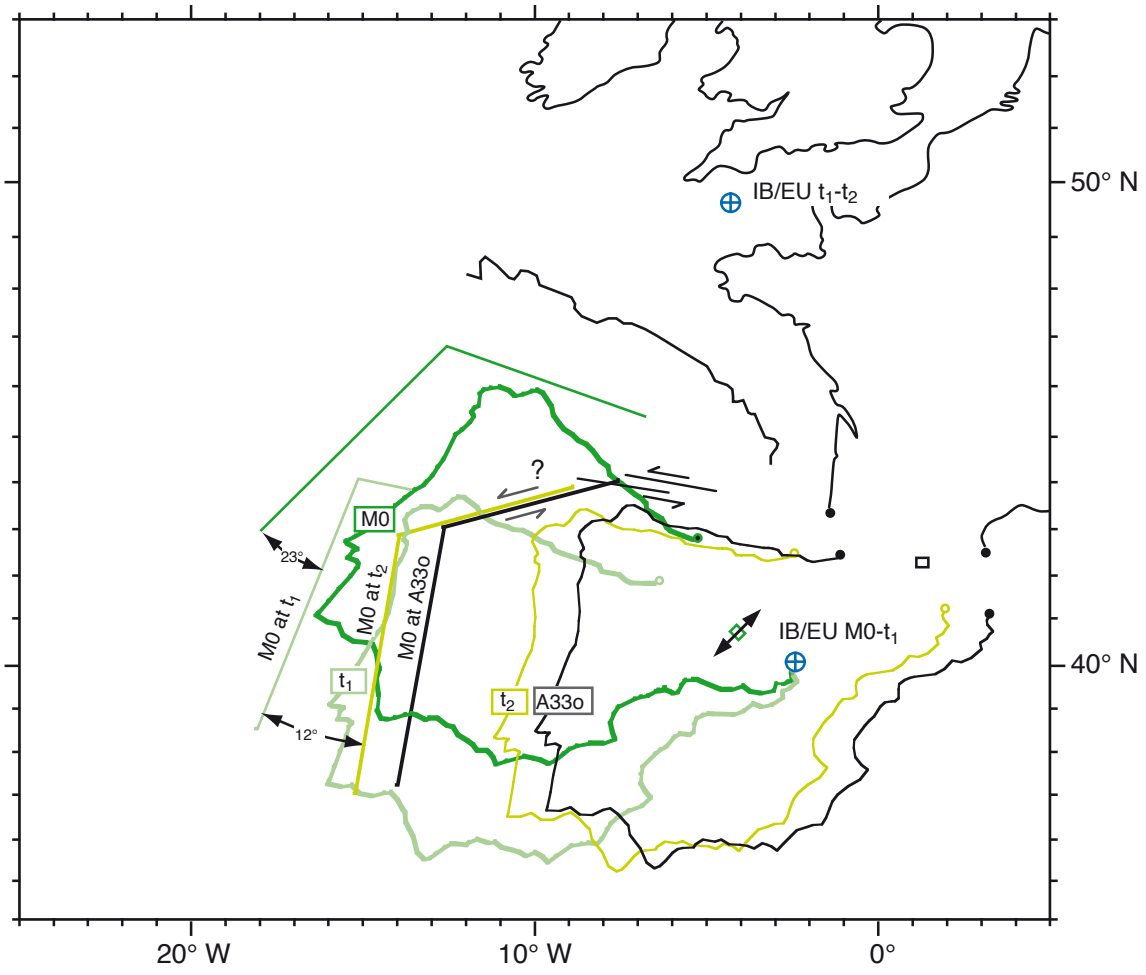

Figure 7 Sketch map illustrating the motion history of Iberia as suggested in this study, with the positions of Iberia and the Iberian M0 anomaly at times M0 (dark green), t_1 (sometime during the Aptian, mild green), t_2 (early Albian, light yellowish green), and A33o (black). Note two steps in Iberian rotation, from M0 to t_1, and from t_1 to t_2, respectively. Circles with crosses denote inferred locations of pertinent stage poles. The distance of M0 to Iberia increases (between t_1 and t_2) caused by late Aptian stretching. Note that for the Organyà Basin in the Pyrenean domain the net effect of this motion history involved an initially NE-SW oriented stretching and rifting phase during the early stages of Iberia rotation, followed by a predominantly strike slip tectonic regime during and after ongoing rotation of Iberia.

that the A33o position of Iberia, inferred by Srivastava (2000) on the basis of the A33o and younger anomalies, is essentially correct, the more because the inferred post-A33o motion in the Pyrenean domain fits remarkably well with shortening estimates of around 165-175 km obtained from restored sections including ECORS (e.g. Muñoz, 1992; Beaumont et al., 2000; Rosenbaum et al., 2002).

We suggest that at M0 times Iberia was located in a position close to that inferred by Olivet (1996), but with an orientation more back-rotated with respect to the Armorican margin as in the Srivastava (2000) and Sibuet et al. (2004) reconstructions (Fig. 7). As shown by Sibuet et al. (2004) for Olivet's (1996) model, such an initial position of Iberia clearly leads to overlapping M0 anomalies, an effect that we ascribe to the stretching of the western Iberian (and Newfoundland?) margin during the late Aptian as outlined above.

In order to accommodate the Aptian opening of the Bay of Biscay and concurrent rifting of the northern Iberian margin, we suggest that the stage pole during this opening was located close to the eastern termination of the margin, leading to some 20-25° of rotation during early Aptian times (Fig. 7). The consequent stretching direction in the Pyrenean domain during this first stage of rifting and opening of the Bay was oriented tangential to the pertinent rotation, i.e., NE-SW as suggested by our (restored) AMS data. Motions on the SW side of Iberia may have been accomodated by NW-SE trending fault segments of the developing Azores-Gibraltar fracture zone, as shown for example on the structural map of the North Atlantic ocean (Miles, 2008).

Ongoing rotation of Iberia by an additional 10-15° occurred during the later Aptian. This late Aptian rotation of the Iberian mainland may have had two components: i.e., a component of rotation due to ongoing spreading in the central Atlantic and Bay of Biscay, leading to rotation and eastward motion of the M0 anomaly (Fig. 7), and perhaps a component of probably small rotation due to intraplate deformation. During this second stage of rotation (shown in Fig. 7 between time t_1 in the late Aptian and time t_2 in the early Albian), the distance between the Iberian mainland and the Iberian M0 anomaly increased due to stretching of the deeper Iberian margin, such that the Iberian mainland moved eastward with respect to the (Iberian) M0 anomaly. It follows that the rotation and motion of Iberia at this stage cannot be expressed in one single stage pole: the stage pole for the rotating M0 anomaly may be located somewhere between Wales and Brittany (Fig. 7) but the motion of the Iberian continent with respect to M0 due to intraplate stretching implies that this same stage pole cannot describe the motion of the Iberian mainland.

The third and last stage of Mesozoic motion of Iberia spans the Albian-Campanian (from time t_2 onward in Fig. 7), and involved a distant stage pole, effectively leading to eastward motion of Iberia towards its A33o position without significant vertical axis rotation, and largely accommodated by strike slip motion along the North Pyrenean Fault and allied structures offshore.

As shown in Fig. 7, the net effect of these three stages is first a significant rotation of Iberia, followed by a smaller rotation and simultaneous ongoing eastward motion of the Iberian continent, presumably accomodated along the northern margin by strike-slip faults like the North Pyrenean Fault. A quantitative analysis of the Iberian plate motion kinematics is needed to investigate the full details of this motion history, however, for present purposes our qualitative approach shows that Aptian rifting in the Organyà basin and the allied stretching directions inferred from our AMS data can indeed be consistent with the simultaneous opening of the Bay of Biscay and consequent Iberian rotation.

6 Conclusions

Our AMS study in the weakly deformed Cretaceous sediments of the Organyà Basin demonstrates the existence of three types of intermediate to tectonic magnetic fabrics that in all likelihood reflect increasing strain. There is a marked trend in the orientation of the magnetic lineation with position in the basin. In the eastern part of the basin, lineations are oriented E-W which we interpret as the result of a compressional overprint formed during basin inversion and shortening since Campanian-Maastrichtian times. In the western part of the basin, where the regional shortening was largely accommodated by decollement along the underlying Triassic evaporates, NS directed lineations dominate suggesting NS extension. This NS extension direction is oriented perpendicular to the inverted Bóixols fault bounding the Organyà Basin to the south, and likely represents the original extension direction during rifting and basin foundering. The NW-SE and NE-SW oriented lineations tend to occur in the marginal parts of the basin and are considered to be transitional.

Correction for the Aptian 35° CCW rotation of Iberia brings the NS lineations into a NE-SW orientation, suggesting that the prevailing stretching direction in the basin during the early stages of opening of the Bay of Biscay and allied rotation of Iberia was NE-SW. This result is inconsistent with current plate kinematic models for the rotation of Iberia such as proposed by Olivet (1996), Srivastava et al. (2000) and Sibuet et al. (2004). In order to circumvent this inconsistency, we propose an alternative scenario in which the stage pole for the onset of opening of the Bay of Biscay and allied Iberian rotation during the early Aptian was located near the northeastern corner of the Iberian mainland. During the late Aptian, ongoing opening of the Bay of Biscay and rotation of Iberia proceeded according to a stage pole located near northern France. At this stage, the motion of the Iberian continent was in part accommodated by stretching of the west Iberian margin, leading to an additional component of eastward motion and development in the Pyrenean realm of a strike-slip environment, prior to post-A33o convergence and N-S directed shortening in the Pyrenees since the latest Cretaceous.

Acknowledgements

During the preparation of this manuscript we have benefited from numerous discussions with Paul Meijer on Iberian plate kinematics and from his constructive comments on the qualitative scenario proposed in this paper. We thank Cor Langereis for discussion on different aspects of the existing

paleomagnetic dataset of Iberia. Thanks are due to Jaume Vergés for providing the geological map of the Pyrenees, Rien Rabbers for helping the Organyà Basin map and Jesus García-Senz for allowing us to use his cross-sections of the Organyà Basin. This work was supported by the Vening Meinesz Research School of Geodynamics (VMSG), with financial aid from the Department of Earth Sciences of the Faculty of Geosciences, Utrecht University, The Netherlands.

References

Aubourg, C., Smith, B., Bakhtari, H., Guya, N., Eshragi, A., Lallemant, S., Molinaro, M., Braud, X., Delaunay, S., 2004. Post-Miocene shortening pictured by magnetic fabric across the Zagros-Makran syntaxis (Iran), in: Weil, A.B. (Eds.), Orogenic Curvature: Integrating Paleomagnetic and Structural analyses. Special Paper 383, Geol. Soc. Amer., Boulder, Colorado, pp. 17-40.

Bakhtari, H.R., de Lamotte, D.F., Aubourg, C., Hassanzadeh, J., 1998. Magnetic fabrics of tertiary sandstones from the Arc of Fars (Eastern Zagros, Iran). Tectonophysics 284, 299-316.

Beaumont, C.J., Mufioz, J.A., Hamilton, J., Fullsack, P., 2000. Factors controlling the Alpine evolution of the central Pyrenees inferred from a comparison of bservations and geodynamical models. Journal of Geophysical Research 106, 8121-8145.

Becker, E., 1999. Orbitoliniden-Biostratigraphie der Unterkreide (Hauterive-Barrême) in den spanischen Pyrenäen (Profil Organyà, Prov. Lérida). Rev. Paléobiol., Genève 18, 359-489.

Bernaus, J.M., Arnaud-Vanneau, A., Caus, E., 1999. La sedimentación "Urgoniense" en la cuenca de Organyà (NE España). Libro homenaje a José Ramírez del Pozo. De Geol. Y Geofis. Españoles del Petróleo AGGEP, 71-80.

Bernaus, J.M., 2000. L'Urgonien du Bassin d'Organyà (NE de l'Espagne): micropaléontologie, sédimentologie et stratigraphie séquentielle. Mém. H. S. 33, 138.

Bernaus, J.M., Caus, E., Arnaud-Vanneau, A., 2000. Aplicación de los análisis micropaleontológicos cuantittivos en estratigrafía secuential: El Cretácico inferior de la cuenca de Organyà (Pirineos, España). Rev. Soc. Geol. España 13, 55-63.

Bernaus, J.M., Arnaud-Vanneau, A., Caus, E., 2003. Carbonate platform sequence stratigraphy in a rapidly subsiding area: the Late Barremian – Early Aptian of the Organya basin, Spanish Pyrenees. Sedimentary Geology 159, 177-201.

Boillot, G., 1984. Some remarks on the continental margins in the Aquitaine and French Pyrenees. Geological Magazine 121, 407-412.

Borradaile, G.J., Henry, B., 1997. Tectonic applications of magnetic susceptibility and its anisotropy. Earth-Science Reviews 42, 49-93.

Borradaile, G.J., Hamilton, T., 2004. Magnetic fabrics may proxy as neotectonic stress trajectories, Polis rift, Cyprus. Tectonics 23, -.

Bullard, E., Everett, J., Gilbert Smith, A., 1965. A symposium on continental drift. in, Phil. Trans. R. Soc. Lond. Ser. A.,41-51.

Cande, S.C., Kent, D.V., 1992. A new geomagnetic polarity time scale for the late Cretaceous and Cenozoic. Journal of Geophysical Research 97, 13917-13951.

Carey, S.W., 1958. A tectonic approach to continental drift. in, Symposium on Continental Drift.Hobart (Tasmania),177-355.

Choukroune, P., and the ECORS Team, 1989. The ECORS Pyrenean deep seismic profile refelction data and the overall structure of an orogenic belt. Tectonics 8, 23-39.

Choukroune, P., 1992. Tectonic evolution of the Pyrenees. Annual Review of Earth and Planetary Sciences 20, 143-158.

Cifelli, F., Mattei, M., Chadima, M., Hirt, A.M., Hansen, A., 2005. The origin of tectonic lineation in extensional basins: Combined neutron texture and magnetic analyses on "undeformed" clays. Earth and Planetary Science Letters 235, 62-78.

Dinarès-Turell, J., García-Senz, J., 2000. Remagnetization of Lower Cretaceous limestones from the southern Pyrenees and relation to the Iberian plate geodynamic evolution. J. Geophys. Res. 105, 19405-19418.

García-Senz, J., 2002. Cuencas extensivas del Cretacico Inferior en los Pireneos Centrales – formacion y subsecuente inversion. [PhD thesis]. University of Barcelona, Barcelona.

Gibbons, W., Moreno, M.T., 2002. The geology of Spain. The Geological Society, London, pp. 649.

Golonka, J., 2004. Plate tectonic evolution of the southern margin of Eurasia in the Mesozoic and Cenozoic. Tectonophysics 381, 235-273.

Gong, Z., Dekkers, M.J., Dinarès-Turell, J., Mullender, T.A.T., 2008a. Remagnetization mechanism of Lower Cretaceous rocks from the Organyà Basin (Pyrenees, Spain). Studia Geoph. Geod. 52, 187-210.

Gong, Z., Langereis, C.G., Mallender, T.A.T., 2008b. The rotation of Iberia during the Aptian and the opening of the Bay of Biscay. Earth and Planetary Science Letters 273, 80-93.

Gradstein, F.M., Ogg, J.G., Smith, A.G., Agterberg, F.P., Bleeker, W., Cooper, R.A., Davydov, V., Gibbard, P., Hinnov, L.A., House, M.R., Lourens, L., Luterbacher, H.P., McArthur, J., Melchin, M.J., Robb, L.J., Shergold, J., Villeneuve, M., Wardlaw, B.R., Ali, J., Brinkhuis, H., Hilgen, F.J., Hooker, J., Howarth, R.J., Knoll, A.H., Laskar, J., Monechi, S., Plumb, K.A., Powell, J., Raffi, I., Röhl, U., Sadler, P., Sanfilippo, A., Schmitz, B., Shackleton, N.J., Shields, G.A., Strauss, H., Van Dam, J., van Kolfschoten, T., Veizer, J., Wilson, D., 2004. A geologic time scale 2004. Cambridge University Press, Cambridge, pp. 589.

Hirt, A.M., Lowrie, W., Clendenen, W.S., Kligfield, R., 1993. Correlation of Strain and the Anisotropy of Magnetic-Susceptibility in the Onaping Formation – Evidence for a near-Circular Origin of the Sudbury Basin. Tectonophysics 225, 231-254.

Hiscott, R.N., Wilson, R.C.L., Gradstein, F.M., Pujalte, V., García-Mondéjar, J., Boudreau, R.R., Wishart, H.A.,

1990. Comparative stratigraphy and subsidence history of Mesozoic rift basins of the North Atlantic. AAPG Bull. 74, 60-76.

Jelinek, V., 1977. The statistical processing of anisotropy of magnetic susceptibility measured on groups of speciments and its applications. Geofyzyca 1, 1-2.

Jelinek, V., 1981. Characterization of the magnetic fabrics of rocks. Tectonophysics 79, 63-67.

Jelínek, V., 1977. The statistical theory of measuring anisotropy of magnetic susceptibility of rocks and its application. in. Geofyzika Brno,87.

Juárez, M.T., Lowrie, W., Osete, M.L., Meléndez, G., 1998. Evidence of widespread Cretaceous remagnetisation in the Iberian Range and its relation with the rotation of Iberia. Earth and Planetary Science Letters 160, 729-743.

Lagabrielle, Y., Bodinier, J.L., 2008. Submarine reworking of exhumed subcontinental mantle rocks: field evidence from the Lherz peridotites, French Pyrenees. Terra Nova 20, 11-21.

Miles, P.R., 2008. Structural map of the North Atlantic Ocean. in. Commission for the Geological Map of the World (CCGM/CGMW), http://www.ccgm.org.

Montigny, R., Azambre, B., Rossy, M., Thuizat, R., 1986. K-Ar study of Cretaceous magmatism and metamorphism in the Pyrenees: age and length of rotation of the Iberian Penisula. Tectonophys. 129, 257-273.

Muñoz, J.A., 1992. Evolution of a continental collision belt: ECORS Pyrenees crustal balanced cross-section, in: McClay, K.R. (Eds.), Thrust tectonics. Chapman and Hall, London, pp. 235-246.

Muñoz, J.A., Pardo, G., Villena, J., 1992. Evolucion paleogeogra´fica de los conglomerados miocenos adosados al borde norte de la Sierra de Cameros (La Rioja). Act. Geol. Hisp. 27, 3-14.

Olivet, J.L., 1996. Kinematics of the Iberian Plate. Bulletin des Centres de Recherches Exploration-Production Elf Aquitaine 20, 131-195.

Péron Pinvidic, G., Manatschal, G., Minshull, T.A., Sawyer, D.S., 2007. Tectonosedimentary evolution of the deep Iberia-Newfoundland margins: Evidence for a complex breakup history. Tectonics 26, TC2011, doi:10.1029/2006TC001970.

Peybernès, B., Souquet, P., 1984. Basement blocks and tecto-sedimentary evolution in the Pyrenees during Mesozoic times. Geological Magazine 121, 397-405.

Rosenbaum, G., Lister, G.S., Duboz, C., 2002. Relative motions of Africa, Iberia and Europe during Alpine orogeny. Tectonophys. 359, 117-129.

Scotese, C., 2001. Atlas of Earth History, PALEOMAP Project. Arlington, TX, pp. 52.

Sibuet, J.C., Collette, B.J., 1991. Triple junctionsof Bay of Biscay and North-Atlantic – new Constraints on the Kinematic Evolution. Geology 19, 522-525.

Sibuet, J.C., Srivastava, S.P., Spakman, W., 2004. Pyrenean orogeny and plate kinematics. J. Geophys. Res. 109, B08104, doi: 10.1029/2003JB002514.

Soto, R., Casas-Sainz, A.M., Villalaín, J.J., Oliva-Urcia, B., 2007. Mesozoic extension in the Basque-Cantabrian basin (N Spain): Contributions from AMS and brittle mesostructures. Tectonophysics 445, 373-394.

Srivastava, S.P., Roest, W.R., Kovacs, L.C., Oakey, G., Levesque, S., Verhoef, J., Macnab, R., 1990a. Motion of Iberia since the Late Jurassic: results from detailed aeromagnetic measurements in the Newfoundland Basin. Tectonophysics 184, 229-260.

Srivastava, S.P., Schouten, H., Roest, W.R., Klitgord, K.D., Kovacs, L.C., Verhoef, J., Macnab, R., 1990b. Iberian plate kinematics: a jumping plate boundary between Eurasia and Africa. Nature 344, 756-759.

Srivastava, S.P., Sibuet, J.C., Cande, S., Roest, W.R., Reid, I.D., 2000. Magnetic evidence for slow seafloor spreading during the formation of the Newfoundland and Iberian margins. Earth and Planetary Science Letters 182, 61-76.

Tarling, D.H., Hrouda, F., 1993. The magnetic anisotropy of rocks. Chapman & Hall, London, pp. 217pp.

Torsvik, T., Muller, R.D., Van der Voo, R., Steinberger, B., Gaina, C., 2008. Global plate motion frames: Toward a unified model. Rev. Geophys. 46, RG3004, doi:10.1029/2007RG000227.

Van der Voo, R., 1969. Paleomagnetic evidence for the rotation of the Iberian Peninsula. Tectonophysics 7, 5-56.

van Hinsbergen, D.J.J., Zachariasse, W.J., Wortel, M.J.R., Meulenkamp, J.E., 2005. Underthrusting and exhumation: A comparison between the External Hellenides and the 'hot' Cycladic and 'cold' South Aegean core complexes (Greece). Tectonics 24, doi:10.1029/2004TC001692.

Vergés, J., Fernàndez, M., Martínez, A., 2002. The Pyrenean orogen: pre -, syn -, and post – collisional evolution. Journal of the virtual explorer 8, 57 – 76.

Vissers, R.L.M., Drury, M.R., Newman, J., Fliervoet, T.F., 1997. Mylonitic deformation in upper mantle peridotites of the North Pyrenean Zone (France): Implications for strength and strain localization in the lithosphere. Tectonophysics, 279, 303-325.

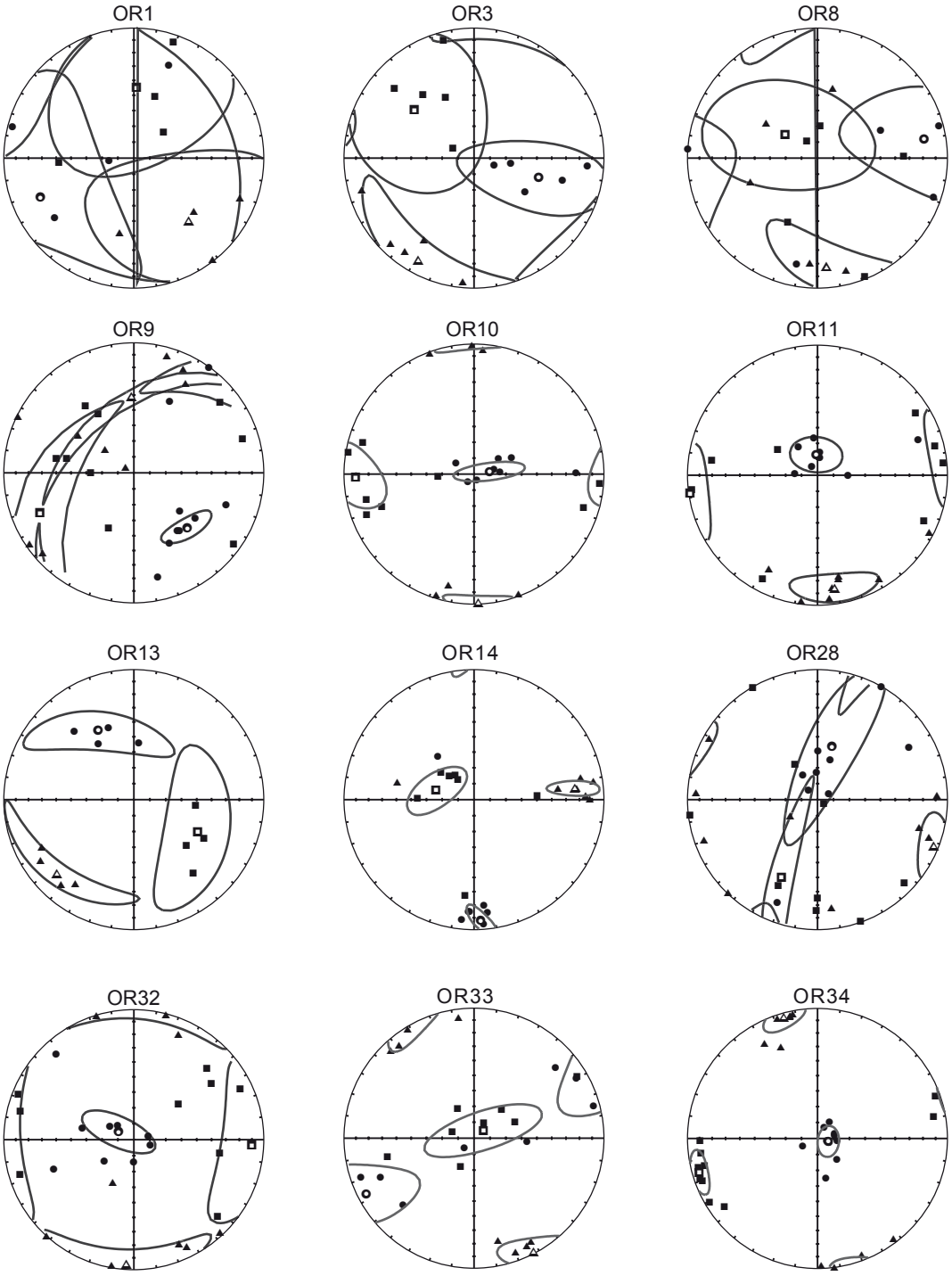

Supplementary Figures 1, 2, 3 and 4 Equal area lower-hemisphere projections showing all AMS data from the measured sites in the Organyà Basin after tectonic correction. Maximum, intermediate and minimum principal anisotropy axes shown as triangles, squares and circles, respectively. Solid symbols show individual directions, open symbols are mean directions, with 95 % confidence zones shown.

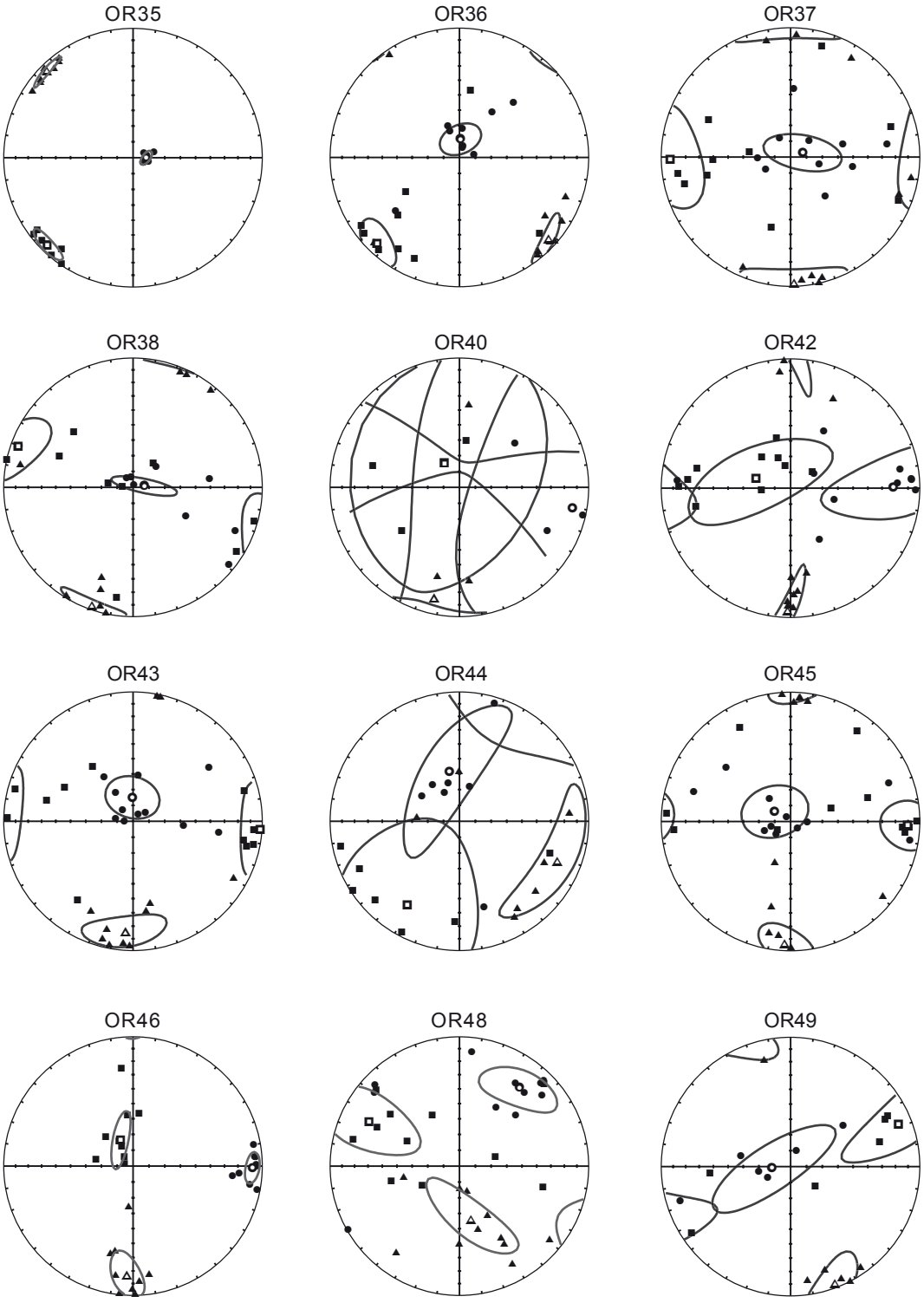
OR35
OR36
OR37
OR38
OR40
OR42
OR43
OR44
OR45
OR46
OR48
OR49

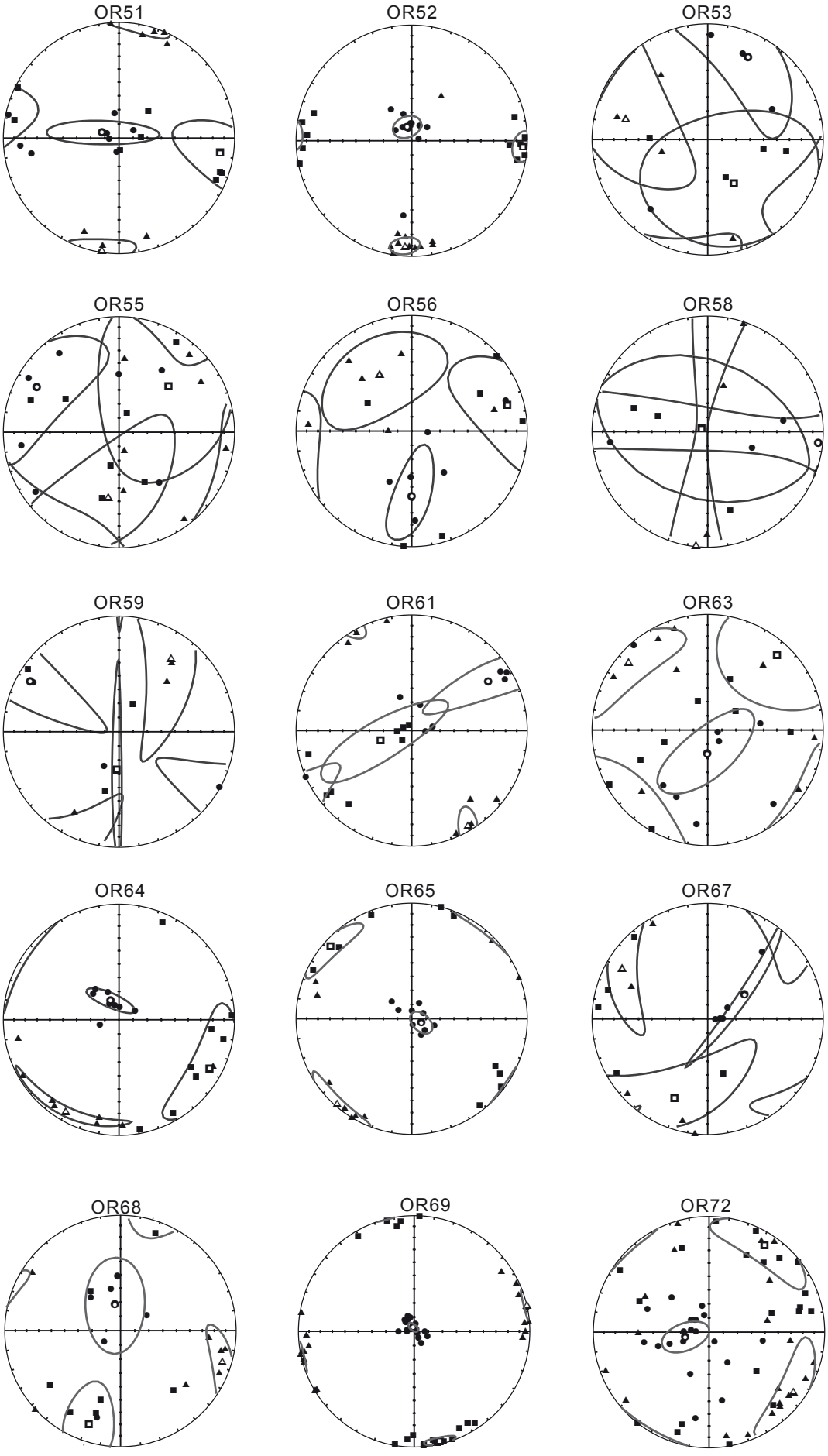
OR51
OR52
OR53
OR55
OR56
OR58
OR59
OR61
OR63
OR64
OR65
OR67
OR68
OR69
OR72

PART 2

Remagnetization

CHAPTER 3

Remagnetization mechanism of Lower Cretaceous rocks from the Organyà Basin (Pyrenees, Spain)

Zhihong Gong[1], Mark J. Dekkers[1], Jaume Dinarès-Turell[2], Tom A.T. Mullender[1]
1 Palaeomagnetic Laboratory "Fort Hoofddijk", Department of Earth Sciences, Faculty of Geosciences, Utrecht University, Budapestlaan 17, 3584 CD Utrecht, The Netherlands (gong@geo.uu.nl)
2 Instituto Nazionale di Geofisica e Vulcanologia, Via di Vigna Murata 605, 00143 Rome, Italy
Reprinted from Stud. Geophys. Geod., 53 (2008), 187-210, with kind permission of Springer Science and Business Media.

Abstract

Widespread Cretaceous remagnetization is documented in several Mesozoic basins in North Central Spain. Organyà Basin (South Central Pyrenean foreland) is atypical in the sense that the lower part of the rock sequence (Berriasian-Barremian limestones) is remagnetized while the upper portion (Aptian-Albian marls) is not (*Dinarès-Turell and García-Senz, 2000*). Here, this view is confirmed by the analysis of 41 new paleomagnetic sites over the entire basin, so that a 3D view is obtained. Thermoviscous resetting of the natural remanent magnetization can be ruled out, hence the remagnetization is chemical in origin. A positive breccia-test on remagnetized strata constrains the remagnetization age to older than the Paleocene-Eocene, when the backthrust system was active. The remagnetization is argued to have occurred early in the geological history of the Organyà Basin either in the elevated geothermal gradient regime during the syn-rift extension or at the earliest phase of the later compression. Burial is considered the most important cause combined with the lithological effect that limestones are more prone to express remagnetization than marls. The observed pressure solution in the remagnetized limestone is likely associated with the remagnetization, whereas it is unlikely that externally derived fluids have played an important role.

Keywords: Natural remanent magnetization, remagnetization mechanism, Cretaceous, Pyrenees

1 Introduction

For a correct interpretation of paleomagnetic data, the recording of the natural remanent magnetization (NRM) in the rocks must be known and the primary nature of the characteristic component should be documented. In sedimentary rocks, the focus of the present contribution, the primary NRM is often considered to be of detrital origin. The exact acquisition timing of the NRM is less critical given the long time scale of plate tectonic processes. Therefore, early diagenetic processes occurring shortly after deposition, are often considered to be part of the 'detrital inventory' which is warranted for paleopole studies. Rocks are not closed systems after their formation and secondary NRM components can be added to existing NRM. Also, primary NRM can be replaced by such components. If secondary components are erroneously interpreted as primary components, evidently incorrect conclusions are the result. Therefore, the recognition of pervasive remagnetization of NRM is essential for a correct interpretation of paleomagnetic data.

Many paleomagnetic studies from the Iberian Peninsula have reported on remagnetization in Mesozoic rocks. Galdeano et al. (*1989*) showed that Late Jurassic to Valanginian sediments near Lisbon (Portugal) had been remagnetized. They hypothesized that the remagnetization would be caused by a complex process during 'prerifting' uplift of sedimentary beds before the Hauterivian. Moreau et al. (*1992*) suggested a primary magnetization for Barremian and Aptian sites in the Maestrazgo basin (southern Iberian Ranges) while older sites are argued to be remagnetized before the Barremian. The age of remagnetization was proposed to be in relation with a rifting phase during Valanginian to Aptian times. In the Algarve region (Portugal) a Barremian-Aptian remagnetization is documented in Jurassic and Cretaceous limestones (*Moreau et al., 1997*). However, the remagnetization time and mechanism was not discussed. Juárez et al. (*1998*), in a study of the Iberian Range (northern Spain), found that their 13 sites of Jurassic age were all remagnetized and argued that the remagnetization may be associated with an extensional phase either during the Early Cretaceous (Barremian-early Albian) or the Late Cretaceous (Cenomanian). Villalaín et al. (*2003*) showed evidence of a Cretaceous remagnetization during the Berriasian and Albian in red beds of the inverted Cameros Basin (northern Spain). The age of the remagnetization was constrained between the Albian and Santonian, most probably Albian, just after the extensional phase of the basin and long before the main compressional events that caused its inversion. Márton et al. (*2004*) pointed out a pre-Aptian remagnetization in Jurassic-Cretaceous sediments in the Lusitanian basin and the Algarve from Portugal. It was suggested that the remagnetization occurred around the transition of the Early and Late Aptian. The remagnetization may be linked to a thermal event due to extensional tectonics. To contribute to solving this widespread remagnetization question in Iberia, ideally a partly remagnetized

and partly unremagnetized basin with the same orogenic history and more or less lithological uniformity is required.

The Organyà Basin (OB) with its Lower Cretaceous sediments (Fig. 1) is a basin along these lines (*Dinarès-Turell and García-Senz, 2000*). The sedimentary sequence consists of 4.5 km thick Cretaceous rocks, mainly limestones and marls. Therefore, the lithology variability is constrained to a minimum. Furthermore, the NRM of the rocks was argued to be unremagnetized in the Aptian-Albian marls, while it was remagnetized in the Berriasian-Barremian limestones (*Dinarès-Turell and García-Senz, 2000*). The transition between remagnetized and unremagnetized rocks is around the Barremian-Aptian boundary. The remagnetization is considered to be a chemical remagnetization but the amount and origin of the fluids involved is currently elusive. The aim of the present paper is to try to unravel the remagnetization mechanism by extending the essentially 2-dimensional cross-section view of the paleomagnetic data along the Segre River (*Dinarès-Turell and García-Senz, 2000*) to three dimensions over the entire basin.

2 Geological setting

During the Cretaceous rotation of Iberia, a series of extensional and transtensional basins formed at its northern margin and also at the southern margin of Europe. One of those basins, the OB (Fig. 1a), is later incorporated in the uppermost thrust sheet of the South Central Pyrenean thrust belt as a consequence of inversion tectonics (*Berástequi et al., 1990*). The southern boundary of the OB (Fig. 1b) is defined by East-West trending normal faults positioned approximately at the place where the Bóixols thrust was developed later (*Muñoz, 1988; Berástequi et al., 1990; García-Senz, 2002*). The northern boundary of the OB is less well defined because the formation of the Pyrenean Axial Zone has resulted in the erosion of the Jurassic-Cretaceous series in the North. However, close to the Morreres back thrust (Fig. 1b), the Jurassic sequence is much thinner (~150 m thick) at the North of a normal fault system than at the South (~1000 m thick) which provides some favor in positioning the northern boundary at the current back thrust (*García-Senz, 2002*). We

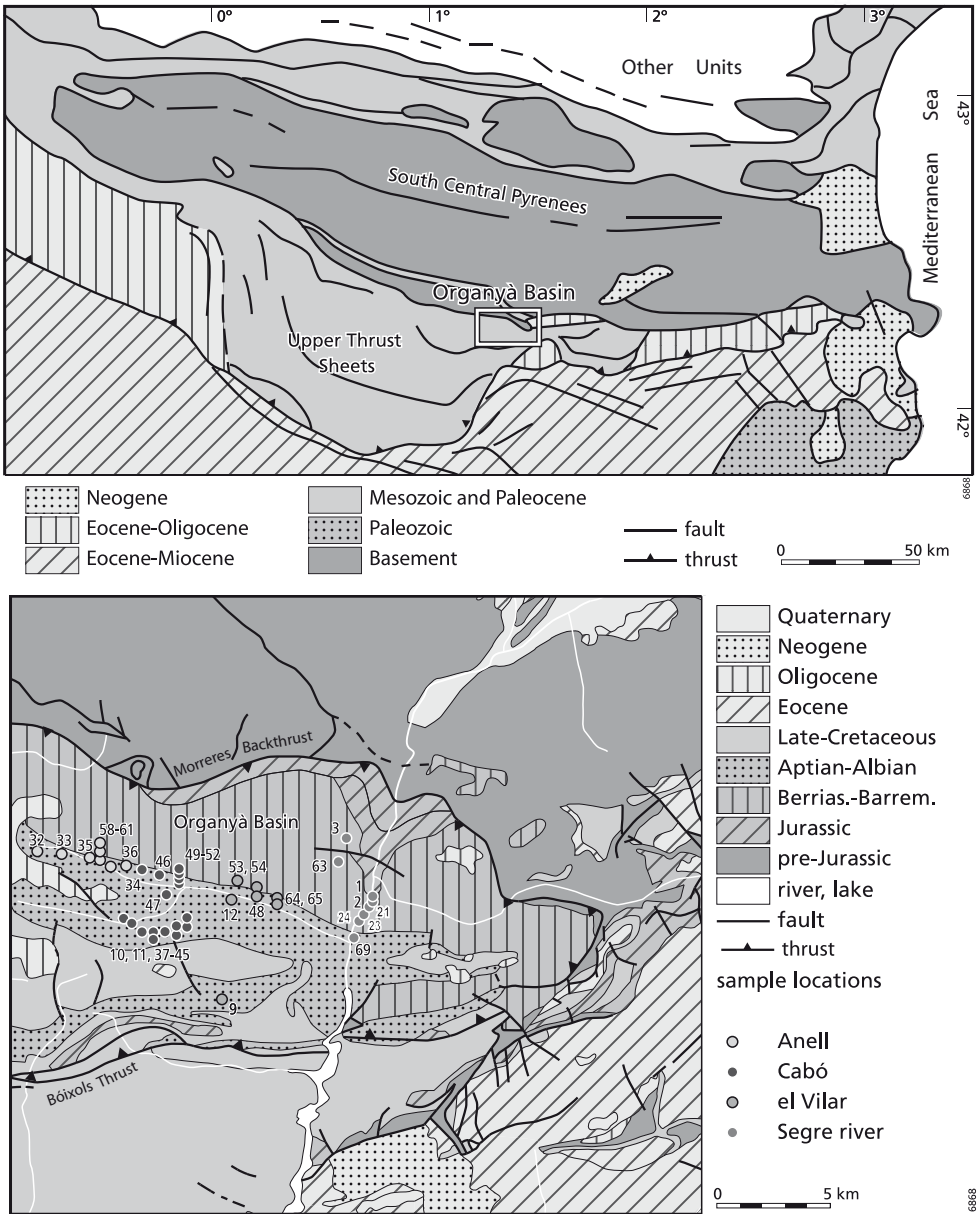

Figure 1 (a) Simplified geological map of the study area. The squared area shows the location of figure (b). (b) Schematized geological map of the Organyà Basin (OB). Dots show sample locations, covering the whole basin. From West to East, four transects can be composed, named after nearby villages: Anell transect, Cabó transect, el Vilar transect, and Segre River transect.

briefly summarize the main aspects of the geological history before describing the formations in the OB.

2.1 Extension

From Late Jurassic to Early Cretaceous times, northern Iberia was mainly covered by a shallow sea, which formed a seaway from the (proto) Atlantic to the Tethys Oceans (e.g. *Vera et al., 2001*). In the Mesozoic, up through the Tithonian-Berriasian, extension is interpreted to be due to flexural subsidence, also referred to as pre-rift phase (in the nomenclature of *Nottvedt et al., 1995*) (*García-Senz, 2002; Gibbons and Moreno, 2002*). Sedimentation was characterized by platform carbonates, both during the Tithonian and the Berriasian-Barremian. Terrigenous input from the south (Ebro block) has always been minor, also on the Montsec platform, south of the OB. The Jurassic-Cretaceous (J/K) boundary is characterized by regression and submergence above sea level (*García-Senz, 2002*); karstification phenomena developed in the limestones. The series was submerged diachronically during the Early Cretaceous.

The Organyà Basin was the largest depocenter during Early Cretaceous times accumulating up to 4850 meters of sediments. In the OB, the syn-rift phase lasted from the Berriasian through the Albian and the post-rift phase comprises the Cenomanian and younger sediments. The OB is in a sense slightly atypical since sedimentation stopped some time before the actual inversion took place (p 281 after *Vergés and García-Senz, 2001; García-Senz, 2002*). There was even substantial erosion in the eastern part of the OB. During the active subsidence of the OB, the region to the south, consisting of the present-day Montsec and Sierras Marginales thrust sheets, always stayed shallow, with Lower Cretaceous sediments with a total thickness of only 400 m.

During Aptian age, accelerating subsidence was caused by the creation of extensional faults in the south. The lithology changed from limestone to marl (Prada Fm vs. Cabó and Senyús Fms). In the Cabó area in the OB, the total thickness of marls is around 2900 m. However, more to the west, it was only ~1100 – 1200 m. During the Albian, sedimentation in the western part of the OB continued, while in its eastern part sedimentation stopped and the sequence was uplifted and eroded. Consequently, the depocenter, which used to be in the Cabó area, moved to the west of the basin. Albian and Cenomanian sedimentation continued in the west. The upper Cenomanian Santa Fè Fm, which covered the entire Pyrenean area, marks the end of the extensional period. It was deposited in so called post-rift conditions (*García-Senz, 2002*).

2.2 Compression

The compression of the Pyrenees began in the upper Cenomanian (*Gibbons and Moreno, 2002*). In the south of the OB, the extensional fault system inverted to a compressional fault system, and became the Bóixols thrust. During the Alpine compressional phase that resulted in the formation of the present-day Pyrenees, the Bóixols thrust sheet was thrusted southward upon the Montsec sheet, that in turn thrusted on the Sierras Marginales sheet that thrusted on the Ebro Basin foreland. This process occurred in a piggy back fashion. The final shortening was accommodated by the Morreres back thrust in the North of the OB (Fig. 1). The dominant structural feature of the OB is an east-west asymmetric syncline, the Santa Fè syncline (*Bernaus et al., 2003*) (Fig. 1b).

The inversion from extension to compression started in the Cenomanian. During Upper Santonian and Maastrichtian compression was most intense, although still considered to be of the 'mild inversion' style as in other Pyrenean basins (*García-Senz, 2002*). Triassic evaporites served as main decollement zone. The latest Cretaceous compression is typified by large folds and associated thrust sheets. During the extensional phase the OB was tilted towards the South along a fault system interpreted to be a basement fault (*García-Senz, 2002*). The compressional direction is somewhat oblique with respect to the earlier extensional system. The OB has undergone a small amount of longitudinal shortening with an orientation oblique to the extensional master faults (*García-Senz, 2002*).

2.3 Geological formations in Organyà Basin

Nine formations (Fig. 2) are distinguished in the Cretaceous sediments from the OB (*Berástequi et al., 1990; García-Senz, 2002; Bernaus et al., 2003*).

Tres Ponts Group (Pont de la Torre, Barranc de la Fontanella, Hostal Nou, Prada Fms)

In the OB, the Lower Cretaceous (Berriasian through Barremian-Lower Aptian) platform carbonates are referred to as Tres Ponts Group (Grupo de Tres Ponts) by García-Senz (*2002*). The ages of the specific formations are mainly derived from biostratigraphy (ammonites, planktonic and benthic foraminifers) recently detailed by Bernaus (*2000*), Bernaus et al. (*1999; 2000*) and Becker (*1999*). The lowermost Cretaceous is represented by the Pont de la Torre limestone breccias (~200m thickness, Tithonian-Berriasian) and the Barranc de la Fontanella limestones (~200m-300m thickness, Berriasian). These are capped by the Hostal Nou Formation (~200m thickness, Berriasian-Valanginian), whereas the topmost limestone formation comprises the Prada Formation (~1125m-460m thickness, Barremian-lowermost Aptian) (*García-Senz, 2002*). Several subunits are recognized in the Prada Formations.

Cabó – Lluçà marls

There are four marl Formations distinguished by García-Senz (*2002*), in stratigraphic order: the Cabó marls (~950m thickness, lower Aptian, most of the Bedoulian in the regional West-European nomenclature), the Senyús marls (~775m thickness, middle Aptian, most of the Gargasian in the regional West-European nomenclature), the Font Bordonera marls (~530m thickness, Upper Aptian, most of the Clansayesian in the regional West-European nomenclature) and the Lluçà marls (Uppermost Aptian, Clansayesian – Albian). Sedimentation kept up with subsidence: throughout marl deposition shallow marine conditions prevailed and occasionally depositional hiatus are recognized. It should be mentioned that in the southern margin of the OB the marls grade into platform carbonates. Towards the West the Senyús marls grade toward platform carbonates whereas the Lluçà marls show an approximately homogeneous lithology throughout the entire the OB.

Santa Fè platform carbonates

The Santa Fè and other post-rift sediments cover a large area: from the Ebro block to within SW France. Before the deposition of the Santa Fè Fm. in a post-rift setting, substantial erosion of the series has occurred in particular east of Organyà where ~600m has been eroded before the Cenomanian platform carbonates were deposited. The amount of erosion rapidly thins in southerly and westerly direction. In the Cabó area about 1500m was eroded and at the actual Santa Fè synclinal axis about 500 m. In the westernmost part sedimentation is more or less continuous up through the Cenomanian. The uplift and erosion in the OB before the Cenomanian Santa Fè Fm is earlier than this post-rifting phase (*García-Senz, 2002, p 276*) and hence should not be considered post-rift. Post-rift sedimentation until the Early Santonian and covered the entire Pyrenean region. In the eastern part of the OB the Prada Fm dips 106-33 S after restoring the Santa Fè Fm to the horizontal (*García-Senz, 2002, p 103*). The amount of angular unconformity decreases towards the West.

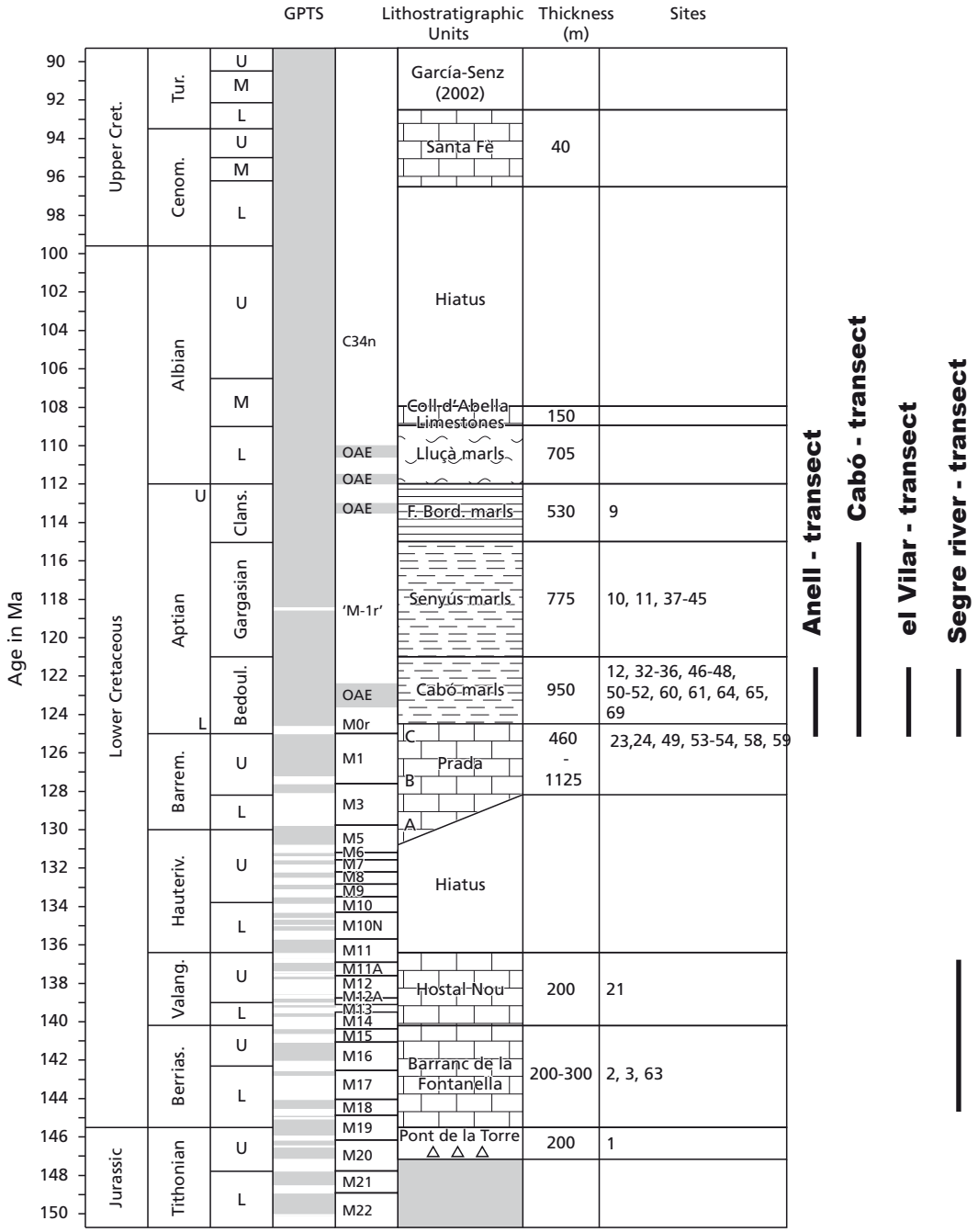

Figure 2 Stratigraphic column of the Organyà Basin with the most recent geological time scale and geomagnetic polarity time scale (GPTS) after Gradstein et al. (2004). Grey indicates normal polarity, white reversed. Lithostratigraphic units and formation thicknesses are after García-Senz (2002). Paleomagnetic sample sites are grouped per formation.

3 Sampling and methods

To test the burial and lithology related remagnetization scenarios in the OB, we sampled four transects (total new 41 sites, 420 cores) by a portable gasoline-powered drill during three fieldworks (Table 1, Figure 2). From west to east, they were named: Anell, Cabó, el Vilar, and Segre river transects. Most of the sites have 8 standard-sized cores. In the laboratory, they were cut into standard specimens of 2.2 cm in length.

To identify the magnetic carriers, 28 hysteresis loops and 29 isothermal remanent magnetization (IRM) curves were measured from the different formations. Hysteresis loops were measured with an alternating gradient magnetometer (AGM, Princeton Measurements Corporation, noise level $2\times10^{-9}Am^2$) also referred to as MicroMag. Sample chips of 30-50 mg were mounted on a so-called P1 phenolic probe. The maximum applied field was 2T. Acquisition curves of the IRM were determined with a PM4 pulse magnetizer with 27 field steps up to 2.2 T, equidistant on a log-scale. They were measured with a 2G 755 DC SQUID magnetometer (noise level 3×10^{-12} Am^2). To analyze the IRM acquisition curves, the cumulative log-Gaussian (CLG) approach was used to identify the different coercivity components with the software developed by Kruiver et al. (*2001*). This allows fitting of symmetric distributions in the log field space. Each coercivity component in magnetic mineral assemblages is characterized by three free parameters: SIRM amount (M_{rs}), the field at which half of the SIRM is reached ($B_{1/2}$), and the standard deviation of the logarithmic distribution (DP). Measured IRM data are fitted using three different plots: the linear acquisition plot (LAP), gradient acquisition plot (GAP) and standardized acquisition plot (SAP). In this paper

Table 1 Paleomagnetic sites with GPS coordinates (Georeference: ED50), formation, age, lithology and bedding attitude. L = limestone, M = marl, ML = marly limestone.

Site	GPS (E)	GPS (N)	Unit / Formation	Age	Lithology	Strike / Dip
OR9	356638	4673823	Font Bordonera	Aptian	dark M	267 / 45
OR10	353783	4676608	Senyús	Aptian	dark M	103 / 47
OR11	354627	4676651	Senyús	Aptian	dark M	104 / 65
OR37	353474	4676149	Senyús	Aptian	dark M&ML	107 / 39
OR38	353737	4676146	Senyús	Aptian	dark M	94 / 45
OR39	353783	4676608	Senyús	Aptian	dark M	105 / 46
OR40	353688	4676609	Senyús	Aptian	dark M	108 / 43
OR41	353678	4676520	Senyús	Aptian	dark M	105 / 51
OR42	353673	4676502	Senyús	Aptian	dark M	106 / 45
OR43	354225	4676657	Senyús	Aptian	dark M	96 / 41
OR44	354627	4676651	Senyús	Aptian	dark M	105 / 48
OR45	354604	4676634	Senyús	Aptian	dark M	103 / 53
OR12	356597	4677761	Cabó	Aptian	dark M	109 / 44
OR32	350548	4679374	Cabó	Aptian	dark M	110 / 45
OR33	350608	4679420	Cabó	Aptian	dark M	111 / 44
OR34	352887	4678412	Cabó	Aptian	dark M	96 / 50
OR35	350663	4679435	Cabó	Aptian	dark M	107 / 50
OR36	352279	4679145	Cabó	Aptian	dark M	98 / 47
OR46	353738	4678324	Cabó	Aptian	dark M	104 / 48
OR47	354093	4677797	Cabó	Aptian	dark M	101 / 39
OR48	356981	4677654	Cabó	Aptian	dark M&ML	97 / 41
OR50	355024	4678049	Cabó	Aptian	dark M	114 / 48
OR51	355021	4678088	Cabó	Aptian	dark M	114 / 51
OR52	354979	4678226	Cabó	Aptian	dark M	111 / 43
OR60	351232	4679751	Cabó	Aptian	dark M	105 / 48
OR61	351293	4679114	Cabó	Aptian	dark M	95 / 45
OR64	358140	4677510	Cabó	Aptian	dark M	106 / 50
OR65	358088	4677405	Cabó	Aptian	dark M	109 / 49
OR69	362557	4676084	Cabó	Aptian	dark M	103 / 51
OR23	362857	4676473	Prada C	Barremian-Aptian	dark L	100 / 60
OR24	362775	4676376	Prada C	Barremian-Aptian	dark L	120 / 67
OR49	354971	4678686	Prada C	Barremian-Aptian	dark L	111 / 57
OR53	356794	4678016	Prada C	Barremian-Aptian	dark L	109 / 42
OR54	357415	4677963	Prada C	Barremian-Aptian	dark L	89 / 46
OR58	351233	4679986	Prada C	Barremian-Aptian	dark L	116 / 50
OR59	351326	4679914	Prada C	Barremian-Aptian	dark L	118 / 54
OR21	363517	4677816	Hostal Nou	Valanginian	dark L	116 / 51
OR1	363464	4678605	Barranc de la Fontanella	Berriasian	light L	106 / 46
OR2	363329	4678296	Barranc de la Fontanella	Berriasian	dark L	97 / 55
OR3	361263	4679885	Barranc de la Fontanella	Berriasian	dark L	97 / 56
OR63	361298	4679700	Barranc de la Fontanella	Barremian	dark L	91 / 57

we mainly use LAPs and GAPs to determine the coercivity components of the OB samples.

To decide on an optimal NRM demagnetization procedure, pilot series were stepwise progressively demagnetized, either thermally (100°C, 200°C, 240°C, 280°C, 300°C, 320°C, 350°C, 380°C, 410°C, 440°C, 460°C, 480°C, 500°C and 520°C) or by alternating field (AF) (5mT, 10mT, 15mT, 20mT, 25mT, 30mT, 40mT, 50mT, 60mT, 70mT, 80mT, 90mT and 100mT) demagnetization. It appeared that the viscous NRM component is best removed by thermal demagnetization. However, thermal demagnetization at temperatures above 400°C often resulted in erratic demagnetization trajectories because of chemical alteration of the samples. The susceptibility at room temperature after each thermal demagnetization step was also measured for a pilot series and showed a dramatic increase after 400°C. This indicated that new magnetite was formed by oxidation of other iron-bearing minerals, possibly pyrite.

AF demagnetization yielded very well defined linear demagnetization paths. However, in marly sediments, surficial oxidation of magnetite particles as a consequence of incipient weathering enhances their coercivity which complicates the separation into secondary and primary components (*Van Velzen and Zijderveld, 1995*). These authors show that upon heating to 150°C the coercivities are reduced and that secondary and primary components are better resolved. The oxidized surface layer is either detached from the bulk of particles or the oxidation gradient in the particles is substantially reduced because of much higher diffusion rates at elevated temperature. The viscous laboratory component (VRM) can be removed by heating to similar temperatures. To take advantage of thermal removal of the VRM and to avoid interference of potentially oxidized rims of magnetic particles, limestones were thermally demagnetized to 150°C and marls up to 210°C after which the remainder of the NRM is AF demagnetized in fields up to 100 mT. During the thermal treatment, potentially present goethite is also demagnetized (Néel temperature 120 °C) (*Dekkers, 1989*). Directions derived from the combined thermal plus AF demagnetization approach were indistinguishable from those derived by thermal demagnetization only. Application of AF without heating to the indicated temperatures, yields poorly defined primary components at demagnetization levels > 70-80 mT.

Remanent magnetization during the thermal demagnetization was measured with the 2G Enterprises DC-SQUID magnetometer and the susceptibility during thermal demagnetization was measured with an AGICO KLY-2 susceptometer (noise level $4x10^{-8}$ SI). AF demagnetization was done with an in-house developed robotized sample handler (*Mullender et al., 2005*) attached to a horizontal pass-through 2G Enterprises SQUID magnetometer (noise level 1 × 10^{-12} Am^2) hosted in the magnetically shielded room in the laboratory (residual field < 200 nT). 96 samples can be AF demagnetized in ~60 hours without operator interference. The standard size cylindrical samples are mounted into dedicated perspex cubes (30 mm edge, magnetic moment << 50 pAm^2) that are magnetically cleaned before in 110 mT AF. These cubes are positioned in twelve rows of eight on a sample plateau. For AF demagnetization they are loaded per row (of eight cubes) on the magnetometer tray and processed fully automatically. The robot protocol allows sample measurement in multiple positions, which is mandatory for getting meaningful results from the relatively weak samples under investigation (Fig. 3a-d).

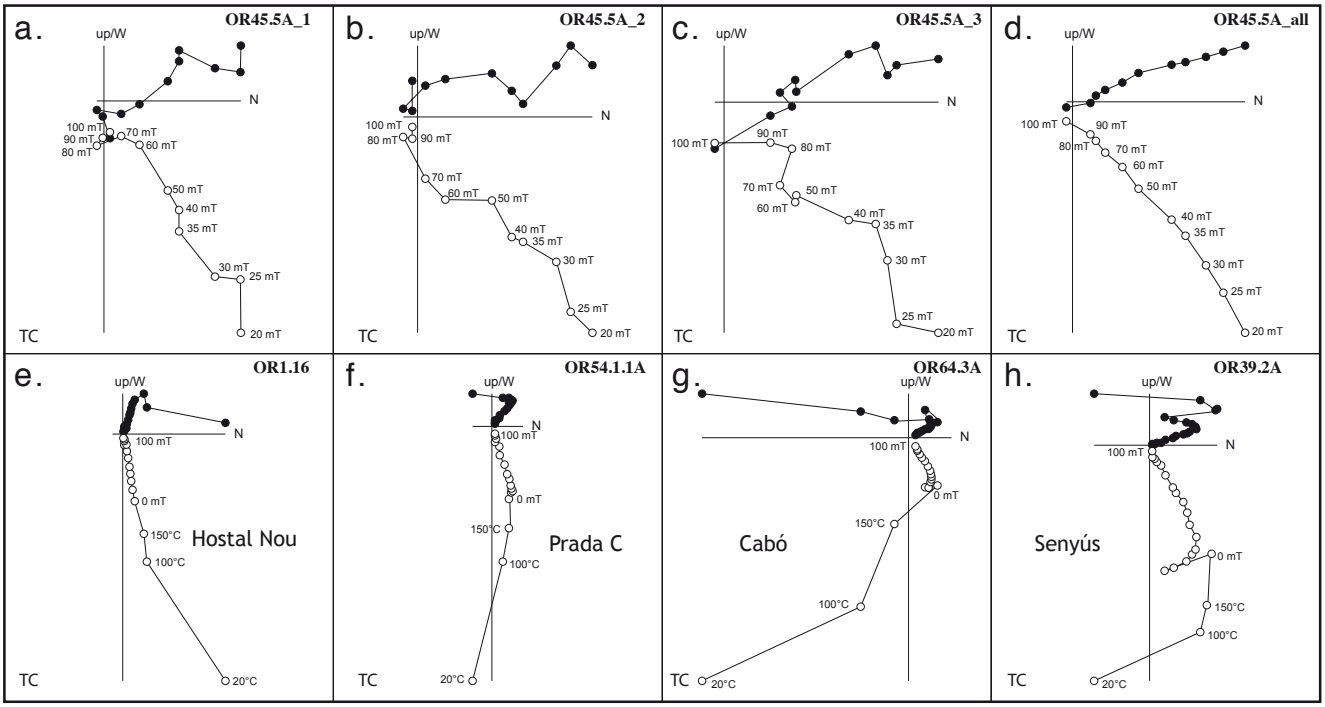

Figure 3 Zijderveld diagrams after tectonic correction (TC), closed (open) circles indicate the projection on the horizontal (vertical) plane. Panels a-d show an example of robotized processing (specimen OR45.5A): the three single position (x, y, z) and the combined '3 position' measurement. Note the "superior behavior" shown in the latter. Panels 3e-h show typical Zijderveld diagrams from the different formations. The Barranc de la Fontanella Formation shows similar demagnetization characteristics as the Hostal Nou Formation.

For the present investigation, the so-called "3 position" protocol has been applied throughout. Fig. 3a-d shows an example of a Zijderveld diagram of each single position ('x', 'y', and 'z'; position 'y' is obtained by 180° rotation of position 'x' around the vertical axis, position 'z' is obtained by rotating position 'y' 180° around the horizontal axis parallel to the magnetometer axis) and the combined three-position result. NRM intensity ranges from 0.5 mA/m to 50 mA/m rendering variability in the perspex cube contribution insignificant. The NRM components were calculated by principal-component analysis (*Kirschvink, 1980*). On average, the linear segments of the characteristic component are defined based on 8 data points for the AF data (and 4 points for thermal demagnetization only, not shown here).

4 Results

4.1 Rock magnetic properties

Hysteresis loops

Two examples of typical hysteresis loops are shown in Figure 4, they are slope-corrected. The limestones often have a diamagnetic matrix contribution, while the marls have paramagnetic slopes. The matrix contribution was very large in 14 samples; no meaningful ferromagnetic hysteresis loop could be extracted. Most hysteresis loops saturate in fields < 500 mT indicative of dominant low-coercivity minerals. It likely indicates magnetite. Some loops have a small high-coercivity contribution indicating hematite or goethite. After slope correction, 8 loops appear to be wasp-waisted (Fig. 4a) indicative of contrasting coercivities (e.g. *Roberts et al., 1995; Tauxe et al., 1996*). They are not entirely saturated at 500 mT indicating a minor contribution of a high-coercivity mineral (hematite or goethite). The wasp-waistedness of the hysteresis loops (Fig. 4a) is plausibly explained by a contribution of superparamagnetic magnetite particles given the low applied fields at which the wasp-waistedness appears. This is in agreement with the fairly large decay of the NRM at low temperatures. The 6 non-wasp-waisted loops (Fig. 4b) indicate

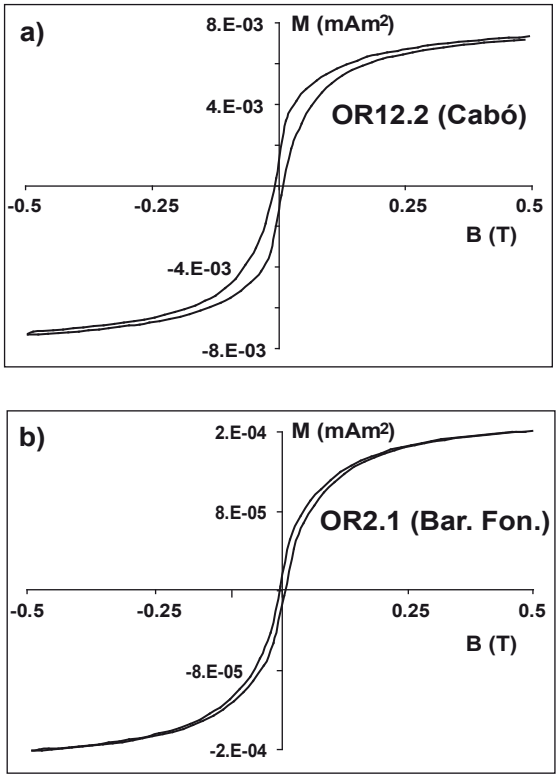

Figure 4 Typical magnetic hysteresis loops after slope correction. The magnetic field B (T) is plotted versus magnetization M (mAm²). (a) shows a sample from the Cabó Formation, marls with paramagnetic slope, unremagnetized. (b) shows a sample from the Barranc de la Fontanella Formation, limestones with diamagnetic slope, and remagnetized.

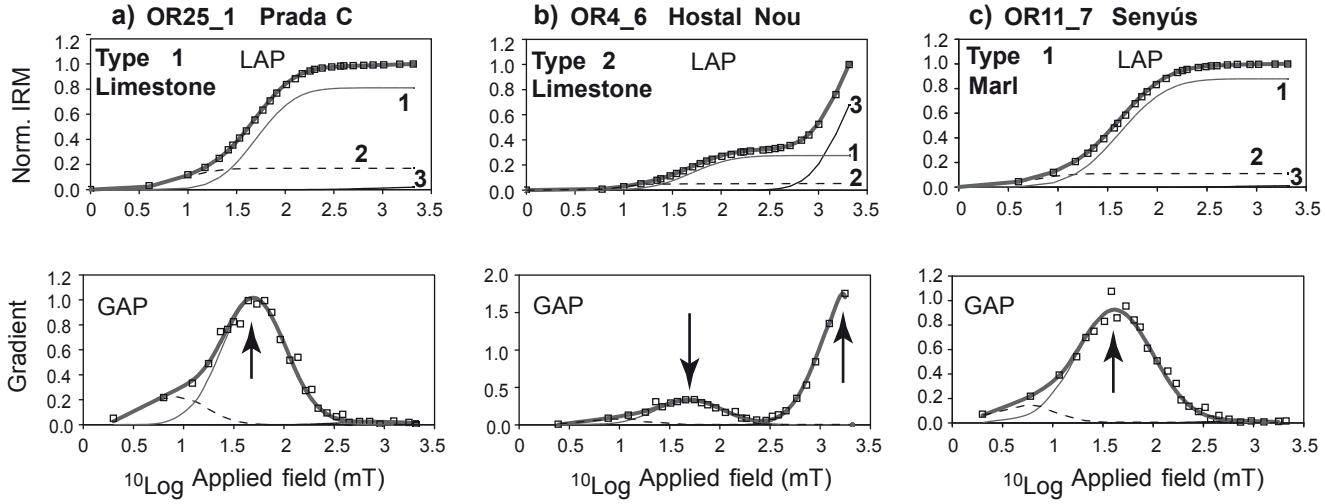

Figure 5 Examples of component analysis of IRM acquisition curves processed with the cumulative log-Gaussian model (Kruiver et al. 2001). Linear Acquisition Plot (LAP) and Gradient Acquisition Plot (GAP) are shown. a) Normalized IRM acquisition curve of sample OR25_1 (SIRM 0.92 A/m) from the Prada C Formation. b) Normalized IRM acquisition curve of sample OR4_6 (SIRM 1.53 A/m; Hostal Nou Formation). c) Normalized IRM acquisition curve of samples OR11_7 (SIRM 1.12 A/m) from the Senyús Formation. Open squares represent measured data. Thick line shows the sum of the all components. Thin grey line represents the component 1. Dark short-dashed line represents component 2. Solid dark line represents component 3. For clarity the component numbers have been added as well.

pseudo-single-domain particles. The (remagnetized) limestone samples broadly range in coercivity between 5 to 20 mT, mainly between 5 and 7 mT. The marls appear more homogeneous, their coercivity ranges between 5 and 10 mT.

IRM component analysis

To supplement the hysteresis loop measurements, IRM component analysis was done as well. Three components were used to fit the IRM acquisition curves in the CLG approach (*Kruiver et al., 2001*). We distinguish two types of IRM curves in the limestones, and one type of IRM curve in the marls. Type one curves (Figure 5a and 5c) occurred in both limestones and marls. In this type of IRM curve, component 1 constitutes 81% of the saturation IRM (SIRM). Component 2 contributes 17% to the SIRM; component 3 has only 2% and is not considered further. The dominant component 1 has a $B_{1/2}$ of 50 mT, the softer component 2 ($B_{1/2}$ = 8.3 mT) is likely due to thermal activation (*Heslop et al., 2004*), magnetic interaction is not important given the low concentration for magnetic material in these samples. This concurs with SP particles as determined from the hysteresis loops. The DP of three components is: 0.32 for component 1, 0.30 for component 2, and 0.38 for component 3. The dominant component in this type of IRM curve is interpreted to be magnetite.

The other type of curves (Figure 5b), only found in the limestones, shows one low-coercivity component 1 contributing 17% to the SIRM, and a dominant high-coercivity component 3 which contributes 80% to the SIRM. Component 2, a very low field component, only constitutes 3% of the SIRM. In all curves component 2 is only required to fit the skewed-to-the-left distribution of component 1; it is not given physical meaning other than being the result of thermally activated component 1 particles. Again, $B_{1/2}$ of component 1 is around 50 mT, is almost same value as the one from the low-coercivity component 1 of type 1. However for the component 3, $B_{1/2}$ is much higher, around 2 T. The parameter DP of the two dominant components is 0.33 for component 1 and 0.30 for component 3. This is quite similar to those of type one. In the limestone samples, a high-coercivity component is present interpreted to be goethite while the other two low-coercivity components are magnetite (similar to type one).

The limestone samples have their $B_{1/2}$ ranging from ~30 to ~64 mT (N = 24, average: 47.4 mT, standard deviation: 8.4 mT) for component 1 interpreted to be magnetite, and 1000 – 3200 mT for component 3 (N = 24, average: 1552 mT, standard deviation: 557 mT) interpreted to be goethite. $B_{1/2}$ values are too high for hematite that typically ranges from c. 300-800 mT (*Kruiver and Passier, 2001*). Meanwhile, for the marl samples, the $B_{1/2}$ range are more homogeneous ranging from 40 to 55 mT for component 1 (N = 5, average: 47.2 mT, standard deviation: 5.0 mT), and from 300 to 1000 mT for component 3 (N = 5, average: 610 mT, standard deviation: 250 mT). Component 1 is again magnetite and component 3 could be either hematite or, less likely, very fine-grained goethite. It should be realized, however, that its (magnetic) presence in small amounts precludes a precise characterization.

Limestone DPs for component 1 range from ~0.25 to ~0.40 (N = 24, average: 0.334, standard deviation: 0.055). Data for component 3 are respectively N = 24, range 0.24-0.39, average: 0.312, standard deviation: 0.081. For the marls component 1 data are N = 5, range 0.34-0.38, average: 0.351, standard deviation: 0.017 and component 3 data are N = 5, range 0.24-0.38, average: 0.316, standard deviation: 0.062. $B_{1/2}$ and DP values of component 1 are compatible with other data for detrital magnetite (*Kruiver and Passier, 2001; Kruiver et al., 2003*).

4.2 NRM demagnetization diagrams

In general, marls have a higher NRM intensity (~2 to ~50 mA/m) than limestones (~0.5 to ~3 mA/m). Mainly the combined thermal and AF demagnetization treatment was used for the NRM component analysis. The directions of viscous components were fairly random for all formations as can be seen from the Zijderveld diagrams (Figure 3e-h). Samples show generally only one high field component, between 30 mT to 100 mT. No gyroremanent magnetization was observed when demagnetizing, except in some samples from the lowest Cabó Fm site (site 69) in the Segre River transect.

Figure 3e-h shows representative Zijderveld diagrams of each formation. After tectonic correction, the declination of the ChRM in the limestone formations (Hostal Nou and Prada C) (Figure 3e, f) is more westerly than that of the marl formations (Cabó and Senyús) (Figure 3g, h). The Hostal Nou formation (Figure 3e) has a ChRM declination around 290° and inclination around 57°, while the declination of the of the top part of the Prada Formation, Prada C, (Figure 3f) is around 315° with an inclination of c. 60°. There was no significant declination and inclination difference between the two marl formations (Cabó and Senyús). The common declination is c. 335° and inclination is around 55°. Table 2 gives the paleomagnetic results, both in situ and tilt corrected, from all sites in the OB. They can be conveniently grouped into four transects, from West to East: Anell, Cabó, el Vilar, and Segre river transects.

In the westernmost Anell transect, the Prada C and Cabó formations have almost the same declination after tectonic correction (328.9° for Prada C with α_{95} = 6.7 and 326.1° for Cabó with α_{95} = 4). Furthermore, the Prada C site has a somewhat suspect steep inclination of around 67° with α_{95} = 6.7°. In the Cabó Formation, the mean inclination of 5 sites is less steep than that in the Prada C formation, c. 58.5° with α_{95} = 4° after tectonic correction.

The Cabó transect is located nearby the village of Cabó, to the east of the Anell transect. It contains three Formations: Prada C, Cabó and Senyús. The mean declination and inclination of the Prada C and Cabó Formations are virtually identical after tectonic correction (declination/inclination: 316.1°/60.1° with α_{95} = 7.0° versus 325.8°/57.3° with α_{95} = 3.6°). The Cabó Formation is also indistinguishable from the mean direction from the Anell transect (326.1°/58.5° with α_{95} = 4°). The mean declination in the Senyús formation is around 334.3° and the inclination is 53.9° with α_{95} = 2°. The limestone site in the Senyús Fm (site 38) in this transect was excluded from the average paleomagnetic direction for the Senyús marls because of the different lithology (349.5°/58.5° with α_{95} = 9.9°). After tectonic correction, the Senyús marls in the Cabó transect have a shallower inclination compared to the Prada C and Cabó Fms.

Table 2 Paleomagnetic data before and after tectonic correction. N = number of the samples contributing to the mean from each site, n = number of measured samples from each site, Dg = declination in geographic coordinates, Ig = inclination in geographic coordinates, Ds = declination in stratigraphic coordinates, Is = inclination in stratigraphic coordinates. κ and α_{95} are the statistical parameters. For site OR1 only the results from strata above the breccia are included. Sites OR32b, OR38b and 65b are excluded from mean direction calculations. J21, J23 and J31 are taken from Dinanès-Turell and García-Senz (2000).

Site	Unit/Formation	N/n	In Situ				Tectonic Corrected			
			Dg	Ig	κ	α_{95}	Ds	Is	κ	α_{95}
Anell-transect										
OR58	Prada C	7/8	4.5	24.6	52.4	8.4	330.0	66.3	52.4	8.4
OR59	Prada C	2/3	8.5	26.2	-	-	324.3	70.8	-	-
Mean	**Prada C**	**9/11**	**5.4**	**25.0**	**61.9**	**6.6**	**328.9**	**67.3**	**60.9**	**6.7**
OR60	Cabó	6/7	8.4	21.4	56.5	8.4	341.4	58.0	52.4	9.3
OR61	Cabó	8/8	350.1	20.5	84.2	6.1	333.5	62.7	84.2	6.1
OR33	Cabó	5/5	342.1	17.7	79.9	8.6	319.5	47.3	79.9	8.6
OR32b	Cabó	10/11	5.4	17.0	114.7	4.8	353.0	59.0	126.3	4.3
OR35+36	Cabó	9/11	343.5	21.7	92.8	5.4	313.4	60.1	127.0	5.4
Mean	**Cabó**	**28/31**	**350.4**	**20.9**	**40.2**	**4.4**	**326.1**	**58.5**	**48.5**	**4.0**
Cabó-transect										
OR49	**Prada C**	**7/8**	**342.3**	**25.2**	**75.7**	**7.0**	**316.1**	**60.1**	**75.7**	**7.0**
OR34	Cabó	7/8	340.6	26.5	35.5	10.3	300.2	64.8	35.5	10.3
OR46	Cabó	9/9	347.3	16.1	147.3	4.3	324.5	55.5	147.3	4.3
OR51	Cabó	8/8	354.7	18.1	24.9	11.3	325.0	56.9	24.9	11.3
OR50	Cabó	9/9	1.3	18.0	23.6	10.8	338.6	59.1	23.6	10.8
OR52	Cabó	8/9	356.2	18.8	63.6	7.0	336.3	55.3	63.6	7.0
OR47	Cabó	11/11	341.5	20.5	34.0	7.9	322.7	52.0	34.0	7.9
Mean	**Cabó**	**52/55**	**350.2**	**19.7**	**29.5**	**3.7**	**325.8**	**57.3**	**31.4**	**3.6**
OR10	Senyús	11/13	351.7	18.8	672.9	1.8	337.2	59.4	672.9	1.8
OR11	Senyús	12/13	347.6	13.5	76.6	5.6	330.7	51.2	55.3	5.9
OR37	Senyús	12/14	352.7	16.7	50.5	6.2	338.4	50.8	50.5	6.2
OR38b	Senyús	8/9	356.3	14.2	32.2	9.9	349.5	58.5	32.2	9.9
OR39	Senyús	5/7	357.8	15.4	420.5	3.7	337.3	59.8	117.5	6.2
OR40	Senyús	4/4	346.6	11.6	325.6	5.1	330.6	45.9	324.2	5.1
OR41	Senyús	4/7	2.4	8.9	308.4	7.0	338.2	60.5	29.4	17.2
OR42	Senyús	8/11	353.3	12.9	109.5	5.3	338.0	52.3	109.7	5.3
OR43	Senyús	12/14	346.1	22.9	116.3	4.0	327.7	59.7	116.1	4.0
OR44	Senyús	7/8	343.5	8.8	49.0	8.7	326.1	46.7	49.1	8.7
OR45	Senyús	7/8	348.8	2.6	111.5	5.7	334.3	49.0	111.3	5.7
Mean	**Senyús**	**80/99**	**350.4**	**14.3**	**55.7**	**2.1**	**334.3**	**53.9**	**66.2**	**2.0**
el Vilar-transect										
OR53	Prada C	6/9	350.4	30.1	67.3	8.2	318.0	61.7	67.3	8.2
OR54	Prada C	4/8	333.8	22.5	73.3	10.8	306.9	60.1	73.3	10.8
Mean	**Prada C**	**10/17**	**343.5**	**27.5**	**41.8**	**7.6**	**313.4**	**61.2**	**71.1**	**5.8**
OR12	Cabó	6/8	353.8	18.4	166.7	5.2	333.5	55.4	166.7	5.2
OR48	Cabó	7/10	340.6	15.7	21.9	13.2	324.8	50.2	21.9	13.2
OR64	Cabó	9/9	348.3	12.5	60.1	6.7	327.2	52.9	60.1	6.7
OR65b	Cabó	7/8	7.8	24.6	24.7	12.4	0.1	72.2	17.3	13.7
Mean	**Cabó**	**22/27**	**347.4**	**15.2**	**39.2**	**5.0**	**328.0**	**52.8**	**45.2**	**4.7**
OR9	**Font Bordonera**	**8/14**	**138.3**	**82.4**	**158.8**	**4.4**	**4.2**	**50.6**	**156.3**	**4.4**
Segre river-transect										
OR1+J34	Barranc de la Fontanella	12/12	340.1	34.5	59.4	5.7	298.3	55.5	63.7	5.5
OR2+J32	Barranc de la Fontanella	10/10	336.5	33.5	174.9	3.7	280.2	55.7	179.3	3.6
OR3+J33	Barranc de la Fontanella	16/16	340.2	12.9	64.0	4.6	307.7	51.9	64.6	4.6
OR63	Barranc de la Fontanella	8/9	329.6	20.9	26.0	12.1	292.3	58.2	21.7	12.2
Mean	**Barranc de la Fontanella**	**40/47**	**336.6**	**26.0**	**30.9**	**4.1**	**295.8**	**55.9**	**42.0**	**3.5**
OR21+J31	**Hostal Nou**	**20/20**	**341.3**	**31.5**	**87.3**	**3.5**	**278.8**	**54.4**	**70.1**	**3.9**
OR23+J23	Prada C	10/11	346.3	10.0	70.0	5.5	316.4	60.4	66.1	5.7
OR24+J21	Prada C	9/9	358.4	10.7	52.3	7.2	316.9	57.5	52.3	7.2
Mean	**Prada C**	**19/20**	**350.0**	**8.3**	**42.0**	**5.2**	**316.4**	**55.2**	**68.7**	**4.1**
OR69	**Cabó**	**70/71**	**354.4**	**7.3**	**112.6**	**1.6**	**336.6**	**48.6**	**112.6**	**1.6**

In the el Vilar transect, the Font Bordonera formation (1 site) is found in addition to the Prada C (2 sites) and Cabó (4 sites) Fms. After tectonic correction, the declination of the Prada C and Cabó Fms differs c. 15° (313.4° with α_{95} = 5.8° versus 328.0° with α_{95} = 4.7°), their inclination is also quite different (61.2° for Prada C with α_{95} = 5.8° and 52.8° for Cabó with α_{95} = 4.7°). The Font Bordonera formation has a mean declination 4.2° and inclination 50.6° with α_{95} = 4.4°.

In the Segre River transect there are (stratigraphic order) the Barranc de la Fontanella, Hostal Nou, Prada C, and Cabó Formations. From old to young, the declination after tectonic correction is increasing, with 296° (α_{95} = 3.5°) for the Barranc de la Fontanella Fm., 279° for Hostal Nou (α_{95} = 3.9°), 316° for Prada C (α_{95} = 4.1°), and 337° for Cabó (α_{95} = 1.6°). Compared to the declination, the inclination is quite consistent, with 55.9° for Barranc de la Fontanella, 54.4° for Hostal Nou, 55.2° for Prada and 48.6° for Cabó.

All directions have a normal polarity, while the Lower Cretaceous before the Cretaceous Normal Superchron (CNS) should contain many reversed polarity levels. Therefore, the older rocks (primarily Barranc de la Fontanella and Hostal Nou formations) must be remagnetized, having a declination around 279-295°. The Aptian and Albian marls (Cabó and Senyús formations) have a declination of c. 330° and are deposited during the CNS. The declinations fit the expected directions of Iberia (*Dinarès-Turell and García-Senz, 2000*), so they are considered primary (in line with the positive fold test published by Dinarès-Turell and García-Senz, 2000). Prada C is considered somehow 'transitional' between remagnetized and unremagnetized. Together with deviating rock-magnetic properties Dinarès-Turell and García-Senz (*2000*) argue that they are remagnetized,. We conclude that the data of the four transects agree with the results along the Segre river (*Dinarès-Turell and García-Senz, 2000*).

5 Discussion

Figure 6 shows an overview of the paleomagnetic results after tectonic correction. They can be slightly different for the same formations in the different transects. The declination of the Prada C formation in the Anell transect (328.9°) is c. 10° higher than in the Cabó, el Vilar and Segre river transects (316.1°, 313.4° and 316°). For the Cabó formation, the declination in the three westernmost transects is statistically indistinguishable (326.1°, 325.8° and 328.0°). However, the declination of the Segre river transect is higher (336.6°). Inclinations from this formation remain the same in the Anell and Cabó transects (58.5° and 57.5°), then decrease slightly from the el Vilar to Segre River transects (52.8° to 48.6°). Paleoslopes differ in the eastern tip of the OB (*García-Senz, 2002*), one could speculate that the minor changes in inclination are related to paleogeography. When looking at different formations in the same transect, declinations show a geographically

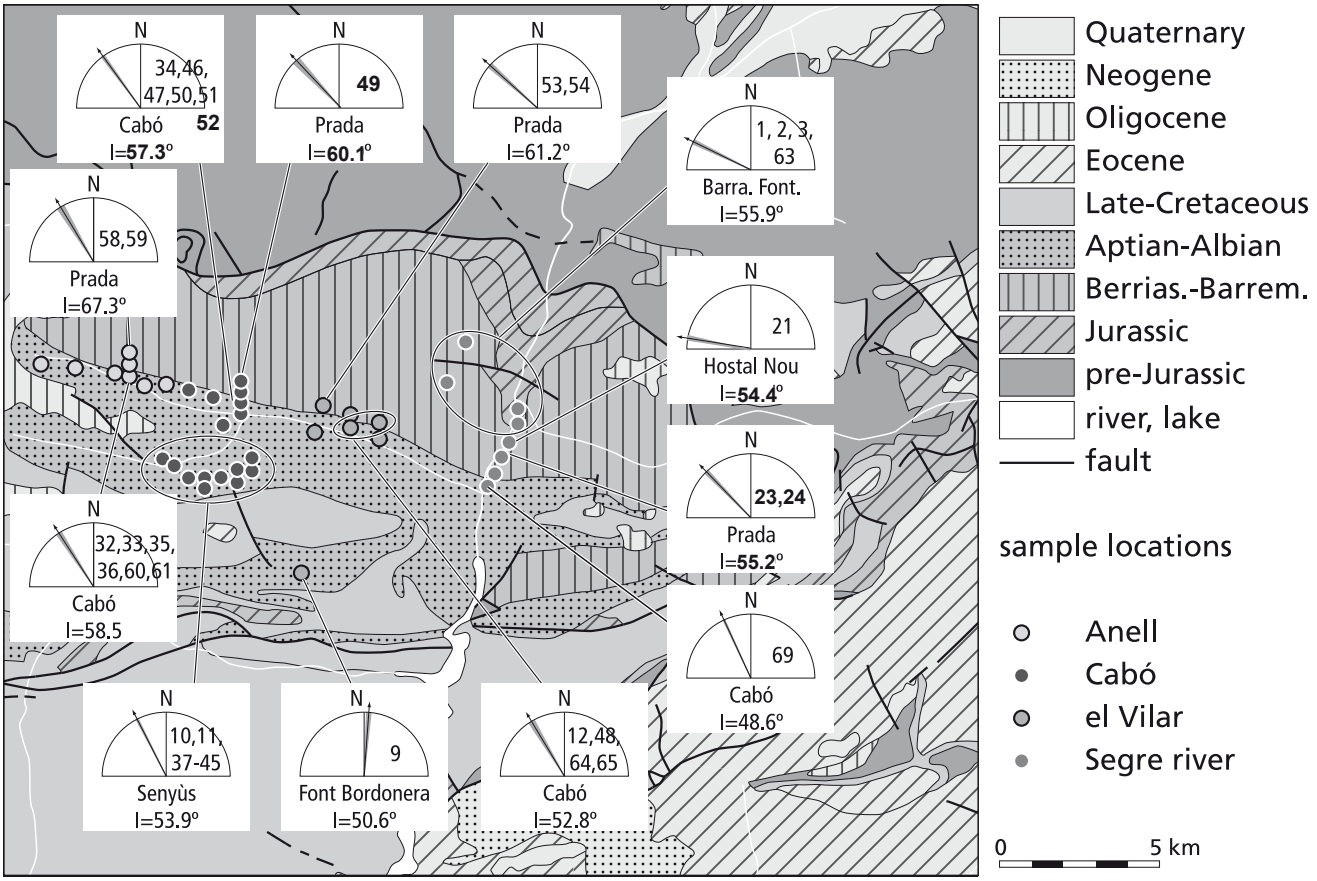

Figure 6 Overview of the paleomagnetic data (after tectonic correction) from the different transects and different formations. In the insets, the arrows show the mean declination per formation in each transect. The shaded areas around the arrow show the α_{95} ranges. Mean inclinations are also shown. Site numbers are written on the right side of the insets. On the map, circles show the groups of averaged sites.

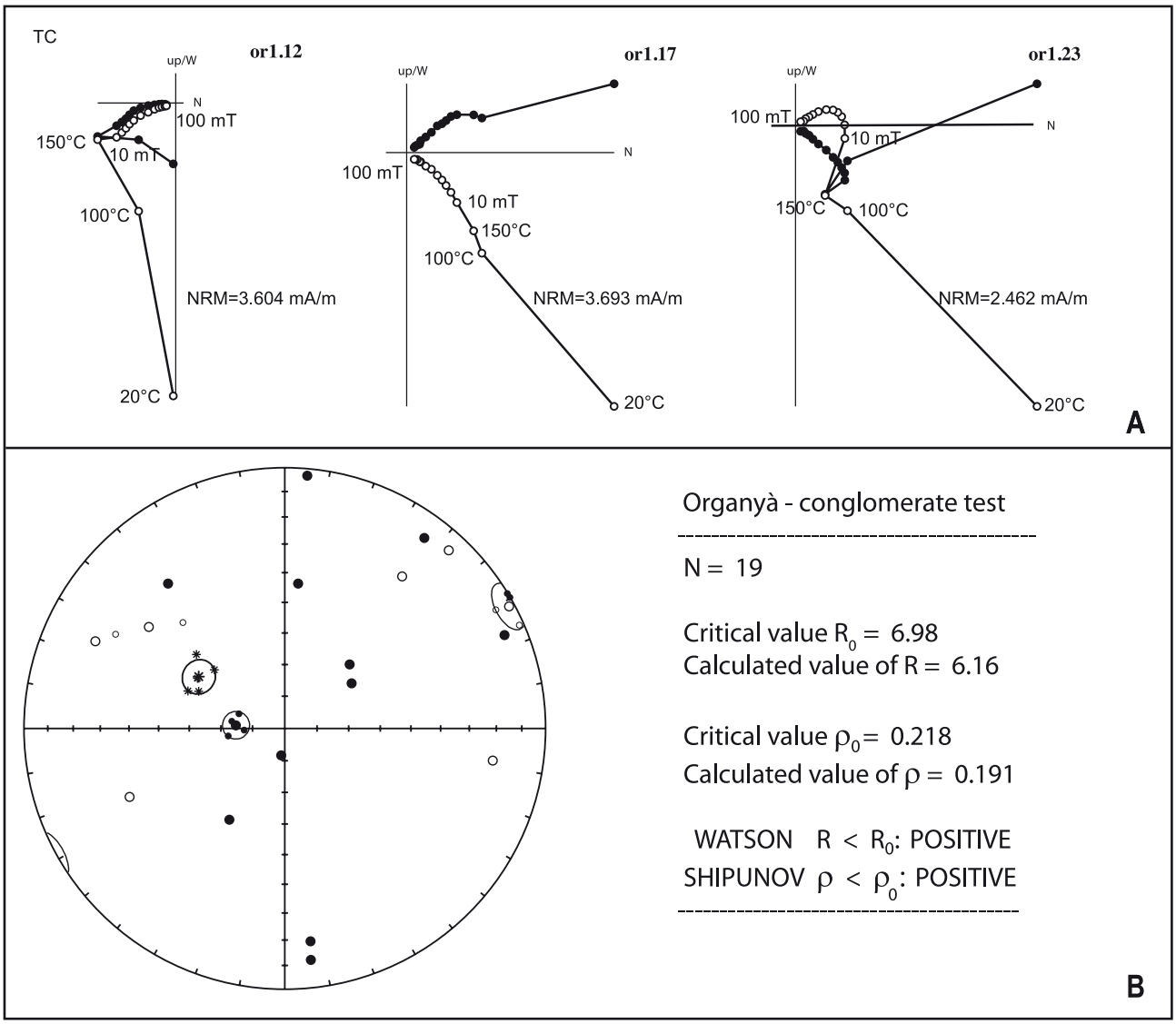

Figure 7 A: Zijderveld diagrams of three selected specimens from the breccia at the J/K boundary after tectonic correction (TC). B: Equal area plot of HT components from site OR1. Data from the same clasts (small symbols) have been averaged. Open/closed dots: up/down-pointing direction from clasts. Asterisks: directions from the Berriasian limestones above the breccia. The statistical results of Shipunov's conglomerate (Shipunov et al., 1998) and Watson's randomness test (Watson, 1956) show that the conglomerate test is positive.

coherent pattern in the Segre River transect. The Barranc de la Fontanella and Hostal Nou formations are remagnetized with a declination around 279-296°, while the Cabó formation has an unremagnetized direction with a declination of c. 337°. The Prada C formation has a declination in between at c. 316°. From the el Vilar transect, it seems that the Font Bordonera Formation is not remagnetized with declination around 4.2°. The Senyús marl Formation also has not been remagnetized, giving the directions with a declination of c. 334°.

At the Barremian-Aptian boundary, in the lowermost Cabó Fm, the topmost reversed polarity zone M0r of the M-sequence is not found. However, this could be because of a small hiatus in the sequence as suggested by García-Senz (*2002*). Site 69, which possessed a gyroremanence possibly caused by greigite, corresponds to the Ocean Anoxic Event 1a with an age of ~124-123 Ma (*Gradstein et al., 2004*). The sulfide magnetic mineralogy would be in line with the anoxic depositional environment.

5.1 'Fault breccia' test

At the Tithonian-Berriasian boundary (site 1), the occurrence of a synsedimentary breccia offered the possibility to constrain the timing of the remagnetization. Nineteen clasts close to a small fault possibly related to the back-thrust system were sampled. Cores were also drilled in the Berriasian strata directly above the brecciated zone.

After demagnetization, the limestones gave very well defined ChRM components (Figure 7A showing results from some clasts). The ChRM from the matrix samples is well grouped with a direction equivalent to the remagnetized direction (298°/56°). Samples from different clasts showed different NRM directions both with and without tilt correction. For all clasts, the ChRM components appear to be randomly distributed (Fig. 7B left). Both Watson's (*Watson, 1956*) and Shipunov's tests (*Shipunov et al., 1998*) for randomness are positive (Watson test R = 6.16 vs. a critical R_0 of 6.98; Shipunov test ρ = 0.191 vs. a critical ρ_0 of 0.218). So, we are left with a rather

puzzling result: clast directions of a conglomerate are random with respect to a remagnetized direction. This can be explained in two ways. Firstly, the Berriasian rocks are remagnetized but that the clasts escaped remagnetization. This is unlikely because their demagnetization behaviour and intensities are comparable. Secondly, which is our preferred interpretation, is that the clasts have moved after the remagnetization which is interpreted to have occurred during faulting related to later compression including the final back-thrusting. Consequently, the remagnetization is older than the back-thrust, which was active around 40 Ma (*Gibbons and Moreno, 2002*).

5.2 Remagnetization mechanism

Several models for remagnetization have been proposed over the last decades (*McCabe and Elmore, 1989; Katz et al., 1998; Katz et al., 2000; Evans and Elmore, 2006*). In the OB thermoviscous resetting of the NRM is highly unlikely as we will argue below. The remagnetized limestones contain goethite, a high coercivity mineral in variable concentrations, while the marls, which have not been remagnetized, are characterized by minute amounts of hematite. On a molar basis these concentrations imply an appreciable amount of goethite or hematite, and these phases are confined to stylolites similar to observations by Evans and Elmore (*2006*). This would suggest that recent weathering is not responsible for goethite, but that the goethite formed during burial diagenesis. Although the burial history of the OB is less well known than that of the Devonian formations studied by Evans and Elmore (*2006*) their geological history bears similarities. In both cases, ~5 km thick sedimentary sequences of limestones and marls were subjected to later shortening by thrusting. Evans and Elmore's (*2006*) model calculations and experimental data from Langmuir (*1971*) limits burial temperatures to ~150˚C. This concurs with the observation of slightly plastically deformed carbonates in thin sections. A temperature of ~150˚C is too low to explain the remagnetization by means of thermoviscous resetting during the Cretaceous long Normal Superchron, the only period with a sufficiently long duration of normal polarity. Also the prograde epidiagenetic setting makes a purely physical process like thermoviscous resetting implausible.

Therefore some form of a chemical remanent magnetization (CRM) must have occurred. The current debate of CRM models focus on the source of the new magnetic minerals. During the rock history, "orogenic" or "basinal" fluids could have passed through the rock pile (e.g. *Oliver, 1986*). Either externally or internally derived fluids could have caused magnetite formation along with mineralization, potassium metasomatism, dedolomitization and dolomitization (*Suk et al., 1990; Brothers et al., 1996; Xu et al., 1998; Elmore et al., 2006*). Meanwhile, burial diagenesis could also play an important role because the transformation of smectite to illite would serve as a source for the iron in CRM magnetite without the need for extensive volumes of fluid (*Elmore et al., 1993; Katz et al., 1998; Katz et al., 2000; Woods et al., 2002; Blumstein et al., 2004*). The potential effects of pressure solution that occurs prominently in limestones (*Passchier and Trouw, 1996*) on remagnetization remain equivocal (e.g. *Evans et al., 2003*).

Along the lines of reasoning developed by Dinarès-Turell and García-Senz (*2000*) we relate remagnetization primarily to burial. If buried sufficiently deep, remagnetization would occur in the lower part of the sequence while its top part would not be remagnetized, nicely in line with our observations. It is difficult to invoke large amounts of basinal fluids in the OB setting. There are no low-temperature ore deposits known and the rocks do not look heavily 'fluidized'. Moreover, Machel and Cavell (*1999*) argue in the case of Paleozoic carbonate basins in the Canadian Rocky Mountain foreland basin that the volume of basinal fluids is too low to be able to account for pervasive remagnetization. This makes a local source plausible, like the smectite to illite transition during burial whereby some iron is liberated that precipitates as magnetite (*Katz et al., 1998; Katz et al., 2000*).

However, the burial depth in the OB varies depending on the position within the basin. The topmost remagnetized formation, the Prada C Formation, yet shows a coherent paleomagnetic behavior in the E-W sense, seemingly independent of burial depth. So, burial alone may not be the sole explanation. A possibility would be that remagnetization is earlier noticed in the limestones because they are simply considerably less magnetic than marls, noting that the platform carbonates that have not been remagnetized often yielded very low NRM intensities. An added remagnetized component would be much quicker traceable in that case.

Observations in the field show that the remagnetized limestones clearly have undergone pressure solution. It indicates that there must have been dissolution, diffusive transport, and reprecipitation. Therefore, pressure solution certainly may be associated with remagnetization.

Another possibility would be exploring the possibility of remagnetization during folding, i.e. compression. Unfortunately it is hard to relate the remagnetization explicitly to the folding because in the OB only one remagnetized fold limb is exposed. So, establishing an early or late acquisition depending on position in the orogenic front as proposed for Paleozoic limestones in North America (*Stamatakos et al., 1996; Enkin et al., 2000*) is not possible for the OB. Whether remagnetization is acquired during partial tilting to the South (as anticipated in the extensional setting) is currently being explored. Dinarès-Turell and García-Senz (2000) argue for remagnetization by means of elevated geothermal gradient during the syn-rift deposition of the marls, something which we consider realistic.

Also, the different deformational behavior of limestones and marls may provide a lead. Limestones are more prone to pressure solution than marls and neoformation of magnetite in a tectonic or burial stress field may have occurred. In this matter the suggestion by Zegers et al. (*2003*) and the experimental data of Moreau et al. (*2005*) could be meaningful. The latter authors document that differential stress assists magnetite formation. If this can be extended to the setting in the OB, it provides a provisional explanation for the limestones being more prone to remagnetization than marls. It should be realized that the remagnetization – once formed – is quite stable: it survives the tectonic action of later faulting.

So, it is most plausible that the neoformation of the magnetite occurred early, either in the elevated temperature regime prevailing during the half-graben style extension, or in the earliest stage of the compression (See also *Villalaín et al., 2003*). This concurs with arguments developed by Evans and Elmore

(*2006*) for the Devonian Helderberg and Tonoloway formations. In the OB the role of external fluid remains currently elusive; field observation suggests that it is not prominent. Machel and Cavell (*1999*) argue for Devonian aquifers in the foreland of the Rocky Mountains (Canada) that the flux of such fluids is low confining their expression to late-stage overgrowths. To further constrain the role of external fluids, strontium isotope analysis of our samples is currently being planned.

6 Conclusion

Analysis of new paleomagnetic data from most of the Organyà Basin shows that the remagnetization in the OB is confined to the limestone part of the lithological sequence. Thermoviscous resetting can be ruled out as remagnetization mechanism because inferred maximum burial temperatures are ~150°C, too low to make thermoviscous resetting a viable option. Epidiagenetic processes have caused neoformation of magnetite; which could have been assisted by deformational processes. Pressure solution certainly must have played a role in the remagnetization. A large effect of external fluids is not likely but cannot entirely be excluded. To shed light on this issue strontium isotope analysis is being planned. The elevated thermal gradient that prevailed during the syn-rift extension is likely to have caused remagnetization in other basins in similar setting. Whether or not it is possible to better constrain the timing of the remagnetization is currently being investigated.

Acknowledgements

R. Rabbers is thanked for helping with some of the figures. The project is supported by the Vening-Meinesz research School of Geodynamics, a collaboration between the Department of Earth Sciences (Utrecht University, The Netherlands) and the Department of Earth Observation and Space Systems of the Faculty of Aerospace Engineering (Delft University of Technology, The Netherlands).

References

Becker E., 1999: Orbitoliniden-Biostratigraphie der Unterkreide (Hauterive-Barrême) in den spanischen Pyrenäen (Profil Organyà, Prov. Lérida). *Revue Paléobiol. Genève*, **18**, 359-489.

Berástequi X., García-Senz J. and Losantos M., 1990: Tecto-sedimentary evolution of the Organyà extensional basin (central south Pyrenean unit, Spain) during the Lower Cretaceous. *Bull. Soc. Géol. France*, **8(VI)**, 251-264.

Bernaus J.M., 2000: L'Urgonien du Bassin d'Organyà. *Géologie Alpine,Mémoire HS 33*, 138pp.

Bernaus J.M., Arnaud-Vanneau A. and Caus E., 1999: La sedimentación "Urgoniense" en la cuenca de Organyà (NE España). Libro homenaje a José Ramírez del Pozo. *De Geol. Y Geofis. Españoles del Petróleo, AGGEP*, 71-80.

Bernaus J.M., Arnaud-Vanneau A. and Caus E., 2003: Carbonate platform sequence stratigraphy in a rapidly subsiding area: the Late Barremian-Early Aptian of the Organya basin, Spanish Pyrenees. *Sedimentary Geology*, **159(3-4)**, 177-201.

Bernaus J.M., Caus E. and Arnaud-Vanneau A., 2000: Aplicación de los análisis micropaleontológicos cuantittivos en estratigrafía secuential: El Cretácico inferior de la cuenca de Organyà (Pirineos, España). *Rev. Soc. Geol. España*, **13**, 55-63.

Blumstein A.M., Elmore R.D., Engel M.H., Elliot C. and Basu A., 2004: Paleomagnetic dating of burial diagenesis in Mississippian carbonates, Utah. *Journal of Geophysical Research-Solid Earth*, **109(B4)**, -No. B4, B04101, 04110.01029/02003JB002698.

Brothers L.A., Engel M.H. and Elmore R.D., 1996: A laboratory investigation of the late diagenetic conversion of pyrite to magnetite by organically complexed ferric iron. *Chemical Geology*, **130**, 1-14.

Dekkers M.J., 1989: Magnetic properties of natural goethite – II. TRM behaviour during thermal and alternating field demagnetization and low-temperature treatment. *Geophysical Journal*, **97**, 341-355.

Dinarès-Turell J. and García-Senz J., 2000: Remagnetization of Lower Cretaceous limestones from the southern Pyrenees and relation to the Iberian plate geodynamic evolution. *Journal of Geophysical Research-Solid Earth*, **105(B8)**, 19405-19418.

Elmore R.D., Dulin S., Engel M.H. and Parnell J., 2006: Remagnetization and fluid flow in the Old Red Sandstone along the Great Glen Fault, Scotland. *Journal of Geochemical Exploration*, **89(1-3)**, 96-99.

Elmore R.D., London D., Bagley D., Fruit D. and Gao G., 1993: Remagnetization by basinal fluids: testing the hypothesis in the Viola Limestone, southern Oklahoma. *Journal of Geophysical Research B: Solid Earth*, **98**, 6237-6254.

Enkin R.J., Osadetz K.G., Baker J. and Kisilevsky D., 2000: Orogenic remagnetizations in the Front Ranges and Inner Foothills of the southern Canadian Cordillera: Chemical harbinger and thermal handmaiden of Cordilleran deformation. *GSA Bull.*, **112(6)**, 929-942.

Evans M.A. and Elmore R.D., 2006: Fluid control of localized mineral domains in limestone pressure solution structures. *Journal of Structural Geology*, **28**, 284-301.

Evans M.A., Lewchuk M., T. and Elmore R.D., 2003: Strain partitioning of deformation mechanisms in limestones: examining the relationship of strain and anisotropy of magnetic susceptibility (AMS). *Journal of structural geology*, **25(9)**, 1525-1549.

Galdeano A., Moreau M.G., Pozzi J.P., Berthou P.Y. and Malod J.A., 1989: New Paleomagnetic Results from Cretaceous Sediments near Lisbon (Portugal) and Implications for the Rotation of Iberia. *Earth and Planetary Science Letters*, **92(1)**, 95-106.

García-Senz J., 2002: Cuencas extensivas del Cretacico Inferior en los Pireneos Centrales – formacion y subsecuente inversion. *PhD thesis, University of Barcelona*, 310pp.

Gibbons W. and Moreno M.T., 2002: The geology of Spain. *The Geological Society*, London, 649 pp.

Gradstein F.M., Ogg J.G., Smith A.G., Agterberg F.P., Bleeker W., Cooper R.A., Davydov V., Gibbard P., Hinnov L.A., House M.R., Lourens L., Luterbacher H.P., McArthur J., Melchin M.J., Robb L.J., Shergold J., Villeneuve M., Wardlaw B.R., Ali J., Brinkhuis H., Hilgen F.J., Hooker J., Howarth R.J., Knoll A.H., Laskar J., Monechi S., Plumb K.A., Powell J., Raffi I., Röhl U., Sadler P., Sanfilippo A., Schmitz B., Shackleton N.J., Shields G.A., Strauss H., Van Dam J., van Kolfschoten T., Veizer J. and Wilson D., 2004: A geologic time scale 2004. *Cambridge University Press*, 589 pp.

Heslop D., McIntosh G. and Dekkers M.J., 2004: Using time- and temperature-dependent Preisach models to investigate the limitations of modelling isothermal remanent magnetization acquisition curves with cumulative log Gaussian functions. *Geophys. J. Int.*, **157**, 55-63.

Juárez M.T., Lowrie W., Osete M.L. and Meléndez G., 1998: Evidence of widespread Cretaceous remagnetisation in the Iberian Range and its relation with the rotation of Iberia. *Earth and Planetary Science Letters*, **160**, 729-743.

Katz B., Elmore R.D., Cognoini M., Engel M.H. and Ferry S., 2000: Associations between burial diagenesis of smectite, chemical remagnetization, and magnetite authigenesis in the Vocontian trough, SE France. *J. Geophys. Res.*, **105(B1)**, 851-868.

Katz B., Elmore R.D., Cogoini M. and Ferry S., 1998: Widespread chemical remagnetization: Orogenic fluids or burial diagenesis of clays? *Geology*, **26(7)**, 603-606.

Kirschvink J.L., 1980: The least-squares line and plane and the analysis of palaeomagnetic data. *Geophysical Journal of the Royal Astronomical Society*, **62**, 699-718.

Kruiver P.P., Dekkers M.J. and Heslop D., 2001: Quantification of magnetic coercivity components by the analysis of acquisition curves of isothermal remanent magnetisation. *Earth and Planetary Science Letters*, **189**, 269-276.

Kruiver P.P., Langereis C.G., Dekkers M.J. and Krijgsman W., 2003: Rock-magnetic properties of multicomponent natural remanent magnetization in alluvial red beds (NE Spain). *Geophys. J. Int.*, **153**, 317-332.

Kruiver P.P. and Passier H.F., 2001: Coercivity analysis of magnetic phases in sapropel S1 related to variations in redox conditions, including an investigation of the S-ratio. *Geochemistry Geophysics Geosystems*, **doi: 2001GC000181**.

Langmuir D., 1971: Particle size effect of the reaction goethite = hematite + water. *American Journal of Science*, **271**, 147-156.

Machel H.G. and Cavell P.A., 1999: Low-flux, tectonically-induced squeegee fluid flow ("hot flash") into the Rocky Mountain Foreland Basin. *Bulletin of Canadian Petroleum Geology*, **47(4)**, 510-533.

Márton E., Abranches M.C. and Pais J., 2004: Iberia in the Cretaceous: new paleomagnetic results from Portugal. *Journal of Geodynamics*, **38(2)**, 209-221.

McCabe C. and Elmore R.D., 1989: The occurrence and origin of Late Paleozoic remagnetization in the sedimentary rocks of North America. *Reviews of Geophysics*, **27**, 471-494.

Moreau M.G., Ader M. and Enkin R.J., 2005: The magnetization of clay-rich rocks in sedimentary basins: low-temperature experimental formation of magnetic carriers in natural samples. *Eart Planet. Sci. Lett.*, **230**, 193-210.

Moreau M.G., Berthou J.Y. and Malod J.-A., 1997: New paleomagnetic Mesozoic data from the Algarve (Portugal): fast rotation of Iberia between the Hauterivian and the Aptian. *Earth and Planetary Science Letters*, **146(3-4)**, 689-701.

Moreau M.G., Canerot J. and Malod J.A., 1992: Paleomagnetic study of Mesozoic sediments from the Iberian Chain (Spain). Suggestions for Barremian remagnetization and implications for the rotation of Iberia. *Bulletin de la Societe Geologique de France*, **163(4)**, 393-402.

Mullender T.A.T., Frederichs T., Hilgenfeldt C., Fabian K. and Dekkers M.J., 2005: Fully automated demagnetization and measurement of NRM, ARM and IRM on a '2G' SQUID magnetometer. *IAGA, abstract number: IAGA2005-A-00898*.

Muñoz J.A., 1988: Estructura de las unidades surpirineaicas en la tranversal del corte ECORS. *Reun. Extraord. ECORS – Pirineos. Soc. Geol. España – Soc. Géol. France. Guía de Campo.*

Nottvedt A., Gabrielsen R.H. and Steel R.J., 1995: Tectonostratigraphy and sedimentary architecture of rift basins, with reference to the northern North Sea. *Marine and Petroluem Geology*, **12**, 881-901.

Oliver J., 1986: Fluids expelled tectonically from orogenic belts: their role in hydrocarbon migration and other geologic phenomena. *Geology*, **14**, 99-102.

Passchier C.W. and Trouw R.A.J., 1996: Microtectonics. *Springer*, New York.

Roberts A.P., Cui Y.-L. and Verosub K.L., 1995: Wasp-waisted hysteresis loops: mineral magnetic characteristics and discrimination of components in mixed magnetic systems. *Journal of Geophysical Research B: Solid Earth*, **100**, 17,909-917,924.

Shipunov S.V., Muraviev A.A. and Bazhenov M.L., 1998: A new conglomerate test in palaeomagnetism. *Geophys. J. Int.*, **133**, 721-725.

Stamatakos J., Hirt A.M. and Lowrie W., 1996: The age and timing of folding in the central Appalachians from paleomagnetic results. *GSA Bull.*, **108(7)**, 815-829.

Suk D.-W., Peacor D.R. and Van der Voo R., 1990: Replacement of pyrite framboids by magnetite in limestone and implications for paleomagnetism. *Nature*, **345**, 611-613.

Tauxe L., Mullender T.A.T. and Pick T., 1996: Potbellies, wasp-waists, and superparamagnetism in magnetic hysteresis. *Journal of Geophysical Research B: Solid Earth*, **101**, 571-583.

Van Velzen A.J. and Zijderveld J.D.A., 1995: Effects of weathering on single-domain magnetite in Early Pliocene marine marls. *Geophys. J. Int.*, **121**, 267-278.

Vera J.A., Salas R., Bitzer K. and Mas R., 2001: Iberia and Western Mediterranean; Aptian-Albian 121-98.8 Ma. *In: Stampfli G., Borel G., Cavazza W., Mosar J., Ziegler P.A. (eds) The Paleotectonic Atlas of the PeriTethyan Domain (CD-ROM) EGS.*

Vergés J. and García-Senz J., 2001: Mesozoic evolution and Cainozoic inversion of the Pyrenean Rift. *In: Ziegler P.A., Cavazza W., Robertson A.H.F. and Crasquin-Soleau (eds) Peri-Tethyan rift/wrench basins and passive margins. Mém. Mus. Natn.Hist. nat. Paris*, **186**, 187-212.

Villalaín J.J., G. F.-G., M. C.A. and A. G.-I., 2003: Evidence of a Cretaceous remagnetization in the Cameros Basin (North Spain): implications for basin geometry. *Tectonophysics*, **377**, 101-117.

Watson G.S., 1956: Analysis of dispersion on a sphere. *Mon. Not. Roy. Astron. Soc. Geophys. Supp.*, **7**, 153-159.

Woods S., Elmore R.D. and Engel M.H., 2002: Paleomagnetic dating of the smectite-to-illite conversion: testing the hypothesis in Jurassic sedimentary rocks, Skye, Scotland. *Journal of Geophysical Research*, **107(10.1029/2000JB000053)**, EPM 2-1-2-12.

Xu W., van der Voo R. and Peacor D.R., 1998: Electron microscopic and rock magnetic study of remagnetized Leadvillle carbonates, central Colorado. *Tectonophysics*, **296**, 333-362.

Zegers T.E., Dekkers M.J. and Bailly S., 2003: Late Carboniferous to Permian remagnetization of Devonian limestones in the Ardennes: Role of temperature, fluids, and deformation. *Journal of Geophysical Research-Solid Earth*, **108(B7)**, 2357.

CHAPTER 4

Diachronous pervasive remagnetization in northern Iberian basins during Cretaceous rotation and extension

Z. Gong, D.J.J. van Hinsbergen, M.J. Dekkers
Paleomagnetic Laboratory Fort Hoofddijk, Dept. of Earth sciences, Utrecht University, Budapestlaan 17, 3584 CD Utrecht, The Netherlands
(submitted to EPSL)

Abstract

Northern Iberia exposes a series of Mesozoic sedimentary basins, of which the final formation history is tied to the rotation episode during the Aptian (Gong et al., 2008b), related to the opening of the Bay of Biscay. Many of these basins experienced widespread remagnetization, previously loosely tied to a 'Mid-Cretaceous thermal event'. Here we make use of the improved apparent polar wander path (APWP) of Iberia to narrowly constrain the age of their remagnetization to show that several basins experienced a regional diachronous remagnetization.

We apply the small circle intersection (SCI) method (Waldhör and Appel, 2006), to restore the paleomagnetic field during remagnetization in the Organyà Basin in the Southern Pyrenees, Spain, where both the age of remagnetization is stratigraphically well-dated to around the Barremian-Aptian boundary, and where the paleomagnetic direction during remagnetization has been well-established. The resulting direction of D/I = 316.8°/54.8° (with a_{95} = 3.3) corresponds closely to a recently improved APWP of Iberia (Gong et al., 2008b), providing support for the applicability of this method. Application of the SCI method allows us to show that the older portion of the remagnetized beds were already tilted by ~15-20° to the South during the remagnetization as a result of half-graben formation in the Organyà Basin. Moreover, the positive outcome of the SCI technique enables us to argue that previously published results from three other basins – the Cabuérniga and Cameros basins and the Iberian range – can be straightforwardly compared to the APWP. Hence, we show that the four pervasively remagnetized basins under consideration all acquired their remagnetization at different times. The remagnetization events were thus confined to these sedimentary basins on an individual 'per basin' scale – albeit occurring on a regional scale over a period of at least ~10-15 Myr. Therefore, we propose that the Cretaceous remagnetization events in northern Iberia are related to the extensional tectonic rifting. The pervasive remagnetization is most likely basin confined because there is no apparent overall regional or temporal trend among the basins. Reasonable explanations for remagnetization are those that can occur on the scale and within the context of individual sedimentary basins. These include the interplay of burial depth and an elevated geothermal to reach the diagenetic temperatures required for magnetite-producing reactions. In the Iberian situation, there is no need to invoke more speculative regional Iberia-wide mechanisms.

Keywords: Remagnetization, Small Circle Intersection, Organyà Basin, Pyrenees, Aptian, Iberian rotation

1 Introduction

Paleomagnetism is a frequently used, quantitative tool for (plate) tectonic studies. Pervasive remagnetization, common in many geological environments, evidently complicates the geological interpretation of the natural remanent magnetization (NRM) for the paleomagnetic studies. Remagnetized strata do not carry a primary NRM, i.e. an NRM of the same age as the rock unit, making those sample collections unsuited for classic paleogeographic or tectonic reconstructions. Remagnetization was considered a fairly rare phenomenon in the 1960s but became increasingly documented since the early 1980s (McCabe et al., 1983), in particular in limestones and marls that make up large portions of orogenic belts and their forelands. At present, remagnetized rock units are common place in many orogens and paleomagnetic data sets are tested to identify possible remagnetization. Often such analyses are based on the application of field-tests, in particular (versions of) the fold test, and comparing paleomagnetic pole positions to the apparent polar wander path (APWP) of the respective tectonic unit.

The recognition of the causes, and possibly, correction for remagnetization has been subject of many studies (e.g. Katz et al., 1998; Machel and Cavell, 1999; Elmore et al., 2006a). One notorious problem with identification of the mechanisms behind remagnetization concerns the timing and regional extent of such events: a remagnetization event restricted to a sedimentary basin may make other mechanisms plausible than one that occurs continent-wide. A region which has been shown to be remagnetized regionally during the Cretaceous concerns the Iberian Peninsula (e.g. Galdeano et al., 1989; Moreau et al., 1992; Villalain et al., 1994; Moreau et al., 1997; Juárez et al., 1998; Dinarès-Turell and García-Senz, 2000; Villalaín et al., 2003; Márton et al., 2004; Casas et al., 2008; Gong et al., 2008a; Soto et al., 2008). This remagnetization is related to

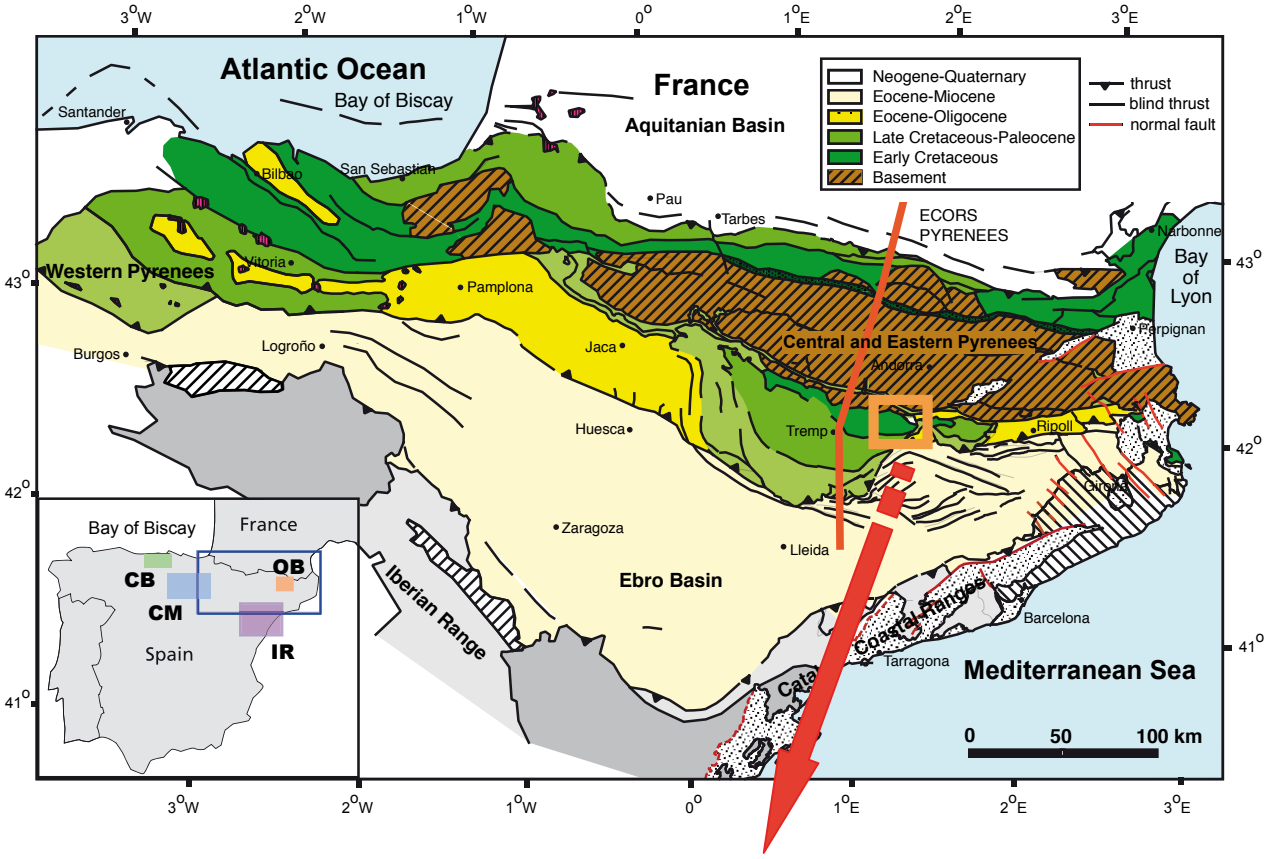

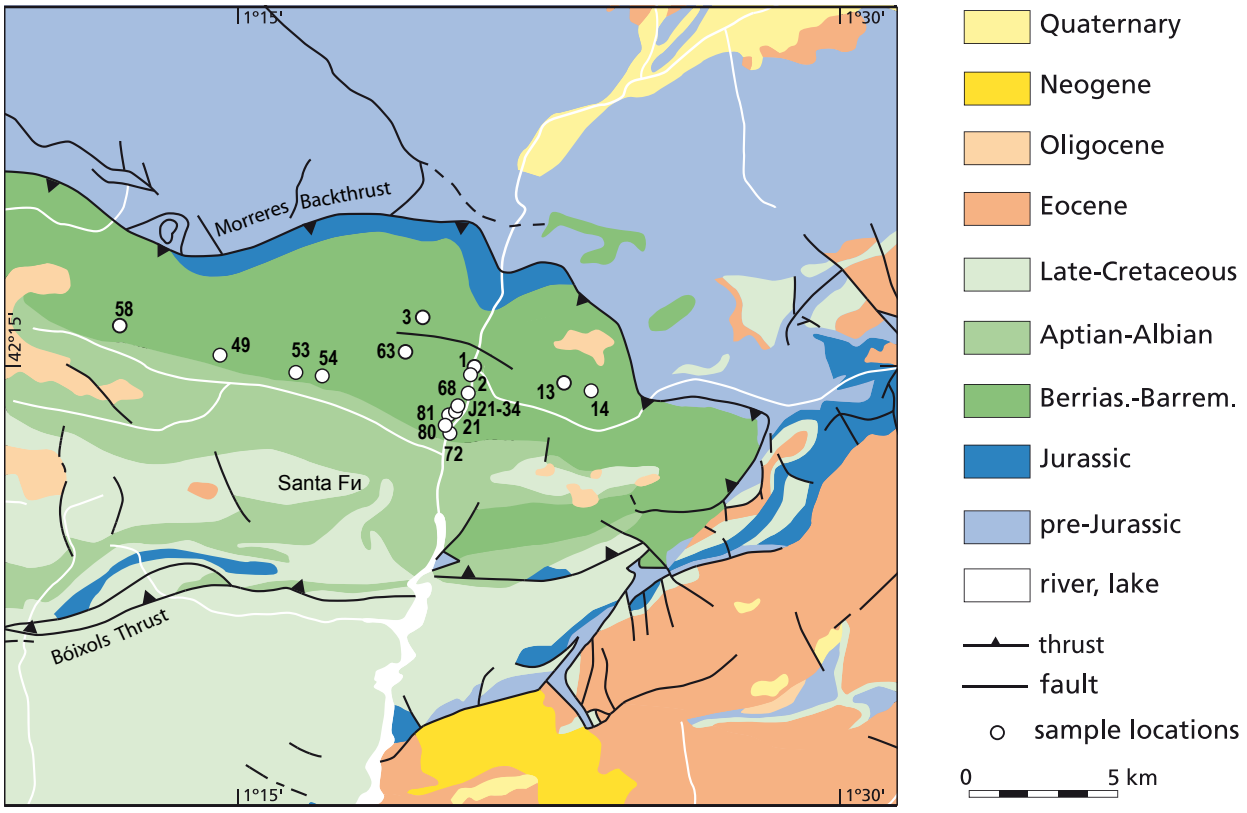

Figure 1 Geological map of the Pyrenees modified after Vergés et al. (2002) and the Organyà Basin with the locations of the sampling sites; numbers refer to those reported in Table 1. At the bottom left in the top map, the Organyà Basin (OB), Cabuérniga Basin (CB), Iberian Range (IR), Cameros Basin (CM) are indicated by pale orange, pale green, pale purple, pale blue solid rectangles respectively. The map area of the geological map of the Pyrenees is indicated with the blue rectangle on the topographic map.

the 'Mid Cretaceous thermal anomaly that prevailed during the extensional phase' (e.g. Juárez et al., 1998; Dinarès-Turell and García-Senz, 2000). This extensional phase refers to the opening of the Bay of Biscay, during a contemporaneous Aptian counter-clockwise rotation phase of Iberia. The Cretaceous remagnetization has regionally been documented from the Cabuérniga Basin to the Iberian Range (Figure 1).

Remagnetization may occur well after sedimentation and the beds may have been tilted prior to remagnetization. Correction for bedding tilt thus does not necessarily yield the paleomagnetic direction during remagnetization. Proper reconstruction of this direction, which allows comparison to the APWP, however, may put important constraints on the timing of remagnetization, which in turn is essential in assessing its cause. The small circle intersection (SCI) method which is proposed by Shipunov (1997) and later perfected by Enkin et al. (2002); Enkin (2003); Waldhör and Appel (2006), can be used to determine the paleomagnetic direction during remagnetization from a series of remagnetized sites. This method has recently been applied to remagnetized Mesozoic basins in the Iberian Peninsula (Casas et al., 2008; Soto et al., 2008). The SCI method uses of the inherent variability in bedding strike of a folded tilted basin. Upon rotation around the bedding strike the NRM component directions of individual sites describe small circles. The only possible direction that fits all small circles is their common crossing point and by seeking the maximum concentration of small circle crossings, the paleomagnetic direction during remagnetization can be calculated.

The Organyà Basin in north-eastern Iberia contains a Berriasian-Barremian remagnetized and an Aptian-Cenomanian non-remagnetized, syn- and post-rift sedimentary sequence (García-Senz, 2002). From these syn-rift sedimentary sequences, Gong et al. (2008b) reconstructed and dated the Aptian rotation history of Iberia, further constrained by a review of Iberian paleomagnetic and marine magnetic anomaly data. From the stratigraphic relationships Dinarès-Turell and García-Senz (2000) already inferred that remagnetization occurred around the onset of the intensive rifting phase in the basin. Because the timing and the paleomagnetic direction of the remagnetization in the Organyà Basin are well constrained, this basin provides a unique opportunity to further investigate the validity of the SCI method in the reconstruction of syn-remagnetization paleomagnetic directions, using new and published data. The reconstructed direction of Organyà Basin, as well as published remagnetization directions, will then be compared to the recently improved Iberian APWP to determine their ages.

By analysing the Cretaceous northern Iberian basins we thus investigate whether the remagnetization was a single event that has operated 'Iberia-wide' or whether it was active more regionally on a 'per basin' scale. Either option has its bearing on remagnetization scenarios, an item that we address at the end of this contribution.

2 Remagnetization mechanisms

The regular occurrence of remagnetization in anchimetamorphic and very low grade metamorphic rocks has motivated research into its mechanism. Broadly speaking two main categories of mechanisms have been proposed. The first involves viscous resetting of existing magnetic minerals at the burial temperature for the burial duration, referred to as the thermoviscous remagnetization (TVRM) model (Kent, 1985). This mechanism may have some credibility for rocks that are at their most elevated burial temperature during a long single polarity chron, for example the reversed Kiaman superchron during the Hercynian orogeny, and could occur on a regional scale. However, in many cases the prevailing burial temperatures are too low to make the TVRM model plausible and neoformation of magnetic minerals has been put forward as an alternative. This model is referred to as the chemical remanent magnetization (CRM) model (e.g. McCabe and Elmore, 1989). Fluids are presumed to have delivered the constituents for the newly formed magnetic minerals. Older scenarios involved vast amounts of 'orogenic fluids' that would have moved orogen-wide (e.g. Oliver, 1986; Morris and Robertson, 1993). More recent remagnetization studies take a more conservative approach and do not involve (large amounts of) external fluid (sometimes referred to as squee-gee fluid) (e.g. Katz et al., 1998; Machel and Cavell, 1999; Katz et al., 2000; Blumstein et al., 2004). These document that diagenetic reactions deliver iron, required to form magnetite, amongst others by reactions involving clay minerals obviating the need for external fluids. This scenario can also occur in a more confined regional scale. When dolomitization of the carbonates is occurring, evolved fluid is reported to have migrated in relation to remagnetization and oil generation (e.g. O'Brien et al., 2007). The role of pressure solution in remagnetization is equivocal (e.g. Evans et al., 2003; Elmore et al., 2006b) but it requires compression and would be less likely in an extensional setting.

3 Organyà Basin: Geological setting and sampling

The Organyà Basin is located in the Bóixols thrust sheet in the southeast Pyrenees, Spain (Fig. 1). During the Cretaceous opening of the Bay of Biscay, the Iberian microplate rotated ~35° counter-clockwise (CCW) with respect to Eurasia (Carey, 1958; Bullard, 1965; Van der Voo, 1967, 1969; Srivastava et al., 1990; Sibuet et al., 2004; Gong et al., 2008b). Based on both paleomagnetic data from Iberia and ocean floor magnetic anomaly data from the Bay of Biscay, the timing of the Iberian rotation is now well constrained to the Aptian (Gong et al., 2008b). During the Iberian rotation, several syn-rotational extensional basins including the Organyà Basin, formed along northern Iberia, which later inverted since ~80 Ma during the Pyrenean orogeny.

The Organyà Basin, an west-east trending inverted half-graben, is now exposed in the hanging wall of the Bòixols thrust (Dinarès-Turell and García-Senz, 2000). Its extensional history is characterized by Tithonian-Barremain proto to early syn-rift, Aptian syn-rift and a post-Aptian post-rift covers. The bulk of the inversion occurred during the Santonian-Maastrichtian compression. The southern margin of the graben was inverted as the Bòixols thrust sheet (Bond and McClay, 1995). The original northern margin is less certainly known since exposures coincide with a passive-roof backthrust, located in the contact with

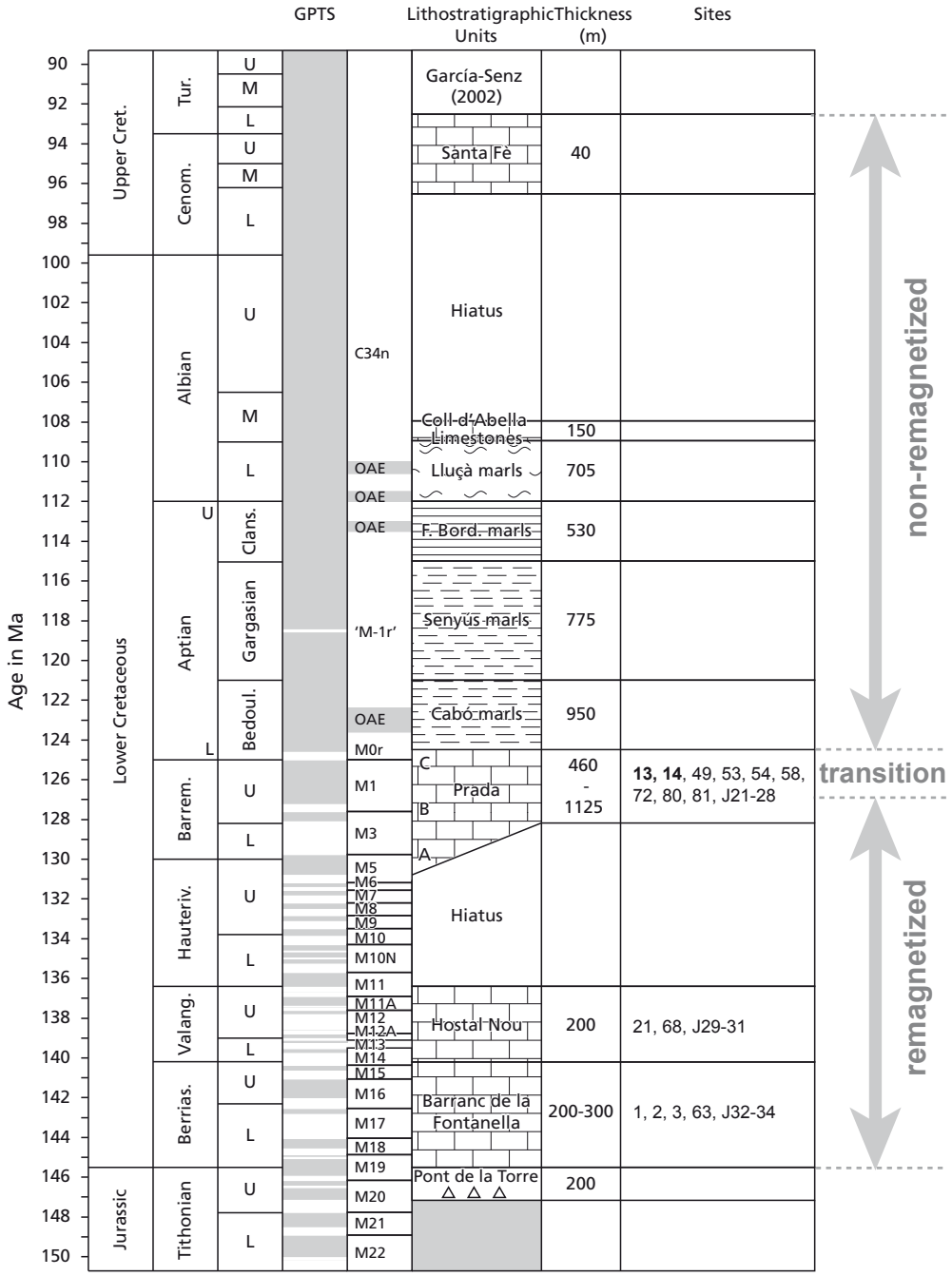

Figure 2 Stratigraphic column of the Organyà Basin with lithologies, formations, and broad stratigraphic locations of paleomagnetic sites (new sites in bold), correlated to the geological time scale (Ogg et al., 2004). The geomagnetic polarity time scale (GPTS) is also included: grey (white) is normal (reversed) polarity. Chron nomenclature follows CK92 (Cande and Kent, 1992). The Berriasian – lower Barremian limestones are remagnetized; the Aptian – Cenomanian sediments are non-remagnetized; the uppermost Barremian Prada C Formation is the transition between the remagnetized and non-remagnetized rocks (Dinarès-Turell and García-Senz, 2000; Gong et al., 2008b).

the Axial Zone antiformal stack (Dinarès-Turell and García-Senz, 2000). The compressive tectonics led to the development of folds in the basin, such as the present main structure, the approximately E-W trending Santa Fè syncline (Fig. 1).

The Organyá Basin comprises about 4.5 km of hemipelagic to pelagic Cretaceous sediments (Fig. 2). These are mainly limestones and marls. Their age is well constrained by biostratigraphy in stages and sub-stages (Becker, 1999; Bernaus et al., 1999; Bernaus, 2000; Bernaus et al., 2000; Bernaus et al., 2003). The lower sediments include Berriasian-Barremian platform carbonates with a lagoonal depositional environment (García-Senz, 2002). The limestones grade into Aptian-Albian marls and depositional conditions changed to coastal-marine with a high sedimentation rate (~27 cm/kyr). Before the post-rifting Cenomanian sediments were deposited, the top of the Albian sediments was eroded in the eastern end of the Organyá Basin, producing an upper Albian to lower Cenomanian hiatus leading to an angular unconformity.

Previous studies (Dinarès-Turell and García-Senz, 2000; Gong et al., 2008a) show that the upper part of the statigraphy

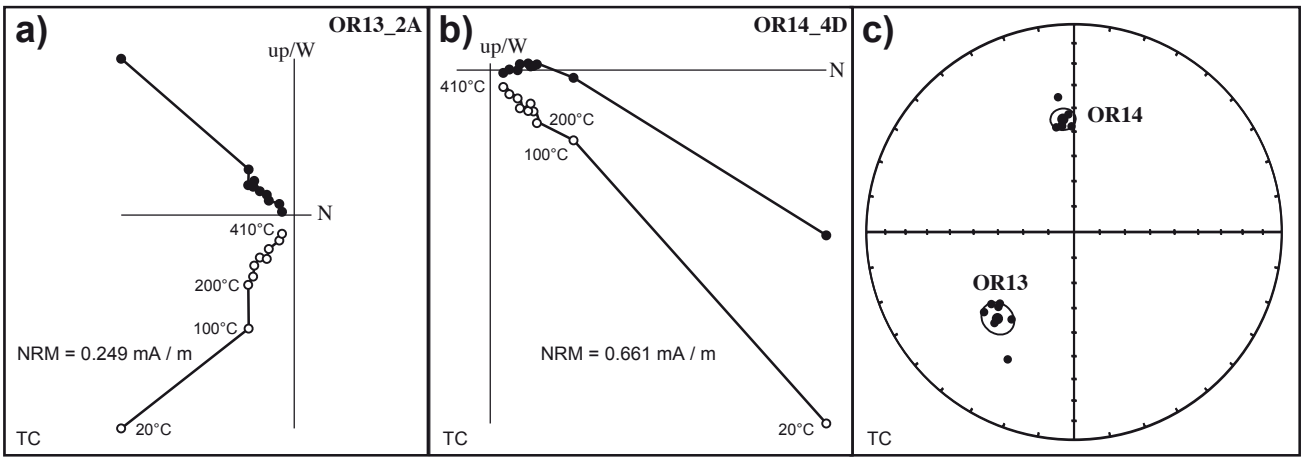

Figure 3 Demagnetization results of the new sites (OR13 and OR14) after bedding tilt correction (TC). (a, b). Representative orthogonal vector diagrams (Zijderveld, 1967) from OR13 and OR14. Closed (open) circles indicate the projection on the horizontal (vertical) plane. (c). Equal – area projections of the characteristic remanent magnetization (ChRM) distributions of sites OR13 and OR14. The open circles indicate their cone of confidence (a_{95}).

in the Organyá Basin has a primary NRM. This is supported by positive fold tests, normal polarities in the Cretaceous Normal Superchron, and rock magnetic results. The non-remagnetized formations include Cabó marls, Senyús marls, Font Bordonera marls, Lluçà marls, Coll d'Abella limestones and Santa Fè limestones (Fig. 2). However, the sediments from the lower part of the stratigraphy, from the Berriasian to Barremian, are remagnetized. These involve the Prada A, Prada B, Hostal Nou and Barranc de la Fontanella formations (Fig. 2). The Prada C formation represents the transition from remagnetized to non-remagnetized rocks. These remagnetized sediments all show normal polarity, whereas biostratigraphy would suggest that approximately half of the sites should have a reversed polarity (Dinarès-Turell and García-Senz, 2000; Gong et al., 2008a; Gong et al., 2008b) (Fig. 2). The associated rock magnetic studies show that the magnetic mineral is mainly magnetite with minor hematite and goethite (Dinarès-Turell and García-Senz, 2000; Gong et al., 2008a).

For this study, twenty nine sites covering the entirely remagnetized as well as transitional series in the Organyá Basin were used (Table 1). Two new sites (OR13 and OR14) (Fig. 1) from the east of the basin were sampled by a portable gasoline-powered drill, and combined with 13 other sites (labelled OR#) from our previous studies (Gong et al., 2008a; Gong et al., 2008b). Furthermore, 14 of sites (labelled J#) from Dinarès-Turell and García-Senz (2000) were used (Table 1, Fig. 1).

4 Paleomagnetic analysis and small circle intersection (SCI) results

4.1 Paleomagnetic analysis

Thermal demagnetization for sites OR13 and OR14 was processed in a laboratory-built furnace with small steps from room temperature up to 500°C; the NRM was measured with a 2G Enterprises DC-SQUID magnetometer. Zijderveld diagrams (Zijderveld, 1967) and principal component analysis (Kirschvink, 1980) were used to determine the characteristic remanent magnetisation (ChRM) directions. The NRM intensity of these limestone samples ranges between ~ 0.1 and ~ 1.1 mA/m. A low-temperature component (lower than 240°C) with normal polarity before tilt correction was interpreted as the present-day geomagnetic field overprint and was not analyzed further. An univectorial high-temperature component in both sites, from 240°C to 410°C, is considered to be the ChRM component (Fig. 3). After tectonic correction, the ChRMs from both sites have a positive inclination and also a normal polarity, however, their declinations are distinctly different with a northerly direction for OR14 and south-westerly direction for OR13, respectively (Fig. 3, Table 1). Previous results from the same formation (Prada A, B), also revealed a single, normal polarity component with a similar demagnetization behaviour. Therefore, these two sites are also considered to be remagnetized and used together with the other remagnetized sites for further analysis.

4.2 Small Circle Intersection (SCI) results

The SCI method (Waldhör and Appel, 2006) assumes that a tilted remanence has been rotated around a horizontal axis parallel to the bedding strike. Following this presumption, if no differential vertical axis rotation has occurred between the sites of a folded sequence or area, the paleomagnetic directions can be restored by the intersection of the remanence small circles (Shipunov, 1997). This method can be applied not only to syn-folding, but also to pre-folding NRMs (Waldhör and Appel, 2006). In the Organyà Basin, it is impossible to apply the fold test on the remagnetized and transitional limestones because of the low variety of bedding tilts and the non-exposure of northerly dipping strata. However, a post-folding origin of the remagnetized and transitional magnetization is unlikely because it gives an uninterpretable remanence inclination in geographic coordinates (Dinarès-Turell and García-Senz, 2000) (see also Table 1). Therefore, the secondary remanent magnetization in the Organyà Basin is either syn-folding or pre-folding. In this case, we can use the SCI method to restore the remagnetization direction. According to the geological record in the Organyà Basin, all sites in this study belong to the same overall fold structure. Thus, the local geological background fits the SCI criteria. In Figure 4, we applied the SCI method to the transitional and remagnetized directions (29 sites) from east

Table 1The remanent magnetization parameters of the paleomagnetic sites in the Organyà Basin. The OR sites are from our studies (the new sites in bold) (Gong et al., 2008a; Gong et al., 2008b) and numbers as plotted in Figure 1; the J sites are from Dinarès-Turell and García-Senz (2000). N/n, is number of the samples contributing to the mean/measured samples from each site. D and I, are declination and inclination in degrees. κ and $a_{95,}$ are the precision parameter and their cone of confidence (Fisher, 1953).

				In Situ				Tectonic Corrected				Corrected to D = 316.8°. I = 54.8°	
Site	**Lithology**	**Strike / Dip**	**N / n**	**D**	**I**	**κ**	**α_{95}**	**D**	**I**	**κ**	**α_{95}**	**D**	**I**
Barremian-Aptian (Prada C Fm)													
OR49	dark L	111 / 57	7/ 8	342.3	25.2	75.7	7.0	316.1	60.1	75.7	7.0	315.0	51.7
OR53	dark L	109 / 42	6 / 9	350.4	30.1	67.3	8.2	318.0	61.7	67.3	8.2	322.1	60.4
OR54	dark L	89 / 46	4 / 8	333.8	22.5	73.3	10.8	306.9	60.1	73.3	10.8	316.6	54.3
OR58	dark L	116 / 50	7 / 8	4.5	24.6	52.4	8.4	330.0	66.3	52.4	8.4	327.6	67.0
OR72	dark L	105 / 65	28 / 34	345.3	8.6	131.8	2.4	306.2	53.0	28.3	4.7	316.9	54.7
OR80	dark L	108 / 68	30 / 31	347.1	9.6	325.5	1.5	305.8	57.9	325.5	1.5	316.9	54.7
OR81	dark L	105 / 66	30 / 32	341.8	6.4	287.7	1.6	308.4	53.6	287.7	1.6	314.3	51.4
J21	dark L	120 / 67	9 / 9	358.4	10.7	52.3	7.2	316.9	57.5	52.3	7.2	317.9	57.2
J22	dark M and L	104 / 62	5 / 5	337.6	4.9	220.5	5.2	311.0	48.5	222.1	5.1	312.0	48.0
J23	dark L	100 / 60	10 / 11	346.3	10.0	70.0	5.5	316.4	60.4	66.1	5.7	321.3	58.2
Barremian (Prada B, A Fm)													
OR13	**light L**	**98 / 42**	**7 / 7**	**280.7**	**66.1**	**97.0**	**6.2**	**221.6**	**43.8**	**93.0**	**6.3**	**319.9**	**57.0**
OR14	**light L**	**296 / 18**	**6 / 7**	**339.9**	**58.9**	**216.5**	**4.6**	**354.5**	**44.8**	**216.3**	**4.6**	**324.9**	**64.9**
J24	dark L	104 / 55	6 / 6	343.9	28.0	108.4	6.5	290.8	63.6	108.7	6.5	319.3	57.1
J25	dark L	120 / 50	7 / 7	348.9	24.4	72.2	7.2	311.8	52.3	72.3	7.1	315.5	51.6
J26	dark L	114 / 58	7 / 7	346.3	22.4	358.2	3.2	300.4	55.3	359.3	3.2	315.6	52.5
J27	dark L	110 / 45	5 / 5	339.6	33.5	63.1	9.7	296.2	57.1	63.1	9.7	315.8	53.1
J28	dark L	110 / 50	5 / 5	349.2	30.2	253.1	4.8	301.7	63.1	251.7	4.8	320.5	59.1
Valanginian (Hostal Nou Fm)													
OR21+J31	dark M and L	116 / 51	20 / 20	341.3	31.5	87.3	3.5	278.8	54.4	70.1	3.9	314.9	50.7
OR68	dark L	110 / 60	70 / 80	343.1	24.0	96.3	1.7	290.8	57.1	97.7	1.7	315.6	52.9
J29	dark L	116 / 59	7 / 7	337.0	29.7	70.1	7.3	284.5	47.9	69.4	7.3	313.4	46.6
J30	dark L	116 / 51	5 / 8	345.0	33.7	304.6	3.2	290.5	57.5	305.0	3.2	316.6	54.3
Berriasian (Barranc de la Fontanella Fm)													
OR1+J34	light L	106 / 46	12 / 12	340.1	34.5	59.4	5.7	298.3	55.5	63.7	5.5	331.9	65.6
OR2+J32	dark L	97 / 55	10 / 10	336.5	33.5	174.9	3.7	280.2	55.7	179.3	3.6	318.3	55.7
OR3+J33	dark L	97 / 56	12 / 12	337.6	15.0	72.9	5.1	307.0	53.4	66.2	5.4	308.8	45.1
OR63	dark L	91 / 57	8 / 9	329.6	20.9	26.0	12.1	292.3	58.2	21.7	12.2	306.4	44.2

to west throughout the Organyà Basin. The bedding strikes range from 89°-120 (except for one bedding with strike/dip: 296°/18°), and the remanence small circles are intersecting. Our restored paleomagnetic direction is D = 316.8°, I = 54.8° (a_{95} = 3.3), which is very close to the transitional direction (Prada C) in the Organyà Basin (Fig. 4).

5 Discussion

5.1 Bedding tilt of the Organyà Basin during remagnetization

Application of the SCI method to the remagnetized sites of the Organyà Basin shows that the best clustering of paleomagnetic directions almost coincides with the 100% tilt-corrected directions from the Prada C Formation. From this we can infer that the Prada C Formation was subhorizontal during remagnetization. However, the SCI results show that a full tilt-correction of the remagnetized paleomagnetic directions obtained from older strata in the Organyà Basin gives an overcorrection to the south of approximately 10-20°. From this we can infer that the older strata below Prada C were already mildly tilted to the south by approximately 10-20° when the remagnetization occurred. It is plausible this tilt relates to the early moderate extension history of the Organyà Basin in pre-Aptian time, back-tilting the stratigraphy against the then normal fault which later became the Bòixols thrust. A comparable conclusion was recently reached for the bedding tilt during remagnetization in the Cabuérniga Basin by Soto et al. (2008).

5.2 Timing of the Iberian-wide remagnetization

In the Organyà Basin, the paleomagnetic direction of the Prada C Formation (uppermost Barremian-lowermost Aptian) was reported as transitional between the remagnetized and non-remagnetized sequences. In the equal angle projection (Fig. 4), the transitional directions plot in a narrow range closer to the restored direction. The restored paleomagnetic field declination (D = 316.8°) is virtually the same as the direction derived from the oceanic magnetic anomaly pattern at M0 (~ 317°) (Sibuet et al., 2004), which defined the beginning of the Iberian rotation at the base of the Aptian (Fig. 5). Meanwhile, the obtained inclination (I = 54.8°) agrees as well with the APWPs of

Iberia and Eurasia at the beginning of the Aptian (Besse and Courtillot, 2002; Gong et al., 2008b; Torsvik et al., 2008) (Fig. 5).

The stratigraphy shows that the boundary between remagnetized and non-remagnetized rocks occurred at the beginning of intensive rifting at the Barremian/Aptian boundary (Fig. 2). Therefore, both the results from SCI method and geological evidence yield the same age for the timing of the remagnetization, which supports the approach of the SCI method. Thus, we can use the SCI method in other Iberian basins without stratigraphic control at the age of the remagnetization to obtain its timing by comparison of the restored remagnetized direction to the well defined Iberian APWP.

Many paleomagnetic studies have reported on the widespread Iberian remagnetization during the Cretaceous (e.g. Galdeano et al., 1989; Moreau et al., 1992; Villalain et al., 1994; Moreau et al., 1997; Juárez et al., 1998; Dinarès-Turell and García-Senz, 2000; Villalaín et al., 2003; Márton et al., 2004; Casas et al., 2008; Gong et al., 2008a; Soto et al., 2008). Based on the recent study from Gong et al. (2008b) which combined all the available paleomagnetic data sets in Iberia and oceanic magnetic anomaly data in the Bay of Biscay together, the APWP of Iberia was calculated: the pre-rotation direction (D = 323.4° ± 9.7°, I = 50.2° ± 9.7°) by averaging the Tithonian-Barremian paleomagnetic results; the post-rotation direction (D = 357.5° ± 4.0°, I = 47.1° ± 4.0°) by averaging the Albian-Campanian data (Fig. 5). The Iberian rotation happened during the Aptian, ~35° CCW with respect to Eurasia (Gong et al., 2008b). Hence, for this study, we have a well defined APWP for Iberia. Meanwhile, recently the SCI method has been used to restore the paleomagnetic directions in the remagnetized sediments from the Cabuérniga Basin in the westernmost sector of the Basque-Cantabrian Basin (Soto et al., 2008) and Cameros Basin in the north-westernmost part of the Iberian Chain (Casas et al., 2008) (Fig. 1). Both of these basins have a similar basin development history as the Organyà Basin. The preserved sediments in the Cabuérniga Basin were entirely remagnetized with a syn-tectonic secondary NRM: a SCI restored paleomagnetic direction of D = 335.4°, I = 49.1° (a_{95} = 3.4) was obtained (Soto et al., 2008). Soto et al. (2008) constrained the remagnetization age to between the Valanginian and the Cenomanian. Comparison of this direction to our APWP now suggests an early to middle Aptian age of remagnetization. The different restored declination indicates a smaller amount of rotation in the Cabuérniga Basin than in the Organyà Basin. Its remagnetization must be younger than that in Organyà Basin.

Juárez et al. (1998) reported a Cretaceous remagnetization in the Iberian Range. The direction of the Cretaceous overprint is defined as D = 344.9°, I = 45.2° (with a_{95} = 6.8), suggesting middle-late Albian remagnetization (Fig. 5). The Cretaceous sediments in the Cameros Basin (Fig.1) are also completely remagnetized (Villalaín et al., 2003). Application of the SCI method here gives a paleomagnetic direction of D = 359.0°, I = 51.5° (with a_{95} = 4.2) (Casas et al., 2008), which suggests a post-Aptian remagnetization, with an upper age limit defined by the onset of the Pyrenean orogeny (Santonian) (Fig. 5). Therefore, from old to young, remagnetization of these four Iberian locations happened in the order: Organyà Basin (earliest Aptian), the Cabuérniga Basin (early-middle Aptian), the Iberian Range (middle-late Aptian) and the Cameros Basin (post Aptian, but before Pyrenean compression).

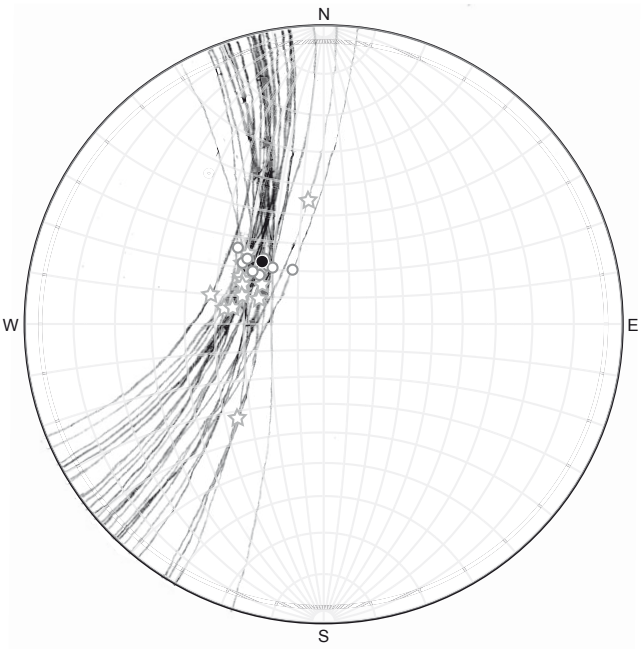

Figure 4 Equal angle (Wulff net) projection of the small circles of the mean paleomagnetic directions (after tectonic correction) in the Organyà Basin. Open dots (open stars) indicate the transitional (remagnetized) bedding tilt corrected directions (see Table 1). The black dot (D = 316.8°, I = 54.8°, a_{95} = 3.3) indicates the resulting paleomagnetic direction after applying the small circle intersection (SCI) method (Waldhör and Appel, 2006).

5.3 Implications for remagnetization mechanism

The Cretaceous evolution of Iberia is related to the opening of the Bay of Biscay and North Atlantic Ocean, and Iberia was mainly in a lithospheric stretching regime. The Iberian remagnetization was thus loosely linked to an elevated geothermal regime due to the extensional tectonics (e. g. Juárez et al., 1998; Márton et al., 2004). Here we assemble available information basin by basin.

In the Organyà Basin, the remagnetization occurred exactly at the beginning of the intensive rifting. As remagnetization mechanism, thermoviscous resetting was excluded because the burial temperature of ~ 150°C is too low (Gong et al., 2008a). In the CRM model, burial essentially without external fluid is considered to be the most likely remagnetization mechanism in the elevated geothermal gradient regime during the syn-rift extension (Gong et al., 2008a).

In the Cabuérniga Basin, Soto et al. (2008) pointed out that the remagnetization is related to the basin extension when a high level of subsidence was reached because of thick syn-rift deposits (that have been eroded since). Further details were not provided. Because the remagnetization is syn-rotational, its duration (a few Myrs only) is too short for thermoviscous resetting being a viable option. Therefore, we consider a CRM most probably for this basin.

In the Iberian Range, Juárez et al. (1998) argue that the remagnetization could well have been caused by a thermoviscous process related to the thermal event(s). However, their data do

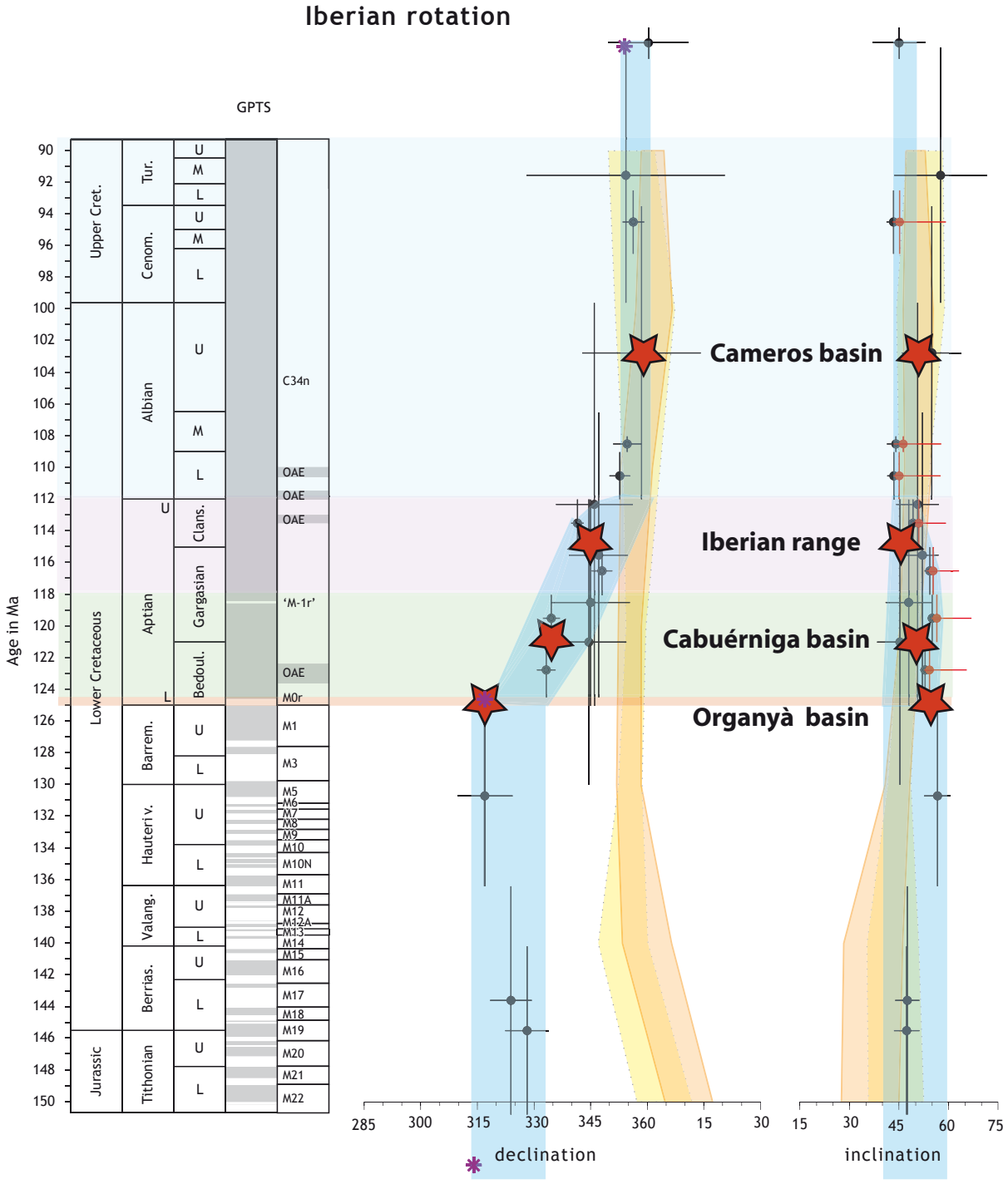

Figure 5 The SCI based paleomagnetic directions (Organyà Basin, Cabuérniga Basin, Iberian Range and Cameros Basin) plot onto the APWP of Iberia of Gong et al. (2008b). The red stars indicate the mean directions after application of the SCI method: Organyà Basin (D = 316.8°, I = 54.8°, a_{95} = 3.3), Cabuérniga Basin (D = 335.4°, I = 49.1°, a_{95} = 3.4) (Soto et al., 2008), Iberian Range (D = 344.9°, I = 45.2°, a_{95} = 6.8) (Juárez et al., 1998) and Cameros Basin (D = 359.0°, I = 51.5°, a_{95} = 4.2) (Casas et al., 2008). Interpretational error boundaries of the ages of the remagnetization from the different locations are shown as different color shadings: pale orange (Organyà Basin), pale green (Cabuérniga Basin), pale purple (Iberian Range) and light blue (Cameros Basin). The Iberian rotation path (blue) is calculated: Tithonian-Barremian (pre-rotation: 323.4°/50.2° ± 9.7°); Albian-Campanian (post-rotation: 357.5°/47.1° ± 4.0°). The solid dots indicate the data used for APWP recontruction by Gong et al. (2008b). Vertical error bars denote age uncertainty, horizontal error bars denote ΔD (= a_{95}/cos (I)) and ΔI (=a_{95}). The light yellow and orange shaded areas are the APWP for Eurasia from Besse and Courtillot (2002) and Torsvik et al. (2008), respectively. The purple asterisks give the declinations as derived from the sea-floor anomaly data from the Bay of Biscay (Srivastava et al., 2000; Sibuet et al., 2004), notably the M0 anomaly at the Barremian/Aptian boundary, and the A33o anomaly in the late Cretaceous. The geological time scale is from Ogg et al. (2004).

not make this argument entirely clear and a chemical origin of the remagnetization cannot be excluded (as actually realized by authors). Juárez et al. (1998) favoured the TVRM model in absence of a precise Cretaceous APWP for Iberia which left the whole Cretaceous Superchron available, sufficient for the TVRM acquisition time. The age of their remagnetization is now much narrower constrained to the late Aptian being syn-rotational. The TVRM model is unlikely in this part of the Iberian range and a CRM remagnetization model related to the thinner lithosphere during the rotation is a plausible alternative.

In the Cameros Basin, the remagnetization (Villalaín et al., 2003) is suggested between the Albian and Santonian, the ages of the extensional and compressional deformation stages. Villalaín et al. (2003) prefer to relate the remagnetization that resides in hematite to the Albian, early in the possible window. The syn-rift deposits (Kimmeridgian to Early Albian; fluvial and lacustrine sandstones, siltstones and shales, at least 4 km thick) in the Cameros Basin underwent low-grade thermal metamorphism; isotopic dating of illite yields an age around 100 Ma (between 86 and 108 Ma) for the peak conditions (Goldberg et al., 1988; Casquet et al., 1992) that post-dates the extensional phase. It is also younger than cleavage-related folding because of textural relationships of the metamorphic minerals (Mata et al., 2001). The maximum temperature was 350°C in the deepest buried rocks (uniquely high for the Iberian Chain) that were at a low pressure of < 2 kbar (Mata et al., 2001). The geothermal gradients are 27-41°C/km for the extensional stage and 70° C/km during the thermal peak (Mata et al., 2001). Fluid inclusions in quartz veins point to a local, within basin scale, origin of the fluid (Mata et al., 2001). While the hematite is formed or recrystallized during the metamorphism, it is unlikely that the remagnetization is thermoviscous because the available temperature-time period is too short to explain the maximum unblocking temperatures observed in the hematite. Indeed Villalaín et al. (2003) relate the remagnetization to subsidence – first mainly tectonic and later also thermal – in an elevated geothermal gradient regime in a stretched lithosphere. This situation is feasible since Iberia was moving eastward with respect to stable Europe as a consequence of the opening of the Atlantic Ocean.

This study shows that although the remagnetization in the four basins occurred at different times, they are all somehow related to the rifting phase in their geological history, in line with other remagnetization found in Iberian sedimentary basins formed under basinal rifting (e.g. Galdeano et al., 1989; Moreau et al., 1992; Moreau et al., 1997; Márton et al., 2004). Under syn-rift and early post-rift conditions an elevated geothermal regime prevails. It is the interplay of the geothermal gradient and burial depth that determines when the diagenetic reactions set in that result in the remagnetization. In Iberia this has led to a mozaic of remagnetized basins without a clear regional trend. Because of their distinct timing a single Iberia-wide mechanism can now be excluded and mechanisms that operate on a basin scale are favoured. We envisage that the approach applied here can be utilized elsewhere to constrain the remagnetization timing and mechanism where remagnetization can be broadly related to rotation of (micro) plates.

6 Conclusions

To determine the timing of the regional Cretaceous remagnetizations in northern Iberia, we provide new data from the Organyà Basin, where both the age and the corresponding paleomagnetic direction of the remagnetization is well-established. To this end, we apply the small circle intersection (SCI) method, and restore a direction of D/I = 316.8°/54.8° (with a_{95} = 3.3) closely corresponding to a recently improved apparent polar wander path (APWP) of Iberia. We also compare previously published results from three other basins – the Cabuérniga and Cameros Basins and the Iberian range – to the APWP of Iberia. We draw the following conclusions:

1. Application of the SCI method allows us to show that most of the remagnetized beds of the Organyà Basin were already tilted by ~15-20° as a result of half-graben formation starting prior to remagnetization.
2. Each of the four remagnetized basins provides a different paleomagnetic direction during remagnetization and, therefore, each basin acquired its remagnetization at different moments. Comparison of these directions to the Iberian APWP shows that the remagnetizations occurred at the onset of, during, and at the end of, or after the Iberian rotation in Aptian to early Albian times.
3. The remagnetization events were – albeit occurring on a regional scale over a period of at least ~10-15 Myr – confined to these individual sedimentary basins.
4. Although the remagnetization in all four locations occurred at the different times, they are all temporally related to the rifting phase in their geological history. The Cretaceous Iberian remagnetization events in northern Iberia are hence temporally related to the extensional tectonics.
5. Existing explanations for remagnetization that can occur on the scale and within the context of sedimentary basins, including elevated temperatures during diagenesis and circulating basin fluids may therefore be the most reasonable explanations. There is no need to infer more speculative Iberia-wide mechanisms.

Acknowledgements

We thank Cor Langereis for discussion, and motivating us to prepare this paper. Thanks to Rien Rabbers for helping the Organyà Basin map. This PhD project is supported by the Vening Meinesz Research School of Geodynamics (VMSG), with financial aid from the Department of Earth Sciences of the Faculty of Geosciences, Utrecht University, The Netherlands.

References

Becker, E., 1999. Orbitoliniden-Biostratigraphie der Unterkreide (Hauterive-Barrême) in den spanischen Pyrenäen (Profil Organyà, Prov. Lérida). Rev. Paléobiol., Genève 18, 359-489.

Bernaus, J.M., Arnaud-Vanneau, A., Caus, E., 1999. La sedimentación "Urgoniense" en la cuenca de Organyà (NE

España). Libro homenaje a José Ramírez del Pozo. De Geol. Y Geofis. Españoles del Petróleo AGGEP, 71-80.
Bernaus, J.M., 2000. L'Urgonien du Bassin d'Organyà (NE de l'Espagne): micropaléontologie, sédimentologie et stratigraphie séquentielle. Mém. H. S. 33, 138.
Bernaus, J.M., Caus, E., Arnaud-Vanneau, A., 2000. Aplicación de los análisis micropaleontológicos cuantittivos en estratigrafía secuential: El Cretácico inferior de la cuenca de Organyà (Pirineos, España). Rev. Soc. Geol. España 13, 55-63.
Bernaus, J.M., Arnaud-Vanneau, A., Caus, E., 2003. Carbonate platform sequence stratigraphy in a rapidly subsiding area: the Late Barremian – Early Aptian of the Organya basin, Spanish Pyrenees. Sedimentary Geology 159, 177-201.
Besse, J., Courtillot, V., 2002. Apparent and true polar wander and the geometry of the geomagnetic field over the last 200 Myr. J. Geoph. Res. 107, doi:10.1029/2000JB000,050.
Blumstein, A.M., Elmore, R.D., Engel, M.H., Elliot, C., Basu, A., 2004. Paleomagnetic dating of burial diagenesis in Mississippian carbonates, Utah. Journal of Geophysical Research 109, B04101, doi: 10.1029/2003JB002698.
Bond, R.M.G., McClay, K.R., 1995. Inversion of a Lower Cretaceous extensional basin, south central Pyrenees, Spain, in: Buchanan, P.G. (Eds.), Basin Inversion. Geol. Soc. Spec. Publ., pp. 88.
Bullard, E., Everett, J., Gilbert Smith, A., 1965. A symposium on continental drift. in, Phil. Trans. R. Soc. Lond. Ser. A.,41-51.
Cande, S.C., Kent, D.V., 1992. A new geomagnetic polarity time scale for the late Cretaceous and Cenozoic. Journal of Geophysical Research 97, 13917-13951.
Carey, S.W., 1958. A tectonic approach to continental drift. in, Symposium on Continental Drift.Hobart (Tasmania),177-355.
Casas, A.M., Villalaín, J.J., Soto, R., Gil-Imaz, A., del Río, P., Fernández, G., 2008. Multidisciplinary approach to an extensional syncline model for the Mesozoic Cameros Basin (N Spain). Tectonophysics in press.
Casquet, A., Galindo, C., González-Casado, J.M., Alonso, A., Mas, R., Rodas, M., García, E., Barrenechea, J.F., 1992. El metamorfismo en la cuenca de los Cameros.Geocronologíae implicaciones tectónicas. Geogaceta 11, 22-25.
Dinarès-Turell, J., García-Senz, J., 2000. Remagnetization of Lower Cretaceous limestones from the southern Pyrenees and relation to the Iberian plate geodynamic evolution. J. Geophys. Res. 105, 19405-19418.
Elmore, R.D., Dulin, S., Engel, M.H., Parnell, J., 2006a. Remagnetization and fluid flow in the Old Red Sandstone along the Great Glen Fault, Scotland. Journal of Geochemical Exploration 89, 96-99.
Elmore, R.D., Foucher, J.L.E., Evans, M.A., Lewchuk, M.T., Cox, E., 2006b. Remagnetization of the Tonoloway Formation and the Helderberg Group in the Central Appalachians: testing the origin of syntilting magnetizations. Geophys, J. Int. 166, 1062-1076.
Enkin, R.J., Mahoney, J.B., Baker, J., Kiessling, M., Haugerud, R.A., 2002. Syntectonic remagnetization in the southern Methow block: Resolving large displacements in the southern Canadian Cordillera. Tectonics 21, ISI:000179018800001.
Enkin, R.J., 2003. The direction-correction tilt test: an all-purpose tilt/fold test for paleomagnetic studies. Earth and Planetary Science Letters 212, 151-166.
Evans, M.A., Lewchuk, M., T., Elmore, R.D., 2003. Strain partitioning of deformation mechanisms in limestones: examining the relationship of strain and anisotropy of magnetic susceptibility (AMS). Journal of structural geology 25, 1525-1549.
Fisher, R.A., 1953. Dispersion on a sphere. Proceedings of the Royal Society London 217A, 295-305.
Galdeano, A., Moreau, M.G., Pozzi, J.P., Berthou, P.Y., Malod, J.A., 1989. New Paleomagnetic Results from Cretaceous Sediments near Lisbon (Portugal) and Implications for the Rotation of Iberia. Earth and Planetary Science Letters 92, 95-106.
García-Senz, J., 2002. Cuencas extensivas del Cretacico Inferior en los Pireneos Centrales – formacion y subsecuente inversion. [PhD thesis]. University of Barcelona, Barcelona.
Goldberg, J.M., Guiraud, M., Maluski, H., Séguret, M., 1988. Caractères pétrologiques etâge du métamorphisme en contexte distensif du bassin sur décrochement de Soria Crétacéinférieur, Nord Espagne). Comptes rendus de l'Académie des sciences, Paris 307, 521-527.
Gong, Z., Dekkers, M.J., Dinarès-Turell, J., Mullender, T.A.T., 2008a. Remagnetization mechanism of Lower Cretaceous rocks from the Organyà Basin (Pyrenees, Spain). Studia Geoph. Geod. 52, 187-210.
Gong, Z., Langereis, C.G., Mallender, T.A.T., 2008b. The rotation of Iberia during the Aptian and the opening of the Bay of Biscay. Earth and Planetary Science Letters 273, 80-93.
Juárez, M.T., Lowrie, W., Osete, M.L., Meléndez, G., 1998. Evidence of widespread Crataceous remagnetisation in the Iberian Range and its relation with the rotation of Iberia. Earth Planet. Sci. Lett. 160, 729-743.
Katz, B., Elmore, R.D., Cogoini, M., Ferry, S., 1998. Widespread chemical remagnetization: Orogenic fluids or burial diagenesis of clays? Geology 26, 603-606.
Katz, B., Elmore, R.D., Cognoini, M., Engel, M.H., Ferry, S., 2000. Associations between burial diagenesis of smectite, chemical remagnetization, and magnetite authigenesis in the Vocontian trough, SE France. J. Geophys. Res. 105, 851-868.
Kent, D., 1985. Thermoviscous remagnetization in some Appalachian limestones. Geophyscal research letter 12, 805-808.
Kirschvink, J.L., 1980. The least-squares line and plane and the analysis of palaeomagnetic data. Geophysical Journal of the Royal Astronomical Society 62, 699-718.
Machel, H.G., Cavell, P.A., 1999. Low-flux, tectonically-induced squeegee fluid flow ("hot flash") into the Rocky Mountain Foreland Basin. Bulletin of Canadian Petroleum Geology 47, 510-533.
Márton, E., Abranches, M.C., Pais, J., 2004. Iberia in the Cretaceous: new paleomagnetic results from Portugal. Journal of Geodynamics 38, 209-221.

Mata, M.P., Casas, A., Cil, A., Pocovi, P., 2001. Thermal history during Mesozoic extension and Tertiary uplift in the Cameros Basin, northern Spain. Basin Res. 13, 91-111.

McCabe, C., Van der Voo, R., Peacor, D.R., Scotese, C.R., Freeman, R., 1983. Diagenetic magnetite carries ancient yet secondary remanence in some Paleozoic sedimentary carbonates. Geology 11, 221-223.

McCabe, C., Elmore, R.D., 1989. The occurrence and origin of Late Paleozoic remagnetization in the sedimentary rocks of North America. Reviews of Geophysics 27, 471-494.

Moreau, M.G., Canerot, J., Malod, J.A., 1992. Paleomagnetic study of Mesozoic sediments from the Iberian Chain (Spain) Suggestions for Barremian remagnetization and implications for the rotation of Iberia. Bull. Soc. Géol. France 163, 393-402.

Moreau, M.G., Berthou, J.Y., Malod, J.-A., 1997. New paleomagnetic Mesozoic data from the Algarve (Portugal): fast rotation of Iberia between the Hauterivian and the Aptian. Earth and Planetary Science Letters 146, 689-701.

Morris, A., Robertson, A.H.F., 1993. Miocene remagnetisation of carbonate platform and Antalya Complex units within the Isparta Angle, SW Turkey. Tectonophysics 220, 243-266.

O'Brien, V.J., Moreland, K.M., Elmore, R.D., Engel, M.H., Evans, M.A., 2007. Origin of orogenic remagnetizations in Mississippian carbonates, Sawtooth Range, Montana. J Geophys. Res. 112, B06103, doi:10.1029/2006JB004699.

Ogg, J.G., Agterberg, F.P., Gradstein, F.M., 2004. The Cretaceous Period, in: Smith, A.G. (Eds.), A Geologic Time Scale 2004. Cambridge University Press, Cambridge, pp. 589.

Oliver, J., 1986. Fluids expelled tectonically from orogenic belts: their role in hydrocarbon migration and other geologic phenomena. Geology 14, 99-102.

Shipunov, S.V., 1997. Synfolding magnetizations: detection, testing and geological applications. Geophys. J. Int. 130, 405-410.

Sibuet, J.C., Srivastava, S.P., Spakman, W., 2004. Pyrenean orogeny and plate kinematics. J. Geophys. Res. 109, B08104, doi: 10.1029/2003JB002514.

Soto, R., Villalaín, J., J., Casas-Sainz, A., M., 2008. Remagnetizations as a tool to analyze the tectonic history of inverted sedimentary basins: A case study from the Basque-Cantabrian basin (north Spain). Tectonics 27, doi:10.1029/2007TC002208.

Srivastava, S.P., Schouten, H., Roest, W.R., Klitgord, K.D., Kovacs, L.C., Verhoef, J., Macnab, R., 1990. Iberian plate kinematics: a jumping plate boundary between Eurasia and Africa. Nature 344, 756-759.

Srivastava, S.P., Sibuet, J.C., Cande, S., Roest, W.R., Reid, I.D., 2000. Magnetic evidence for slow seafloor spreading during the formation of the Newfoundland and Iberian margins. Earth and Planetary Science Letters 182, 61-76.

Torsvik, T., Muller, R.D., Van der Voo, R., Steinberger, B., Gaina, C., 2008. Global plate motion frames: Toward a unified model. Rev. Geophys. 46, RG3004, doi:10.1029/2007RG000227.

Van der Voo, R., 1967. The rotation of Spain: palaeomagnetic evidence from the Spanish Meseta. Palaeogeography, Palaeoclimatology, Palaeoecology 3, 393-416.

Van der Voo, R., 1969. Paleomagnetic evidence for the rotation of the Iberian Peninsula. Tectonophysics 7, 5-56.

Vergés, J., Fernàndez, M., Martínez, A., 2002. The Pyrenean orogen: pre -, syn -, and post – collisional evolution. Journal of the virtual explorer 8, 57 – 76.

Villalain, J.J., Osete, M.L., Vegas, R., Garciaduenas, V., Heller, F., 1994. Widespread Neogene Remagnetization in Jurassic Limestones of the South-Iberian Palaeomargin (Western Betics, Gibraltar Arc). Physics of the Earth and Planetary Interiors 85, 15-33.

Villalaín, J.J., G., F.-G., M., C.A., A., G.-I., 2003. Evidence of a Cretaceous remagnetization in the Cameros Basin (North Spain): implications for basin geometry. Tectonophysics 377, 101-117.

Waldhör, M., Appel, E., 2006. Intersections of remanence small circles: new tools to improve data processing and interpretation in palaeomagnetism. Geophys, J. Int. 166, 33 – 45.

Zijderveld, J.D.A., 1967. A.C. Demagnetization of rocks: analysis of results, in: Runcorn, S.K. (Eds.), Methods in Palaeomagnetism. Elsevier, New York, pp. 254-286.

CHAPTER 5

End-member modeling of isothermal remanent magnetization (IRM) acquisition curves: a novel approach to diagnose remagnetization

Z. Gong[1], M. J. Dekkers[1], D. Heslop[2], T.A.T. Mullender[1]
[1] Paleomagnetic Laboratory Fort Hoofddijk, Dept. of Earth sciences, Utrecht University, Budapestlaan 17, 3584 CD Utrecht, The Netherlands
[2] Universität Bremen, FB Geowissenschaften, Postfach 330440, 28334 Bremen, Germany
(submitted to GJI)

Abstract

To identify remagnetization is essential for paleomagnetic studies and their geodynamic implications. The traditional approach is often based on directional analysis of paleomagnetic data and field tests which may be inconclusive if the apparent polar wander path (APWP) is poorly constrained or the remagnetization predates folding. In several cases, rock magnetic work, particularly, measurement of hysteresis loops allows identification of the so-called "remagnetized" and "non-remagnetized" trends. However, for weakly magnetic samples this approach can be equivocal.

Here, in order to improve the diagnosis of remagnetization, we investigated 192 isothermal remanence magnetization (IRM) acquisition curves (up to 700 mT) of remagnetized and non-remagnetized limestones from the Organyà Basin, northern Spain. Also 96 IRM acquisition curves from non-remagnetized marls were studied as a cross-check for the non-remagnetized limestones.

A non-parametric end-member modeling is used to explain of the IRM acquisition data sets. First remagnetized and non-remagnetized groups were treated separately. Two or three end-members were found to adequately describe the data variability: one end-member represents the high-coercivity contribution while the low-coercivity part can be described by either one end-member or two reasonably similar end-members. In the remagnetized limestones the low coercivity end-members tend to saturate at higher field values than in the non-remagnetized limestones. When the entire data set was processed together, a three end-member model was judged optimal. This model consists of a high coercivity end-member, a low-coercivity end-member that saturates at ~300-400 mT and a low-coercivity end-member that approximately saturates in 700 mT. Higher contributions of the latter end-member appear to occur dominantly in the remagnetized limestones while the reverse is true for the non-remagnetized limestones, so they plot in clearly distinguishable areas. Meanwhile, the IRM curves from non-remagnetized marls show a behavior similar to the non-remagnetized end-member in the limestones. Therefore, this new approach can be a very useful tool to diagnose remagnetization in weakly magnetic limestones and marls. We recommend applying it to other areas of potentially remagnetized low intensity sediments.

Keywords: Remagnetization, End-member modeling, IRM acquisition curves, Organyà Basin, limestone, marl

1 Introduction

Remagnetization in sedimentary rocks often provides important information on geological features and processes (i.e., diagenesis, tectonic motion, fluid migration, thermal events). It has only recently become apparent that remagnetization may be much more widespread than previously considered. Sediments in forelands and outer margins of orogenic zones, which were often supposed to deliver high-quality paleomagnetic data, are increasingly reported to be remagnetized. This applies as well to many of the Mesozoic Iberian basins (e.g., Galdeano et al., 1989; Moreau et al., 1992; Moreau et al., 1997; Juárez et al., 1998; Dinarès-Turell and García-Senz, 2000; Villalaín et al., 2003; Márton et al., 2004; Gong et al., 2008a; Soto et al., 2008).

To diagnose remagnetization, classical methods focus on the analysis of paleomagnetic directions and polarity patterns. By comparing the observed paleomagnetic polarities to the standard geomagnetic polarity time scale (GPTS) for the age range of interest or the paleomagnetic directions to the regional apparent polar wander path (APWP), remagnetization may be recognized. Also field tests (e.g., the fold test) are used in many cases to distinguish remagnetized natural remanent magnetization (NRM). In most studies, a pre-folding magnetization is taken to be primary, however, this is not always the case. Remagnetization can occur any time during the geological history: pre-folding (e.g. Perroud and Van der Voo, 1984), syn-folding (e.g. Kent and Opdyke, 1985) or post-folding (e.g. Stearns and Van der Voo, 1987). When the remagnetized component has completely overprinted the original NRM component and passes field tests, its recognition is hard. Furthermore, directional NRM analysis to establish a remagnetized rock sequence is not an entirely independent method of analysis. Hence if there is a consistent way to describe (differences in) the properties of remagnetized and non-remagnetized rocks, it would provide an independent method with which to identify the remagnetization.

For limestones, in a number of cases remagnetized rocks have distinct magnetic hysteresis properties and the so-called remagnetized and non-remagnetized trends are recognized on the 'Day plot' (Day et al., 1977; Jackson, 1990; Channell and McCabe, 1994). It should be noted, however, that in a strict sense these trends on the Day plot apply to samples that only contained magnetite. Mixed magnetic mineralogy biases the area where the samples would plot. The neoformed magnetite particles are very fine-grained and close to the superparamagnetic threshold. This is supported by fairly low maximum unblocking temperatures in remagnetized limestones ranging between 480 and 530°C (e.g. Zegers et al., 2003). Dunlop (2002a; 2002b) modelled the hysteresis parameters for different proportions of superparamagnetic and larger magnetite particles and could reproduce the trends observed by Channell and McCabe (1994). However, the amount of magnetic minerals in limestones is often very low yielding low-intensity remanences that may complicate their meaningful measurement. Also it is not uncommon that remagnetized rocks plot in between those two trends (e. g. Katz et al., 2000; Zegers et al., 2003). Indeed Lanci and Kent (2003) modeled positions on the Day plot intermediate between the two trends if thermal activation was included in the modeling. Relying solely on whether or not a sample suite plots on the remagnetized trend is therefore somehow equivocal. As mentioned before, mixed magnetic mineralogy may have a biassing effect. Hence, other types of analysis are needed.

Rock magnetic properties are used in this context, in particular the analysis of anhysteretic remanent magnetization (ARM) and isothermal remanent magnetization (IRM) properties. Because the specific ARM of magnetite – particularly when it is fine-grained – is so high, ARM is biased with respect to magnetite. IRM gives a more complete picture of the magnetic mineralogy because the high-coercivity minerals are included. As is the case for ARM, IRM is also sensitive to the grain size of the magnetic particles. Compared to other rock magnetic parameters, IRM can be faithfully measured on very weak magnetic samples because high applied fields are used for its acquisition. When a small amount of a high-coercivity mineral (like hematite) is present together with a dominant low-coercivity mineral (like magnetite) it is often difficult to detect the former on hysteresis loops, but it is easily identifiable with IRM acquisition curves. These advantages make IRM acquisition curves suitable for the analysis of remagnetization in generally weak limestones.

To investigate the coercivity contributions of different minerals to measured IRM acquisition curves, a number of techniques have been developed (Robertson and France, 1994; Stockhausen, 1998; Kruiver et al., 2001; Heslop et al., 2002; Egli, 2003; Heslop et al., 2004). For IRM acquisition curves consisting of at least of 25 data points, cumulative log Gaussian (CLG) modeling can be applied (Kruiver et al., 2001; Heslop et al., 2002; Heslop et al., 2004). However, this modeling is based on base function fitting, it relies on the assumption that all coercivity components conform to a cumulative Gaussian distribution in the log-field space. Also the more generalized

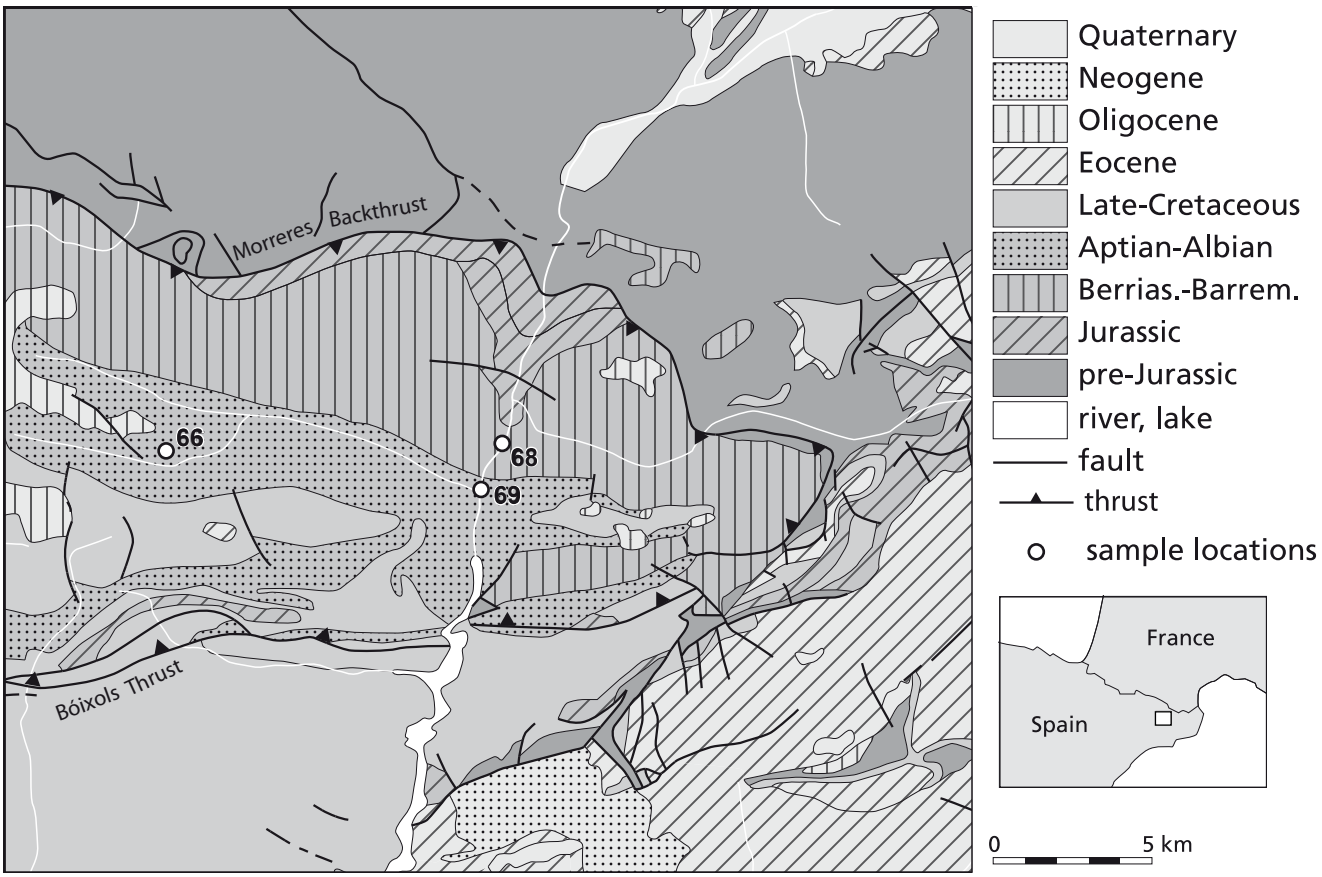

Figure 1 Schematic geological map of the Organyà Basin with the locations of the sampling sites; numbers refer to those with "OR" reported in text and the Supplementary Table. At the bottom right, the study area is indicated by a white square on the topographic map.

Skewed Generalized Gaussian fitting approach proposed by Egli (2003) relies on a set of base functions. To avoid potential problems with proper base function selection, here we apply end-member modeling, a non-parametric technique (e.g. Weltje, 1997; Heslop and Dillon, 2007). It has been tested to evaluate its usefulness for unraveling basin fills in complex geotectonic settings (Weltje, 1997) and was applied to rock-magnetic analysis of diagenetic processes by Heslop and Dillon (2007). There is no assumption on base functions or even the end-members required. As end-member modeling makes use of inherent variability within a data set, a fair number of IRM acquisition curves (> 30) must be used as input. The only criterion is that the input curves must be monotonic. To this end, the measured IRM acquisition curves are normalized and smoothed. Another advantage of the end-member modeling is its rapidity that makes it possible to process the large IRM data sets within a reasonable amount of time. In this study, we will try to diagnose remagnetization in limestone by using the end-member method for the analysis of the IRM acquisition curve data sets.

The selected study area, Organyà Basin, is a Cretaceous Pyrenean basin, located in northern Spain (Fig. 1). It is a typical foreland basin. Therefore, the method developed in the Organyà Basin, may well be applicable elsewhere. The previous studies (Dinarès-Turell and García-Senz, 2000; Gong et al., 2008a) show that the Berriasian-Barremian limestone strata inside the Organyá Basin are remagnetized while the Aptian-Cenomanian strata have a primary magnetization. The lithologies are limited to limestones and marls. There are remagnetized and non-remagnetized limestones, in contrast, all marls in the basin are non-remagnetized. Therefore we focus on the limestones, and use the marls only as a cross-check to investigate to what extent they would compare to the non-remagnetized limestone. If IRM properties can be consistently unraveled into non-remagnetized and remagnetized groups, it will provide a directionally independent method to recognize remagnetization that would complement existing remagnetization criteria.

2 Geological setting and sampling

The Organyà Basin is located in the southern Pyrenees, northern Spain (Fig. 1). It is an inverted basin, and experienced early Cretaceous extension as well as late Cretaceous to Miocene compression which led to the Pyrenean orogeny. There are around 4.5 km of Cretaceous limestones and marls deposited. Platform carbonates in a coastal lagoonal environment were deposited from the Berriasian to Barremian-lower Aptian. Three formations are distinguished: Barranc de la Fontanella, Hostal Nou and Prada Formations. From the Aptian to the Albian, the limestones change to marls when the basin rifting was maximal. The marls include the Cabó, Senyús, Font Bordonera and Lluçà Formations. In the marls, some limestone intercalations occur. The depositional environment became costal-marine. In the late Cretaceous, a post-rift platform carbonate formation was deposited, named the Santa Fè Formation.

In the Organyà Basin, the previous studies (Dinarès-Turell and García-Senz, 2000; Gong et al., 2008a) show that the carbonate rocks which comprise the lower part of the stratigraphy, from Berriasian to Barremian, are remagnetized. However, the upper part of the stratigraphy, which includes the marl formations and intercalated limestones and the youngest Santa Fè limestones, is not remagnetized. The associated rock magnetic studies show that the magnetic carrier is mainly magnetite with a small amount of goethite and hematite (Dinarès-Turell and García-Senz, 2000; Gong et al., 2008a; Gong et al., 2008b). Therefore, the remagnetization in the Organyà Basin cannot be precisely diagnosed by plotting on the Day plot.

We sampled 144 drilling cores from 3 sites (OR66, OR68 and OR69) in the Organyà Basin, 48 cores for each site, using a portable gasoline-powered drill (Fig. 1). Sites OR66, OR68, OR69 are from the top Senyús intercalation limestone (non-remagnetized), Hostal Nou limestone (remagnetized), and Cabó marls (non-remagnetized), respectively. Note that there is no remagnetized marl in the Organyà Basin. The paleomagnetic results from their sister samples were published by Gong et al. (2008b).

3 Methodology

In previous studies (Gong et al., 2008a; Gong et al., 2008b), we found that the optimal NRM demagnetization procedure for the low intensity samples in the Organyà Basin is: limestones thermally demagnetized to 150°C and marls thermally demagnetized to 210°C, followed by alternating field (AF) demagnetization up to 100 mT. The selected temperatures were considered to be an efficient method to remove the viscous remanence magnetization (VRM) with the advantage of avoiding the potential interference of oxidized rims of the magnetic particles (Van Velzen and Zijderveld, 1995). It may well be that the heating enhances the discrimination of the different IRM components. So, in this study, we also want to investigate how the IRM acquisition curves are influenced by the pre-heating treatment.

Two hundred and eighty eight specimens (2 specimens from each drilling core) were processed in six groups: remagnetized limestone with and without pre-heating to 150°C (48 samples in each group); non-remagnetized limestone with and without pre-heating to 150°C (48 samples in each group); non-remagnetized marls with and without pre-heating to 210°C (48 samples each). In order to compare the results, two specimens were taken from most of the individual cores (one reference specimen and one specimen which would be subjected to preheating).

For the determination of the IRM acquisition curves, the specimens were first AF demagnetized (three orthogonal axes at 300 mT) to minimize the influence of magnetic interaction and thermal activation (Heslop et al., 2004). The IRM was acquired until 700 mT with 30 small steps. IRM measurements were processed by an in-house developed robot, which let the samples pass-through a 2G Enterprises SQUID magnetometer (noise level 10^{-12} Am^2). The pre-heating treatment was done in a magnetically shielded, laboratory-built, furnace in the paleomagnetic laboratory at the University of Utrecht.

The end-member modeling algorithm (Weltje, 1997) is used for the interpretation of the IRM curves in this study. It assumes that the measured data can be represented by a linear mixture of a number of invariant constituent components, which are

referred to as end-members. The use of least-squares estimation procedures enables the objective minimization of differences between measured compositions and calculated normative compositions, eliminating the need for prior knowledge of the magnetic minerals' properties (cf. Weltje, 1997). An underlying assumption of the end-member modeling algorithm is that the acquisition curves are monotonic, i.e. all the derivatives of the input data should be ≥ 0 (e.g. Heslop et al., 2007). When normalized to their maximum value the IRM curves form a closed data set, thus the abundances of the various end-members will not be independent and changes in the abundance of an end-member will naturally affect the abundances of the other end-members. Therefore to achieve a quantitative analysis, the signatures of the individual end-members must be understood.

After correction for the magnetic background and tray contributions, the IRM acquisition curves were processed as follows: (1) to be able to get meaningful components from the samples, IRM data were expressed on a mass-specific basis. (2) The end-member algorithm required data smoothing because it appeared to be sensitive to small deviations from a monotonically increasing curve. Therefore, small negative IRM data points at low fields were transferred to zero in order to comply with the requirements of the end-member modeling. The IRM acquisition curves were smoothed using an optimally smooth monotonic spline (e.g. Zhang, 2004). (3) Samples which appeared to be either too sensitive to small deviations in the tray contribution during the IRM acquisition or which showed the effects of gyroremanent magnetization (GRM) (Dankers and Zijderveld, 1981) were removed from the data set. (4) The coefficient of determination (r^2) for different numbers of end-members (from 2 to 9) was calculated by running the end-member model in MATLAB, version 7.4.287 (R2007a). (5) The optimum number of end-members was determined based on the result from the previous step (detailed criteria will follow in next paragraph). (6) The end-member parameters were calculated for each end-member model.

In end-member modeling, estimation of the number of end members is a crucial step for the decomposition of the dataset. To decide how many meaningful end-members should be included in the end-member modeling procedure, the selection criterion is based on the calculation of the coefficient of determination (r^2, range from 0 to 1) between the input data and the end-member model (Heslop et al., 2007). If the number of the end-members is not sufficient to describe adequately the variance of the input dataset, the r^2 value will be low (< 0.5). For an optimum model, the r^2 value is high and the inclusion of additional end-members provides little improvement in the quality of the model. For this purpose, r^2 was calculated from 2 to 9 end-members for each of the analyzed datasets.

4 End-member modeling results

The end-member modeling results show that r^2 is ~ 0.7 for the 2 end-member models and 0.75 – 0.8 for the 3 end-member models for all limestone datasets. Previous rock magnetic studies have suggested that the magnetic carriers in these limestones are magnetite with a small amount of goethite and hematite (Dinarès-Turell and García-Senz, 2000; Gong et al., 2008a; Gong et al., 2008b). Based on the r^2 value and the mineralogy, two or three end-member models were selected.

In this study, we will mainly compare the end-member modeling results from IRM of the remagnetized and non-remagnetized limestones. After the selection process discussed above, 32 IRM acquisition curves from each remagnetized group and 48 IRM acquisition curves from each non-remagnetized group were used for the end-member model (Fig. 2). Compared to the IRM curves without pre-heating (Fig. 2a, g), those with pre-heating (Fig. 2b, h) show a somewhat more dispersed distribution. For the end-member modeling, the main difference between the pre-heated and non-pre-heated groups emerges in the lower coercivity components (solid line in the 2 end-member model and solid & long dashed line in the 3 end-member model), whilst the high coercivity component (short dashed line) remains similar in both the 2 and 3 end-member models.

In the remagnetized datasets with 2 end-members (Fig. 2c, d), the lower coercivity component (Fig. 2d) is saturated at ~500 mT in the pre-heated dataset. However, it is not saturated at 700 mT in the non-preheated dataset (Fig. 2c). The 3 end-member models (Fig. 2e, f) separate this lower coercivity component into two components. In the non-pre-heated group (Fig. 2e) the low coercivity components include a saturated component at ~700 mT and an unsaturated component until 700 mT; while in the pre-heated group (Fig. 2f) they involve a component saturated at ~400 mT and an unsaturated component until 700 mT.

For the non-remagnetized datasets (Fig. 2g, h), the behavior of the components between the pre-heated and non-pre-heated groups is very similar in both the 2 and 3 end-member models. In the case of 2 end-member (Fig. 2i, j), the low coercivity component saturates at ~400 mT; while in the 3 end-member model (Fig. 2k, l), one low coercivity component is saturated at ~300 mT and another one is not saturated until 700 mT. Note that the high coercivity components in the 2 end-member models (Fig. 2i, j) are different from the ones (Fig. 2k, l) from the 3 end-member models in the non-remagnetized groups. This may be caused by a high coercivity component that combines in the 2 end-member model with a separate low coercivity component while it remains a separate high coercivity component in the 3 end-member model. Therefore, by end-member modeling, we can see that the remagnetized data sets with pre-heating can be separated into the different coercivity components better than the ones without pre-heating. Also the 3 end-member model is better to identify the magnetic mineralogical properties for the remagnetized and non-remagnetized groups than the 2 end-member model.

Now we will merge the data sets to investigate whether the end-member algorithm can separate remagnetized and non-remagnetized limestones. The analysis will focus on comparing results from the datasets with pre-heating by a 3 end-member model.

5 Discussion and conclusions

Notable differences between the remagnetized and non-remagnetized rocks emerge in the 3 end-member model from the pre-heated limestone groups (Fig. 3b, d). The low coercivity

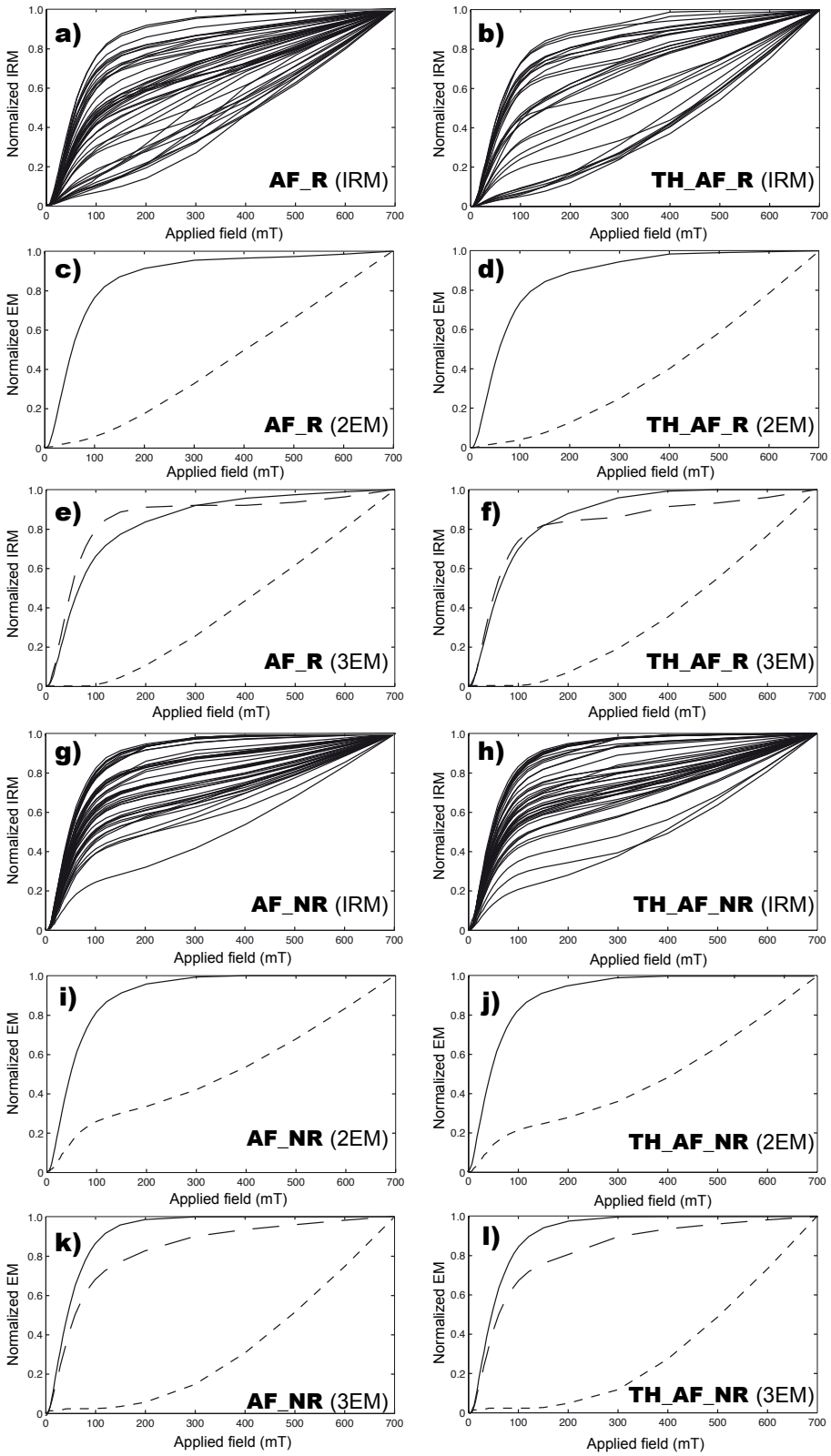

Figure 2 End-member models for the IRM acquisition curves from limestones. a) and b) are the IRM curves from the remagnetized datasets without pre-heating and with pre-heating (150°C), respectively. g) and h) are the IRM curves from the non-remagnetized datasets without pre-heating and with pre-heating (150°C), respectively. The examples of the 2 end-member and 3 end-member models are shown: c) and e) for the remagnetized datasets without pre-heating; d) and f) for the remagnetized datasets with pre-heating; i) and k) for the non-remagnetized datasets without pre-heating; j) and i) for the non-remagnetized datasets with pre-heating. In the end-member diagrams, short dashed lines indicate the high coercivity component (end-member 2 in the 2 end-member model and end-member 3 in the 3 end-member model); long dashed lines indicate the low coercivity component (end member 2 in the 3 end-member model); the solid lines indicate the low coercivity component (end-member 1 in both models).

component (end member 1, solid line) saturates at ~400 mT for the remagnetized limestone and at ~300 mT for the non-remagnetized limestones. Meanwhile, the other low coercivity component (end member 2, long-dashed line) and high coercivity component (end member 3, short-dashed line) are quite similar. For all the normalized IRM curves of limestone (Fig. 3e), 3 end-member models are considered to best describe the dataset because the 4 and 5 end-member models give an un-interpretable result. Based on all the normalized IRM distribution curves for the limestones only (Fig. 3e), however, we can not distinguish between the remagnetized and non-remagnetized groups by observation. Therefore, we turn to the end-members to find the solution.

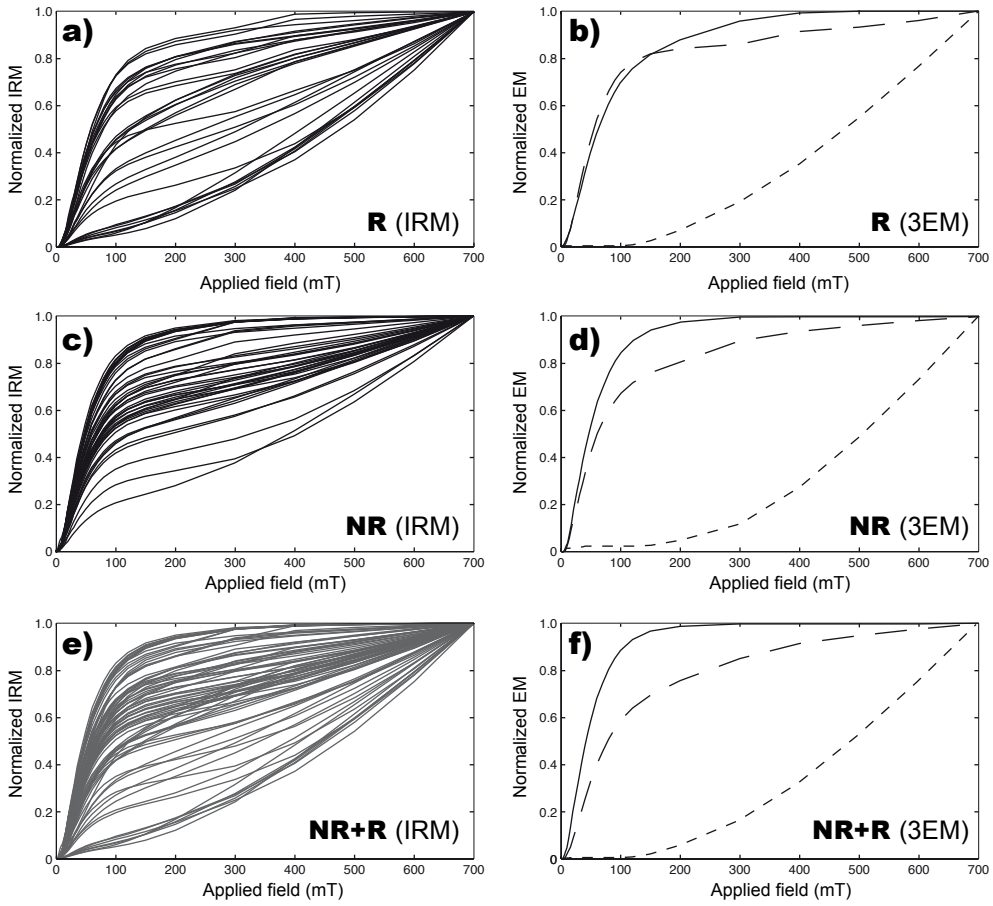

Figure 3 End-member models for IRM acquisition curves from limestone groups with pre-heating at 150°C. a). Normalized IRM curves from the remagnetized limestones. b). Derived 3 end-members for the remagnetized limestones. c). Normalized IRM curves from the non-remagnetized limestones. d). Derived 3 end-members for the non-remagnetized limestones. e). Normalized IRM curves from both the remagnetized and non-remagnetized limestones. f). Derived 3 end-members for the pre-heated limestones. In the end-member diagrams (b, d, f), the solid lines indicate the low coercivity component (end-member 1); long dashed lines indicate the low coercivity component (end-member 2); short dashed lines indicate the high coercivity component (end-member 3).

For the limestones with pre-heating in the 3 end-member models (Fig. 3b, d), end-member 1 is interpreted to be the magnetite component because it saturates at ~300 mT for the non-remagnetized dataset and ~ 400 mT for the remagnetized dataset. End-member 3 is not close to saturation at the maximum applied field (700 mT) and is interpreted to be hematite or goethite. End member 2 is close to saturation around 700 mT. We consider that end-member 2 could be very fine-grained magnetite, close to the SP threshold size. Also clusters of magnetically interacting yet formally superparamagnetic particles of a few nanometers in size may cause this effect. It should be kept in mind that large SP particles saturate in fairly low applied fields leading to wasp-waisted hysteresis loops as regularly observed. Small SP particles may not even be saturated in 2 Tesla fields as shown by Dekkers and Pietersen (1992) for IRM acquisition curves of industrial fly ash. This neoformed fine-grained magnetite is the major contributor to the remagnetization in the Organyà Basin limestones. This interpretation is in line with the remagnetization studies in Paleozoic carbonates (Jackson, 1990) and the Vocontian trough (Katz et al., 2000). In the Organyà Basin, because of the low-intensity of the limestones, hysteresis measurements could not provide reliable data for many samples to investigate the existence of SP magnetite (Gong et al., 2008a). For a more robust analysis in the Organyà Basin, future work could include scanning electron microscopy (SEM) and particularly transmission electron microscopy (TEM) analysis to visualize the SP particles.

The 3 end-members from the limestone datasets with pre-heating (Fig. 4, Supplementary Table) show distinguishable distributions between the remagnetized and non-remagnetized groups. In the remagnetized group (Fig. 4a), the percentage of end-member 1 varies from 0-50% with most samples having less than 10%. End-members 2 and 3 have a broad distribution, varying from 0 to 90%. End-member 2 mostly contributes a high percentage (50-90%) to the IRM, while end-member 3 generally has low contributions below 10%. On the contrary, in the non-remagnetized dataset, end-member 1 is found to contribute mostly in the region of 40% to 80%, indicating a large influence on the IRM. The contribution of end-member 2 is mostly less than 40% and end-member 3 is typically less than 50%. Comparing the percentage of the end-members in the IRM curves from the pre-heated limestones, the low coercivity component end-member 1 dominates in the non-remagnetized limestones while the other low coercivity component end-member 2 dominates in the remagnetized limestones. The high

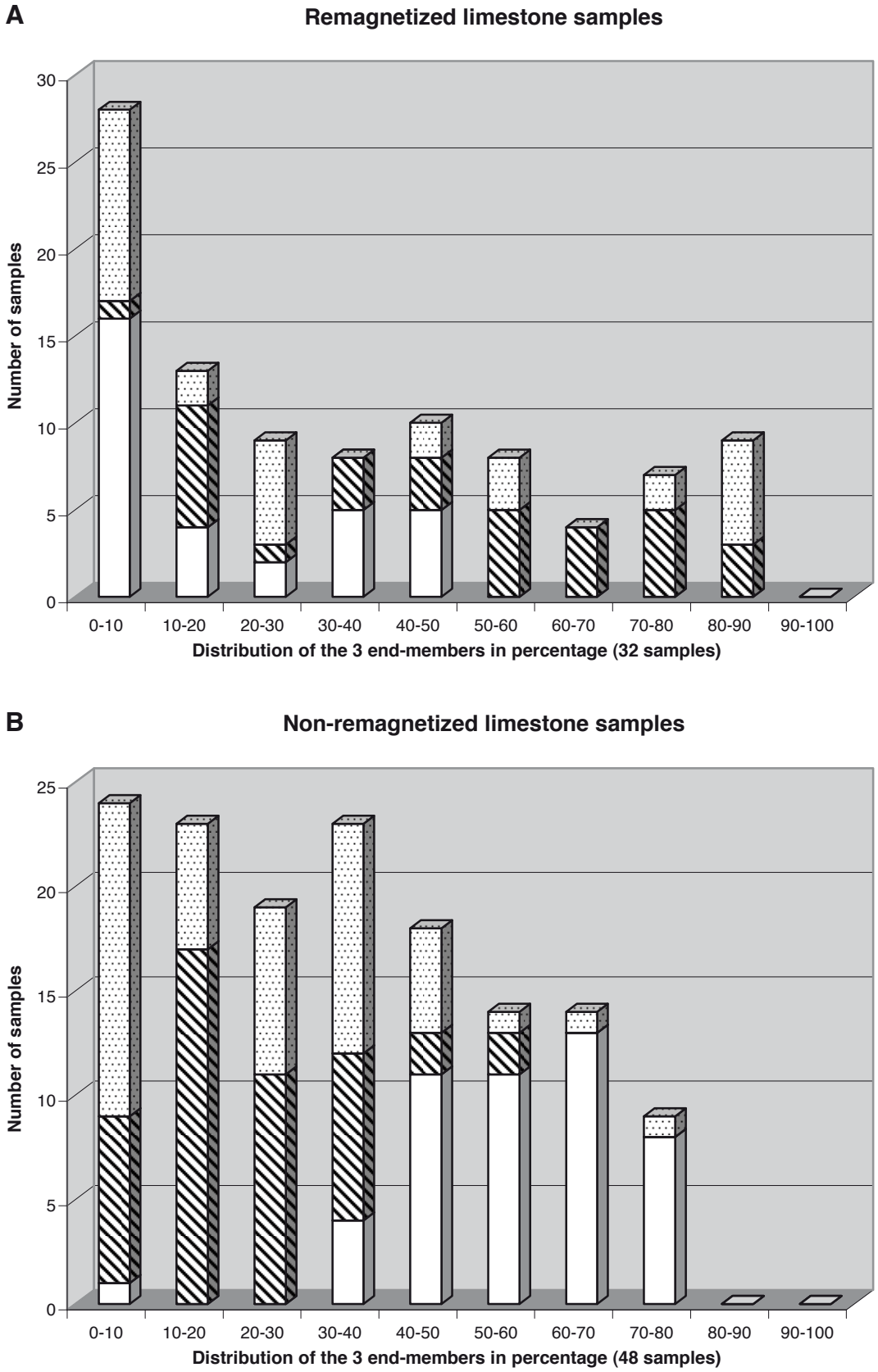

Figure 4 Histograms of the percentage of the 3 end-members in the end-member model from the limestones with pre-heating. White bars indicate end-member 1; obliquely shaded rectangles denote end-member 2; doted bars represent end-member 3. A). End-member partitioning in the remagnetized limestones. B) End-member partitioning in the non-remagnetized limestones expressed as percentages.

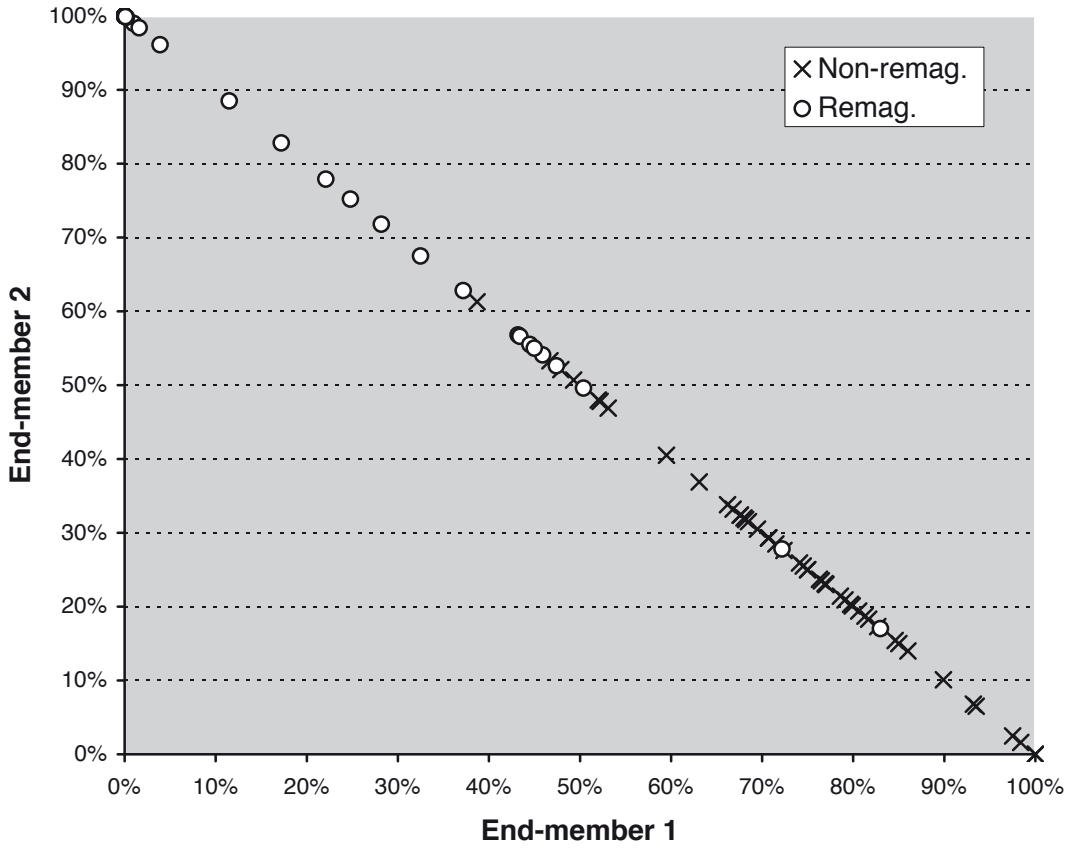

Figure 5 The contribution of end-member 1 vs end-member 2 corrected for the (variable) contribution of end-member 3 (the high coercivity end member) for the limestone dataset with pre-heating at 150°C. The open dots indicate the remagnetized data, while the crosses denote the non-remagnetized data. Note that the remagnetized and non-remagnetized designation is independent of the end-member model.

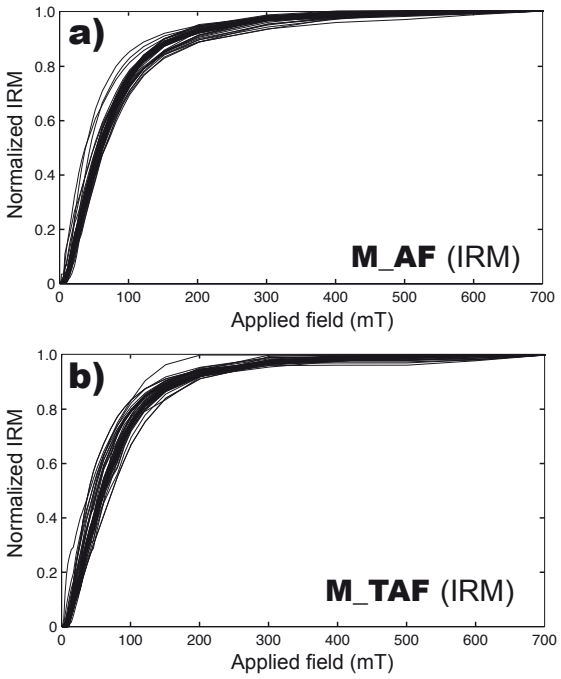

Figure 6 IRM acquisition curves from the marl groups with and without pre-heating at 210°C. a). Normalized IRM curves from the marls dataset without pre-heating. b). Normalized IRM curves from the marls dataset with pre-heating. Solid lines indicate end-member 1; long dashed lines indicate end member 2.

coercivity component end-member 3 contribution is low in general.

After correction for the contribution of end-member 3, the diagram with end-member 1 versus end-member 2 (Fig. 5) demonstrates a clear separation of the remagnetized and non-remagnetized limestones with pre-heating. Generally speaking, the remagnetized limestones have a high percentage of end-member 2, while the non-remagnetized limestones have a high percentage of end-member 1. This remarkable discovery can lead to an alternative method in the future to recognize remagnetization independently from the analysis of paleomagnetic directions.

The end-member modeling results from the non-remagnetized marls shows a very similar behavior for the non-heated and pre-heated groups (Fig. 6). This concurs with the observation in the non-remagnetized limestones that there is no distinguishable difference between the pre-heated and non-heated datasets. Here we concentrate on the pre-heated marl data set for the sake of comparison. The marl data are very uniform and the IRM acquisition curves tend to saturate at 300 mT (without a meaningful high-coercivity contribution), strongly supporting their non-remagnetized nature. The curves can be considered as a single end-member because if calculated for two or a higher number of end-members their shape appears to be very similar which makes an interpretation hard. This low coercivity end-member is very similar to end-member 1 from the heated non-remagnetized limestone samples.

Acknowledgements

This PhD project is supported by the Vening Meinesz Research School of Geodynamics (VMSG), with financial aid from the Department of Earth Sciences of the Faculty of Geosciences, Utrecht University, The Netherlands. The robotized 2G SQUID magnetometer was financed by the Netherlands Organization for Scientific Research (NWO). Thanks to Rien Rabbers for helping the Organyà Basin map.

References

Channell, J.E.T., McCabe, C., 1994. Comparison of Magnetic Hysteresis Parameters of Unremagnetized and Remagnetized Limestones. J Geophys Res-Sol Ea 99, 4613-4623.

Dankers, P., Zijderveld, J.D.A., 1981. Alternating field demagnetizatiof rocks, and the problem of gyromagetic remanence. Earth Planet. Sci. Lett. 53, 89-92.

Day, R., Fuller, M.D., Schmidt, V.A., 1977. Hysteresis properties of titanomagnetites: Grain size and composition dependence. Phys. Earth Planet. Int. 13, 260-266.

Dinarès-Turell, J., García-Senz, J., 2000. Remagnetization of Lower Cretaceous limestones from the southern Pyrenees and relation to the Iberian plate geodynamic evolution. J. Geophys. Res. 105, 19405-19418.

Dunlop, D.J., 2002a. Theory and application of the Day plot (Mrs/Ms versus Hcr/Hc) 2. Application to data for rocks, sediments, and soils. J Geophys Res-Sol Ea 107, 10.1029/2001JB000487.

Dunlop, D.J., 2002b. Theory and application of the Day plot (Mrs/Ms versus Hcr/Hc) 1. Theoretical curves and tests using titanomagnetite data. J Geophys Res-Sol Ea 107, 10.1029/2001JB000486.

Egli, R., 2003. Analysis of the field dependence of remanent magnetization curves. J Geophys. Res. 108, 2081, doi:10.1029/2002JB002023.

Galdeano, A., Moreau, M.G., Pozzi, J.P., Berthou, P.Y., Malod, J.A., 1989. New Paleomagnetic Results from Cretaceous Sediments near Lisbon (Portugal) and Implications for the Rotation of Iberia. Earth Planet. Sci. Lett. 92, 95-106.

Gong, Z., Dekkers, M.J., Dinarès-Turell, J., Mullender, T.A.T., 2008a. Remagnetization mechanism of Lower Cretaceous rocks from the Organyà Basin (Pyrenees, Spain). Studia Geoph. Geod. 52, 187-210.

Gong, Z., Langereis, C.G., Mallender, T.A.T., 2008b. The rotation of Iberia during the Aptian and the opening of the Bay of Biscay. Earth Planet. Sci. Lett. 273, 80-93.

Heslop, D., Dekkers, M.J., Kruiver, P.P., Van Oorschot, I.H.M., 2002. Analysis of isothermal remanent magnetisation acquisition curves using the expectation-Maximisation algorithm. Geophys, J. Int. 148, 58-64.

Heslop, D., McIntosh, G., Dekkers, M.J., 2004. Using time- and temperature-dependent Preisach models to investigate the limitations of modelling isothermal remanent magnetization acquisition curves with cumulative log Gaussian functions. Geophys. J. Int. 157, 55-63.

Heslop, D., Dillon, M., 2007. Unmixing magnetic remanence curves without a priori knowledge. Geophys, J. Int. 170, 556-566.

Heslop, D., Dobeneck, T.v., Höcker, M., 2007. Using non-negative matrix factorization in the "unmixing" of diffuse reflectance spectra. Marine Geology 241, 63-78.

Jackson, M., 1990. Diagenetic Sources of Stable Remanence in Remagnetized Paleozoic Cratonic Carbonates – a Rock Magnetic Study. J Geophys Res-Solid 95, 2753-2761.

Juárez, M.T., Lowrie, W., Osete, M.L., Meléndez, G., 1998. Evidence of widespread Cretaceous remagnetisation in the Iberian Range and its relation with the rotation of Iberia. Earth and Planetary Science Letters 160, 729-743.

Katz, B., Elmore, R.D., Cognoini, M., Engel, M.H., Ferry, S., 2000. Associations between burial diagenesis of smectite, chemical remagnetization, and magnetite authigenesis in the Vocontian trough, SE France. J. Geophys. Res. 105, 851-868.

Kent, D., Opdyke, N., 1985. Multicomponent magnetizations from the Mississippian Mauch Chunk Formation of the central Appalachians and their tectonic implications. J Geophys. Res. 90, 5371-5383.

Kruiver, P.P., Dekkers, M.J., Heslop, D., 2001. Quantification of magnetic coercivity components by the analysis of acquisition curves of isothermal remanent magnetisation. Earth Planet. Sci. Lett. 189, 269-276.

Lanci, L., Kent, D., 2003. Introduction of thermal activation in forward modeling of hysteresis loops for single-domain magnetic particles and implications for the interpretation of the Day diagram. J Geophys. Res. 108, 10.1029/2001JB000944.

Márton, E., Abranches, M.C., Pais, J., 2004. Iberia in the Cretaceous: new paleomagnetic results from Portugal. J. Geodyn. 38, 209-221.

Moreau, M.G., Canerot, J., Malod, J.A., 1992. Paleomagnetic study of Mesozoic sediments from the Iberian Chain (Spain) Suggestions for Barremian remagnetization and implications for the rotation of Iberia. Bull. Soc. Géol. France 163, 393-402.

Moreau, M.G., Berthou, J.Y., Malod, J.-A., 1997. New paleomagnetic Mesozoic data from the Algarve (Portugal): fast rotation of Iberia between the Hauterivian and the Aptian. Earth Planet. Sci. Lett. 146, 689-701.

Perroud, H., Van der Voo, R., 1984. Secondary magnetizations from the Clinton-type iron ores of the Silurian Red Mountain Formation, Alabama. Eart Planet. Sci. Lett. 67, 391-399.

Robertson, D.J., France, D.E., 1994. Discrimination of remanence-carrying minerals in mixtures, using isothermal remanent magnetisation acquisition curves. Phys. Earth Planet. Inter. 82, 223-234.

Soto, R., Villalaín, J., J., Casas-Sainz, A., M., 2008. Remagnetizations as a tool to analyze the tectonic history of inverted sedimentary basins: A case study from the Basque-Cantabrian basin (north Spain). Tectonics 27, doi:10.1029/2007TC002208.

Stearns, C., Van der Voo, R., 1987. A paleomagnetic reinvestigation of the Upper Devonian Perry Formation:

Evidence for late Paleozoic remagnetization. Eart Planet. Sci. Lett. 86, 27-38.

Stockhausen, H., 1998. Some new aspects for the modelling of isothermal remanent magnetization acquisition curves by cumulative log Gaussian functions. Geophys. Res. Lett. 25, 2217-2220.

Van Velzen, A.J., Zijderveld, J.D.A., 1995. Effects of weathering on single-domain magnetite in Early Pliocene marine marls. Geophys. J. Int. 121, 267-278.

Villalaín, J.J., G., F.-G., M., C.A., A., G.-I., 2003. Evidence of a Cretaceous remagnetization in the Cameros Basin (North Spain): implications for basin geometry. Tectonophysics 377, 101-117.

Weltje, G.J., 1997. End-member modeling of Compositional data: numberical-statistical algorithms for solving the explicit mixing problem. Mathematical Geology 29, 503-549.

Zegers, T.E., Dekkers, M.J., Bailly, S., 2003. Late Carboniferous to Permian remagnetization of Devonian limestones in the Ardennes: Role of temperature, fluids, and deformation. J Geophys Res-Sol Ea 108, 2357.

Zhang, J.-T., 2004. A simple and efficient monotone smoother using smoothing splines. Journal of Nonparametric Statistics 16(5), 779-769. (doi: 10.1080/10485250410001681167).

Supplementary Table The percentage of each end-member in the 3 end-member model from the limestone dataset with pre-heating. EM = end-member.

Sample Code	EM1	EM2	EM3
OR66_03A	67.6%	32.4%	0.0%
OR66_10A	70.7%	29.3%	0.0%
OR66_11A	75.0%	25.0%	0.0%
OR66_12A	70.7%	29.3%	0.0%
OR66_13A	76.3%	23.7%	0.0%
OR66_17A	74.5%	25.5%	0.0%
OR66_18A	79.7%	20.3%	0.0%
OR66_21A	68.0%	32.0%	0.0%
OR66_23A	59.0%	40.2%	0.9%
OR66_24A	37.2%	34.3%	28.4%
OR66_26A	50.7%	46.4%	2.9%
OR66_27A	47.2%	51.4%	1.4%
OR66_28A	43.0%	37.9%	19.1%
OR66_30A	33.7%	53.5%	12.7%
OR66_31A	58.7%	29.2%	12.1%
OR66_32A	62.2%	36.4%	1.5%
OR66_34A	64.0%	32.7%	3.3%
OR66_35A	61.4%	21.4%	17.2%
OR66_36A	54.8%	25.2%	20.0%
OR66_37A	54.4%	16.7%	28.9%
OR66_38A	42.0%	16.0%	42.0%
OR66_39A	49.9%	16.6%	33.5%
OR66_40A	40.4%	17.7%	41.9%
OR66_41A	40.1%	10.6%	49.3%
OR66_42A	40.1%	0.6%	59.3%
OR66_43A	30.9%	31.8%	37.3%
OR66_44A	45.1%	21.0%	33.9%
OR66_45A	59.3%	14.3%	26.4%
OR66_46A	13.2%	15.1%	71.7%
OR66_47A	42.3%	10.6%	47.1%
OR66_48A	49.0%	13.4%	37.6%
OR66_49A	47.4%	19.7%	32.9%
OR66_04A	53.7%	16.1%	30.2%
OR66_51A	62.7%	1.6%	35.7%
OR66_52A	65.6%	11.6%	22.8%
OR66_54A	59.0%	0.0%	41.0%
OR66_55A	61.6%	14.2%	24.1%
OR66_56A	62.3%	4.3%	33.4%
OR66_57A	66.7%	15.0%	18.3%
OR66_58A	72.7%	5.3%	22.0%
OR66_59A	30.9%	0.0%	69.1%
OR66_05A	61.6%	10.0%	28.5%
OR66_60A	55.5%	6.3%	38.2%
OR66_61A	62.2%	13.0%	24.8%
OR66_62A	52.3%	15.7%	32.0%
OR66_63A	57.4%	10.5%	32.2%
OR66_64A	67.6%	32.4%	0.0%
OR66_7A	70.6%	28.2%	1.3%
OR68_15A	0.0%	22.6%	77.4%
OR68_17A	0.0%	17.3%	82.7%
OR68_18A	0.0%	16.4%	83.6%
OR68_20A	0.0%	15.5%	84.5%
OR68_22A	0.0%	10.7%	89.3%
OR68_23A	0.0%	17.2%	82.8%
OR68_30A	0.0%	13.8%	86.2%
OR68_31A	19.4%	4.0%	76.7%
OR68_33A	40.7%	15.6%	43.7%
OR68_35A	0.7%	69.3%	30.0%
OR68_37A	35.3%	46.3%	18.4%
OR68_38A	39.9%	39.3%	20.8%
OR68_40A	41.9%	49.3%	8.8%
OR68_41A	39.3%	51.2%	9.6%
OR68_42A	44.5%	55.5%	0.0%
OR68_43A	45.0%	55.0%	0.0%
OR68_45A	0.0%	77.6%	22.4%
OR68_46A	0.0%	85.9%	14.1%
OR68_47A	0.0%	73.5%	26.5%
OR68_48A	1.2%	76.8%	21.9%
OR68_50A	0.1%	56.5%	43.4%
OR68_51A	1.6%	39.7%	58.7%
OR68_53A	11.0%	38.6%	50.4%
OR68_55A	32.2%	66.9%	0.9%
OR68_58A	24.8%	75.2%	0.0%
OR68_59A	26.9%	68.4%	4.8%
OR68_60A	17.0%	81.8%	1.1%
OR68_61A	11.1%	85.4%	3.4%
OR68_64A	0.0%	47.2%	52.8%
OR68_67A	35.8%	60.4%	3.8%
OR68_69A	47.4%	52.6%	0.0%
OR68_72A	0.1%	77.6%	22.3%

Epilogue

The title of the proposal of this Ph.D project was: Remagnetization and fluid flow. During executing this project, two main challenges were encountered: (1) In the Organyà Basin, some of the marine sediments appeared to have a very low-intensity NRM and most of them could not be properly analyzed. To improve the paleomagnetic analysis, a new demagnetization protocol was developed consisting of first thermal demagnetization followed by alternating field demagnetization. During the project a fully robotized instrument set-up (a '2G' SQUID magnetometer with alternating field demagnetization) became on-stream. With the so-called '3-position protocol' that measures the paleomagnetic samples automatically in more than one position, the demagnetization results have been dramatically improved. We recommend at least exploring this demagnetization approach in future studies. (2) The second challenge was the absence of external fluid flow in the basin inferred from field observation. Hence, the fluid flow modeling component had to be abandoned and more emphasis than originally anticipated was put on classic paleomagnetic rotation studies that appeared to be very successful.

The timing of the Iberian rotation is now well constrained to the Aptian by this study, based on both paleomagnetic and oceanic magnetic anomaly datasets. This opens opportunities for further refinement of the reconstruction of Iberia rotation during the Cretaceous, and of the evolution of the Pyrenean orogen. Therefore, future kinematic studies are suggested in the following topics. (1) In terms of the geometry of Iberia, how big was the Iberian micro-plate during its rotation? This question may be answered by collecting information from several localities at the edges and outside the present Iberian plate boundary. (2) In terms of the kinematic reconstruction of the movement of Iberia during the Cretaceous, the proposed Iberian reconstruction fits both the geophysical and geological evidence, but still requires numerical model testing. This effort will have bearing on the evolution of small provinces (e.g. Arctic, Greenland, Rockall, Spitsbergen) but also the evolution of big plates (e.g. Eurasia, Africa and North America). (3) In terms of chronology, a more precise Cretaceous geological time scale is in need for linking the Iberian rotation to other global events. The latest geological time scale (2004) has still age errors of around 1 Myr for the Cretaceous stages. Recently, controversies have risen on the age of some of the Cretaceous stages which will need to be solved by improved radiometric dating.

In this thesis, the remagnetization in the Organyà Basin was studied in detail. The remagnetization occurred during the beginning of the Aptian, the onset of the Iberian rotation. The remagnetization mechanism is considered most likely burial in an elevated geothermal gradient during the syn-rifting phase. We also constrain the ages of remagnetization from three other regions. However, to get a solid image of the remagnetization mechanism throughout Iberia, more Mesozoic Iberian sedimentary basins must be investigated in detail, including their rifting and thermal geological history. According to our end-member modeling of the IRM curves, newly formed very fine-grained magnetite was proposed to likely have caused the remagnetization in the limestones from the Organyà Basin. To conclusively test this scenario, further detailed rock magnetic study together with scanning electron microscopy (SEM) and, in particular, transmission electron microscopy (TEM) observation will be needed.

Acknowledgements

I would like to acknowledge the following people for their contribution and support in producing this thesis.

First of all, I would like to thank my promoter Cor Langereis who helped a lot during my fieldworks and drilled thousands of cores for me. I greatly benefited from his patient explanations and accurate advices on the existing knowledge and problems on the tectonic implications of paleomagnetism. Special thanks for rescuing me from the "middle project crisis" and supporting me to explore the rotation of Iberia.

I am grateful to my co-promoter Mark Dekkers for teaching me all the details of rock magnetism and giving me the opportunities to attend conferences and training programs. I also want to thank him to pick up my English bugs and polish my writing. My special appreciation goes out to him for always being available during my final fighting for this thesis.

Not in the least Tom Mullender should be mentioned for all his support. Great thanks for his talent to get the first robot in paleomagnetism up and running during my Ph.D, which made this thesis possible. Thanks for his patience during the introduction of the instrumentation. He also became my initial Dutch language teacher.

I appreciate that Douwe van Hinsbergen gave a big hand in the final stage of this thesis. Thanks for his inspiration, enthusiasm and support as a great team player. Thanks to him for teaching me the "potential rules" for writing a paper and demonstrating me how to write a paper as an art work. It has been really pleasant to work with you and I enjoyed it a lot.

Thanks to Wout Krijgsman for always giving valuable advices during my Ph.D study and supplying useful future opportunities at the end of my Ph.D.

Thanks to Reinoud Vissers who spent his valuable time listening to my Organyà stories no matter how "funny" they were at the beginning stages. I appreciate very much that you were always giving priority to helping with the AMS chapter in your busy time schedule. I also enjoyed having participated in the student field excursion where you with Martyn Drury taught me Pyrenean geology with patience and passion.

Further thanks go out to Jaume Dinarès-Turell for helping me during my first fieldwork and the long distance supervision as well as inspiration for continuing this project. Miguel Garces arranged the permits for several fieldworks. I learned a lot from David Heslop on the ins-and-outs of end-member modeling in rock magnetism. Pim van Maurik taught me how to use the scanning electron microscope (SEM).

Prof. Jianming Wu, Prof. Xirong Jia, Prof. Shuangsuo Yang and Dr. Yinda Zhai, thanks for encouraging me to apply the Ph.D. Thanks to Prof. Pu Su and Prof. Xingzhao Fan for support applying this Ph.D position. Also thanks to Prof. Reidar Løvlie for his recommendation for this Ph.D study.

Several other people have contributed to this thesis perhaps even without realizing it. Simon Vriend taught me geochemistry and administration skills during the student geochemistry fieldwork. I benefited from interesting discussions with Dr. Juan-José Villalaín on the Iberian remagnetization during the Castle meeting. We explored hydrological modeling and support of Prof. Majid Hassanizadeh, Prof. Ruud Schotting and Prof. Erwin Appel for discussing the possibilities for hydrogeological modeling is gratefully acknowledged. I appreciate the interest of Prof. Rinus Wortel and Prof. Wim Spakman for this project. Dr Hans de Bresser discussed with me the intricacies of plastic deformation in carbonates.

Ahmet Peynircioglu was patient, understanding and willing to listen to me during writing this thesis. He also spent his valuable time when I was in trouble with my computer. Many thanks go to him. Iuliana Vasiliev taught me all kinds of tricks of the Adobe Illustrator program and showed me how to use some instruments. Also I thank you and Martijn Deenen for helping the fieldworks in Spain. Thanks to Fatima Martín-Hernández and Christine Franke for sharing their experience during the Ph.D period and inspiring me to move ahead. Yougui Song provided inspiration during his visit in Utrecht. Thanks also to Frits Hilgen, for the nice scientific plus religion and philosophy discussions during the 'borrel'.

During the translation of the summary of this thesis, John, Mark Dekkers and Maud Meijers helped to improve the Dutch version, while Dr. Yougui Song and Jinping Han checked the Chinese version.

I also would like to thank my colleagues and friends: Silja Huesing, Andy Biggin, Arjan de Leeuw, Guillaume Dupont-Nivet, Klaudia Kuiper, Hayfaa Abdul Aziz, Geert Strik, Piet-Jan Verplak, Nuretdin Kaymakci, Pinar Ertepinar, Maartje Hamers, Mariel Reitsma, Gijs Straathof, Jelmer Oosthoek, Floor Boekhout, Lennart de Groot, Marius Stoica, Viktor Popov, Tanja Zegers, Cornelia Köhler, Ayten Koç, Hemmo

Abels, Angel Carrancho, Elisenda Costa, Sergei Yudin, Katya Grundan, Vika Tomsha, Femke Saulus, Roderic Bosboom, Bart Meijninger and Aart-Peter van den Berg van Saparoea for various sorts of aid. Thanks to Marcela Haldan to make me more professional.

Thanks to Liesbeth, Anne Beuwer and her families for improving my Dutch language and showing me the genuine Dutch life and culture. Thanks to Vincent Langereis for fixing my bike and delivering all kinds of nice things.

A special word of appreciation to my Chinese and Norwegian friends: Xiaomei Zhang, Yan Chen, Shenjie Gao, Weiming He, Yanchun Zhang, Meikun Jia, Jinping Han, Qunpeng Luo, Kari Kobbeltvedt and Heidi to make my spare time colorful.

Last but not least I am grateful for the support of my families: John, Conny, Agnes, Mat, Njoekie, Peter, Greetje, Berend, as well as other overseas and Chinese families no matter where they are. 感谢家里所有人在这博士学习期间的理解和支持!

宫志红

Zhihong Gong
September 2008
Utrecht, The Netherlands

Curriculum Vitae

Education

Ph.D. in Paleomagnetism 2004-2008
University of Utrecht, Utrecht, the Netherlands
Dissertation title: "The rotation of Iberia during the Aptian and consequences for pervasive Cretaceous remagnetization"
Promoter: Prof. dr. C.G. Langereis; Co-promoter: Dr. M.J. Dekkers

M. Ph. in Paleomagnetism 2001-2003
University of Bergen, Bergen, Norway
Thesis title: "Magnetostratigraphic correlation between Pleistocene loess/lacustrine sections at Dingcun and Dachai, Shanxi, China"
Supervisors: Prof. dr. R. Løvlie, Dr. H. Walderhang

B.Sc. in Hydrogeology and Engineering Geology 1994-1998
North China University of Water Conservancy and Electric Power, China
Thesis title: "The evaluation of the high slope stability in Xiaoliangdi Hydro project, China"
Supervisors: Prof. dr. Huaye Li, Dr. Rundong Huo

Working experience

Marketing Manager, Grand Environment & Industry Inc., China 2004

Project Manager, Taiyuan Advanced Technology Company, China 2003

Lecturer and research assistant, Taiyuan University of Technology, China 1998-2001

- ***Teaching courses:*** 'The treatment of building foundations', 'Modern mathematic technique', 'Rock mechanics' and 'Earth mechanics' in the Energy and Environment Institute
- ***Assisting project:*** Blake excursion in Salawusu section, Lawusu desert, Inner Mongolia, China – funded by NNSFC *(National Natural Science Foundation of China)*.
- ***Organizing the fourth year undergraduate industrial experience projects*** (4-year bachelor education system in China), mainly in Wangjiazhai Yellow River Hydro project, and Fen River Hydro project.

Personal interests and hobbies

Traveling, hiking, skiing, swimming, painting, rock and classical music